Thèse de doctorat

Université de Paris

Ecole doctorale BIOSPC – Bio Sorbonne Paris Cité – ED 562

Unité de Génétique Moléculaire des Virus à ARN

Host RNA degradation pathways and influenza A virus interplay: Identification of a major role of the cellular exonuclease ERI1 in the influenza A virus life cycle.

Présentée par Marion Declercq

Thèse de doctorat de Microbiologie – Spécialité Virologie

Dirigée par le Pr. Sylvie van der Werf

Présentée et soutenue publiquement à Paris, le 16 septembre 2019

Président du jury : Pr. Pierre Emmanuel Ceccaldi – Université de Paris - France

Rapporteur : Pr. Wendy Barclay – Imperial College London – Royaume-Uni

Rapporteur : Pr. Vigo Heissmeyer – Ludwig Maximilians Universität München – Allemagne

Examinateur : Dr. Cyril Barbezange – Sciensano – Belgique

Examinateur : Pr. Lionel Tafforeau – Université de Mons – Belgique

Directeur de thèse : Pr. Sylvie van der Werf – Université de Paris – France

Résumé détaillé en français

Les mécanismes de dégradation de l'ARN sont essentiels à l'homéostasie cellulaire. En effet, ils contrôlent la stabilité des ARN cellulaires, et par ce biais, régulent de façon globale l'expression des gènes cellulaires. Par ailleurs, la capacité à contrôler largement ou plus précisément l'expression des gènes cellulaires est cruciale à la fois pour l'hôte, mais aussi pour le virus. D'une part, la régulation de la stabilité des transcrits ARN est un élément essentiel au maintien de l'homéostasie cellulaire mais aussi à l'établissement d'une réponse cellulaire adaptée en cas d'infection virale. D'autre part, le succès de l'infection virale dépend fortement de la capacité du virus à prendre le contrôle des machineries d'expression géniques cellulaires. De ce fait, les virus doivent interagir avec les machineries cellulaires de dégradation de l'ARN afin de contrôler à la fois, l'expression des gènes cellulaires, et celle des gènes viraux. De nombreuses études rapportent l'existence d'une interface majeure d'interaction entre les machineries eucaryotes de dégradation de l'ARN et les protéines virales. Les virus ont non seulement la capacité d'échapper aux voies cellulaires de dégradation, mais ils peuvent également manipuler ces mécanismes cellulaires de dégradation de l'ARN afin de promouvoir leur propre réplication.

Les virus influenza de type A (IAV) sont des virus à ARN enveloppés appartenant à la famille des *Orthomyxovirdiae.* Leur génome se compose de 8 segments d'ARN de polarité négative. Chez l'homme, les virus influenza de types A sont responsables avec les virus influenza de type B des épidémies saisonnières de grippe. Les virus influenza de type A infectent non seulement l'homme mais également un grand nombre d'espèces animales, aviaires et mammifères (porc, cheval,..). Selon la nature de leurs glycoprotéines de surface, l'hémagglutinine (HA) et la neuraminidase (NA), différents sous-types d'IAV sont définis. Actuellement, les IAV de sous-types H1N1 et H3N2 circulent dans la population humaine et sont responsables des épidémies saisonnières de grippe. Occasionnellement, des virus venant du réservoir animal peuvent être transmis à l'homme et être responsables de cas d'infections dites zoonotiques (par ex. virus aviaires hautement pathogènes de sous-type H5N1, ou plus récemment, de sous-type H7N9). Episodiquement, l'introduction d'un sous-

type d'IAV antigéniquement nouveau dans la population humaine immunologiquement naïve peut donner lieu à une de pandémie, comme cela a été le cas en 2009.

Au sein de la particule virale chaque segment d'ARN négatif est associé à plusieurs monomères de nucléoprotéines (NP) ainsi qu'au complexe hétérotrimérique de réplication composé des protéines PB2, PB1 and PA, formant ainsi des ribonucléoprotéines virales (RNPv). Ces RNPv constituent l'unité fonctionnelle minimale requise pour la transcription et réplication du génome viral. La transcription virale est dépendante d'un mécanisme de « vol de coiffe » où l'extrémité 5' coiffée des ARNm cellulaires est liée par le domaine de liaison à la coiffe de PB2 et clivée par l'activité endonucléase de PA. Ces courtes amorces cellulaires coiffées servent ensuite à initier la synthèse d'ARNm viraux. La réplication virale dépend quant à elle de la synthèse d'un ARN complémentaire, servant de matrice à la synthèse d'ARN génomiques viraux. Ces processus s'effectuent dans le noyau des cellules infectées, en lien avec les machineries cellulaires. De ce fait, les IAV établissent un vaste et complexe réseau d'interactions avec le protéome cellulaire au cours de leur cycle viral.

Plusieurs études rapportent l'existence de liens étroits et complexes entre les IAV et les machineries de dégradation des ARN. Une étude récente a notamment montré que l'exosome à ARN, une machinerie centrale des processus de dégradation des ARN, était détourné par les IAV afin de promouvoir la transcription virale. De plus, plusieurs études soulignent l'importance des exonucléases XRN1 et XRN2, jouant un rôle majeur dans les processus de dégradation des ARN, dans le cycle des IAV. Cependant, les interactions entre protéines virales des IAV et machineries cellulaires de dégradation de l'ARN n'ont jamais été spécifiquement étudiées. A l'aide d'un test de complémentation protéique développé au laboratoire nous avons criblé une banque de 75 facteurs cellulaires portant des activités exoribonucléases et/ou appartement aux machineries de dégradation de l'ARN (nommée banque ExoRDec pour « Exonucleases and RNA DEcay ») pour leur interaction avec sept protéines virales qui constituent les RNPv (PB2, PB1, PA, NP) ou interagissent avec les RNPv et ont une rôle régulateur de leur activité (NS1, NEP) ou sont impliquées dans leur export du noyau (M1), de deux souches d'IAV : A/Bretagne/7608/2009(H1N1pdm09) et A/Paris/650/2004(H1N1).

Le test de complémentation protéique utilisé repose sur la reconstitution fonctionnelle d'une enzyme luciférase de *Gaussia princeps* (GPCA : *G. princeps* Protein Complementation Assay). Dans ce test, chaque partenaire protéique testé est fusionné à une moitié de la luciférase de *G. princeps*. La détection d'un signal lumineux est ainsi le reflet d'une interaction binaire entre les deux partenaires testés. Le crible systématique de la banque ExoRDec a ainsi permis l'identification de 18 protéines comme interagissant avec au moins une des protéines virales testées. Par ailleurs, l'étude des premiers voisins trouvés dans l'interactome humain des protéines cellulaires identifiées comme interagissant avec les protéines virales testées, d'une part, et celles n'interagissant pas avec les protéines virales d'autre part, a mis en évidence un enrichissement unique et spécifique du groupe de protéines cellulaires interagissant avec les protéines virales dans la voie de dégradation des ARN. Parmi les 18 interacteurs, huit ont également été identifiés comme nécessaires à la réplication des IAV à l'issue d'un crible par ARN interférence, validant ainsi l'utilisation de la GPCA comme technique efficace de criblage permettant l'identification d'interactions fonctionnellement pertinentes. Ainsi, ces deux cribles, interactomique et ARN interférence, complètent la carte des réseaux d'interactions existant entre protéines virales et protéines cellulaires impliquées dans les voies de dégradation ARN et soulignent l'importance du ciblage de ces voies pour la réplication des IAV.

Notre crible GPCA a permis l'identification de l'exoribonucléase ERI1 comme interagissant avec quatre protéines virales : PB2, PB1, NP et, dans une moindre mesure, M1. Ce profil d'interaction a par la suite été confirmé, en contexte infectieux ou non, par des expériences de co-immunoprécipitation qui ont identifié les composants des RNPv PB2, PB1 et NP comme interacteurs majeurs de ERI1. Par ailleurs, ERI1 a également été identifiée dans notre crible par ARN interférence comme requise pour la réplication des IAV. En effet, l'extinction de ERI1 par traitement siRNA est associée à une production réduite de particules virales infectieuses mais aussi à un retard dans l'accumulation des ARN viraux et protéines virales. Cependant, l'extinction de ERI1 ne réduit pas de façon drastique la production virale soulignant que ERI1 est requise mais non essentielle à la réplication des IAV. La caractérisation plus fine du rôle de ERI1 dans le cycle de réplication des IAV a permis de

mettre en évidence que ERI1 était nécessaire à la transcription virale, et notamment à la transcription virale primaire (*i.e.* transcription se faisant à partir des RNPv infectantes).

ERI1 a en particulier été caractérisée pour ses rôles dans la dégradation des ARNm histones en fin de phase S, dans la maturation de l'ARN ribosomique 5.8S, ainsi que dans l'homéostasie des petits ARN régulateurs. Par ailleurs, ERI1 porte deux domaines majeurs : un domaine de liaison à l'ARN (domaine SAP) ainsi qu'un domaine à activité exonucléase 5'-3'. A l'aide d'expériences de surexpression de différents mutants de ERI1 nous avons montré que ces 2 activités étaient essentielles au rôle de ERI1 dans la transcription virale. Nous avons par la suite caractérisé plus précisément l'interface d'interaction entre ERI1 et les protéines virales et montré que ces interactions, à la fois en contexte infectieux et non infectieux étaient sensibles au traitement par la RNase. Alors que le traitement par la RNase en contexte infectieux conduit à la perte totale de l'interaction entre protéines virales et ERI1, en contexte non infectieux, celui-ci n'est associé qu'à une perte partielle de l'interaction. De ce fait, bien que l'interaction soit sensible à la RNase, nous ne pouvons pas exclure que des interactions protéine-protéine directes puissent également être impliquées dans l'interaction entre ERI1 et les protéines virales.

De façon intéressante, les ARN viraux sont également co-purifiés avec ERI1 dans les cellules infectées. Par ailleurs, une plus grande quantité d'ARNm viraux, en comparaison des ARN viraux génomiques, sont co-purifés avec ERI1. Cet enrichissement spécifique, associé à nos résultats d'interactomique ainsi qu'au rôle de ERI1 dans la transcription virale, est en faveur d'un modèle selon lequel les RNPv en cours de transcription cibleraient ERI1.

L'interaction entre ERI1 et les protéines virales étant sensible à la RNase à la fois en contexte infectieux et en contexte non infectieux, celle-ci pourrait donc impliquer un ARN cellulaire, plutôt qu'un ARN viral. La transcription virale a lieu dans le noyau des cellules infectées. Dans le noyau, ERI1 s'associe aux ARNm histones, entre autres liés par la protéine SLBP, et participe à leur maturation avant leur export nucléaire. De façon notable, ERI1, SLBP, mais aussi les ARNm histones, sont co-purifiés avec PB2 dans les cellules infectées. De plus, l'interaction entre SLBP et les protéines virales, tout comme l'interaction entre ERI1 et protéines virales, est sensible au traitement par la RNase. De plus, le mutant de liaison à l'ARN de ERI1, delta SAP, est déficient pour l'association aux ARNm histones mais aussi aux

ARN viraux. En résumé, ces résultats suggèrent que la polymérase virale en cours de transcription et/ou les ARN viraux seraient incapables de s'associer à une forme de ERI1 ayant perdu la capacité de lier les ARNm histones.

Ainsi, nos résultats suggèrent un modèle où le rôle de ERI1 dans le cycle des IAV, ainsi que son interaction avec les protéines virales, nécessite son association avec les ARNm histones. Cette association est dépendante de l'ARN et, est également probablement stabilisée par des interactions protéine-protéine directes. Cependant, le but précis de cette interaction ainsi que le rôle de l'activité exonucléase de ERI1 requise pour promouvoir la transcription virale restent encore à élucider. Deux hypothèses sont toutefois envisageables et sont discutées dans le manuscrit présenté ci-après. i) L'interaction entre la polymérase virale et ERI1 pourrait aider à adresser efficacement les RNPv aux sites actifs de transcription cellulaire, favorisant de ce fait le mécanisme de vol de coiffe, et par ce biais, la transcription virale. ii) L'activité de transcription de l'ARN Polymérase II, requise pour la synthèse de messagers coiffés, nécessaires à l'initiation de la transcription virale, est plus importante en phase G1 du cycle cellulaire. Les ARNm histones sont en revanche largement synthétisés avant l'entrée en phase S des cellules. Ainsi, le ciblage de ERI1 par la polymérase virale permettrait de recruter les RNPv près des sites actifs de transcription cellulaire par l'ARN Polymérase II, favorisant ainsi la transcription virale, en dehors de la phase G1 du cycle cellulaire.

ERI1, *via* ses différents rôles dans l'homéostasie des petits ARN régulateurs, dans la maturation des ARN ribosomiques ou dans la maturation et la dégradation des ARNm histones possède un rôle central dans le contrôle de l'expression génique. Ainsi, le ciblage de ERI1 par les IAV représente un autre exemple du détournement des machineries de dégradation ARN par les virus, visant à créer un environnement cellulaire favorable à la réplication virale.

Mots clés : Virus influenza de type A, polymérase, réplication, transcription, machineries de dégradation de l'ARN, exonucléase, interactions virus-hôte, crible interactomique, crible par ARN interférence, ERI1, SLBP, ARNm histone, liaison à l'ARN

Résumé en français

Les mécanismes de dégradation de l'ARN représentent un processus cellulaire central. En effet, ils contrôlent la stabilité et la qualité de l'ARN et, par conséquent, régulent l'expression des gènes. D'une part, la régulation de la stabilité des transcrits est un élément essentiel au maintien de l'homéostasie cellulaire mais aussi à l'établissement d'une réponse cellulaire adaptée en cas d'infection virale. D'autre part, le succès de l'infection virale dépend fortement de la capacité du virus à prendre le contrôle des machineries d'expression géniques cellulaires. De ce fait, les virus doivent interagir avec les machineries cellulaires de dégradation de l'ARN afin de contrôler à la fois, l'expression des gènes cellulaires, et celle des gènes viraux. De nombreuses études rapportent l'existence d'une interface majeure d'interaction entre les machineries eucaryotes de dégradation de l'ARN et les protéines virales. Les virus ont non seulement la capacité d'échapper aux voies cellulaires de dégradation, mais ils peuvent également manipuler ces mécanismes cellulaires de dégradation de l'ARN afin de promouvoir leur propre réplication.

Les virus influenza de type A (IAV) sont des agents pathogènes majeurs responsables d'épidémies annuelles et de pandémies occasionnelles. Pour leur cycle de réplication, les IAV dépendent de nombreuses protéines cellulaires et établissent ainsi un vaste et complexe réseau d'interactions avec le protéome cellulaire. Par ailleurs, plusieurs études rapportent l'existence de liens étroits entre les IAV et les machineries de dégradation de l'ARN. Ainsi, identifier les interactions mises en jeu lors du cycle viral participe à une meilleure compréhension du cycle viral, nécessaire au développement de stratégies antivirales.

Nous avons recherché des interactions entre les protéines virales impliquées dans la réplication des IAV et un ensemble de 75 protéines cellulaires portant des activités exoribonucléases et/ou associées aux mécanismes de dégradation de l'ARN. Au total, 18 protéines ont été identifiées comme interagissant avec au moins une des protéines virales testées. Par ailleurs, l'analyse du réseau d'interaction a mis en évidence un ciblage spécifique et préférentiel des voies de dégradation de l'ARN par les protéines des IAV. Enfin, parmi les interacteurs validés, un criblage par ARN interférence a identifié neuf facteurs comme étant nécessaires à la multiplication virale.

Nous avons choisi de nous concentrer sur l'exoribonucléase 1 (ERI1), identifiée comme interacteur de plusieurs composants des RNPv (RiboNucleoProtéine virale) (PB2, PB1 et NP). ERI1, *via* ses différents rôles dans l'homéostasie des petits ARN régulateurs, dans la maturation des ARN ribosomiques ou dans la maturation et la dégradation des ARNm histones possède un rôle central dans le contrôle de l'expression génique. En explorant l'interaction entre ERI1 et les protéines virales au cours de l'infection, nous avons mis en évidence que i) ERI1 favorise la transcription virale et que, pour ce faire, ses deux activités - liaison à l'ARN et exonucléase - sont nécessaires, ii) ERI1 interagit avec les protéines virales de manière dépendante de l'ARN, iii) ERI1 interagit avec les RNPv, iv) les protéines virales interagissent avec une forme d'ERI1 associée aux ARNm histones. Ainsi, nos données tendent vers un modèle dans lequel ERI1 associée aux ARNm histones est cooptée par la polymérase virale en transcription, favorisant ainsi la multiplication des IAV par un mécanisme qui reste cependant encore à déterminer. Ainsi, le ciblage de ERI1 par les IAV représente un autre exemple du détournement des machineries de dégradation de l'ARN par les virus, visant à créer un environnement cellulaire favorable à la réplication virale.

Abstract

RNA decay is a central cellular process as it regulates RNA stability and quality and thereby gene expression, which is essential to ensure proper cellular physiology and establishment of adapted responses to viral infection. Global takeover of gene expression machineries and rewiring of the cellular environment is key to the success of viral infection. Cellular proteome and viral replication are tightly connected and cellular RNA processing, stability, quality and decay accordingly influence the fate of the viral cycle. Growing evidence points towards the existence of a large interplay between eukaryotic RNA turnover machineries and viral proteins. Viruses not only evolved mechanisms to evade those RNA degradation pathways, but they also manipulate them to promote viral replication.

Influenza A viruses (IAV) are major pathogens responsible for yearly epidemics and occasional pandemics. To complete their viral cycle, IAVs rely on many cellular proteins and establish a complex and highly coordinated interplay with the host proteome. Growing evidence supports the existence of a complex interplay between IAV viral proteins and RNA decay machineries. Unraveling such interplay is therefore essential to gain a better understanding of the IAV life cycle, required for the development of antiviral strategies.

This led us to systematically screen interactions between viral proteins involved in IAV replication and a selected set of 75 cellular proteins carrying exoribonucleases activities or associated with RNA decay machineries. A total of 18 proteins were identified as interactors of at least one viral protein tested. Analysis of the interaction network highlighted a specific and preferential targeting of RNA degradation pathways by IAV proteins. Among validated interactors, a targeted RNAi screen identified nine factors as required for viral multiplication.

We chose to focus on the 3'-5' exoribonuclease 1 (ERI1), found in our screen as an interactor of several components of the vRNPs (viral RiboNucleoProtein) (PB2, PB1 and NP). The ERI1 protein is a major player in the control of cellular gene expression as it is essential for the maturation and decay of histone mRNA, maturation of 5.8S rRNA and miRNA homeostasis in mammalian cells. Exploring the interplay between ERI1 and viral proteins during the course of IAV infection we found that i) ERI1 promotes viral transcription, and both of its activities – RNA binding and exonuclease – are required, ii) ERI1 interacts with viral proteins in an RNA dependent manner, iii) ERI1 interacts with the transcribing vRNPs, iv) viral proteins interact with a form of ERI1 that is associated to histone mRNA. Ultimately, our data point to a model where ERI1 associated to histone mRNA is co-opted by the transcribing viral polymerase, thereby promoting IAV multiplication, through a mechanism that remains to be precisely determined. Targeting of ERI1 by IAV is another example further supporting the intricate interplay between IAV and RNA decay machineries, used to rewire cellular gene expression in order to create a favorable environment for viral replication.

Keywords: Influenza A virus, polymerase, replication, transcription, RNA decay, exonuclease, host-virus interactions, interactomic screen, RNAi screen, ERI1, SLBP, histone mRNA, RNA binding

Acknowledgements

First, I would like to thank the member of my thesis committee, Pr. Wendy Barclay and Pr. Vigo Heissmeyer, who kindly accepted to review this work during their summer. I would also like to thank Dr. Cyril Barbezange and Pr. Lionel Tafforeau who agreed to be examiners during my defense, and finally Pr. Pierre-Emmanuel Ceccaldi who accepted to chair this thesis committee.

Je remercie ensuite l'université Paris Diderot qui a financé mon doctorat et qui m'a donné la chance de faire 2 années très enrichissantes en tant que moniteur. Je remercie également la Fondation pour la Recherche Médicale qui a financé cette dernière année de thèse et qui m'a permis de terminer ce travail plus sereinement.

Merci au Pr. Sylvie van der Werf qui m'a accueillie dans son laboratoire. Merci de m'avoir fait confiance pendant ces 4 années de thèse. Merci pour votre gentillesse, votre bienveillance ainsi que vos conseils toujours pertinents.

Merci au Dr. Caroline Demeret qui m'a accueillie en stage quand j'étais étudiante de Master 1. Merci de m'avoir fait confiance et initiée à l'interactomique. Merci aussi du fond du cœur pour ta présence, tes conseils et ton implication au quotidien pendant ces 4 années de thèse, qui ont été indispensables à la réussite de ce projet. Enfin, merci de m'avoir aidée à grandir et à m'endurcir.

Merci au Dr. Cyril Barbezange qui m'a d'abord encadrée pendant mon Master 2 puis en thèse. Merci de m'avoir appris la rigueur des titrages par centaines. Merci d'avoir toujours répondu présent quand j'avais besoin d'aide, merci pour tes conseils et tes bonnes idées, même après ton départ en Belgique. Enfin, merci beaucoup d'avoir pris le temps de relire l'introduction de cette thèse.

Je tiens également à remercier le Dr. Yves Jacob, Patricia Cassonnet et Mélanie Dos Santos, pour leur aide, leurs conseils et leur disponibilité sans lesquels je n'aurai probablement pas réussi à dépatouiller les galères de clonages indispensables à la construction de la banque ExoRDec.

Merci à tous les membres passés et présents du laboratoire que j'ai pu côtoyer et en particulier à tous ceux qui m'ont supportée et soutenue au quotidien : Marion Barbet, Sylvie Behillil, Mathilde Benassaya, Solenne Brun (SBrun !), Angela Brisebarre, David Courtney, Bernadette Crescenzo (merci pour tes conseils, tes râleries et nos discussions), Christine Detchepare, Flora Donati (FloFloooo <3 !), Vincent Enouf, Anne-Marie Filodeau, Guillaume Fournier, Tim Krischuns, Marie Lazzerini, Stéphane Léandri, Catherine Isel-Griffiths, Sandie Munier, Nadia Naffakh (merci à toutes les 3 pour vos précieux conseils et votre aide durant ces 4 années), Isabelle Poste, Yannis Rahou (Kakou !) et Sarah Razafindrakoto. Merci à tous pour votre présence et votre aide en tout genre, vos sourires et votre bonne humeur au quotidien. Je vous souhaite à tous le meilleur pour la suite.

To my fellow PhD students colleagues, Usama Ashraf, Kuang-Yu Chen and Marwah Karim, I wish you all the best and good luck for the rest of your PhD.

Merci à mes amis anciens étudiants en thèse du laboratoire. Merci à Elise Biquand qui a été la meilleure co-thésarde de bureau que l'on puisse espérer avoir. Merci à Cédric Diot d'avoir été un grand frère de thèse plein de bons conseils, merci aussi pour toutes tes railleries.

Merci à Mélanie Dos Santos avec qui je suis vraiment très heureuse et chanceuse d'avoir fait un gros bout de chemin au labo depuis notre stage de Master 2. Merci pour ton incroyable gentillesse, merci d'avoir toujours été présente, à l'écoute et disponible.

Un merci tout particulier à mes sœurs de cœur du labo, Mélanie et Nicolas. Merci pour le soutien, pour les pauses à n'importe quelle heure, pour les fous rires, pour le pouvoir des trois, pour les sorties arrière-cuisine mais aussi pour toutes les autres. Merci d'avoir rendu les moments difficiles plus doux et supportables. Merci pout tout. Cette thèse aurait été beaucoup plus dure sans votre présence et vos rires.

Merci à mes 2 copines du nord, Anaïs et Marion qui sont toujours là malgré mes rares visites. Merci d'avoir toujours répondu présentes quand j'avais besoin de râler, que l'on me remonte le moral ou simplement que l'on me change les idées.

Merci à Elise pour sa présence à toute épreuve au quotidien depuis Dublin. Merci d'avoir partagé, suivi et soutenu tous les hauts et bas de cette thèse.

Merci aux super copains du Master de viro : Ghina, Lulu, Mélanie, Sousou, et tous les autres. Merci pour votre soutien, vos sourires et tous les bons moments partagés. Un merci spécial du fond du cœur à Barbara. Merci d'avoir été cette amie magique de galère de la 4ème année de thèse.

Merci aussi à tous mes amis rencontrés à Pasteur, à Agathe, merci d'être cette jolie bouffée de fraicheur et de légèreté à chaque fois que je te vois, à Vincent qui a été un super compagnon de rédaction, à Ségo, Guigui, et tous les autres qui ont égayés de très nombreux moments.

Merci à mes parents, à mes petites sœurs et à toute ma famille pour tout ce qu'ils ont fait pour moi ainsi que pour le soutien indéfectible. Et surtout, merci de m'avoir supportée quand j'étais insupportable.

Mes derniers remerciements vont à Florian, merci de m'avoir supportée et supportée pendant ces 4 années. Merci de ton soutien, de ton amour et de ta présence au quotidien. Merci aussi pour toutes ces discussions science qui ont énormément aidé ce projet. Et surtout, merci de m'avoir aidée à lâcher prise quand il le fallait. Merci pour tout. Je n'aurai pas réussi sans toi.

Table of content

Table of figures

Table of tables

Abbreviations

3'UTR:	**3' U**n**TR**anslated region
5'UTR:	**5' U**n**TR**anslated region
A549:	**A**denocarcinomic human alveolar basal epithelial cells
aa:	**a**mino **a**cid
AP-MS:	**A**ffinity **P**urification followed by **M**ass **S**pectrometry
ARE:	**AU R**ich **E**lement
AREBP:	**ARE B**inding **P**rotein
ASFV:	**A**frican **S**wine **F**ever **V**irus
BMV:	**B**rome **M**osaic **V**irus
cRNA:	**c**omplementary **RNA**
CHX:	**C**yclo**H**e**X**imide
CTD:	**C t**erminal **D**omain of the RNA Polymerase II
Cter:	**C ter**minal
dsDNA:	**d**ouble **s**tranded **DNA**
dsRNA:	**d**ouble **s**tranded **RNA**
EBV:	**E**pstein **B**arr **V**irus
EJC:	**E**xon **J**unction **C**omplex
ER:	**E**ndoplasmic **R**eticulum
ERI1:	3'à5' **E**xo**RI**bonuclease **1**
FluPol:	In**flu**enza virus **Pol**ymerase complex
GPCA:	***G**aussia **p**rinceps* **P**rotein **C**omplementation **A**ssay
GRE:	**GU R**ich **E**lement
HA:	**H**emagglutin
HCC:	**H**istone **C**leavage **C**omplex
HCV:	**H**epatitis **C V**irus
HEK 293T:	**H**uman **E**mbryonic **K**idney cells 293 cells
HSV-1:	**H**erpes **S**implex **V**irus 1
IAV:	**I**nfluenza **A V**irus
IBV:	**I**nfluenza **B V**irus
ID:	**I**nter**D**omain

JEV: **J**apanese **E**ncephalitis **V**irus

KO: **K**nock-**O**ut

KSHV: **K**aposi's **S**arcoma associated **H**erpes **V**irus

lncRNA **l**ong **n**on **c**oding **RNA**

M1: **M**atrix Protein **1**

M2: **M**atrix Protein **2**

MCMV: **M**urine **C**yto**M**egalo**V**irus

MDCK: **M**adin-**D**arby **C**anine **K**idney cells

MDCK Siat: **M**adin-**D**arby **C**anine **K**idney cells overexpressing the human 2,6-**Sial**t**r**ansferase

MHV: **M**urine **H**epatitis **V**irus

MHV68: **M**urine gamma-**H**erpes **V**irus **68**

miRNA **mi**cro **RNA**

moi: **m**ultiplicity **o**f **i**nfection

NA: **N**euraminidase

NEP: **N**uclear **E**xport **P**rotein

ncRNA: **n**on **c**oding **RNA**

NGD : **N**o**G**o **D**ecay

NLR: **N**ormalized **L**uminescence **R**atio

NMD: **N**onsense-**M**ediated **D**ecay

NSD: **N**o**S**top **D**ecay

NP: **N**ucleo**P**rotein

NS1: **N**on **S**tructural Protein **1**

NT: **N**on **T**argeting siRNA

Nter: **N ter**minal

PA: **P**olymerase **A**cidic

PB1: **P**olymerase **B**asic **1**

PB2: **P**olymerase **B**asic **2**

PCA: **P**rotein **C**omplementation **A**ssay

pfu: **p**laque **f**orming **u**nit

PPI: **P**rotein-**P**rotein **I**nteraction

PT: **P**ositive **T**hreshold

ORF: **O**pen **R**eading **F**rame

RISC: **R**NA-**i**nduced **s**ilencing **c**omplex

RdRp: **R**NA **d**ependent **R**NA **p**olymerase

RITS: **R**NA-**I**nduced **T**ranscriptional **S**ilencing

RNAi: **RNA i**nterference

RNA Pol II: **RNA P**olymerase **II**

rRNA: **r**ibosomal **RNA**

RVFV: **R**ift **V**alley **F**ever **V**irus

SARS CoV: **S**evere **A**cute **R**espiratory **S**yndrome **Co**rona**V**irus

SFV: **S**emliki **F**orest **V**irus

SINV: **SIN**dbis **V**irus

siRNA **s**mall **i**nterfering **RNA**

U7 snRNA: **U7 s**mall **n**uclear **RNA**

U7 snRNP: **U7 s**mall **n**uclear **R**ibo**N**uclear **P**rotein

VACV: **VAC**cinia **V**irus

vmRNA: **v**iral **m**essenger **RNA**

vRNA: **v**iral **RNA**

VSV: **V**esicular **S**tomatitis **V**irus

Y2H: **Y**east **two H**ybrid

YFV: **Y**ellow **F**ever **V**irus

WNV: **W**est **N**ile **V**irus

wt: **w**ild-**t**ype

Introduction

I. Influenza A viruses: general features

1. Classification of influenza A viruses

Influenza viruses belong to the *Orthomyxoviridae* family. All influenza viruses are enveloped and their genome consists of seven or eight segments of single stranded RNAs of negative polarity. According to the antigenic properties of the nucleoprotein (NP) and the matrix protein (M1), four types of influenza viruses are described [1]. Influenza A viruses (IAV) and influenza B viruses (IBV) contain eight RNA segments, while influenza C and influenza D viruses have only seven segments.

Influenza A and B viruses are responsible for annual epidemics, while influenza C viruses are less prevalent and usually cause mild infections in humans. Influenza C viruses have also been reported to infect swine and bovine species like influenza D viruses discovered in 2013. So far, influenza D viruses have not been detected in humans [1,2].

Unlike the other influenza virus types, IAVs can infect a wide range of birds and mammalian species including humans. IAVs are further classified into sub-types according to their surface glycoproteins, the hemagglutinin (HA) and the neuraminidase (NA), the two most variable viral proteins encoded by IAVs. To date 16 HA and 9 NA sub-types have been identified among avian strains. In addition, two subtypes have been identified in bats, H17N10 and H18N11 [3].

Currently, seasonal IAVs of the H1N1 and H3N2 sub-types circulate in the human population causing annual epidemics. The H2N2 sub-type is the only other IAV sub-type known to have circulated in the human population in the 20th century (from 1957 to 1968). In addition to yearly epidemics, IAVs zoonotic potential has also led to occasional pandemics. Since 1918, introduction of IAVs from the avian or swine reservoir in the human population has led to four pandemics (in 1918, 1957, 1968 and 2009) [4].

2. The influenza A virus: particle, genome and viral cycle

a. *Influenza A virus particle*

IAVs particles are enveloped (**Figure 1A**) and can display diverse morphologies. Virions are generally of spherical or elliptical shapes with diameters ranging from 80 to 120 nm. Filamentous particles that can reach length up to 20 µm have also been described (**Figure 1B, C**). However, filamentous particles are more frequently found in clinical isolates, whereas most of the laboratory adapted strains are predominantly spherical [5]. Their lipid membrane derives from the host cell and includes three viral proteins: the HA, the NA, both forming characteristic spikes at the surface of the particle, and the membrane channel protein M2. The HA is required for the attachment to the cell surface and for the fusion of viral and cellular envelopes while the NA carries a sialidase activity important for the release of new viral particles. The M2 proteins form ion channels essential during viral entry. Additionally, cellular proteins such as tetraspanins are also incorporated in the viral envelope and contribute to virion structure [6,7].

A recent study characterized the amount of variation within an IAV particle population. Using labeled viruses, Vahey and Fletcher found great variability in the abundance of HA and NA between individual particles (up to 100-fold variation between virions) as well as in the HA to NA ratios. The authors linked this tremendous variability to a low fidelity assembly process inherent to the virion biogenesis mechanism [8]. Overall, this phenotypic heterogeneity contributes to viral population survival when facing challenging environments including the exposure to some antiviral drugs.

The protein M1 lies just beneath the viral envelope where oligomers assemble to form a continuous matrix. M1 is essential to maintain virion morphology and plays a key role in virion assembly and budding. The core of the viral particle is represented by eight viral ribonucleoproteins (vRNPs). Each vRNP is composed of a single strand of negative RNA, associated to oligomers of nucleoprotein NP and to the heterotrimeric viral polymerase, which is composed of the Polymerase Basic 2 protein (PB2), the Polymerase Basic 1 protein (PB1) and the Polymerase Acidic protein (PA). Within the viral particle, the eight vRNPs usually adopt a 7+1 configuration, in which a central vRNP is surrounded by the seven other

vRNPs (**Figure 1D**). Highlighting the importance of such organizational pattern, a recent study reported that in the presence of only seven vRNAs, host-derived 18S and 28S ribosomal RNAs (rRNAs) are specifically incorporated into the virions [9].

Finally, the Non Structural Protein NS1 and the Nuclear Export Protein NEP are also found in the viral particle along with several cellular proteins, such as cytoskeletal proteins, ubiquitin, annexins or cyclophilin A [6,7,10].

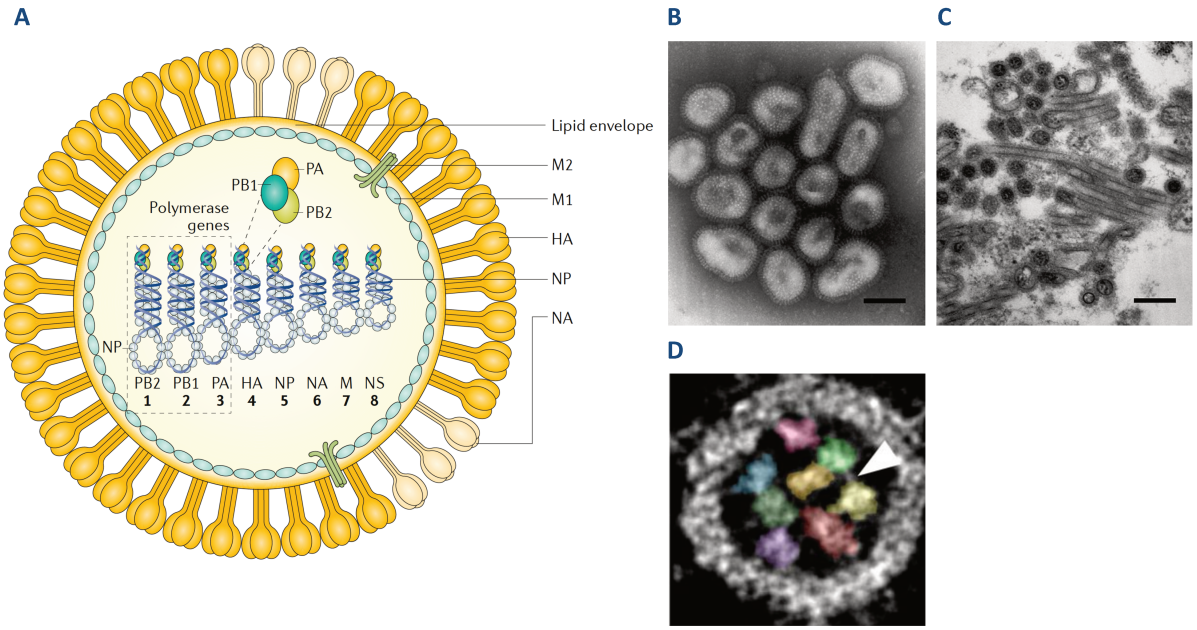

Figure 1: The influenza virus particle.
A. Schematic representation of the IAV particle. The viral envelope incorporates the hemagglutinin (HA), the neuraminidase (NA) and the M2 ion channel protein. The matrix M1 protein lies beneath the viral envelope providing a scaffold that shapes the virion and interacts with the surface proteins and the vRNPs. The vRNPs consist of a negative stranded RNA, associated to the nucleoprotein (NP) and to the trimeric polymerase complex (PB2, PB1 and PA). **From [2].** **B-C.** Electron microscopy images of pandemic H1N1 2009 virus. Negatively stained virions collected from the supernatant of infected cells. Scale bar, 100 nm (**B**). Filamentous particles from sections of infected lungs. Scale bar, 200 nm (**C**). **From [11]**. **D.** Tomograms (0.5 nM thick) of a transversal section of an IAV virion. The vRNPs are organized in a 7+1 pattern with a central segment surrounded by the other seven segments. White arrowhead indicates linkage between vRNPs. **From [12].**

b. *Influenza A viral cycle*

The IAV life cycle begins with attachment of the HA proteins to the cell surface [13] (**Figure 2**). On the surface of the viral envelope, the HA is organized in homotrimers forming

spikes. The HA spikes bind to the sialic acids found on the surface of the host cell membrane. Sialic acids are ubiquitous molecules. However, two major linkages are found between sialic acids and the carbohydrates they are bound to in glycoproteins. The HA proteins of viruses that replicate in different species show different specificities towards sialic acids with different linkages. Human viruses preferentially bind to sialic acids with an α2,6 linkage, whereas viruses from avian origin mostly bind to sialic acids with an α2,3 linkage [14].

The HA is made up of two subunits linked by a disulfide bound: HA1, which contains the receptor binding domain, and HA2, which contains the fusion peptide (reviewed in [15]). Upon binding of the virus to the cell membrane, endocytosis is induced. Endocytosis is mainly clathrin dependent, but clathrin independent pathways, such as macropinocytosis, have been reported [16–18]. The low pH of the endosome induces a conformational change of the HA leading to the exposition of the HA2 fusion peptide allowing fusion of the endosomal and viral membranes (reviewed in [19]). Then, the acidic environment of the endosome opens up the M2 ion channel. M2 is a transmembrane protein organized in tetramers acting as a proton-selective ion channel [20]. Acidification of the viral core weakens the interaction between M1 and the vRNPs allowing their release into the cytoplasm [21]. The vRNPs are then routed to the nucleus using the importin-α-importin-β1-dependent nuclear import pathway, where viral transcription and replication will take place (reviewed in [22]).

Inside the nucleus the viral polymerase carries out the transcription and replication of the viral genome (see section II.2.) (reviewed in [23,24]). The viral mRNAs are then exported to the cytoplasm *via* the NXF1 pathway and translated by the cellular machinery (reviewed in [25]). Newly synthesized proteins required for subsequent rounds of transcription and for replication of the viral genome are imported into the nucleus, whereas the HA, NA and M2 proteins are targeted to the endoplasmic reticulum (ER) before being addressed to the plasma membrane *via* the Golgi network. PA and PB1 proteins are translocated into the nucleus as a heterodimer, while PB2 and NP are imported individually [26,27]. The genomic viral RNA is replicated through the synthesis of a positive sense complementary RNA (cRNA) intermediate that in turn serves as template for synthesis of new vRNAs. Both the cRNAs and the vRNAs are further associated to oligomers of NP and bound by the RNA dependent RNA

polymerase (RdRp) complex, thereby forming new cRNPs or vRNPs. The newly synthesized vRNPs are then exported from the nucleus through interaction with M1. To this end, M1 interacts with the Nuclear Export Protein (NEP), which in turn interacts with the exportin CRM1.

Once in the cytoplasm, newly synthesized vRNPs are trafficked by the RAB11 GTPase to the plasma membrane for assembly. How vRNPs come into contact with RAB11 is still unclear. One model proposes that vRNPs associate with RAB11 on recycling endosomes and use the microtubules for transport to the cell membrane [28,29]. Recently, another model has been proposed where infection causes tubulations of the ER membrane. vRNPs exiting the nucleus would be targeted to the modified ER where they are thought to interact with RAB11. Vesicles carrying RAB11 associated to vRNPs are then proposed to bud from the ER and ensure transport of the vRNPs to the plasma membrane [30]. Eight distinct vRNPs are then incorporated into the viral particle. Specific interactions between vRNPs most likely contribute to the packaging, however the precise mechanism is still largely unknown [31]. A recent study generated a high-resolution structure of the IAV genome, and reported that IAV segments have distinct RNA configurations and form both intra- and intersegment RNA interactions within a viral particle. Those interactions are proposed to drive segment co-segregation during reassortment events as well as selective segment packaging [32].

Once the newly assembled viral particles bud, their release from the cell surface depends on the sialidase activity of the NA. The NA is organized in tetramers at the surface of the particle. By removing sialic acids residues, NA promotes the liberation of viral particles and prevents their aggregation [33]. Furthermore, a proper balance between HA and NA activities is imperative to avoid HA and NA competition during release and entry steps (reviewed in [34]). Still, most of the newly budded virions are non-infectious as they harbor HA proteins that are fusion incompetent. To gain its fusion competency, HA must be cleaved into the HA1 and HA2 subunits. This cleavage occurs either at a monobasic or at a multibasic cleavage site [35]. Human IAVs encode HAs carrying monobasic cleavage sites, which are processed by extracellular proteases found in the respiratory tract. However, highly pathogenic avian strains of the H5 and H7 subtypes harbor HA with a multi-basic site that is cleaved by furin, a ubiquitous protease of the *trans* Golgi network. This major difference

therefore confers a wider tissue tropism to these highly pathogenic avian strains, causing systemic infection and fatal disease.

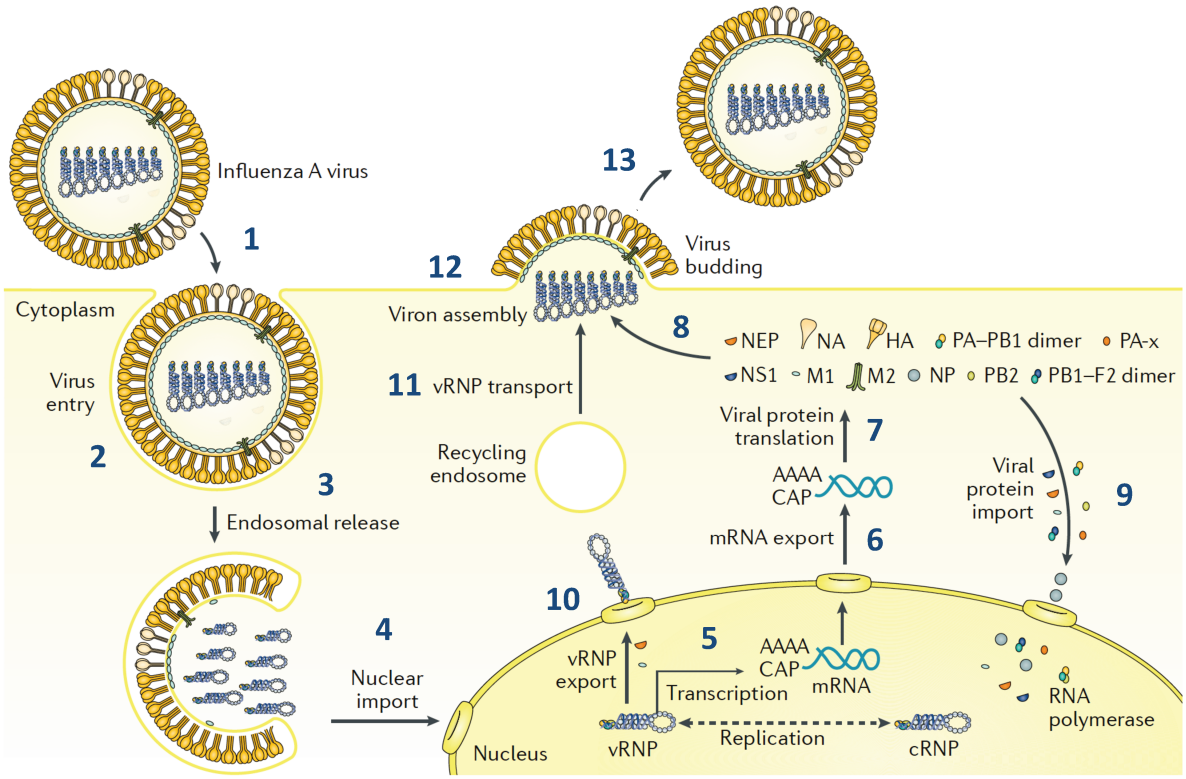

Figure 2: IAV cycle.

1) Attachment of the HA to the cellular receptor. **2)** Fusion of viral and endosomal envelopes. **3)** Release of the vRNPs into the cytoplasm. **4)** Nuclear import of vRNPs. **5)** Transcription and replication of the viral genome. **6)** Nuclear export of viral mRNAs. **7)** Translation of viral proteins. **8)** Trafficking of the envelope proteins (HA, NA and M2) to the plasma membrane. **9)** Nuclear import of viral proteins involved in the viral replication. **10)** Nuclear export of neosynthetized vRNPs. **11)** Transport of the vRNPs to the cellular membrane (only the RAB11 recycling endosome mediated trafficking of the vRNPs model is represented here). **12)** Virion assembly. **13)** Virion budding. **Adapted from [2].** IAV cell entry, replication and virion assembly is reviewed in [36].

c. *Proteins encoded by the influenza A virus genome*

The genome of IAVs encodes 10 essential proteins as well as up to eight specific additional proteins. Due to the limited size of their genome, IAVs have evolved different strategies such as the use of splicing or alternative reading frames to increase their coding capacity (reviewed in [37,38]).

The splicing of M1 and NS1 mRNAs give rise to mRNAs encoding the M2 and NEP proteins essential for IAV replication. The first additional protein discovered was PB1-F2,

expressed from an alternative open reading frame (ORF), most likely through leaky scanning of the upstream AUG codons of the PB1 ORF [39]. PB1-F2 was found to be a virulence factor, expressed in many but not all IAV strains [40]. PB1-N40 is an N-terminally truncated form of PB1 translated as a result of leaky scanning of an upstream AUG codon as well [41].

PA-X, is a ribosomal frame shift product, translated from the PA segment mRNA as a fusion of the N-terminal endonuclease domain of PA (191 aa) and the C-terminal domain (61 aa) encoded by an alternative ORF of PA, called X-ORF. PA-X is involved in the modulation of host responses to influenza virus infection [42] (see section III.3.b.). Truncated forms of the PA protein (PA-N155 and PA-182) are also translated from in frame downstream AUG codons [43].

Besides M2 mRNA, two other spliced transcripts; M3 and M4 mRNAs are expressed from the M segment. All spliced M segment mRNAs use a common acceptor splice site, but different donor splice sites. M3 mRNA does not encode any protein and is thought to act as a negative regulator of the M1 and M2 proteins expression [44]. The M42 protein, which is an M2 variant with an alternative ectodomain, is expressed from the M4 mRNA possibly through leaky scanning [45].

For some viruses, splicing of the NS segment mRNA produces the NS3 mRNAs coding for an NS1 isoform with an internal deletion, while splicing of the PB2 mRNA produces the PB2-S1 protein [46,47]. The NS3 function is poorly understood but is proposed to be involved in host adaptation [46]. PB2-S1 was found to inhibit the RIG-I-dependent signaling pathway *in vitro*; although PB2-S1 deficiency had no effect on viral growth in cell culture nor on virus pathogenicity in mice [47].

Lastly, an unusual long ORF, NEG8, was identified in the negative orientation on the genomic strand of the NS segment. There is still no evidence supporting its transcription into mRNA or translation into protein. However, the NEG8 ORF is very conserved among influenza viruses suggesting an important role in the viral cycle and some biological data in mice would support its existence [48,49].

All the distinct IAV encoded proteins and their major functions are summarized in **Table 1**.

Segment length	Schematic view of the ORFs encoded by the viral segments	Theoric molecular sizes	Principal functions of encoded proteins
PB2 2341 nt		PB2: 86 kDa PB2-S1: 55 kDa	PB2: Component of the vRNP, binds the cap of cellular mRNA PB2-S1: Unkown (inhibition of RIG-I dependent signalling pathway *in vitro*)
PB1 2341 nt		PB1: 87 kDa PB1-F2: 10-kDa PB1-N40: 82kDa	PB1: Component of the vRNP, RNA dependent RNA polymerase PB1-F2: Apoptosis, regulation of polymerase activity PB1-N40: Unkown
PA 2233 nt		PA: 84 kDa PA-X: 29 kDa	PA: Component of the vRNP, endonuclease (cleaves cap of host transcripts for cap snatching) PA-X: Host shut-off PA-N155 and PA-N182: Unkown
HA 1778 nt		HA: 61 kDa	HA: Surface glycoprotein organized in homotrimers, binding to the cell surface, fusion of cellular and endosomal membranes
NP 1565 nt		NP: 56 kDa	NP: Component of vRNP, assembles as oligomers, encapsidation of vRNA
NA 1413 nt		NA: 50 kDa	NA: Surface glycoprotein organized in homotetramers, release of progeny virions
M 1027 nt		M1: 28 kDa M2: 11 kDa M42: 11 kDa	M1: Matrix protein which assembles as oligomers, nuclear export of vRNPs and budding of new virions M2: Proton channel organized in homotetramers, release of vRNPs from the endosome M42: Putative M2-like function
NS 890 nt		NS1: 27 kDa NEP: 14 kDa NS3: 20 kDa	NS1: Repression of innate immune response, host gene expression shut-off, regulation of polymerase activity NEP: Nuclear export of neosynthesized vRNPs NS3: Host adaptation

Table 1: Major proteins encoded by the genome of IAVs.

The ORFs from intronless or unspliced mRNAs are boxed in blue, the ORFs from spliced mRNAs are boxed in red, and the remaining ORFs are boxed in green. The length of the proteins is indicated (amino acids number). For each viral protein, the expected molecular size and the main functions are indicated. **Adapted from [47,49,50] and from Cédric Diot [51].**

3. Epidemiology and ecological features of influenza A viruses

a. *Influenza A virus reservoir and host range*

IAVs can infect a wide range of hosts (**Figure 3**). Aquatic birds such as the Anseriformes (particularly ducks, geese, and swans) and Charadriiformes (gulls, terns, and shorebirds) are thought to constitute the major reservoir of IAVs [52,53]. The greatest diversity of IAVs is found in the avian reservoir, as all HA and NA sub-types have been identified in wild birds, except for the H17N10 and H18N11 sub-types identified in bats [3,54]. In the wild aquatic bird reservoir, IAVs are maintained mostly by asymptomatic infections. Furthermore, IAVs are predominantly transmitted through the fecal-oral route and principally infect cells of the lower intestinal tract. This transmission route thus represents an efficient way to spread viruses between waterfowl, by shedding viruses into the water *via* feces [53].

From the avian reservoir, IAVs can be transmitted to various hosts, such as domestic poultry or several mammals including sea mammals, horses, pigs, or sporadically humans. Due to their large host range, IAVs thus constitute a threat of zoonotic infections. Close proximity of humans to IAV hosts such as domestic poultry or pigs, or live-poultry markets play a key role in those zoonotic transmission events and regular cases of human infection by highly pathogenic avian H5N1, and more recently H7N9 infections, have been reported over the past few years.

However, most of the zoonotic transmissions cases are not followed by emergence, as establishment of a new IAV lineage in the human population requires a few challenging steps: i) a first event of animal to human transmission, ii) an efficient replication in the human host, iii) an efficient human-to-human transmission. As mentioned in section I.1.b., human IAVs preferentially bind sialic acids with an α2,6 linkage, while IAVs from avian origin mostly bind sialic acids with an α2,3 linkage, thus limiting the occurrence of avian to human transmissions [14]. Swine species however display both sialic acid types in their respiratory tract and are believed to constitute “mixing vessels” favoring the emergence of viruses with potential threat for humans [55].

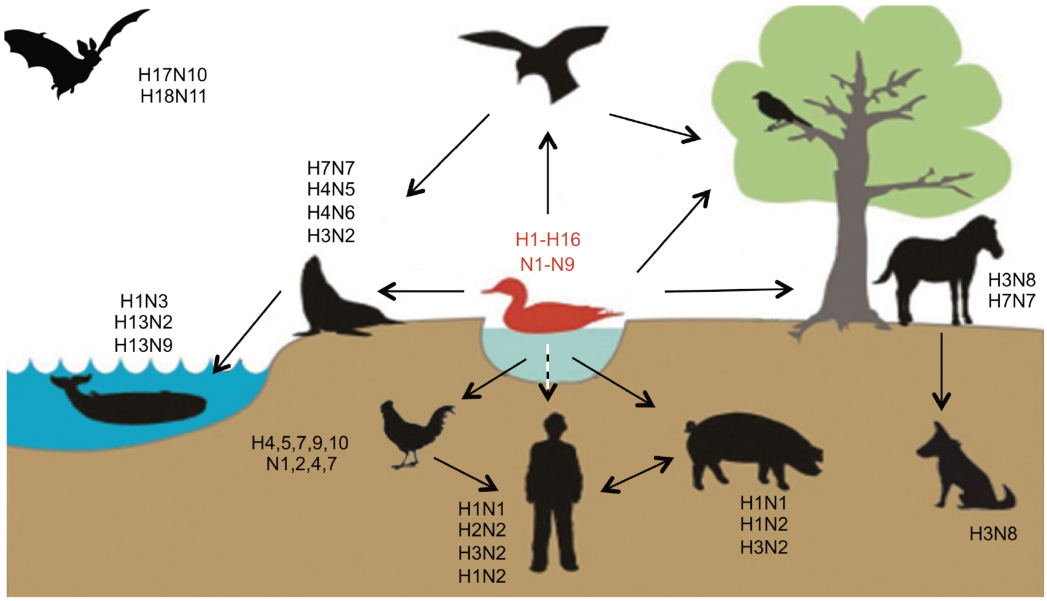

Figure 3: IAVs host range.

Wild aquatic birds constitute the reservoir of IAVs (in red). IAVs can be transmitted to a wide range of other birds and mammal species (in black). Black arrows indicate the major types of interspecies transmissions. Dashed arrow indicates the sporadic avian to human transmissions. The major subtypes having circulated in each host are indicated. **Adapted from [50].**

b. *Influenza A virus evolution: genetic drift and genetic shift*

Epidemiology of IAVs is linked to their great genetic flexibility allowing viral evolution through two different mechanisms: genetic drift and genetic shift (**Figure 4**) [56].

The IAV RdRp does not bear a proofreading activity, leading to the gradual accumulation of mutations in the viral genome [57]. Constant pressure from the host immune system leads to the positive selection of IAV variants that are able to escape antibody neutralization. Accumulation of mutations in the HA and NA proteins causing antigenic changes therefore results in the selection of new variants. This antigenic drift thus explains the need for constant updates of the human influenza vaccines composition.

Genetic shift on the other hand is associated to more drastic changes and is allowed by the segmented nature of IAV genome. Indeed, during co-infection events, reassortant viruses, harboring a segment combination coming from the two infecting strains, can be produced. Such reassortment events, when they involve the HA and/or NA segments, can lead to new IAV sub-types. The introduction of a novel HA and/or NA segment coming from the animal reservoir into the currently circulating human influenza viruses, will result in

major changes in the antigenic properties of the HA and/or NA proteins. Such antigenic shift can be at the origin of devastating pandemics, as the majority of the population would not be immune to the new IAV subtype.

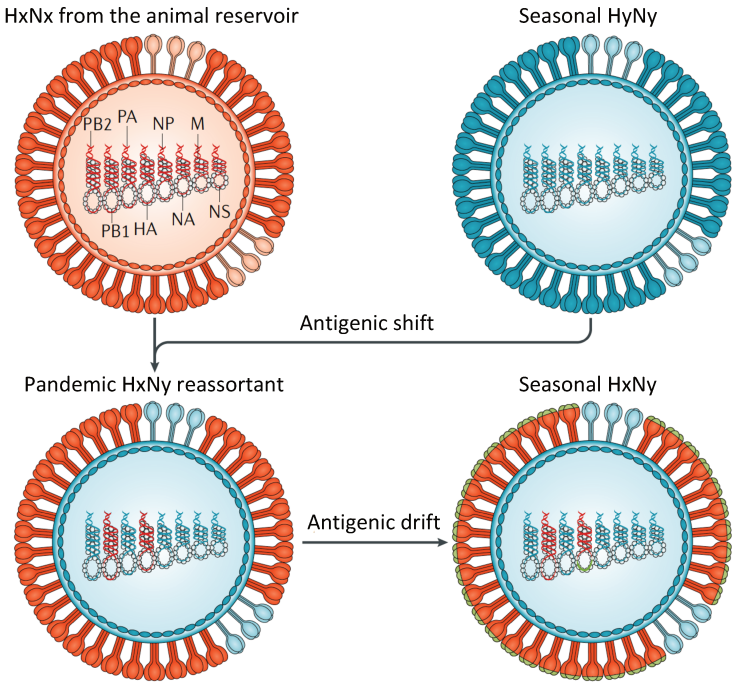

Figure 4: Antigenic drift and antigenic shift.
Co-infection between an HxNx virus from the animal reservoir and a seasonal HyNy virus circulating in the human population can result in the production of an HxNy reassortant with drastically new antigenic properties, termed antigenic shift. Introduced in a population lacking pre-existing immunity, the new HxNy virus can lead to a pandemic. Once the HxNy becomes established in the human population as a seasonal strain, the virus begins to drift. Antigenic changes accumulate in the HA and NA and are selected to promote immune evasion. **Adapted from [2].**

c. *Human influenza A virus epidemiology: seasonal epidemics and pandemics*

In humans, seasonal influenza is an acute respiratory disease. Latest studies estimate that between 300 000 and 650 000 seasonal influenza-associated respiratory deaths occur annually worldwide [58]. In most cases, influenza virus infection is characterized by a sudden onset of fever coupled with symptoms associated to a mild respiratory disease confined to the upper respiratory tract such as sore throat, nasal congestion, cough, and general symptoms such as headache, muscle pain and fatigue. In some cases, influenza virus infection can lead to lethal pneumonia either due to influenza virus infection itself or to secondary bacterial infection of the lower respiratory tract [2]. Human-to-human

transmission usually occurs through respiratory droplets, aerosols or by contact with contaminated surfaces or hands [59]. Persons of all age groups are susceptible to influenza. However, hospitalization and death related to influenza are more frequent among young children (< 5 years), persons aged 65 years and older, and among patients with medical conditions increasing the risk of complications from influenza [60].

On rare occasions, a new strain of IAV that is antigenically different from previously circulating seasonal strains can be introduced in the human population leading to a pandemic. Pandemic IAVs usually are from zoonotic origin and rapidly spread in the human population lacking pre-existing immunity.

By using clinical and epidemiological data as described in [61], it has been estimated that there have been approximately 14 pandemics in the last 500 years [61,62]. The four more recent ones are documented in **Figure 5**. In 1918, the so-called “Spanish flu” caused about 50 million deaths worldwide. The origin of the pandemic 1918 H1N1 virus is not clear. Either it arose by reassortment of an avian and a mammalian virus or it derived from an avian virus by gradual adaptation to humans without reassortment [63,64]. After 1918, the H1N1 virus circulated in the human population as a seasonal virus until 1957, when the H2N2 virus of the Asian pandemic emerged and replaced the circulating H1N1. This H2N2 virus arose from a reassortment between the circulating seasonal H1N1 virus and an H2N2 virus from avian origin. In 1968, a new H3N2 virus emerged leading to the Hong Kong flu pandemic. Again, this H3N2 virus resulted from a reassortment from the previously H2N2 circulating strain and an H3N2 virus from avian origin. In 1977, an H1N1 virus closely related to the H1N1 virus circulating in the 1950’s re-emerged in Russia. This virus co-circulated with the H3N2 virus until 2009. The H1N1 2009 pandemic virus was derived by reassortment between the swine H1N1 virus of the Eurasian avian-like H1N1 virus lineage and the “triple reassortant” swine virus. This “triple reassortment” arose in pigs from multiple reassortment events between an avian virus, the H3N2 seasonal virus and a swine virus of the classical swine lineage related to the 1918 H1N1 pandemic virus [65]. The first cases of the H1N1 2009 pandemic (H1N1pdm09) virus were detected in Mexico in early 2009 and the virus rapidly spread worldwide, causing major outbreaks, before becoming seasonal in the following years. Today, the seasonal H3N2 and H1N1pdm09 viruses, respectively deriving from the 1968 and

2009 pandemics, co-circulate in the human population and are responsible for the seasonal epidemics along with influenza B viruses.

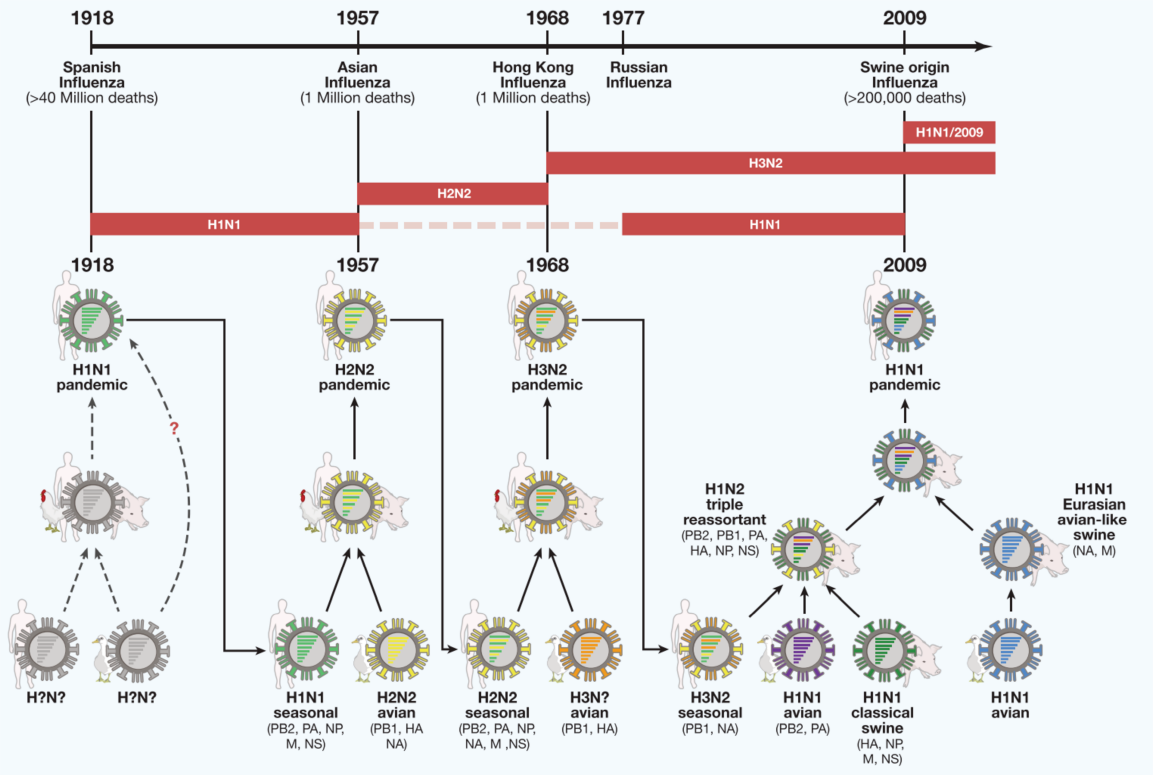

Figure 5: Influenza pandemics since 1918.
Red bars indicate the period of circulation of each virus in the human population. The dashed red bar indicates the period during which the seasonal H1N1 virus disappeared from the human population before its reintroduction in 1977. Segment exchanges through reassortment are indicated. Drawings of human, swine and avian species indicate the host of origin of the viruses involved in the reassortment events. **From [4]**.

d. *Anti-influenza A virus strategies*

Currently approved antivirals for seasonal influenza target viral proteins embedded in the viral envelope. Drugs such as oseltamivir or zanamivir act by mimicking the binding of sialic acid in the active site of the NA. Adamantanes, such as amantadine and rimantadine, target the M2 ion channel. However, adamantanes use is no longer recommended as most of the currently circulating strains (H3N2 and H1N1pdm09 viruses) are naturally resistant to those drugs [2,66]. Due to the concern of potential emergence of viruses with oseltamivir resistance mutations outside of the context of treatment, as it already happened in the past, new therapeutics targeting different viral or cellular functions are being developed. Drugs

such as favipiravir (a nucleoside analog inhibiting the RdRp of several RNA viruses), pimodivir (preventing cap binding), baloxavir (inhibiting the endonuclease activity of PA) or nitazoxanide (inhibiting HA maturation) are thus being tested [67–71].

Vaccination is one of the most efficient public health means for protection against infectious diseases. WHO recommends vaccination especially for pregnant women, young children, elderly, individuals with specific chronic diseases and health-care workers [72]. Influenza vaccine production mainly involves growing the virus in chicken embryonated eggs or in cell culture followed by inactivation. Cell-grown influenza virus vaccines based on Madin–Darby canine kidney (MDCK) were approved by the FDA in 2012 and have the advantage of not being limiting in case of a pandemic unlike vaccines grown on embryonated eggs. Live attenuated vaccines based on temperature sensitive and cold-adapted viruses that are only able to replicate in the nasal cavity are also available in some countries, like in the USA, where their use is recommended for not pregnant individuals in good medical condition aged 2 to 49 [72–74]. Current vaccines are quadrivalent and include selected strains of the two circulating IAV sub-types, H1N1pdm09 and H3N2, and of the two of IBV lineages, Yamagata and Victoria [2,75–77]. To date, attempts to produce a universal influenza vaccine have not been successful, and thus the vaccine composition needs to be updated twice a year upon review of the genetic and antigenic characteristics of circulating influenza viruses obtained within the WHO global influenza surveillance and response system in order to elicit protection against viral genetic variants that arise through antigenic drift [72]. However, this approach is greatly limited by its dependence on the influenza viruses not undergoing major antigenic changes, which may results in the vaccine poorly matching the actual circulating strains and thereby conferring poor protection.

The wide host spectrum of IAVs and the threat of pandemics coming from the animal reservoir have led to the emergence of the “one health concept” where controlling influenza virus emergence relies on both human and veterinary public health institutions. Prevention of transmission from the animal reservoir to humans is essential and measures such as water treatment, indoors raising and increased surveillance (human and veterinary surveillance of disease, virus genetic and antigenic variation, patterns of dissemination) are being implemented [78].

II. Influenza A viruses: structure and function of the vRNPs

Each RNA segment is associated to the NP and bound at its 5' and 3' extremities by the viral polymerase complex (FluPol) composed of PB2, PB1 and PA, thus forming viral ribonucleoproteins (vRNPs) (**Figure 6A**). vRNPs constitute the minimum unit required for the transcription and replication of the viral genome. Unlike most of the other RNA viruses, IAVs replicate in the nucleus of infected cells. After release of the incoming vRNPs in the cytoplasm, they are thus rapidly imported inside the nucleus where viral primary transcription will occur. Newly synthesized viral proteins are then imported into the nucleus where they carry out subsequent rounds of viral transcription and replication of the viral genome. Replication of the viral genome occurs through a positive sense RNA intermediate, the complementary RNA (cRNA). This cRNA serves as a template for the synthesis of new vRNPs that will be exported from the nucleus and packaged into new virions (**Figure 6B, 6C**).

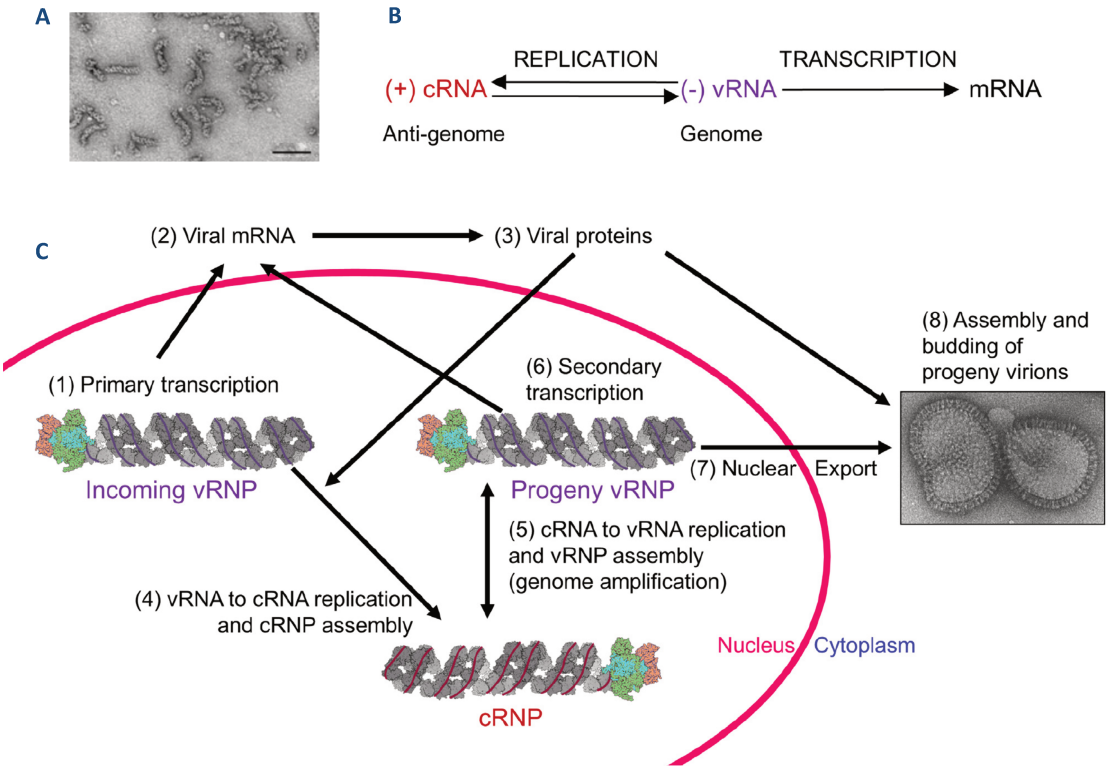

Figure 6: Transcription/Replication of the IAV genome.

A. Negative staining of vRNPs purified from virions. Scale bar, 100 nm. **From [79].** **B.** Summary of RNA synthesis performed by IAV polymerase **C.** Simplified viral cycle displaying successive steps of RNA synthesis: primary transcription, secondary transcription, synthesis of the cRNA and of progeny vRNA. **From [23]**.

1. The viral ribonucleoproteins (vRNPs)

a. *Structure of the vRNPs*

The vRNPs are organized as a double-helical protein-RNA filament. One end is characterized by the presence of a loop while the other end is bound to the trimeric replication complex [80,81]. The vRNPs have a uniform diameter and their length most likely correlates with the size of the different vRNAs (ranging from 0.9 to 2.4 kilobases) [82] (**Figure 7A**).

Each vRNA is wrapped around oligomers of NP *via* the phosphate backbone of the RNA in a neither random nor uniform pattern as suggested by the latest studies [83,84]. Purified monomers of NP can self-arrange in large structures that are morphologically indistinguishable from actual vRNPs, highlighting the key role of NP in organization and stabilization of the vRNP structure [85]. Furthermore, the plasticity of NP-NP interactions gives vRNPs structural flexibility that could facilitate molecular trafficking and packaging, or be functionally important for RNA synthesis. The vRNPs are thus not uniform, rigid structures but they rather display a polymorphism in length and curvature [84] (**Figure 7B**).

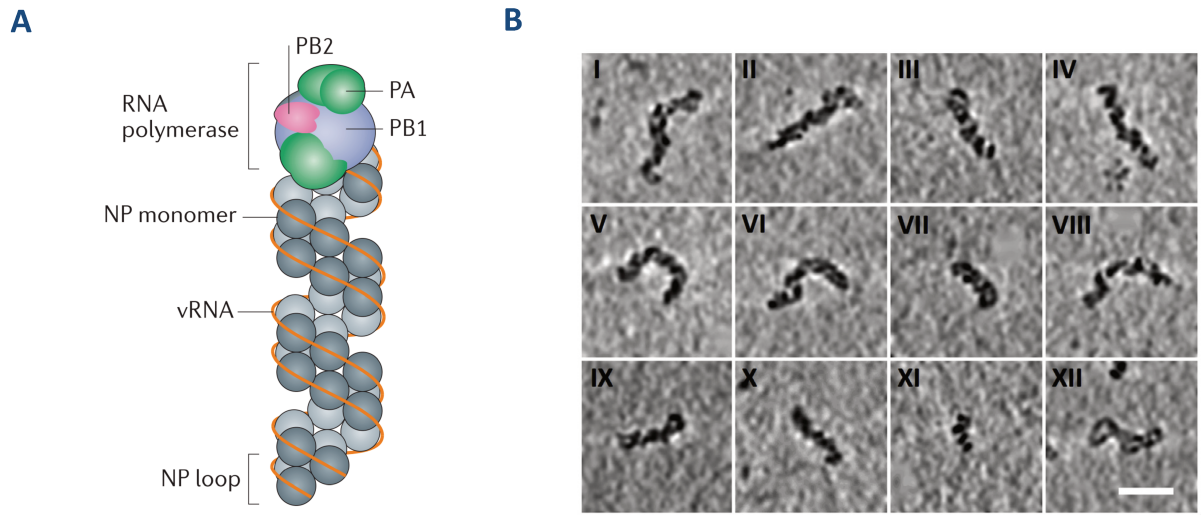

Figure 7: Structure of the vRNPs.
A. Model of the viral ribonucleoprotein (vRNP) complex. In the vRNP, the 5' and 3' extremities of the vRNA are bound by the polymerase complex and the rest of the vRNA is associated to nucleoproteins (NP). The vRNA forms a loop at the end opposite to the polymerase-bound end. **From [86]**. **B.** Analysis of RNPs by cryo-electron tomography. Gallery (I-XII) of sections of individual RNPs displaying straight, twisted and curved appearances. Scale bar, 50 nm. **From [84]**.

b. *The vRNA*

All vRNA genome segments contain 13 and 12 conserved nucleotides at the 5’ and 3’ termini, respectively, showing partial complementarity and annealing with each other to form the viral promoter [87]. Those conserved non-coding sequences flank the anti-sense segment specific non-coding and coding sequences (**Figure 8A**).

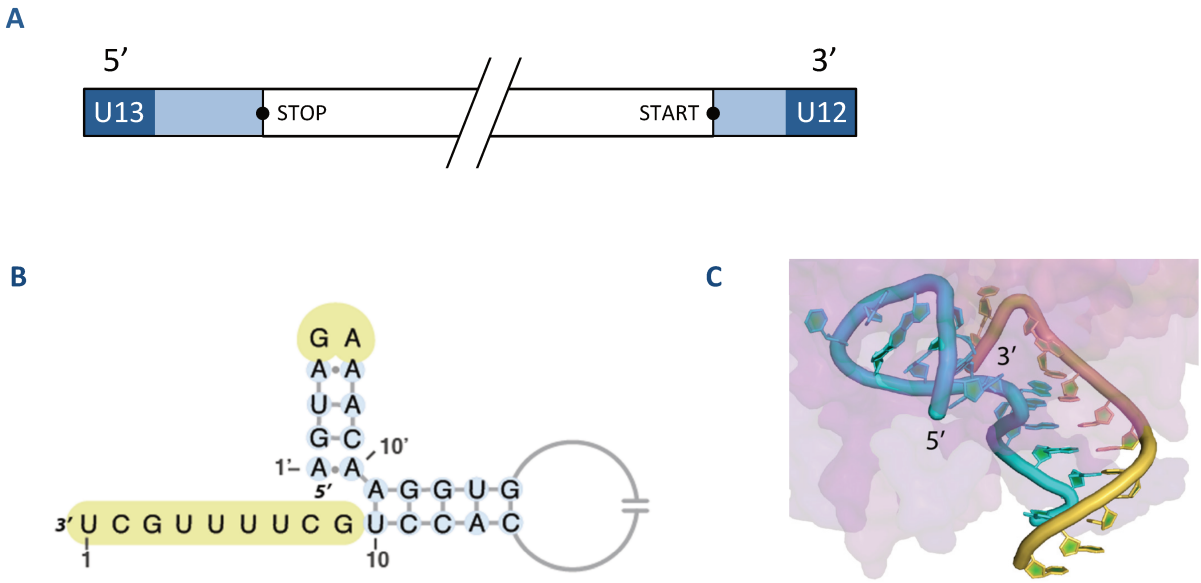

Figure 8: Structure of the vRNA and vRNA promoter.
A. Schematic representation of the vRNA. The 13 and 12 nucleotides respectively conserved at the 5’ and 3’ end of the vRNA are represented in dark blue. The segment specific untranslated regions are represented in light blue, while the coding sequence with start and stop codons is indicated in white. **B.** Half-corkscrew configuration of the vRNA promoter. In the hook (5’ extremity), two canonical base pairs are flanked by two non-canonical A-A base pairs. Unpaired nucleotides are highlighted in yellow. **From [88]. C.** Structure of the vRNA promoter bound to the viral polymerase. The hook present at the 5’ extremity is represented in medium blue. The unpaired 3’ extremity is represented in red. The RNAs involved in the duplex between the 5’ and the 3’ extremities are respectively represented in cyan and yellow. **From [88]**.

The most recent structural studies indicate that the viral RNA promoter adopts a “half-corkscrew” configuration. The 5’ extremity forms a loop or a hook through two canonical base pairs, that are flanked on both sides by one A-A non-canonical base pairing, while the 3’ extremity remains single stranded (**Figure 8B**) [87]. The distal regions of both extremities form an RNA duplex and are followed by the segment specific sequence. The 5’ end of the

viral promoter associates with the viral RNA-dependent RNA polymerase at the interface between PB1 and PA, whilst the 3' end enters the active site cavity to serve as template for RNA synthesis (**Figure 8C**) (reviewed in [88]).

Importantly, segment specific extensions of the RNA duplex can be observed underlying the importance of such RNA duplex for viral transcription and replication. It has been reported that mutations of nucleotides within this RNA duplex in the HA segment are associated to a decreased promoter activity and a defect in segment packaging [89]. In addition, the structure of the promoter including the 5' stem and the RNA duplex is essential for the endonuclease activity of the polymerase that is required to prime viral transcription through cap-snatching [90].

c. *The nucleoprotein*

As mentioned in section II.1.a., association of NP with the vRNA is neither random nor uniform (**Figure 9A**). Furthermore, the nucleotide content of the vRNA may contribute to the degree of NP association as the binding site of NP on vRNA was found to be rather guanine-rich and uracil-poor compared to the overall IAV genome [83]. Interaction between dimers of NP organizes the vRNP into a double helical structure. The vRNP structure is stabilized by two forces: i) interactions between adjacent NP molecules on the same polymer strand, and ii) interactions between NP dimers between the anti-parallel strands. NP forms the scaffold of the vRNP, and disruption of the NP dimers leads to vRNP unwinding. Furthermore, mutants of NP that cannot dimerize are unable to support viral replication [91] (**Figure 9B**).

The NP structure can be structurally divided in three sub-domains: the head, the body and the tail domains (**Figure 9C**). NP binds the RNA through its positively charged groove found between the head and the body domains whereas the tail domain is flexible and involved in oligomerization of NP by its insertion into the neighboring molecule (**Figure 9D**) [92]. Additionally, NP can interact with the subunits of the polymerase PB2 and PB1, primarily through its body domain [93]. Recruitment of NP to nascent vRNP is proposed to occur through NP homo-oligomerization independently of RNA binding by insertion of the tail loop of the incoming NP into the groove of the resident NP [94]. Furthermore, a non-

conventional NLS, mapped to a NP region accessible to solvent and highly flexible, has been shown to be important for nuclear import of free NP molecules and vRNPs [92,95].

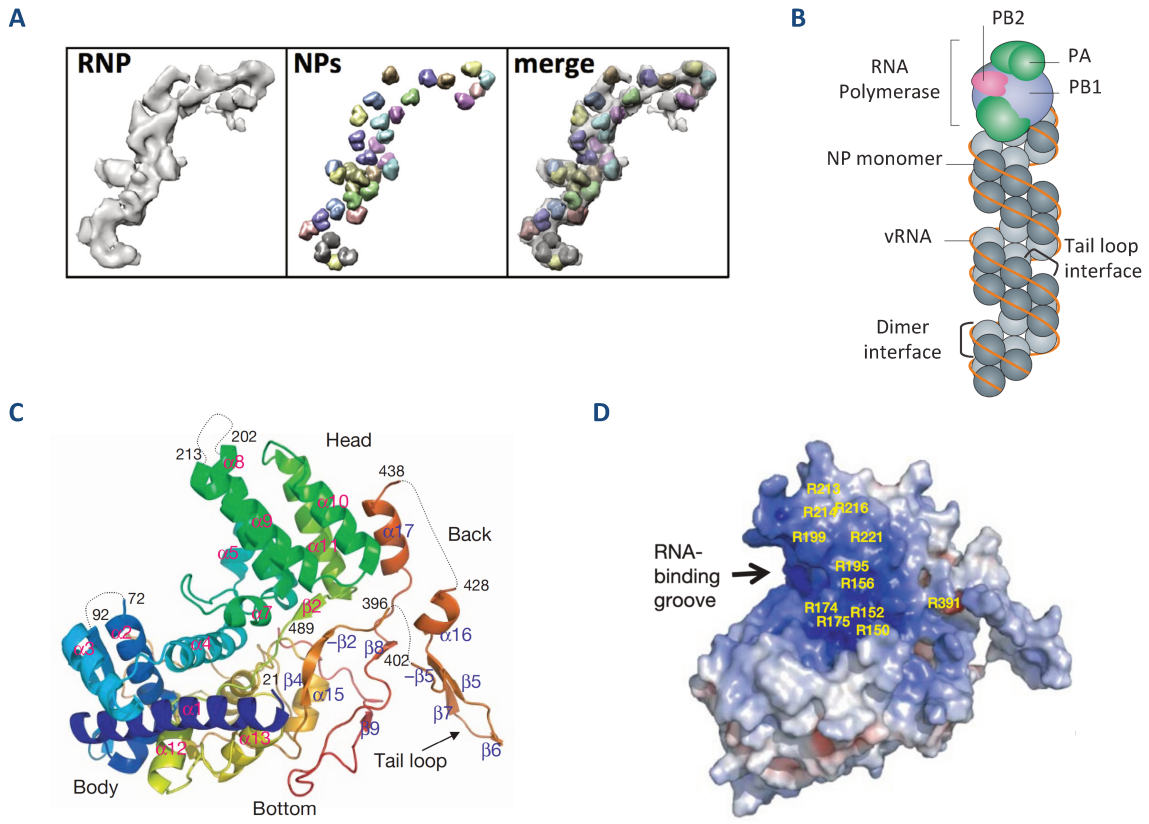

Figure 9: Structure of the nucleoprotein NP.
A. Model of NP monomers distribution on viral RNA by docking of NP into RNP molecular envelopes. **From [84]**. **B.** Interacting forces stabilizing the vRNP structure into a double helical structure: i) interaction between NP molecules on the same strand (tail loop interface), ii) interaction between NP dimers from the two anti-parallel strands (dimer interface). **Adapted from [86]**. **C.** Structure of the nucleoprotein. The head and body domains frame the RNA binding groove. Those domains are formed by non-contiguous polypeptide regions: the head domain is formed by residues 150–272 and 438–452, and the body domain consists of the three polypeptide segments: 21–149, 273–396 and 453–489. The tail loop, which is formed by residues 402–428, participates in NP oligomerization. **From [92]**. **D.** The RNA binding groove is lined with basic residues (blue). Amino acids predicted to interact with the RNA are indicated in yellow. **From [92]**.

Oligomerization of NP is required for vRNP activity as mutants of the tail domain show reduced activity [96]. The IAV polymerase complex is sufficient to promote transcription and replication of a short vRNA-like template in the absence of NP in a cellular context, suggesting that NP is not essential for the priming of those activities [94]. However, NP has a central role in viral transcription and replication by supporting the elongating transcripts and

is an essential cofactor required for the full processivity of the viral polymerase during replication of the viral genome [94,97].

Also, NP plays an important role in defining the host range of IAVs. Mutations allowing escape from cellular restriction and adaptation to new hosts have been mapped to the nucleoprotein, such as mutations enabling escape from the MxA restriction factor [98,99]. Furthermore, due to its prime role in vRNP architecture, NP is an attractive target for antiviral drugs development, and drugs like nucleozin (and its derivatives) or naproxen interfere with NP oligomerization or RNA binding respectively [100–102]. Lastly, the attenuation of cold-adapted and temperature sensitive influenza vaccine strains has also been linked to mutations in components of the vRNPs, including NP (see section I.3.d.) [103].

d. *The viral polymerase*

The viral polymerase is a heterotrimeric complex composed of PB2, PB1 and PA and is involved in the transcription and replication of the viral genome. PB1 carries the RNA-dependent RNA polymerase (RdRp) activity, while PB2 and PA respectively carry the cap binding and endonuclease activities required for viral transcription (**Figure 10A**). The PB1 subunit displays the finger, thumb and palm domains typical of RNA polymerases, surrounding a central active site cavity where RNA synthesis occurs. Protruding from the active site of the polymerase, a β-hairpin, within the PB1 thumb sub-domain, called the priming loop, is required for *de novo* RNA synthesis (*i.e.* unprimed RNA synthesis) (see section II.2.b) [104] (**Figure 10C**). The PB2 cap-binding domain is located in the central region of PB2 while the PA endonuclease domain, which has a core fold characteristic of the nucleases of the PD-(D/E)xK superfamily, is found in the Nter region of PA.

The complete structures of a bat IAV polymerase, evolutionary close to human IAV, and of a human IBV polymerase, both bound to the viral promoter have been resolved [87,105]. The overall structure of the polymerase is U-shaped with two upper protuberances that correspond to the cap binding domain of PB2 and the endonuclease domain of PA (**Figure 10B**). PB1 is stabilized in the center of the polymerase complex by large interfaces of interactions with PA and PB2 (reviewed in [23,106]).

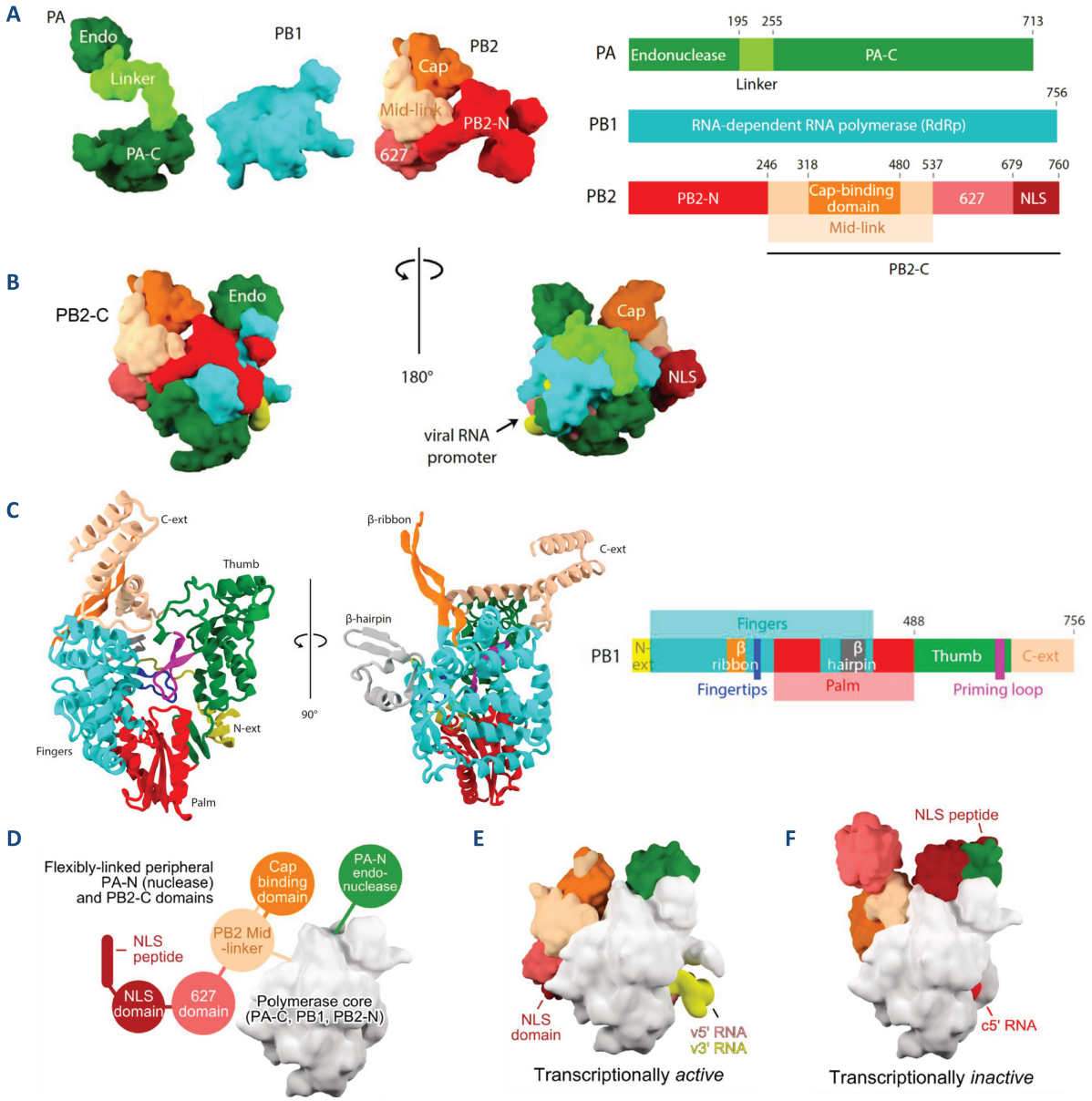

Figure 10: Structure of the influenza virus polymerase subunits and heterotrimer.

A. Structure and schematic domain organization of each subunit. **B.** Assembly of each subunit in the heterotrimer. **C.** Ribbon diagram and schematic domain organization of the PB1 subunit showing the finger, palm and thumb domains along with the priming loop and fingertips in the active site cavity. The β-ribbon carries the PA-PB1 nuclear localization signal, the β-hairpin is involved in promoter binding and the C-extension (C-ext) is at the interface with PB2. **D.** Schematic diagram showing the polymerase core and the flexible peripheral domains. **E, F.** Structures of the influenza B virus polymerase showing different rearrangements of the peripheral domains onto the core. **E.** The polymerase is bound to the full vRNA promoter and is presumed to be configured for cap-snatching and transcription initiation. **F.** The polymerase structure is bound to the 5' end of cRNA. **Adapted from [23]**.

The heterotrimer has great flexibility and can display different conformations depending on the bound RNA. All the resolved structures show the presence of an invariant core composed of PB1 stabilized by the linker domain of PA, and the PA Cter and PB2 Nter domains. However, the PB2-Cter (composed of the cap-binding domain, PB2-mid linker, PB2 627 domain and the NLS domain) and the endonuclease domain of PA are flexible (**Figure 10C**). Indeed, the two conformations of the crystalized influenza B virus polymerase, either bound to the full vRNA promoter or to the 5' end of the cRNA, show striking differences, especially in the PB2 Cter domain [105,107] (**Figure 10D, E**).

Similarly to NP, several residues of the viral polymerase subunits, mostly in the PB2 subunit, are implicated in host adaption. Activity of the avian influenza virus polymerases is severely impaired in mammalian hosts. Most avian virus polymerases contain a glutamic acid (E) residue at position 627 of PB2, whereas this residue is frequently mutated to a lysine (K) in mammal-adapted polymerases. Remarkably, the E627K mutation has been shown to allow activity of avian polymerases in mammalian cells [108]. The 627 domain of PB2 is essential for viral RNA replication and transcription in the cell [109]. Furthermore, a species specific difference in a cellular protein, ANP32, has been linked to the host restriction mediated by the PB2 627 residue [109,110]. However, the precise mechanism by which the PB2 627 residue determines host range has yet to be determined.

2. Transcription and replication of the viral genome

a. *The viral transcription*

Viral transcription is a primed process leading to the synthesis of a capped and polyadenylated viral mRNA from the template genomic vRNA. The resulting viral mRNAs are thus structurally comparable to cellular mRNAs and can therefore exploit cellular machineries for RNA processing and nuclear export.

Synthesis of viral mRNA occurs in four steps: i) nascent cellular RNA Polymerase II (RNA Pol II) capped transcripts bound by the PB2 cap binding domain are cleaved by the endonuclease activity of PA (**Figure 11A**), ii) rotation of the cap binding domain of PB2

towards the PB1 catalytic cavity (**Figure 11B**), iii) elongation of the transcript (**Figure 11C**), iv) polyadenylation of the mRNA by stuttering of the viral polymerase on an oligo-U stretch located near the 5' end of the vRNA template (**Figure 11D**).

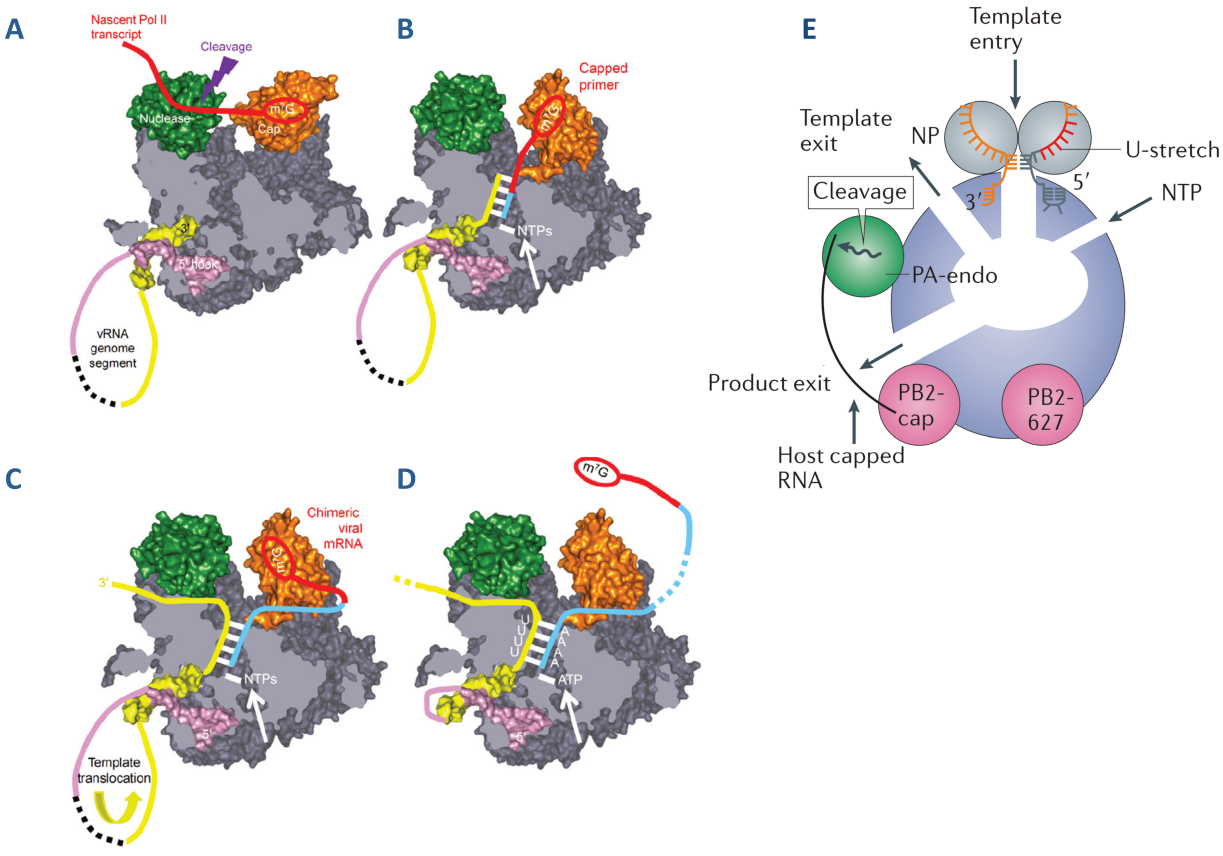

Figure 11: Key steps of viral transcription and schematic representation of FluPol in the transcription pre-initiation state.

A. Cap-snatching: the PB2 cap binding domain (orange) binds capped nascent RNA Pol II transcripts (red), while the PA endonuclease (green) cleaves the cellular transcript to prime viral transcription. 3' (yellow) and 5' (pink) ends of the vRNA are represented. **B.** The PB2 cap-binding domain rotates to direct the capped primer towards the PB1 active site. **C.** Elongation of the viral transcript. The vRNA template translocates through the catalytic site to be copied into mRNA. The produced viral mRNA is chimeric with cap and 5' end coming from cellular transcripts (red) followed by viral specific sequence (cyan). **D.** Polyadenylation of viral mRNA by iterative copy of the oligo-U sequence located near the 5' end of the template. **Adapted from [23]**. **E.** Channels for template entry, template exit, NTPs entry and product exit are represented. The PB2 cap and PA-endonuclease (PA-endo) domains are rearranged in a transcription active conformation. Host capped RNA (black) is bound by the PB2 cap-binding domain (PB2-cap, pink) and cleaved by the PA endonuclease domain (PA-endo, green). Once cleaved, the capped primer will enter the catalytic cavity and anneal to the 3' end of the vRNA. **Adapted from [86]**.

The 5’ terminal N7-methyl guanosine methylated cap is acquired through a cap-snatching mechanism (reviewed in [111]). Cap-snatching requires an intricate connection between the viral polymerase and the host RNA Pol II. The large subunit of the RNA Pol II, RPB1, has a flexible C-terminal domain (CTD), which is composed of 52 heptad repeats: Tyr1–Ser2–Pro3–Thr4–Ser5–Pro6–Ser7. This CTD can be phosphorylated on Ser2 and Ser5. Phosphorylated Ser5 is recognized by cellular machineries such as RNA capping enzymes that are required for early RNA Pol II transcription. During transcript elongation by the RNA Pol II, Ser2 becomes phosphorylated while Ser5 phosphorylation is gradually lost. Hence, the Ser5 phosphorylation is most predominant at the transcription start site and its presence decreases along gene bodies (*i.e.* the transcriptional region of the gene) (reviewed in [112]). Through residues within the PA Cter domain, the FluPol interacts with the RNA Pol II CTD specifically when it is phosphorylated on Ser5 [113–115] (reviewed in [116]). This interaction thereby allows vRNPs to hijack RNA Pol II for cap-snatching.

The FluPol conformation compatible with transcription is proposed to be stabilized through the interaction between FluPol and RNA Pol II CTD which further allows binding to nascent host transcripts and cap-snatching [117] (**Figure 10**). Once the capped nascent transcript is bound to the PB2 cap-binding domain, it is cleaved by the PA endonuclease domain 10 to 13 nucleotides downstream of the cap. The size of the capped primer is limited by the 50 angstroms distance found between the PB2 cap-binding and PA endonuclease domains. Whether specific cellular RNAs are preferentially targeted for cap-snatching is still unclear to date, but the FluPol was shown to target host mRNAs as well as a wide range of RNA Pol II non coding RNAs such as small nucleolar RNAs and small nuclear RNAs [118–120]. Overall, it appears that the probability for a given RNA to be targeted for cap-snatching is linked to its abundance within the cell [111]. In addition, cap-snatching contributes to the viral-induced host shut-off by reducing RNA Pol II occupancy on gene bodies and interfering with termination of RNA Pol II transcription [121] (see section II.3.d.).

The 3’ end of the capped primer is then used to prime viral transcription. To do so, the cap-binding domain of PB2 rotates by 70° to place the capped primer towards the PB1 active site where it base-pairs with the 3’ end of the vRNA template [105]. Cap-snatching most frequently occurs after a guanine residue within a 5’-GC-3’ motif [122] and the interaction

between the 3' end of the snatched primer and the vRNA template is thus stabilized by base-pairing complementarity. Transcription is initiated by the addition of a G or C residue at the 3' end, directed by the penultimate C residue (C2) or the G residue at position 3 (G3) present in the vRNA template (**Figure 12**). Some snatched primers are not directly complementary to the vRNA template end and are subject to a prime-and-realign mechanism before transcription initiation, where the cap leader is first extended by a few nucleotides [118,119].

Figure 12: Schematic arrangement of RNA during transcription initiation.
Host capped primer is represented in red, while 3' and 5' ends of the vRNA are respectively represented in yellow and pink. Transcription is initiated by addition of a CTP (represented here) complementary to the G residue at position 3 or addition of a GTP complementary to the C residue at position 2 (not represented). **From [23].**

The structure of the active initiating polymerase as it transitions towards processive elongation has recently been crystalized [123]. Although it is not required for the primed mRNA synthesis, an essential element of the RdRp cavity is the priming loop, which protrudes from the PB1 thumb sub-domain and is critical for *de novo* initiation (see section II.2.b.) (**Figure 13**) [104]. The transition between the initiation and elongation conformations of the RdRp occurs by progressive extrusion of this priming loop associated to a widening of the active site cavity. Once the addition of nine nucleotides has been catalyzed, strand separation is enforced by the PB2 helical lid and the template is directed towards the template exit channel while the capped mRNA exits from the PB2 cap binding domain. Concomitantly, as the RdRp elongates, the template progressively translocates into the active site, which leads to the disruption of the base pairing within the vRNA promoter, thereby allowing the elongation to further continue (**Figure 13**).

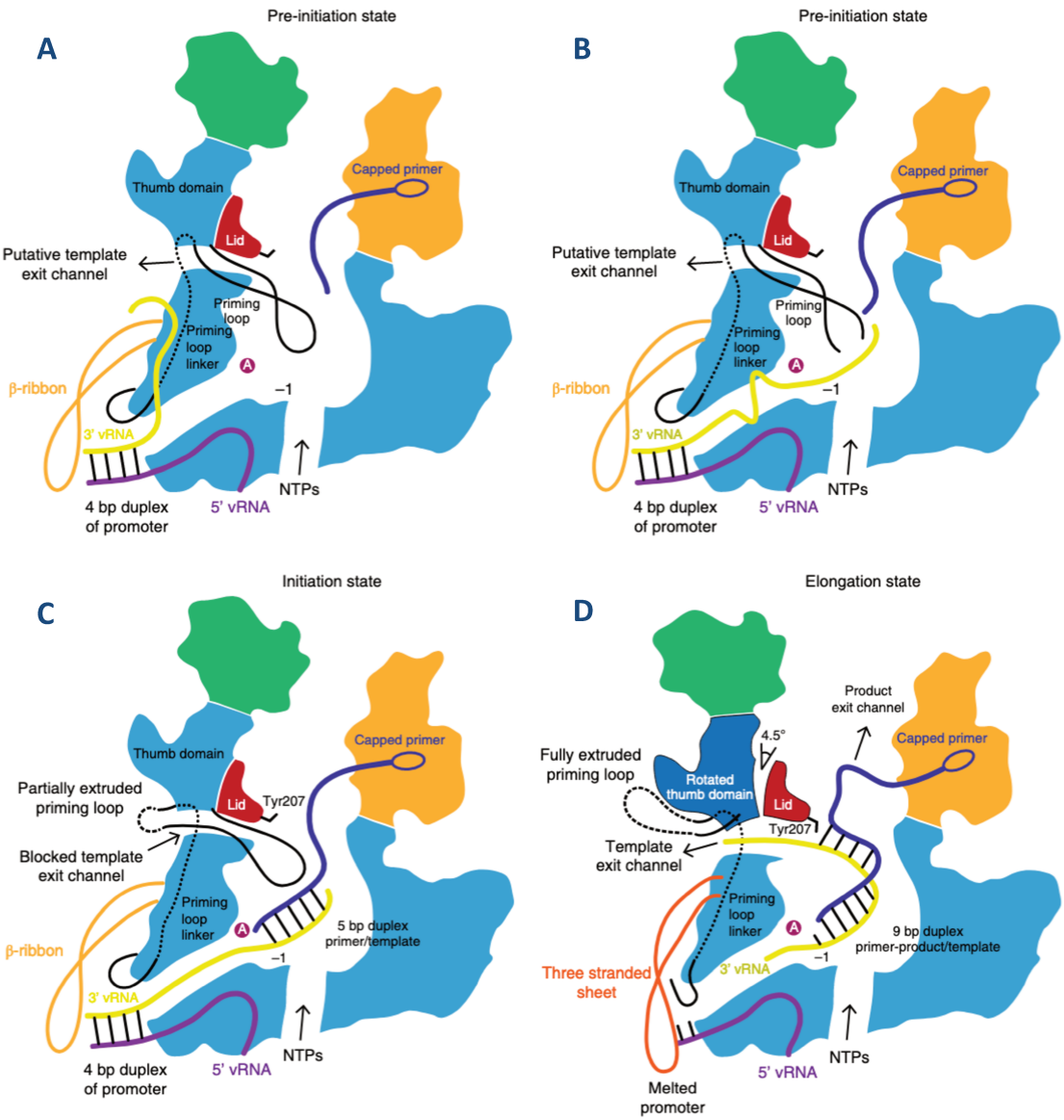

Figure 13: Schematic representation of the transitions between the pre-initiation, initiation and elongation states of the transcribing FluPol.

A. The vRNA promoter is represented by the association of the 5' end (purple) and 3' end (yellow) of the vRNA. The template 3' end is located on the surface of the polymerase and the capped primer (deep blue) is bound to the PB2 cap-binding domain. **B.** The template 3' end enters the active site cavity. Displacement of the priming loop (in black) allows primer-template hybridization and incorporation of the first NTPs. **C.** NTP incorporation as well as the growing occupancy of the active site cavity lead to the progressive extrusion of the priming loop from the template exit channel. **D.** The thumb domain rotation and the opening of the active site cavity allow growth of the template-product duplex up to nine base pairs, at which point the product abuts against the PB2 helical lid forcing strand separation. **From [123].**

Template entry and exit channels are in close proximity possibly allowing dissociation of the template vRNA from the NP scaffold at the entry site and reassociation to it at the exit site, once it has translocated through the PB1 active site [86] (**Figure 11E**). Elongation continues until a five to seven stretch of U nucleotides, located 16 nucleotides from the 5' end of the vRNA template, reaches the active site. The 5' end of the vRNA template remains associated to the polymerase throughout transcription leading to steric constraints and stuttering of the RdRp on the U stretch, resulting in the repeated incorporation of ATP and the production of a polyadenylated tail [124]. The cap of the viral mRNA is most likely released from the PB2 cap-binding domain during elongation and subsequently bound by cellular cap-binding proteins allowing its further handling by cellular machineries for nuclear export and translation [25,125].

b. *The viral replication*

Replication of the viral genome is a two-step process. The first step is the primer independent synthesis of a positive replication intermediate, the cRNA, which will, in a second step, serve as a template for the unprimed synthesis of vRNA. Compared to the primer dependent synthesis of mRNA, *de novo* RNA synthesis (cRNA and vRNA) is drastically less efficient and initiation is the rate-limiting step. Indeed, Reich and colleagues showed that supplying full length recombinant influenza B polymerase with ready-made pppApG dinucleotides as primers largely bypasses this rate-limiting step rendering *de novo* RNA synthesis as efficient as the primed mRNA synthesis [126].

One major difference between cRNA and vRNA synthesis lies in the initiation mode. Although both syntheses are unprimed, cRNA synthesis at the vRNA promoter is terminally initiated, while vRNA synthesis at the cRNA promoter is internally initiated (**Figure 14**). Precise mechanisms involved are further described below.

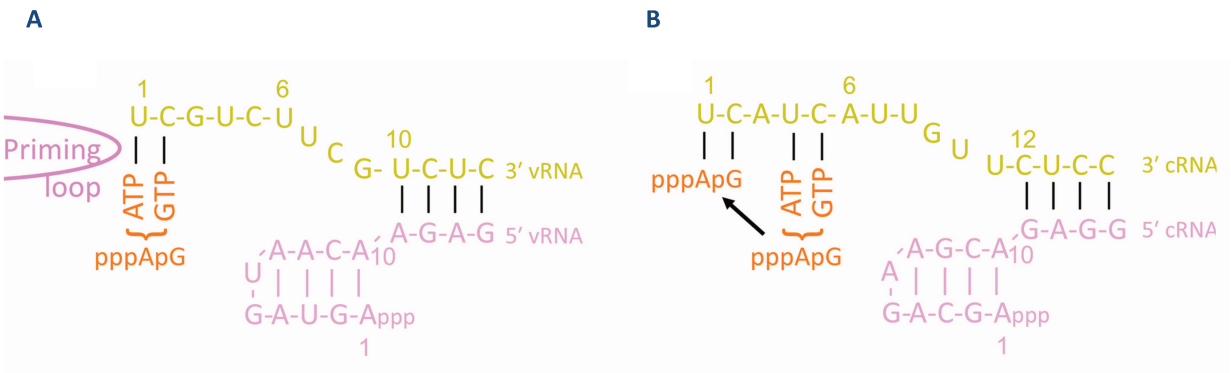

Figure 14: Comparison of terminal and internal initiation at the vRNA and cRNA promoters.
A. Terminal initiation at the vRNP promoter allows synthesis of cRNA and is dependent on the presence of the priming loop. **B.** Internal initiation at the cRNP promoter leads to vRNA synthesis. The alternative base pairing of the 3′ and 5′ ends of the cRNA allows the template to enter deeper into the polymerase active site. vRNA synthesis is initiated by internal assembly of ATP and GTP. Prior to elongation, the pppApG dinucleotide primer reanneals to the end of the template (black arrow). **From [23]**.

cRNA synthesis:

The resident polymerase, *i.e.* the RdRp present on the vRNA, is able to catalyze cRNA synthesis by itself as vRNPs isolated from virions are able to catalyze both mRNA and cRNA synthesis *in vitro* [127]. The priming loop, protruding from the active site of the polymerase, ensures the accuracy of terminal initiation required for proper cRNA synthesis and acts as a stacking platform to stabilize initiating NTPs (**Figure 14**) [104]. This priming loop also prevents dsRNA from entering the active site, thus ensuring that only ssRNA is positioned in the active site. Terminal initiation is primed by addition of a pppApG dinucleotide by base pairing to the U1 and C2 residues found at the 3′ end of the vRNA template (**Figure 15A&B**).

Base pairing of the 3′ and 5′ ends of the vRNA promoter is required to prime RNA synthesis, most likely to correctly position the 3′ end of the template in the active site. However, to allow template translocation and further elongation, the base pairing must be broken. Reich and colleagues proposed a model in which the energy cost of breaking the base pairing between the vRNA 3′ and 5′ ends is compensated by the energy gain obtained from the base pairing between the template RNA and the newly synthesized RNA at the exit of the active site [126] (**Figure 15C-E**). As the elongation further proceeds, the newly

synthesized cRNA and the template vRNA are progressively separated, most likely by action of the PB2 helical lid, which directs each strand through their respective exit channels (**Figure 15F & 11E**) [105].

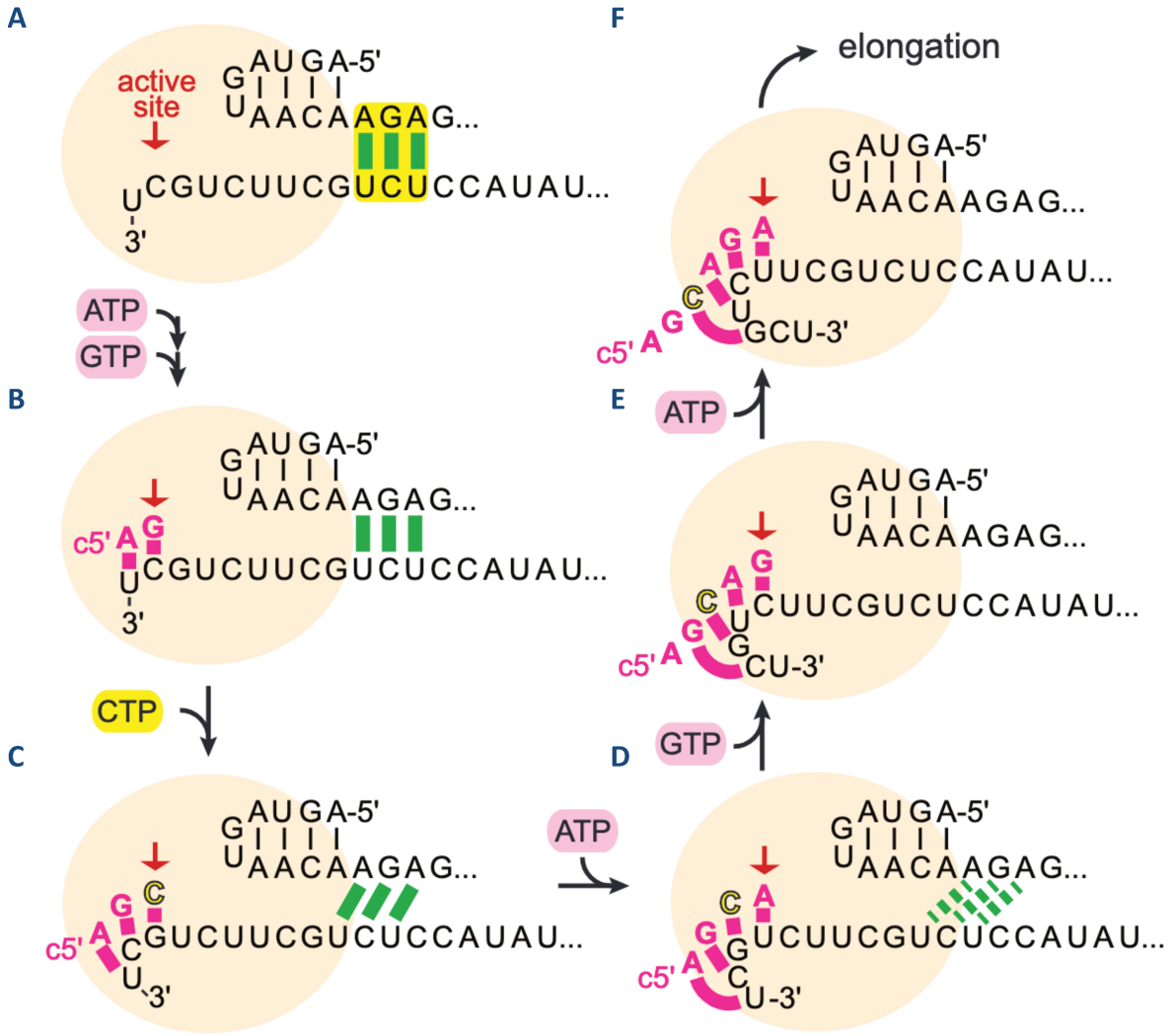

Figure 15: Schematic model of cRNA terminal initiation at the vRNA promoter.
A. The 5’ end of the vRNA is anchored to the viral polymerase (beige sphere), while the 3’ end of the vRNA template is positioned within the active site. Base pairing between 5’ and 3’ ends of the vRNA is indicated in green. **B.** Binding of ATP followed by GTP at the active site is followed by the formation of the first phosphodiester bond. **C.** Directed by the G3 residue, CTP is incorporated next. **D.** To allow further elongation, base pairing of the vRNA promoter must be broken. **E.** Breaking of the 5’-3’ ends base-pairing region is proposed to be coupled with progressive base-pairing of the newly synthesized product with the vRNA template downstream the active site. **F.** Elongation further continues and product cRNA and template vRNA are progressively separated and exit through their respective channels (cf. **Figure 12**). **Adapted from [126].**

Unlike mRNA synthesis, the 5’ end of the vRNA template must be released from the polymerase to achieve synthesis of full-length cRNA. The precise mechanism involved is however still unknown. cRNAs are then assembled into cRNPs where the cRNA is associated to NP and its 3’ and 5’ ends are bound to the FluPol complex [128]. The assembly of cRNA into cRNP is thought to occur as soon as the 5’ end the cRNA emerges from the product exit channel. First, the 5’ end of the cRNA is bound by a newly synthesized polymerase that will recruit the first NP monomer which will in turn recruit successive NP monomers [86].

vRNA synthesis:

Truncation of the priming loop residues is associated to an impaired vRNA to cRNA synthesis but has however little effect on cRNA to vRNA synthesis [129]. Indeed, in contrast to terminal initiation of RNA synthesis at the vRNA promoter 3′ end, RNA synthesis at the cRNA promoter has been demonstrated to initiate internally at U4/C5 residues (**Figure 14**) [130]. This dinucleotide is subsequently re-aligned (or back-tracked) to the terminal 3′ end prior to elongation, where it will act as a primer for vRNA synthesis (**Figure 14**) [131].

For internal initiation, the priming loop is not required as this mechanism is more energetically favorable compared to terminal initiation. Indeed, due to sequence differences, the template cRNA-dinucleotide duplex is more stable compared to the template vRNA-dinucleotide duplex [129] (**Figure 14**). To allow initiation at the U4/C5 residues, the 3’ end of the cRNA must project deeper into the active site compared to the 3’ end of the vRNA. This is explained by the alternative base pairing of the cRNA promoter compared to the vRNA promoter due to sequence differences (**Figure 14**). Indeed, the distal cRNA promoter region is predicted to involve nucleotides 11 to 13 of the 5’ end base pairing with nucleotides 12 to 14 of the 3’ end, compared to the vRNA promoter where nucleotides 10 to 12 of the 3’ end are involved in base pairing. The duplex region of the promoter therefore allows correct positioning of the 3’ end of the cRNA template within the RdRp active site.

As for cRNA synthesis, further elongation requires rupture of the promoter base pairing and is proposed to follow the same model as described for the breakage of the vRNA

promoter [126]. Similarly, strand separation is then proposed to occur as for cRNA synthesis by clashing of the vRNA product-cRNA template duplex against the PB2 helical lid. Newly synthesized vRNA is finally associated to a trimeric polymerase complex and monomers of NP before being exported from the nucleus.

Interestingly, in contrast to cRNA synthesis, vRNA synthesis requires the presence of a second polymerase in addition to the resident polymerase. However, the precise role of this second polymerase remains unclear. Supported by the observation that a second polymerase defective for vRNA synthesis is still able to promote vRNA synthesis, York and colleagues propose a model involving a *trans* activating non-resident polymerase rather than a *trans* acting one [128]. In this model, the *trans* activating polymerase could stimulate vRNA synthesis by inducing or stabilizing a specific configuration of the resident polymerase. Furthermore, this non-resident polymerase would also fulfill the role of the polymerase that binds to the 5' end of the emerging nascent vRNA and recruits the first NP to start the assembly of a vRNP. On the other hand, by using *trans*-complementation experiments, Jorba and colleagues propose a second model, which involves a *trans* acting and catalytically active second polymerase, which would carry out internal initiation on the cRNA template and replication [132]. In this model, the *trans* acting polymerase, possibly associated with small viral RNAs (svRNAs; see section II.2.c.), accesses the 3' terminus of the cRNA template and carries out vRNA synthesis as described above. However, this model requires a third polymerase that would bind to the 5' end of the nascent vRNA to initiate vRNP assembly. Furthermore, Jorba and colleagues propose that the 3' end of the parental cRNA is used repetitively for several initiation rounds, thereby leading to numerous progeny vRNPs generated from a single cRNP template. This model is further supported by the observation of branched vRNPs by cryo-electron microscopy [80].

c. *Transcription/Replication balance*

Early in the viral cycle, the polymerase activity is biased towards mRNA synthesis and later switches to vRNA synthesis for the production of new vRNPs for virion assembly.

However, how the polymerase switches from a transcriptase to a replicase is still not fully understood.

NEP has been proposed to regulate transcription and replication activities [133]. More specifically, expression of NEP in RNP reconstitution assays is associated to a decreased mRNA synthesis and an increased cRNA and vRNA synthesis. However the precise mechanism and whether NEP supports RNA synthesis or stability still remains to be determined.

Interestingly, NEP was also found to be required for the generation of small viral RNAs (svRNAs) which are 22 to 27 nucleotides long viral RNAs corresponding to the 5' end of each genomic viral RNA [134]. Expression of svRNAs correlates with the accumulation of vRNAs and is thought to promote the switch from transcription to replication. svRNAs regulate vRNA replication in a segment specific way and are required to ensure the stoichiometric balance of each of the eight segments. Perez and colleagues propose a model where nascent svRNAs generated from cRNAs bind to PA. The RdRp carrying a segment specific svRNA then interacts with the cognate cRNA template and synthesizes full-length vRNA [135].

Furthermore, NP and NS1 have been found to stimulate viral RNA synthesis. Indeed, NP is required for vRNA synthesis, cRNA stability and template elongation [94,97,136,137]. In addition, also supporting a role of NS1 in viral RNA synthesis, temperature sensitive NS1 mutants show a defect in viral replication [138].

On the other hand, Vreede and colleagues propose that the synthesis of mRNA and cRNA could be stochastic events and that no such switch between transcription and replication exist [139]. In their proposed model, incoming vRNPs can synthesize both mRNA and cRNA. However, due to their cap and polyadenylated tail, only mRNAs are protected against degradation by cellular nucleases at the early stages of the viral cycle. Later in infection, when sufficient amount of polymerase and NP have been synthesized, cRNAs could be protected leading to the formation of cRNPs, and vRNA synthesis could occur. In this model, the stability of the cRNP replicative intermediate thus controls the transition to the replicative phase.

3. Cellular proteins involved in viral transcription/replication

In addition to viral factors as described previously in section II.2.c., many cellular host factors have been reported to be involved in viral transcription and replication, and a wide range of methods, including proteomics analysis as well as RNA interference (RNAi) and CRISPR/Cas9 screens, have been devoted to their identification [140–151] (reviewed in [86,152–154]). Cellular factors required for viral transcription and replication are summarized in **Figure 16**.

a. *Cellular factors required for viral transcription*

Viral transcription requires the involvement of the cellular transcription machinery. Indeed, to initiate mRNA synthesis, vRNPs need to localize close to cellular transcription sites in order to snatch caps from nascent host mRNAs. Viral transcription and replication are proposed to take place in close proximity with nuclear matrix and chromatin components [155–157]. This is promoted through multiple interactions between vRNPs (most likely through NP) and the histones, or with cellular proteins involved in chromatin structure [158]. Chromatin remodelers, such as the CHD1 and CHD6 proteins, modulate the initiation and elongation steps of cellular transcription by regulating the dynamics of chromatin structure and thus the binding of transcription factors. CHD1 and CHD6 were found to associate with IAV polymerase and to respectively negatively regulate viral replication or positively modulate viral RNA transcription and virus multiplication [159,160]. CHD1 is associated to open chromatin, where mRNAs are being synthesized, and targeting of CHD1 by the viral polymerase is thus proposed to support cap-snatching. Furthermore, the RNA Pol II regulator, hCLE, is required for viral replication and is incorporated into virions, and the nuclear matrix associated protein, NXP2, is required for viral transcription [161–163]. The nucleolar protein RRP1B, involved in ribosomal biogenesis, translocates from the nucleolus to the nucleoplasm upon IAV infection where it facilitates binding of the FluPol to capped cellular mRNAs, thereby supporting cap-snatching and viral transcription [164].

Besides facilitating access to the cap of the host nascent mRNA, interaction of FluPol with RNA Pol II also brings viral transcription close to sites where RNA processing factors are

concentrated [113–115]. Notably, a number of those factors have been identified as being important for influenza virus replication, like cellular factors involved in splicing such as NS1-BP and its associated factor hnRNP K, or SF2/ASF involved in M segment splicing, or the RED-SMU1 complex involved in NS segment splicing [165–167]. Moreover, the splicing factor SFPQ/PSF is required for viral transcription and more specifically could play a role during viral mRNA polyadenylation. The precise mechanism involved is unknown, however SFPQ/PSF has been reported to specifically cross-link to oligo U sequences and could therefore interact with the viral polymerase and the polyadenylation signal to promote stuttering of the polymerase on the oligo U tract [168]. Lastly, the CHD3 protein, through its association with NEP, and the DExD box helicase DDX19 both promote export of viral transcripts from the nucleus [169,170].

b. *Cellular factors required for viral replication*

The minichromosome maintenance (MCM) complex stimulates viral replication by increasing the stability of the viral RNA polymerase that would otherwise produce abortive short RNAs in its absence [171]. The MCM interacts with vRNPs through PA and most likely promotes RNA replication by acting as a scaffold between nascent cRNA and the viral polymerase, thereby stabilizing the elongation complex during the transition from *de novo* initiation to processive elongation on the vRNA template.

Other cellular factors also act as scaffold or chaperones supporting viral replication. RAF-1/Hsp90, which regulates the assembly and nuclear import of viral RNA polymerase subunits, could also act as molecular chaperone during early stages of RNA synthesis [172,173]. The cellular splicing factor, RAF-2p48/UAP56/BAT1, also known as the RNA helicase DDX39B, as well as Tat-SF1, a transcription elongation factor, interact with NP and facilitate the formation of NP–RNA complexes, thus stimulating viral RNA synthesis [174,175]. Likewise, FMRP acts transiently to stimulate vRNP assembly through RNA-mediated interaction with NP, thus supporting viral replication [176]. DnaJA1, a member of the Hsp40 family, interacts with the FluPol subunits and was demonstrated to enhance viral polymerase activity [177]. Lastly, the pre-mRNA processing factor PRP18, stimulates vRNA

synthesis *in vitro* through its interaction with NP and might act as an elongating factor and help association of newly synthesized RNA with NP [178].

Long noncoding RNAs (lncRNAs) participate in host antiviral defense by modulating immune responses (reviewed in [179]) and have also recently been found to be required for IAV replication. PA-associated non-coding RNAs (called 'lncRNAs PPAN'), are induced during IAV infection, interact with PA and promote FluPol assembly [180]. Interferon-independent lncRNAs (called 'IPAN') are also induced during IAV infection and have been found to modulate IAV replication in a loss-of-function screen. Silencing of IPAN is associated with PB1 degradation and impaired viral replication. IPAN was found to associate with PB1 thereby stabilizing the viral polymerase and enabling efficient viral RNA synthesis [181].

Members of the ANP32 family are involved in many cellular pathways including proliferation, differentiation, transcriptional regulation, mRNA export, and, as already mentioned, were found to promote IAV replication. More specifically, human ANP32A (also known as pp32) and ANP32B (also known as APRIL) are functionally redundant and essential for the IAV life cycle [182]. ANP32A and ANP32B interact with the viral polymerase and were found to support unprimed vRNA synthesis from the cRNA template [183,184]. Furthermore, ANP32A has been linked to IAVs host restriction. Indeed, the avian form of ANP32A contains an additional 33 aa between its leucine rich repeats and its Cter low complexity acidic region compared to its mammalian homolog. This sequence difference is responsible for the suboptimal activity of avian polymerase in mammalian cells. Acquisition of host adapting mutations, such as the PB2 627K mutation, allows adaptation of avian polymerase to mammalian ANP32 proteins [110,185,186].

Lastly, some posttranslational modifications are also involved in the regulation of IAV replication. For example, a balanced spatiotemporal NP acetylation is required for efficient replication. Indeed, mutations mimicking a constant acetylated NP are associated to a severely reduced polymerase activity [187]. Phosphorylation is also required, as highlighted by the role of the PPP6 phosphatase, which interacts with PB1 and PB2, and affects viral replication [150,188].

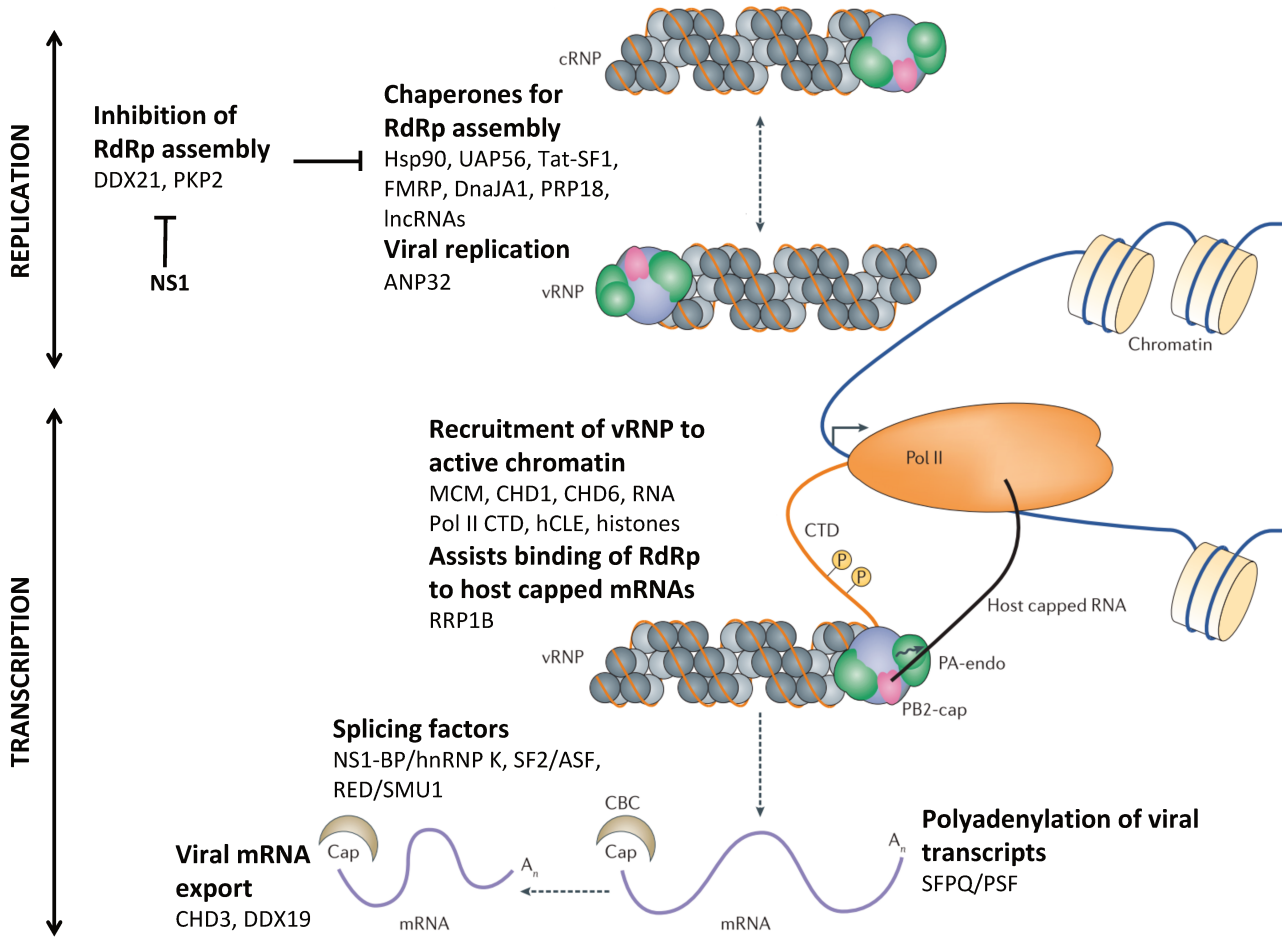

Figure 16: Cellular factors involved in viral transcription and replication.

Viral RNA synthesis is carried out in close proximity to chromatin and nuclear matrix enabling targeting of sites of RNA Pol II transcription by interaction with histones and chromatin associated factors such as the MCM complex, the chromatin remodelers CHD1 and CHD6, and hCLE. During viral transcription, the vRNPs bind the RNA Pol II CTD to access cap of nascent host RNAs for cap-snatching. Polyadenylation of viral mRNA is stimulated by SFPQ/PSF factors and both CHD3 and DDX19 promote export of viral transcripts. NS1-BP/hnRNP K, SF2/ASF and the RED/SMU1 complex participate in viral mRNA processing. For viral replication, cRNA acts as a template for vRNA synthesis. Host Hsp90, UAP56, Tat-SF1, FMRP, DnaJA1 and PRP18, as well as recently identified lncRNAs stimulate vRNA synthesis by supporting the assembly of the FluPol subunits. Assembly of the FluPol complex is inhibited by DDX21 and PKP2. DDX21 is counteracted by NS1. The ANP32 proteins are also implicated in replication of the viral genome. **Adapted from [86]**.

c. *Cellular factors interfering with viral transcription/replication*

Conversely, some cellular factors were found to inhibit viral transcription/replication. The RNA helicase DDX21 inhibits FluPol assembly by binding to PB1 leading to a decreased RNA synthesis. However, this DDX21 antiviral activity is counteracted by NS1, which, by

binding to DDX21, releases PB1 [189]. Similarly, PKP2 has been described as an IAV restriction factor by competing with PB2 for PB1 binding, leading to a defect in the FluPol assembly, thus limiting the RdRp activity and subsequently impairing viral replication [190].

Interestingly, the latest revised models of vRNPs organization suggest a non-uniform association of vRNAs with NP, with regions tightly associated with NP and others that may dynamically associate and dissociate from NP, thus producing regions free of NP [83] (see section II.1.a.). Lee and colleagues proposed that host RNA binding proteins could bind those regions free of NP [83]. The RNA-binding protein DAI (DNA-dependent activator of IFN-regulatory factors), a host antiviral sensor, was found to associate with vRNAs inside infected cells [191]. No apparent overlap between DAI-associated regions and NP binding sites was observed, thus supporting the proposed hypothesis.

d. *Viral induced host shut-off*

This large interplay between cellular host factors and the viral proteins involved in transcription/replication of the viral genome provides direct access to cellular machineries for cap-snatching, viral transcription and replication, mRNA processing, as well as export of mRNAs and vRNAs. In addition, accumulation of viral proteins is associated to a global reduction of host proteins production, progressively leading to host shut-off (reviewed in [192,193]). Indeed, eight hours post infection, more than half of all mRNAs within the cell are viral mRNAs, highlighting the striking takeover of cellular machineries by IAV. Furthermore, host shut-off may also interfere with antiviral cellular responses and promote immune evasion. IAV infection leads to host shut-off through three main mechanisms: i) blocking of cellular mRNA processing and nuclear export, ii) degradation of the RNA Pol II, iii) widespread mRNA degradation.

Notably, the NS1 protein interferes with the 3’ end formation of host mRNAs by interacting with the human cleavage-polyadenylation specificity factor 30 (CPSF30) [194,195]. The CPSF30 complex recognizes the polyadenylation signals at the 3’ end of mRNAs during transcription, cleaves the pre-mRNA and recruits polyadenylation complexes. Polyadenylation is crucial for transcripts as it promote their export, stability and translation.

Therefore, inhibition of polyadenylation and RNA processing of host mRNAs ultimately leads to a defect in host gene expression. In contrast, viral mRNA synthesis is not hindered, as polyadenylation of viral transcripts does not require CPSF complexes (see section II.2.a.). NS1 also interferes with cellular mRNA splicing and disrupts complexes between small nuclear RNAs (snRNAs), which are major components of spliceosomes [196–199]. Furthermore, NS1 interacts with the polyA-binding protein (PABPI) required for elongation of the polyadenylated tail. This interaction results in the synthesis of cellular transcripts harboring short polyadenylated tails, which further interferes with cellular mRNA export [200,201].

The viral endonuclease PA-X plays an essential and specific role in host shut-off by degrading host mRNAs and its role is further discussed in section III.3.b. However, cap-snatching can also alter host RNA transcription and contribute to host shut-off. Association of the FluPol with the RNA Pol II inhibits RNA Pol II elongation thereby reducing cellular gene transcription [121,202]. Bauer and colleagues reported that IAV infection leads to a global defect in host gene RNA Pol II transcription. Indeed, infection leads to a drastic decrease in RNA Pol II occupancy along gene bodies and an impaired termination of host mRNA transcription. As this effect is still observed upon infection with NS1 deficient viruses, this effect is most likely directly triggered by the viral polymerase and is therefore independent of NS1 interaction with CPSF30, which, as described above, interferes with mRNA 3' end processing. This dysregulation of host transcription triggers different consequences. First, impairing RNA Pol II transcription allows IAV to counteract cellular antiviral responses. Indeed, during viral infection, antiviral genes would represent hot-spots of RNA Pol II occupancy and their transcription would therefore be impaired by viral polymerase induced RNA Pol II dysregulation. Furthermore, premature RNA Pol II termination is beneficial in the context of cap-snatching, as RNA Pol II would be more rapidly freed from cellular genes, and therefore be able to re-initiate transcription, thus providing more capped transcripts to prime viral transcription [121]. Lastly, Bauer and colleagues propose that cap-snatching could also directly trigger RNA Pol II release from gene bodies. Indeed, generation of uncapped cellular transcripts can lead to their recognition by the cellular exonuclease XRN2, leading to premature transcription termination [121].

Additionally, IAV infection leads, later in infection, to the degradation of the RNA Pol II, once capped primers derived from host nascent mRNAs are no longer required for viral transcription [203,204]. RNA Pol II is ubiquitinated and targeted to proteosomal degradation leading to a subsequent loss of host gene transcription. This plays a role in circumventing the host antiviral response as it leads to inhibition of interferon stimulated gene transcription.

III. Viruses and the cellular RNA decay machineries

1. Interplay between RNA viruses and RNA decay pathways

a. *Overview of RNA decay pathways*

RNA decay is essential as it controls RNA stability and thus regulates gene expression in eukaryotic cells. Furthermore, the ability to control global or specific gene expression is crucial for both the virus and the host. On the one hand, regulation of transcript stability is central to ensure proper cell physiology and adapted response to the viral infection. On the other hand, successful viral infection relies on a global takeover of the cellular gene expression machineries. Therefore, viruses must interface with RNA decay machineries to control the levels of cellular and viral RNAs. There is growing evidence underlying the existence of a large interplay between the eukaryotic RNA turnover machineries and the viral proteins. Not only have viruses evolved mechanisms to evade those degradation pathways, but they can also manipulate them to promote viral replication (reviewed in [205–210]).

Regulation of gene expression occurs at many different levels in the cell, and RNA can be degraded either from its 3' end by the RNA exosome or the exoribonuclease DIS3L2, or from its 5' end by RNases from the XRN family (**Figure 17**).

Control of mRNA decay rates in the cytoplasm plays a crucial and essential role in transcriptional regulation, as highlighted by the many cellular proteins and partially redundant pathways involved. Those mechanisms involve the action of several endoribonucleases and exoribonucleases, as well as a large number of regulatory factors, which specifically recruit degradative enzymes to their respective targets. Generally, mRNA decay implicates modifications of mRNA ends leading to exposure of the transcripts (*i.e.* loss of the 5' cap and/or of the 3' polyadenylated tail). Shortened polyadenylated tails are recognized by the LSM1-7/PAT1 complex, which stimulates de-capping and subsequent 5'-3' degradation by XRN1. Otherwise, the multi-subunit RNA exosome complex may further degrade the polyadenylated tail and continue the 3'-5' decay into the transcript body. Alternatively, requirement of de-adenylation for mRNA degradation can be bypassed by

untemplated addition of uridine at the 3' end of transcripts. Degradation then proceeds as for de-adenylated transcripts (reviewed in [211,212]).

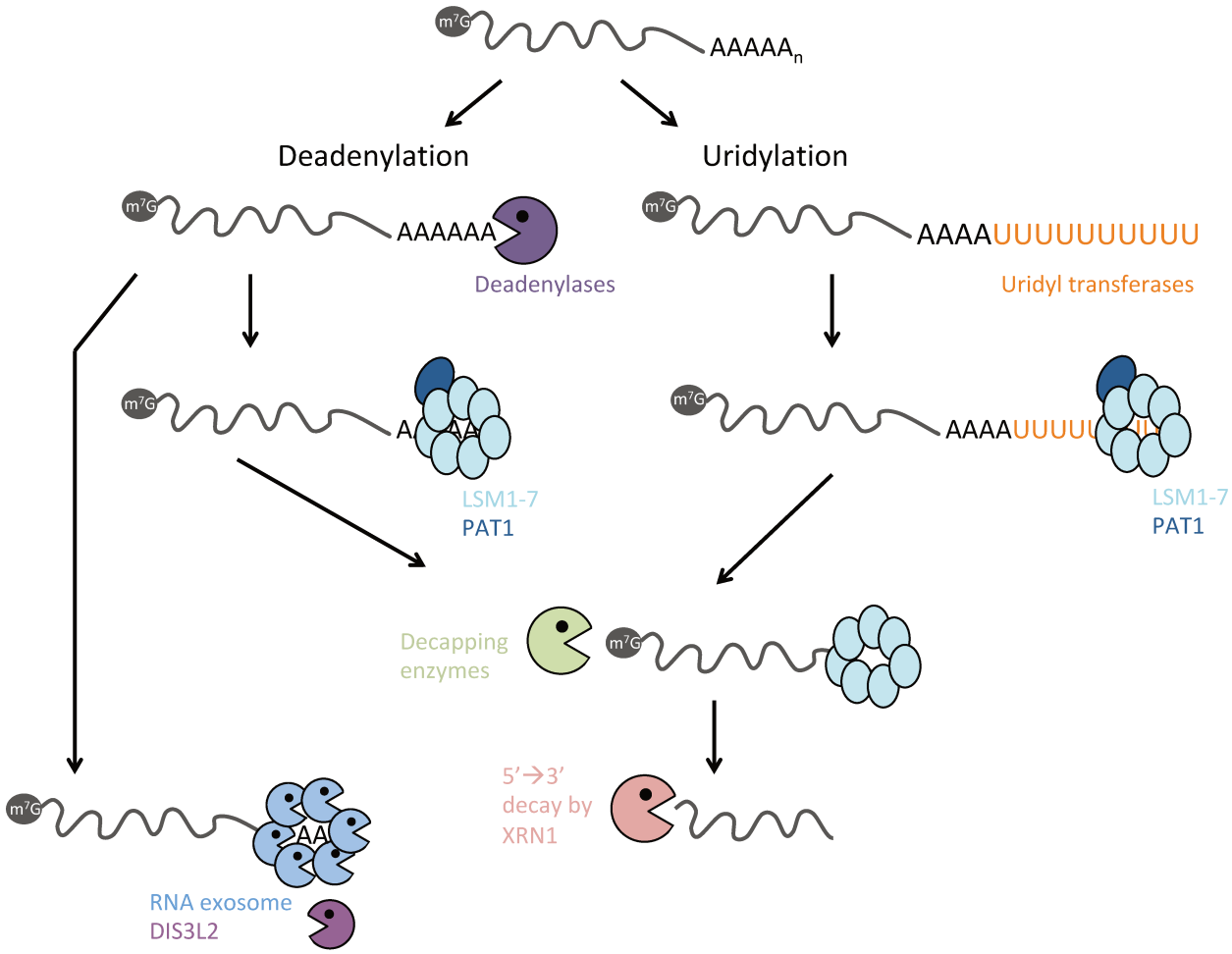

Figure 17: Cellular basal mRNA decay.
Cellular mRNA decay is initiated by de-adenylation or alternatively by uridylation of mRNAs. Subsequently, the LSM1-7/PAT1 complex binds the 3' region (3'UTR) of the de-adenylated or oligouridylated transcripts and stimulates de-capping. The transcript is then further degraded by XRN1. Alternatively, de-adenylated mRNAs can be degraded by the RNA exosome or DIS3L2.

Besides its central role in gene expression regulation, RNA decay is also crucial for co-translational RNA surveillance. Indeed, grossly aberrant RNAs, such as RNAs lacking a 5' cap or a 3' polyadenylated tail are unlikely to be translated. However, mRNAs containing errors such as premature stop codons or abnormal secondary structures can be translated, leading to the synthesis of aberrant proteins that can be detrimental to the cell. Cellular mRNA

surveillance pathways thus exist to recognize and degrade those abnormal transcripts. There are three predominant forms of co-translational mRNA surveillance: nonsense-mediated decay (NMD), which targets transcripts containing a premature stop codon, no-go decay (NGD), which targets transcripts that contain sequences that have the potential to induce stalling during elongation (such as stable stem-loops, pseudoknots, GC-rich sequences or damaged RNA bases), and nonstop decay (NSD), which targets transcripts missing a stop codon (reviewed in [213]) (**Figure 18**).

Although DNA viruses and retroviruses have evolved mechanisms to evade or hijack RNA decay pathways, the following sections will only address RNA viruses.

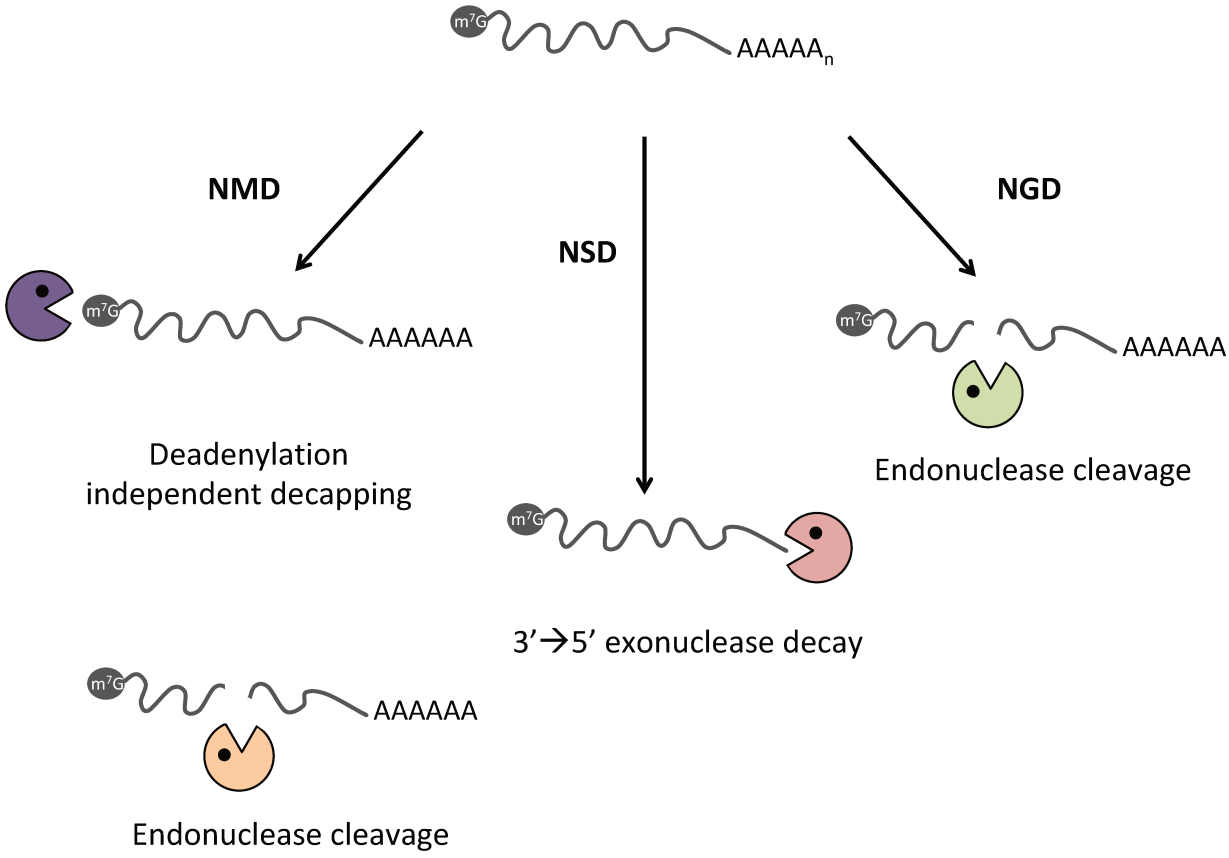

Figure 18: Cellular mRNA surveillance pathways: NMD, NGD and NSD.
Nonsense-mediated decay (NMD) substrates can be de-capped without requirement of de-adenylation or endonucleolytically cleaved and then degraded. No-go decay (NGD) leads to endonucleolytic cleavage of mRNAs with strong stalls in translation elongation, while nonstop decay (NSD) leads to 3' to 5' degradation of mRNAs that do not contain translation termination codons. **Adapted from [214].**

b. *RNA granules and mRNA decay*

RNA granules are structures found in all types of eukaryotic cells and are involved in gene regulation. The most common types of RNA granules are stress granules and processing bodies. Stress granules are dynamic structures enriched in translation initiation factors as well as 40S ribosomal subunits, while processing bodies are enriched in mRNA decay factors. Therefore, RNA granules control gene expression and can typically be exploited by viruses to promote replication. Manipulation of stress granules by viruses will not be discussed further here as this section specifically focuses on mRNA decay. This subject is thoroughly reviewed in [215,216].

Processing bodies have been shown to contain several mRNA decay enzymes, such as the de-adenylation complexes PAN2/PAN3 and CCR4/NOT, the LSM1-7 complex, XRN1 and the de-capping enzyme complex DCP1/DCP2 [214]. Several viruses are known to interfere with those mRNA decay factors either globally, by disrupting processing bodies, or more specifically by co-opting some processing body components.

For instance, poliovirus disrupts processing bodies through a combined action of viral and cell proteases. The de-adenylase complex component PAN3 is subject to degradation by the viral proteinase 3C, while DCP1 and XRN1 involved in de-capping and degradation are most likely degraded by cell proteases [217]. Since de-adenylation is required for processing body formation, viral inhibition of de-adenylation through PAN3 degradation is thought to lead to processing body disruption [218]. Disrupting processing bodies could thus be beneficial for viral replication by increasing viral RNA stability. Likewise, Cricket Paralysis Virus (CrPV) infection also leads to processing body disassembly [219].

Specific targeting of processing body components by viruses will be discussed in dedicated sections below.

c. *ARE and GRE dependent RNA decay*

The mRNA decay process is notably regulated by two *cis*-acting elements - AU-rich elements (ARE) and GU-rich elements (GRE) - and their *trans*-acting regulating factors. Upon binding to *cis*-regulating elements, those *trans*-acting factors can recruit de-adenylases, thus

initiating mRNA decay. Numerous studies report that AREs and GREs are manipulated by viruses to differentially regulate host mRNA stability and gene expression.

AREs and GREs are well-characterized sequences promoting rapid decay found in the 3' untranslated region (3'UTR) of some cellular transcripts. Interestingly, many cytokine gene transcripts contain AREs [220]. AREs control mRNA stability by interacting with ARE binding proteins (AREBP), which either promote transcript stability or its decay. Several studies report that viruses manipulate AREs and GREs to specifically control subsets of ARE- or GRE-containing host transcripts.

Remarkably, the genomic RNA of coxsakievirus B3 (CVB3) contains AREs and is therefore susceptible to decay. However, to counteract this, CVB3 infection leads to the overexpression of a host chaperone, Hsp70-1, which binds and stabilizes ARE-containing viral transcripts, thus facilitating viral replication [221]. Moreover, AUF1, an AREBP promoting mRNA decay, is cleaved upon CVB3 infection, further promoting viral RNA stability and viral replication [222]. Likewise, AUF1 is methylated upon West Nile Virus (WNV) infection, affecting its RNA binding capacities, thus facilitating viral replication [223].

Additionally, Hepatitis C Virus (HCV) NS5A protein binds and stabilizes GRE-containing host transcripts. Especially, NS5A targets host transcripts involved in the regulation of cell growth and apoptosis [209].

d. *De-adenylation*

Most of cellular mRNAs are protected at their ends by a 5' 7-methylguanosine cap and a 3' polyadenylated tail. De-adenylation is the first, and often the rate-limiting step, of cellular mRNA degradation. In eukaryotes, two multiprotein complexes, PAN2-PAN3 and CCR4-NOT, carry out de-adenylation of mRNAs to initiate decay [224,225].

To date, there is no evidence of direct hijacking of de-adenylation pathways by viral proteins. However, several RNA viruses have evolved mechanisms to avoid de-adenylation. Genomic RNAs of the Sindbis virus (SINV) and Venezuelan Encephalitis virus (VEEV) are both capped and polyadenylated like cellular mRNAs. Sequences in their 3'UTR were reported to

stall de-adenylation, presumably by recruiting a protective cellular factor, which displaces cellular de-adenylation factors from the 3'UTR [226].

Although de-adenylation is the initial step towards mRNA degradation, it can be reversible. Indeed, rather than inducing transcript degradation, de-adenylation can induce transient mRNA translation silencing [227]. However, the following step towards mRNA decay, removal of the 5' cap, is irreversible and allows degradation by RNases of the XRN family.

e. *The de-capping activator LSM1-7/PAT1/DHH1 complex*

Once de-adenylation has been completed, the de-capping co-activator LSM1-7/PAT1 complex is recruited to the transcript (**Figure 17**). The LSM complex is an heptameric ring-shaped complex composed of LSM1-7 proteins that act as RNA chaperones [228]. The LSM1-7 ring can bind short polyadenylated tails, while PAT1 interacts with the DCP1 and DCP2 de-capping enzymes, as well as with another de-capping activator, the DHH1 helicase (DDX6) [229]. Although the LSM complex is mostly associated to cellular mRNA decay in eukaryotes, it has also been found in yeast to protect mRNA 3' end from trimming [230,231]. Similarly, there is multiple evidence suggesting that the LSM complex is hijacked by viruses to promote viral RNA stability and viral replication.

The segmented genome of Brome Mosaic Virus (BMV) is composed of three strands of positive RNAs that are capped but not polyadenylated. Instead, their 3' end is stabilized by a tRNA-like structure. Although BMV is a plant virus, it can also replicate in yeast, which greatly facilitates its study. After entry into the cell, the positive genomic RNAs of BMV are directly translated into proteins. Once sufficient amount of viral proteins has been synthesized, translation is repressed and genomic RNAs are recruited to replication complexes to serve as template for replication, which occurs through synthesis of a negative replicative intermediate. Translation and replication are mutually exclusive processes and therefore need to be tightly regulated. LSM1-7, PAT1 and DHH1 have been found to be required for BMV replication and translation, and play a key role in controlling the translation/replication balance [232–235]. The current model proposes that LSM1-7, PAT1

and DHH1 bind to *cis*-elements in the viral RNA, which would remodel RNA secondary structures and promote its circularization and translation. Then, binding of the viral helicase 1A to the LSM1-7/PAT1 complex would break 3'-5' circularization, thereby repressing translation and subsequently allowing recruitment of the genomic RNAs for replication [232,236].

This recruitment of LSM1-7, PAT1 and DHH1 may be a general mechanism for positive-strand RNA viruses as some studies have highlighted their requirement for the replication of several viruses including HCV, Dengue virus, West Nile Virus (WNV) and Flock House Virus (FHV) [237–240].

f. *5'-3' RNA decay by XRN1*

Once the cap has been hydrolyzed by DCP1 and DCP2 de-capping enzymes, RNA degradation can further proceed *via* the XRN1 RNase (**Figure 17**). Thus, viral RNAs lacking a 5' cap are susceptible to XRN1 degradation. Various strategies are therefore employed by viruses to shield their RNA from XRN1-mediated degradation, such as the formation of complex secondary RNA structures or the recruitment of protective protein complexes.

Remarkably, some viruses also exploit XRN1 activity. The 3'UTR genomic region of flaviviruses, such as Yellow Fever Virus (YFV), WNV or Dengue virus, folds into a highly structured sequence that is able to stall XRN1 thereby protecting it from degradation [241,242]. Furthermore, flaviviruses exploit XRN1 stalling on their 3'UTR pseudoknot-like structure to produce 3' subgenomic RNAs, termed sfRNAs, that contain most of the genomic 3'UTR, and are essential for viral pathogenicity and replication [241,243–245] (**Figure 19**). In addition, sfRNAs bind and inhibit XRN1, both in mammalian and mosquito cells. Moreover, sfRNAs are likely to cause major disruption in cellular gene expression as the half-life of numerous cellular transcripts was found to be modified by sfRNAs. By interfering with XRN1, a major cellular decay factor, sfRNAs could therefore alter global host mRNA stability, quality control and decay [243,245].

Repression of XRN1 appears to be a shared feature among flaviviruses. Indeed, as for WNV and Dengue virus, HCV and Bovine Diarrhea Virus (BDV) both encode RNA structures

that induce stalling of XRN1. However, those sequences are located in the 5'UTR. Similarly to what as been described above, repression of XRN1 by HCV or BDV 5'UTR is associated to a dramatic dysregulation of host transcripts stability. Indeed repression of this major 5'-3' decay pathway leads to a striking increase in the stability and abundance of several cellular mRNAs, which normally display a short half-life [246]. Furthermore, this dysregulated cellular gene expression could also play a role in the pathogenesis associated to HCV infection, such as the establishment of hepatocellular carcinoma.

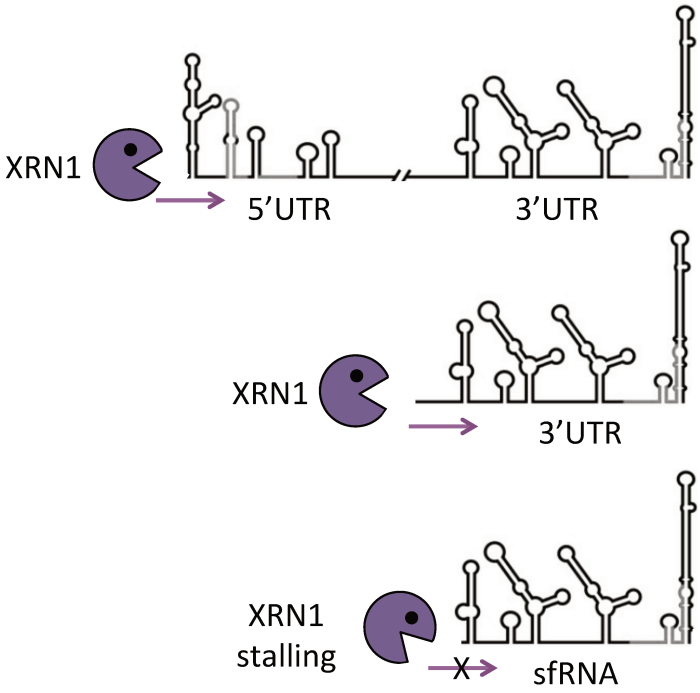

Figure 19: Mechanism of sfRNA formation.
Flaviruses sfRNAs are produced by stalling of the RNase XRN1 on the pseudoknot-like structures found in the 3'UTR of viral genomic RNA.

g. *3'-5' RNA exosome mediated decay*

The 3'-5' RNA decay process is essentially mediated by the RNA exosome (**Figure 17**). This multi-subunit complex is composed of six proteins, organized in a hexameric barrel, associated to a "cap" structure composed of three proteins containing RNA binding domains. This core associates with the processive 3' to 5' exo- and endoribonuclease DIS3 at the bottom of the barrel and/or with the distributive 3' to 5' exonuclease RRP6 at the top. The internal channel, within the barrel structure, is only wide enough to accommodate ssRNA, which is the only type of RNA degraded by the RNA exosome (reviewed in [247]) (**Figure 20**).

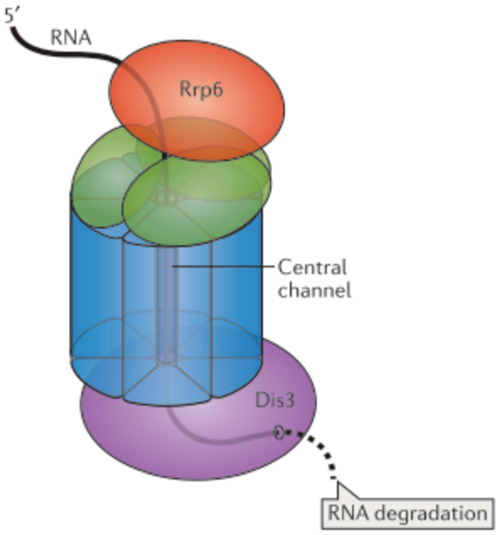

Figure 20: Structure of the exosome.
Schematic representation of an RNA molecule threading in the 3' to 5' direction through the exosome. The RRP6 exonuclease is represented in red. The barrel shaped nine subunits core is composed of the "cap" structure in green and of the hexameric barrel in blue. The endonuclease DIS3 is represented in purple and the substrate RNA in black. **From [247]**.

The two exonucleases associated with the RNA exosome, RRP6 and DIS3, as well as some core components of the RNA exosome, RRP4 and RRP41, and some exosome TRAMP co-factors, such as the helicase MTR4 and zinc finger RNA-binding protein ZCCHC7, are known to restrict replication of Vesicular Stomatitis Virus (VSV), Sindbis virus (SINV) and Rift Valley fever virus (RVFV) [248]. Upon infection, MTR4 and ZCCHC7 are relocalized to the cytoplasm where they associate with the exosome and the viral RNAs. Viral mRNAs of VSV, SINV and RVFV are targeted by the exosome. Indeed, upon exosome disruption, 3' ends of viral mRNAs, that are otherwise normally shortened, are stabilized. Additionally, in the case of RVFV, this exosome-mediated decay has been found to be directed by signals in the viral mRNA 3'UTR.

Some RNA helicases such as DDX17 and DDX60, known to associate with the RNA exosome, respectively inhibit RVFV and VSV [249,250].

Conversely, although examples discussed above support an anti viral role of the RNA exosome, it has recently been found to be hijacked by IAVs to promote cap-snatching (see section III.3.a.) [251].

h. *mRNA quality control*

Eukaryotic cells possess many RNA quality machineries that recognize and degrade aberrant transcripts thus preventing the synthesis of potentially harmful abnormal proteins (**Figure 18**). There is increasing evidence that viruses have evolved mechanisms to interfere with or modulate the cell mRNA quality control machineries (reviewed in [208]). Among those pathways, the nonsense-mediated decay (NMD) is by far the best characterized [252].

A common feature between all classes of NMD substrates is that translation terminates at an unusual position, either distant from the polyadenylated tail or with an exon junction complex (EJC) located between the stop codon and the polyadenylated tail. EJCs are normally removed by the elongating ribosome. Therefore, EJCs remaining after translation are abnormal, and can serve as anchoring points for the assembly of the NMD complex, subsequently leading to mRNA degradation [253]. Transcripts targeted by NMD include transcripts with a premature stop codon, either in an internal exon or in the terminal exon, transcripts containing upstream ORFs, transcripts containing introns downstream of the transcription termination site, or transcripts with long 3'UTRs (**Figure 21**).

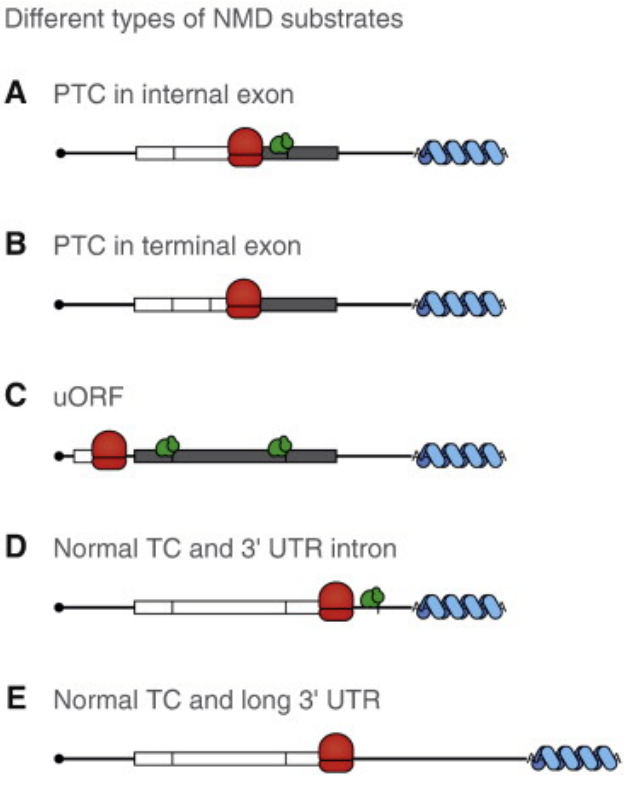

Figure 21: Substrates of nonsense-mediated decay (NMD).
Substrates of NMD comprise mRNAs containing a premature termination codon (PTC) either in an internal (**A**), or in the terminal (**B**) exon, on which one or several exon junction complexes (EJC) are expected to remain after translation termination. The presence of an upstream ORF (uORF) (**C**), of introns in the 3'UTR region, that will lead to EJC remaining associated to the ORF after translation termination (**D**) or long 3'UTR regions (**E**), also trigger NMD. mRNAs are represented as black lines with a 5' cap and a polyadenylated tail bound to the polyA binding protein (PABP) (blue). White boxes represent ORFs, grey boxes refer to the portion of the ORF that is not translated due to PTC or presence of a uORF. Ribosomes are represented in red and EJCs in green. **From [253].**

Due to the limited size of their genome, RNA viruses use various mechanisms to optimize their coding capacities. However, usage of such mechanisms can also render viral RNAs susceptible to NMD. Multiples ORFs, and thereby, multiple termination codons, are usually found on the same vRNA, which can elicit NMD. Some viral mRNAs also harbor long 3'UTR or sequences resembling upstream ORFs (**Figure 22**). Nonetheless, viruses still replicate in the cell, suggesting the existence of mechanisms to shield viral transcripts from NMD [208].

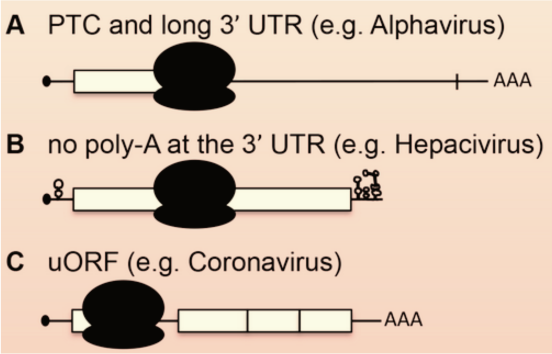

Figure 22: Features of viral RNAs that can elicit NMD.
Viral RNAs contain features that can make them susceptible to NMD, such as the presence of premature termination codons (PTC) or long 3'UTR regions (**A**), the absence of 5' cap and polyadenylated tail (**B**), or the presence of upstream ORFs (uORF) (**C**). **From [208].**

Activation of NMD requires regulatory factors, UPF1-3 (for 'up-frameshift'), as well as some additional factors, SMG1 and SGM5-9, that control UPF1 and trigger mRNA decay by recruiting specific degradation machineries (**Figure 23**). During normal translation, upon reaching the termination codon, the ribosome recruits eRF1 and eRF3 to catalyze peptide release. The PolyA Binding Protein 1 (PABPC1) enhances recruitment of the eRF proteins, thereby promoting correct end efficient translation termination. However, in the context of NMD, UPF1 is thought to compete with PABPC1 for binding to eRF3. In this model, premature stop codons or long 3'UTRs (*i.e.* sequences distant from PABPC1 binding sites) would lead to preferential UPF1 recruitment, which would in turn bind eRF3 at the terminating ribosome, and thereby activate NMD. Alternatively, if a stop codon is found upstream of an exon-exon junction, EJCs that are not displaced by translating ribosomes can also trigger NMD. RNA degradation can then be induced by three different ways as presented in **Figure 23** [208,252,254].

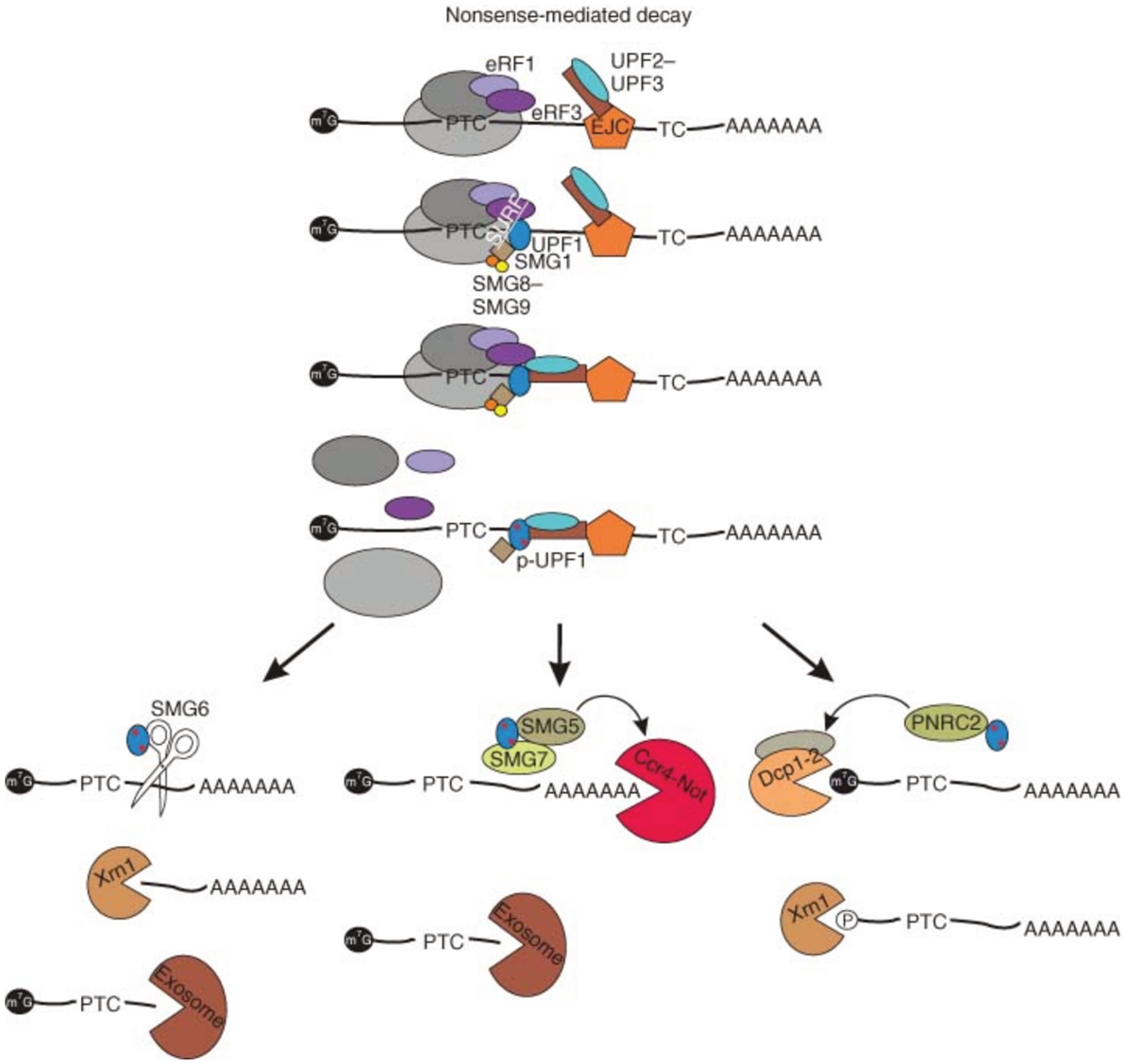

Figure 23: Nonsense meditated decay pathways.

When the ribosome reaches a premature stop codon (PTC) it associates with eRF1–eRF3 factors. Together with SMG1 and UPF1, this association forms a SURF complex (for SMG-1-UPF1-eRF1-eRF3). The SURF complex can then interact with the Exon Junction Complex (EJC) located on the downstream exon-exon junction by interacting with UPF2 and UPF3. Displacement of the SMG8-SMG9 dimer allows UPF1 phosphorylation at different sites. RNA degradation then proceeds *via* three possible pathways depending upon UPF1 phosphorylation status: i) the endonuclease SMG6 cleaves the mRNA near the terminating ribosome (bottom left), ii) the SMG5/SMG7 factors recruit the CCR4/NOT de-adenylation complex, which catalyzes degradation of the polyadenylated tail and eventually stimulates de-capping (bottom middle), iii) UPF1 directs the recruitment of the de-capping complex either directly or indirectly in a PNRC2-dependent manner (bottom right). Lastly, exonucleases involved in normal mRNA turnover ensure final degradation. **From [254].**

The UPF1, SMG5 and SMG7 proteins have been identified as host factors restricting replication of both Semliki Forest Virus (SFV) and SINV [255]. The genome of those alphaviruses is a polycistronic RNA that can directly be used for the synthesis of viral non-structural proteins. Structural proteins are translated later in infection from a subgenomic RNA that contain a very large 3'UTR. SFV genomic RNA has been shown to be a substrate for NMD, since depletion of UPF1 increases SFV genomic RNA stability. However, the long 3'UTR is unlikely to be the trigger for NMD, as viral RNAs with shortened 3'UTR still induce NMD [255]. The current model proposes that association of newly synthesized viral replicase proteins with the vRNAs and the translation machinery triggers translation termination; this could thereby create a RNP environment susceptible to elicit NMD [208].

Conversely, NMD can also be hijacked by viruses to manipulate cellular gene expression. Approximately 3 to 10% of the cellular transcriptome is affected by NMD, suggesting that, besides its RNA surveillance role, NMD has also a function in controlling transcript abundance [256]. HCV infection is associated with a progressive inhibition of NMD, notably highlighted by the accumulation of cellular RNAs that are known targets of NMD. Moreover, the viral core protein is able to bind PYM1, an EJC recycling factor, disrupting its interaction with MAGOH and Y14, two central components of the EJC, and therefore inhibiting NMD [257]. Inhibition of NMD could lead to the stabilization of several cellular transcripts and thereby create a cellular environment favorable to viral replication and pathogenesis. Through a similar mechanism, other flaviviruses such as WNV, Dengue and Zika viruses have also recently been shown to inhibit NMD. The EJC protein Y14 is able to bind WNV viral RNA, which can elicit NMD. Similarly to what has been reported for the HCV core protein, this is counteracted by WNV capsid, which binds PYM1, thereby preventing recycling of the EJC proteins resulting in EJC proteins sequestration and cellular mislocalization. Sequestration of EJC proteins therefore leads to stabilization of both viral RNAs and host mRNAs [258].

No-go decay (NGD) and nonstop decay (NSD) factors have also been found to be essential for the replication of several viruses. The NGD factor, PELO, involved in the rescue of non-productive ribosomes, is required for the replication of the Drosophila C Virus (DCV) [259]. PELO inactivation is associated with increased levels of aberrant 80S ribosomes not engaged in productive translation and to reduced synthesis of viral proteins. PELO thus

ensures the availability of pools of ribosomes through the dissociation of stalled 80S ribosomes, as well as the clearance of aberrant viral RNAs and proteins, both mechanisms being essential for efficient viral translation [259,260].

i. *RNase L*

The RNase L is an interferon-induced ribonuclease playing an essential role in innate immunity. The RNase L pathway is triggered upon activation of the 2',5'-oligoadenylate synthetase (OAS) by dsRNA and leads to the apoptosis of the infected cell. In response to dsRNA, OAS generates 2',5'-oligoadenylate that in turn activates the RNase L which cleaves ssRNAs, preferentially after an UA or UU dinucleotide, and initiates RNA decay. It thus contributes to antiviral defense by cutting both viral and cellular RNAs that are needed for viral replication, and inducing apoptosis [261].

Although RNase L restricts numerous viruses, some have evolved various mechanisms to counteract it. The NS2 protein of the Murine Hepatitis Virus (MHV) cleaves 2',5'-oligoadenylate, thereby preventing activation of RNase L and degradation of viral RNAs. Enteroviruses of the group C encode small RNAs (called 'ciRNA' for 'competitive inhibitor RNA') that compete with RNase L for binding to its RNA substrates. The ciRNAs thus inhibit the endoribonuclease activity of the RNase L and therefore stabilize viral and cellular mRNAs [262,263]. Other viruses such as HCV do not block RNase L activity or activation, but are however less sensitive to RNase L cleavage by limiting the frequency of UA and UU dinucleotides in their genome [264]. Interestingly, in patients under interferon therapy, viral genomes accumulate silent mutations preferentially at UA and UU dinucleotides. This could suggest a correlation between the sensitivity of HCV in patients treated with interferon and the efficiency of HCV mRNA cleavage by RNase L [264].

2. Viral endonucleases and de-capping enzymes directing cellular RNA decay

Instead of interrupting or manipulating cellular RNA decay pathways, some viruses directly encode ribonucleases to rewire cellular gene expression to their benefit. Viruses induce global mRNA degradation either by endonucleolytic cleavage or by promoting de-capping. In both strategies, viruses bypass the rate-limiting step of de-adenylation, ensuring direct translation inactivation and RNA degradation. Viral endonucleases and mechanisms employed by viruses to promote mRNA decay are summarized in **Table 2** (see [207] for review).

Virus	Viral protein	Mechanism	References
DNA viruses			
ASFV	g5R	De-capping enzyme	[265]
Gamma-herpes viruses	BGLF5 (EBV), SOX (KSHV), muSOX (MHV68)	Endonucleases Targeting of RNA stem-loop and bulges (KSHV) Nuclear relocalization of PABPC1	[207,266–268]
HSV-1	VHS	Endonuclease Binds translation factors eIF4A and eIF4H as well as the eIF4F cap-binding complex	[269,270]
VACV	D10, D9	De-capping enzymes	[271,272]
RNA viruses			
IAV	PA-X	Endonuclease	[42,273]
SARS-CoV	NSP1	NSP1 renders the 40S ribosome subunit and the bound cellular transcripts translation incompetent Recruits an unknown cellular endonuclease	[274,275]

Table 2: Viral endonucleases and de-capping enzymes that restrict gene expression.

a. *Endonucleases encoded by herpes viruses*

The Herpes Simplex 1 (HSV1) VHS (for 'Viral Host Shut-off') endonuclease induces the turnover of many host and viral mRNAs. It thus decreases the abundance of cellular transcripts and ensures proper balance between viral transcripts, thereby facilitating the transition between the immediate early, early, and late phases of herpes virus infection. The translation initiation factors eIF4A and eIF4H play a key role in cap-dependent ribosome scanning and are known to interact with VHS [269]. Furthermore, the eIF4A helicase, along

with the eIF4E and eIF4G factors, form the cap-binding complex eIF4F. VHS is targeted to the mRNAs and to the regions of translation initiation mainly through its association with the eIF4F complex. Furthermore, VHS has a broad substrate specificity and can cleave RNAs at many different sites, thus ensuring efficient mRNA degradation [270].

Gamma-herpesviruses encode a viral endonuclease that broadly targets cytoplasmic mRNAs for cleavage leading to their subsequent degradation. This protein, termed SOX in Kaposi's Sarcoma-associated Herpes Virus (KSHV), muSOX in Murine gamma-Herpes Virus 68 (MHV68), and BGLF5 in Epstein–Barr virus (EBV), is a PD-(D/E)XK endonuclease [207]. SOX-induced host shut-off is a coordinated mechanism, which first involves the endonucleolytic cleavage of cellular mRNAs by SOX, followed by further degradation by the cellular exoribonuclease XRN1 [267]. Primary endonucleolytic cleavage by SOX is thought to occur without sequence specificity and generates 5' ends that can be directly processed by XRN1, hence by-passing the steps of de-adenylation and de-capping that are classically required for XRN1 activation [268]. This leads to global depletion of cellular mRNAs from polysomes, thus liberating the host translation machinery and creating a favorable environment for viral replication.

b. *Viral de-capping enzymes*

The vaccinia virus (VACV) D9 and D10 de-capping proteins and the g5R protein from the African Swine Fever Virus (ASFV) contain a Nudix domain essential for their de-capping activity [265,271,272]. While the D10 de-capping enzyme binds both the methylated cap and the RNA body, the g5R protein only recognizes the RNA body. It is not known why VACV encodes two de-capping enzymes. However, there are a few differences between the two enzymes. D9 requires a longer capped RNA substrate than D10 to exert its de-capping activity. Moreover, D9 and D10 are thought to manipulate cellular gene expression in a complementary and overlapping manner, as D9 is expressed early in infection while D10 is expressed later [272]. De-capped transcripts are then most likely degraded by XRN1.

Although they do not encode de-capping enzymes, IAVs, Bunyaviruses and Arenaviruses, by snatching the cap of cellular mRNAs, lead to the accumulation of cellular transcripts

bearing an unprotected 5’ end that are therefore susceptible to XRN1 degradation (see section II.2.a) [276,277].

c. *Endonucleases and exonucleases encoded by RNA viruses*

The Severe Acute Respiratory Syndrome Coronavirus (SARS-CoV) NSP1 binds the 40S ribosome subunit, inactivating the ribosome and inducing cleavage of mRNAs. NSP1 binding to the 40S subunit inactivates its translation activity, thus allowing a global targeting of cellular transcripts and leading to the inhibition of host protein synthesis. Furthermore, ribosomes bound to NSP1 induce RNA modification in the capped mRNAs, rendering them incompetent for translation [274]. However, NSP1 itself does not have an endonuclease activity and is thought to activate a yet unknown cellular endonuclease to cleave the mRNAs. NSP1 induces endonucleolytic RNA cleavage mainly near the 5’UTR region of capped mRNA templates, with no apparent preference for a specific nucleotide sequence at the RNA cleavage site [275]. Although CoV mRNAs are capped and polyadenylated like cellular mRNAs, they are not susceptible to NSP1 mediated degradation. Indeed, the presence of their 5’ end leader sequence protects them from NSP1 endonucleolytic cleavage, thus leading to the accumulation of viral mRNAs and viral proteins during infection.

Although it is not associated to RNA decay, several viruses encode exoribonucleases required for viral replication. Lassa fever virus nucleoprotein possesses a 3’-5’ exoribonuclease activity that specifically digests viral dsRNAs, thereby suppressing activation of innate immunity [278,279]. The SARS-CoV NSP14 carries a DEDD exoribonuclease activity crucial to ensure viral replication fidelity [280].

3. Influenza virus replication and host RNA decay pathways

a. *IAV and the cellular RNA decay machineries*

Like reported for other RNA viruses (see section III.1.c.), IAV infection leads to the formation of stress granules and processing bodies. RAP55, a component of the processing bodies, inhibits viral protein synthesis at early phases of the viral cycle, most likely through the recruitment of RAP55-associated processing bodies. This is however counteracted later in the infection by NS1, whose interaction with RAP55 leads to the disruption of processing bodies [281].

The NS1 protein is also essential to counteract the endonucleolytic cleavage by RNase L [282]. The NS1 Nter RNA-binding domain is able to bind dsRNA [283]. This dsRNA-binding activity is required to protect IAVs from the antiviral state induced by IFN-β. Indeed, NS1 sequesters dsRNA thereby inhibiting the activation of the IFN-α/β-induced 2'-5'-oligoadenylate synthetase (OAS)/RNase L pathway (see section III.1.i.) [282].

IAV infection leads to up-regulation of the interferon induced 3'-5' exonuclease ISG20 expression. ISG20 colocalizes with NP in infected cells and inhibits viral replication and transcription [284]. It has been proposed that ISG20 exerts its antiviral activity by directly degrading viral RNAs as no antiviral effect is observed in cells expressing an ISG20 protein with a defective exonuclease activity [285].

Although the RNA exosome is known to restrict many RNA viruses (see section III.1.g.), it is hijacked by IAVs to promote viral transcription [251]. In the nucleus, the RNA exosome is involved in co-transcriptional RNA quality control and induces degradation of aberrant mRNAs and non-coding RNAs (ncRNA) with unprotected 3' ends. FluPol interacts with the exosome core subunits and silencing of these core subunits is associated to an impaired viral replication. Interaction with the RNA exosome allows the FluPol to snatch 5' caps from ncRNAs and aberrant mRNAs that would otherwise be rapidly cleared by the RNA exosome. IAV have thus evolved mechanisms to exploit the cellular RNA quality control by recycling "junk" cellular RNAs for cap-snatching, therefore promoting their transcription.

b. *IAV PA-X endonuclease*

The IAV PA-X protein is expressed by ribosomal frameshift during translation of the PA segment (see section I.2.c.) and is produced by all IAV strains, underlying its essential role for IAV replication [42,286]. PA-X is a PD(D/E)XK endonuclease (similar to the endonuclease encoded by herpesviruses) that is involved in modulation of the host response following infection. Host RNA degradation observed in IAV infected cells is not solely the consequence of cap-snatching, and PA-X plays a key role in the induction of host shut-off. Like VHS, SOX or SARS-CoV NSP1, PA-X preferentially destabilizes RNA Pol II transcripts and requires the activity of the cellular RNase XRN1 to complete RNA degradation after initial direct fragmentation [273] (see sections III.2.a and III.2.c.). However, unlike VHS, SOX or NSP1, PA-X acts predominantly in the nucleus, where it can target long ncRNAs as well as mRNAs. While other viral RNases access cellular transcripts through translation, PA-X is proposed to interact with cellular factors involved in transcription in order to associate to its target transcripts [193]. Gaucherand and colleagues recently showed that PA-X selectively targets spliced RNA Pol II transcripts as PA-X has little effect on the degradation of intron-less mRNAs and susceptibility to PA-X degradation increases with exon number. This splicing based strategy therefore allows to efficiently discriminates viral RNAs from cellular RNAs for PA-X mediated degradation. Although some IAV mRNAs are spliced, they were remarkably found to be PA-X resistant. Indeed, splicing of IAV mRNAs occurs differently from cellular mRNAs splicing, as in the case of viral mRNAs, the splicing machinery needs to be recruited separately from the RNA Pol II, which is proposed to prevent targeting by PA-X. Hence, in this model, RNAs that are not canonically processed, including viral RNAs, are spared from PA-X degradation [287].

IV. The 3'-5' cellular exoribonuclease 1 (ERI1)

1. General features of ERI1: structure and substrate specificity

The cellular exonuclease ERI1 (also known as 3'hEXO) was first described in *Caenorhabditis elegans* in a screen for mutants demonstrating an "enhanced RNAi" (*i.e.* "ERI") phenotype in neurons (see section IV.2.a.) and is conserved from fission yeast to humans. ERI1 can process small regulatory RNAs, ribosomal RNAs as well as histone mRNAs and therefore has a pivotal role in the control of cellular gene expression (reviewed in [288]).

a. *ERI1 structure*

ERI1 is a 3'-5' exoribonuclease of the DEDDh family (**Figure 24**). DEDD exonucleases all share a characteristic core composed of four invariant acidic residues associated to several other residues organized in three separate sequence motifs [289]. According to the identity of a fifth invariant residue within motif III, DEED exonucleases are further subdivided in two subfamilies: DEDDy exonucleases bearing a Y-x(3)-D sequence and DEDDh exonucleases bearing instead an H-x(4)-D sequence (**Figure 25**). This sequence difference however appears to have little effect on the enzymatic activity, as both subfamilies include DNases as well as RNases.

In addition to its DEDDh catalytic core, ERI1 also has a conserved "SAF-box, Acinus and PIAS" (SAP) domain (**Figure 24**), which binds double-stranded nucleic acids *via* conserved amphipathic helices [290,291]. ERI1 SAP/Interdomain (ID) mutants bind and process less efficiently rRNA or histone mRNA, supporting the role of the SAP domain in recruiting RNA substrates to ERI1 [292–294].

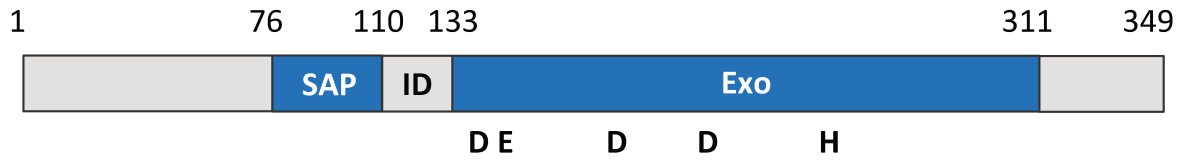

Figure 24: Schematic organization of ERI1.
The conserved "SAF-box, Acinus and PIAS" (SAP), inter-domain (ID) and DEDDh exonuclease (Exo) (D134, E136, D234, D298 and H293) domains are represented. aa numbers and conserved residues of the catalytic core are indicated.

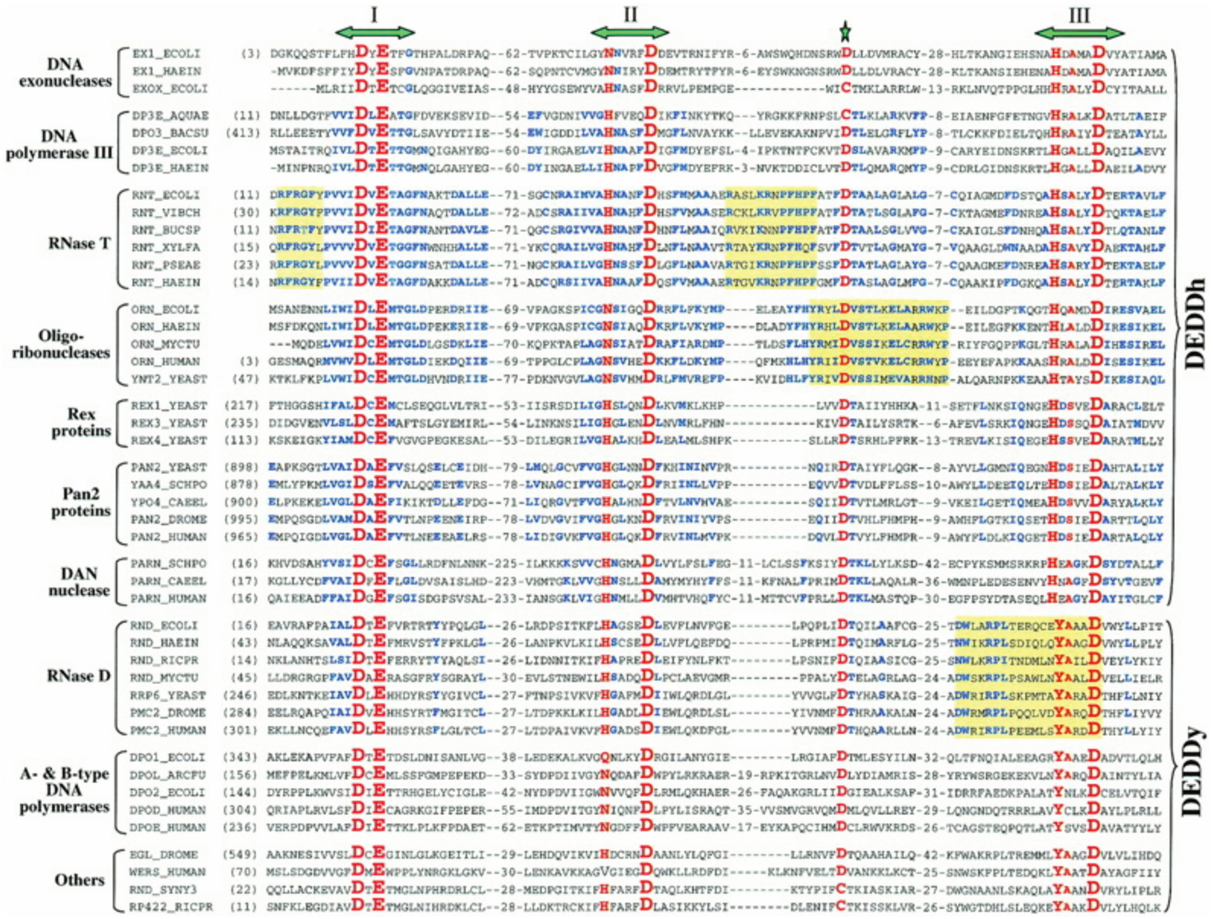

Figure 25: Alignment of exonucleases of the DEDD family.

Sequence alignment of DEDD exonucleases. Sequences are mainly representative of RNases but DNases are also represented. The three conserved motifs (I, II and III) are indicated at the top. Highly conserved residues among all family members are represented in red. The star at the top indicates a conserved residue found between motifs II and III. Residues that are conserved within a subfamily are indicated in blue. Yellow squares highlight sequence motifs characteristic of some subfamilies (aromatic residues specific to the RNase T family, the sequence motif surrounding the conserved residue found between motifs II and III and the characteristic motif III of RNases D). **From [289]**.

In *Caenorhabditis elegans,* two ERI1 isoforms produced by alternative splicing, ERI1a and ERI1b, have been found. The ERI1a isoform is similar to human and murine ERI1, however the ERI1b isoform is longer and displays an extended Cter required for interaction with DICER [295]. Snipper (SNP) is an ERI1 homolog found in *Drosophila melanogaster* that lacks the SAP domain. However, unlike its ERI1 homologs, SNP plays neither a role in histone mRNA degradation, nor in regulation of RNAi (see section IV.2.a.) [296].

b. *ERI1 substrate specificity*

The conserved DEDD residues of the ERI1 catalytic core form a negative patch that coordinates two Mg^{2+} ions within the active site, and thus assist in the binding and orientation of the terminal phosphate group of the substrate RNA. The conserved histidine residue deprotonates Mg^{2+}-coordinated H_2O molecules, thereby allowing it to attack the last phosphorus atom and cleave the terminal phosphodiester bond of the oligoribonucleotide substrate [297].

The ERI1 exonuclease domain binding pocket cannot accommodate RNA substrates longer than a dinucleotide. The structure of ERI1 bound to rAMP shows the rAMP molecule well sat in the ERI1 cavity, leaving enough space to potentially accommodate the penultimate nucleotide of an RNA chain (**Figure 26**). Therefore, 3' ssRNA overhangs, such as those found in siRNA, rRNA or at the 3' end of replication dependent histone mRNA (*i.e.* the only known eukaryotic mRNAs that are not polyadenylated, see section IV.2.c.), can be efficiently cleaved by ERI1 (see section IV.2.). On the contrary, RNAs lacking 3' overhangs, RNA duplexes and DNA have been found to be very poor substrates for ERI1 [292,293,295,298]. The drosophila ERI1 homolog, SNP, is however able to degrade structured DNA and RNA substrates bearing two to five nucleotides long 3' overhangs in the presence of Mg^{2+} with no apparent sequence specificity [296].

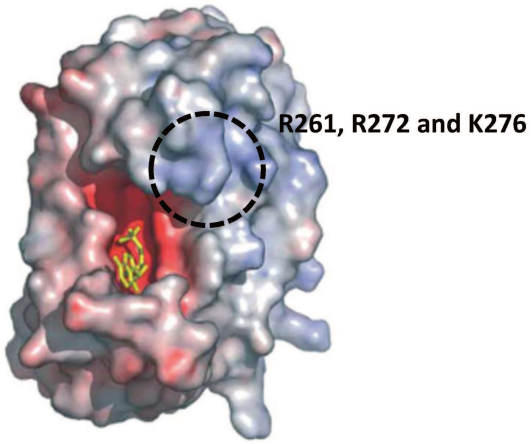

Figure 26: Structure of the ERI1 exonuclease domain.
The ERI1 exonuclease domain potential electrostatic surface is colored from blue (basic) to red (acidic) and bound to rAMP (shown in yellow). R261, R272 and K276 are indicated by a circle and form a basic patch on the surface for binding to the phosphate backbone of the substrate RNA. This potentially allows accommodation of dinucleotide RNA substrates in the binding pocket. **Adapted from [297]**.

2. ERI1 and regulation of cellular gene expression

a. *ERI1 role in the regulation of small RNAs*

ERI1 has a conserved function as a negative regulator of the RNA interference (RNAi) pathway as reported in *C. elegans*, *S. pombe*, mice and humans. Indeed, ERI1 was reported to degrade siRNAs, thereby blocking the RNAi pathway [295]. In *C. elegans* and *S. pombe*, RNAi is dominated by small interfering RNAs (siRNAs), while in metazoan somatic cells, silencing pathways involve both siRNAs and micro RNAs (miRNAs).

Regulation of RNA interference in *C. elegans*

Introduction of foreign dsRNA into an organism usually causes degradation of the mRNA that is homologous to the foreign dsRNA through a mechanism called RNA interference (RNAi). dsRNAs are cleaved by the DICER RNase into siRNAs leaving a two to four nucleotides long 3' ssRNA overhang. Those 3' ssRNA overhangs are essential as they are required for siRNA-mediated degradation or translational silencing of the targeted mRNAs. Each siRNA duplex is composed of a guide strand (antisense) and a passenger strand (sense). The guide strand is incorporated into the RNA-induced silencing complex (RISC), while the passenger strand is targeted to degradation. The RISC complex then binds the targeted transcript through base pairing between the siRNA and the targeted mRNA, either leading to its degradation or to its translational repression (**Figure 27**) (reviewed in [299]).

The vast majority of mRNAs found in *C. elegans'* nervous system are refractory to RNAi. ERI1 was identified in a genetic screen searching for mutants with an enhanced sensitivity to dsRNAs. In *C. elegans*, ERI1 is predominantly cytoplasmic and is highly expressed in gonads and in a subset of neurons. Upon introduction of siRNAs or dsRNAs, ERI1 mutants displayed a higher accumulation of siRNAs compared to their wild type counterparts. *In vitro, C. elegans'* ERI1 was able to degrade siRNAs with 3' overhangs, but was inactive on siRNAs with no overhangs or on internally hybridized siRNAs (*i.e.* siRNAs containing dsRNA portions). ERI1 was thus proposed to inhibit RNAi by degrading siRNAs 3' overhangs, thereby blocking their loading onto the RISC complex or leading to their destabilization and subsequent degradation [295].

ERI1 also promotes the biogenesis of some endogenous siRNAs. Interestingly, only the *C. elegans'* specific ERI1b isoform was found to associate with DICER, and ERI1b ectopic expression was solely able to rescue endogenous siRNA biogenesis [300]. Models involving a competition for DICER between endo- and exogenous siRNA pathways are proposed to explain how ERI1 can promote biogenesis of endogenous siRNAs while restricting exogenous siRNAs. However, the precise mechanism involved is largely unknown [288].

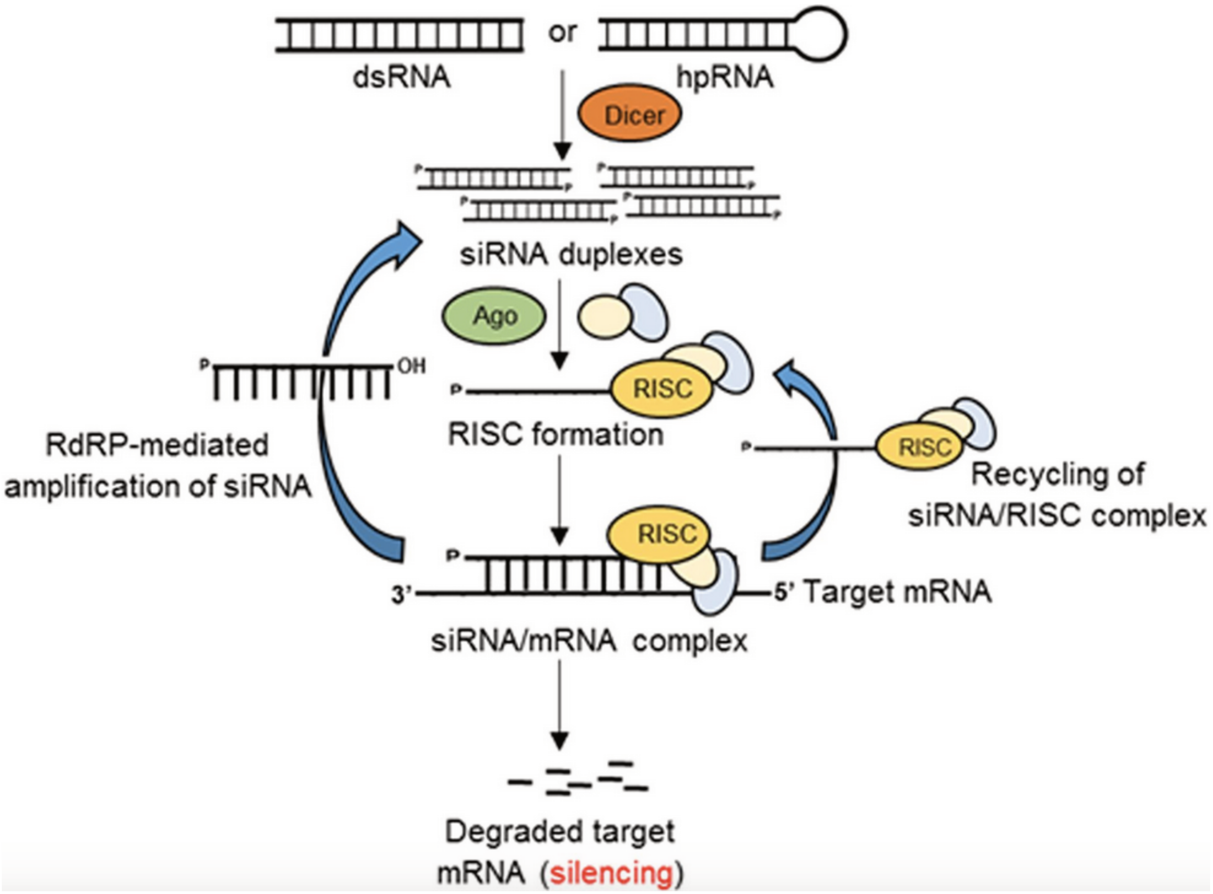

Figure 27: RNAi pathway.
By the action of DICER, siRNA duplexes are generated from double-stranded RNAs (dsRNA) or hairpin RNAs (hpRNAs) Association of the guide strand, Argonaute protein (Ago) and other proteins forms the RNA-induced silencing complex (RISC). The RISC complex then binds its target mRNA resulting either in inhibition of its translation or in its degradation. The components of the RISC complex can then be recycled or stimulate an amplification of the siRNA response by generating more siRNA duplexes by the action of an RNA-dependent RNA-polymerase (RdRP). **From [301].**

Regulation of heterochromatin assembly in *S. pombe*

RNAi is a gene silencing mechanism that has widespread roles in RNA degradation, as mentioned above, but also in translational repression and epigenetic control of chromatin structure. In fission yeast, heterochromatin is primarily found at centromers and telomers. DICER processes transcripts deriving from heterochromatin into siRNAs. Those siRNAs then target the RNA-induced transcriptional silencing (RITS) complex to genomic regions from which they originate. The RITS complex promotes transcripts degradation and controls heterochromatin assembly.

As reported in *C. elegans, Schizosaccaromyces pombe's* ERI1 predominantly localizes in the cytoplasm and represses the accumulation of siRNAs by degrading dsRNAs with two nucleotides 3' ssRNA overhangs into short oligoribonucleotides. Both ERI1 domains (*i.e.* the SAP and exonuclease domains) are required to degrade dsRNAs, even though a large excess of the sole exonuclease domain was found to be able to degrade dsRNAs. Depletion of ERI1 is associated with an increased abundance of siRNAs, an enhanced heterochromatin silencing and an increased level of histone H3-K9 methylation and SWI6 protein. SWI6 targets methylated histone H3-K9 and triggers the formation of silent heterochromatin. Therefore, ERI1 negatively regulates the accumulation of heterochromatic siRNAs and thereby downregulates the amount of RITS complexes containing siRNAs. ERI1 affects heterochromatin in the nucleus, even though it is mainly localized in the cytoplasm. This localization suggests that ERI1, like many siRNA processing enzymes, functions in the cytoplasm. Therefore, how ERI1 regulates nuclear heterochromatin is unclear. Iida and colleagues propose that a small fraction of ERI1 may function in the nucleus, targeting siRNAs close to heterochromatin [298].

Regulation of miRNA abundance

miRNAs are generated from long hairpin-containing primary transcripts that undergo successive cleavage by the Microprocessor complex and DICER. With the exception of germ cells, the mammalian small RNA repertoire is dominated by miRNAs.

Sequencing of small RNAs of lymphocytes from ERI1$^{-/-}$ mice showed a two-fold increase in general miRNA abundance [302]. However, contrary to what is observed in *C. elegans*,

miRNAs are the only RNA population affected by ERI1 knock-out [303]. ERI1 is known to cleave 3' ssRNA overhangs, but it is unclear how ERI1 can regulate miRNAs abundance. ERI1 could degrade mature or precursors miRNAs, or cleave 3' overhangs from pre- or mature miRNAs, thus blocking their loading onto the RISC complex or their export into the cytosol. Alternatively, miRNA trimming by ERI1 could prime them for degradation [288]. In addition, regulation of miRNA abundance appears to be critical for NK cell maturation, expansion and effector function in mice. In ERI1$^{-/-}$ mice, NK cells failed to expanded in response to Murine Cytomegalovirus (MCMV) infection, suggesting that ERI1 could be important for antiviral immunity [302].

Interestingly, even though miRNAs appear to be the only RNA population affected in ERI1$^{-/-}$ mice, ERI1 was upregulated in response to high doses of exogenous siRNAs. Furthermore, upregulation of ERI1 was associated to a reduced RNAi efficiency in mouse, while its silencing rescued RNAi effectiveness, suggesting that it may regulate different RNAi pathways [304,305].

b. *ERI1 role in the regulation of ribosomal RNAs*

The 5.8S rRNA is a very conserved target of ERI1. ERI1 catalyzes trimming of the 5.8S rRNA 3' end in *C. elegans, S. pombe* and in mammalian cells [294,300]. rRNAs are abundant cellular RNAs involved in the formation of the catalytic core of ribosomes. The biogenesis of ribosomes is a highly controlled and coordinated mechanism, and its regulation is essential for translation regulation. The importance of this regulation is highlighted by the strong growth defects and the high neonatal mortality rates observed in ERI1$^{-/-}$ mice [294]. Furthermore, unlike endogenous siRNAs biogenesis, both *C. elegans* ERI1 isoforms are able to process 5.8S rRNA [300].

The ribosomal 40S subunit is composed of the association of the 18S rRNA with 32 ribosomal small subunit proteins, while the 60S subunit is composed of 47 ribosomal subunit proteins associated to the 28S, 5.8S and 5S rRNAs. The 18S, 5.8S and 28S rRNAs all derive from a single precursor transcript that is processed in the nucleolus. Due to base pairing between the 3' end of the mature 5.8S rRNA and the 5' end of the mature 28S rRNA, those

two rRNAs form a duplex and remain associated during ribosome maturation [306]. This base pairing leaves a 3' ssRNA overhang that can be targeted by ERI1. Indeed, ERI1 associates to ribosomes and degrades the 3' ssRNA overhang of the 5.8S/28S rRNA duplex, leaving a one-or-two-nucleotide- long 3' overhang. Further degradation by ERI1 is inhibited by the presence of dsRNA in the duplex. Moreover, although they were found to increase trimming efficiency, ERI1 SAP and ID domains appear to be dispensable for 5.8S rRNA processing and are most likely involved in the stabilization of the interaction between ERI1 and its substrate. As ERI1 predominantly localizes in the cytoplasm in *S. pombe* and *C. elegans*, 5.8S rRNA processing is most likely cytoplasmic, even though ERI1 is also found in the nucleolus of murine and human cells [294].

Remarkably, ERI1 was found to associate with mature ribosomes, suggesting that ERI1 remains associated to the ribosome after 5.8S rRNA processing is completed. Moreover, ERI1 appears to preferentially associate with inhibited ribosomal particles. As proposed by Ansel and colleagues, this could explain the role of ERI1 in the regulation of miRNAs abundance, since some miRNAs were shown to repress transcript expression by sequestering targeted mRNAs into heavy structures that are not actively engaged in translation [288,294,307,308].

c. *ERI1 role in the regulation of histone mRNAs*

Histone mRNA abundance needs to be tightly regulated and controlled to properly respond to histone demand during the cell cycle. Thus, histone mRNAs are highly transcribed as cells enter the S phase when histones are required for DNA packaging into nucleosomes, and their abundance rapidly decreases when cells enter the G2 phase. Coordination between DNA replication and histone synthesis is crucial, as improper control leads to genomic instability and cell cycle arrest [288,309]. Processing and degradation of histone mRNA is reviewed in [310,311].

Histone mRNA 3’ end

Coordination between histone mRNA abundance and the cell cycle relies on a unique *cis*-regulatory element localized in the histone mRNA 3’UTR. Unlike other cellular mRNAs, replication dependent histone mRNAs are not polyadenylated but are rather stabilized by a conserved 3’ stem-loop [312]. The stem is composed of six bases while the loop contains four bases. In addition, this stem-loop structure is followed by a conserved AC-rich sequence, with the consensus 5’-ACCCA-3’ sequence found in vertebrates (**Figure 28**). The stem-loop is co-transcriptionally bound by the stem-loop binding protein (SLBP), which binds to the 5’ side of the stem-loop as well as to the five nucleotides upstream of the stem. SLBP plays a central role in histone mRNAs fate, as it is involved in histone pre-mRNAs processing and in histone mRNAs nuclear export and translation [313–316]. SLBP is a cell cycle regulated protein that accumulates in cells just before entry into the S phase in order to support histone pre-mRNAs processing and that is degraded as soon as the S phase ends, therefore participating in the control of histone mRNAs abundance throughout the cell cycle [317,318].

Besides the stem-loop, the formation of the 3’ end of histone mRNA requires another *cis*-acting element, a 3’ purine-rich sequence called the histone downstream element (HDE), which associates with the U7 snRNA through base pairing. The HDE is essential to direct cleavage of histone pre-mRNAs (see below).

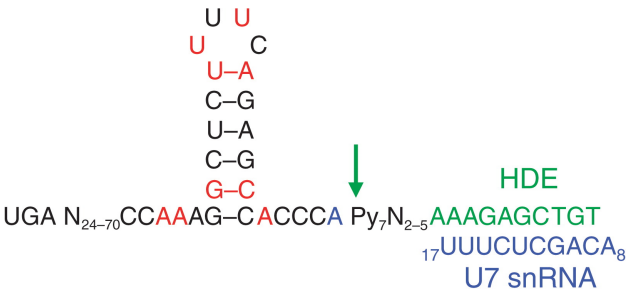

Figure 28: The 3' end of histone mRNAs.
Representation of the stem loop sequence found at the 3’ end of histone mRNAs. Invariant nucleotides are indicated in red. The second and sixth base pairs of the stem, as well as the first and third uridine of the loop are critical for SLBP binding. The consensus sequence of the histone downstream element (HDE) is shown in green and the sequence of the U7 snRNA in blue. The arrow indicates the cleavage site. **From [312].** Reviewed in [319].

Histone pre-mRNA processing

Formation of mature histone mRNA requires cleavage between the stem–loop and the HDE, which is located about 15 nucleotides after the cleavage site. Cleavage of histone pre-mRNA requires both SLBP and the U7 small nuclear ribonucleoprotein (U7 snRNP), a complex composed of a heteroheptameric ring of Sm proteins, including LSM10 and LSM11, and of the U7 snRNA [320]. SLBP stabilizes the interaction between the U7 snRNP and the histone pre-mRNA, with the U7 snRNP being recruited to the HDE through base pairing with the 5' end of the U7 snRNA. LSM11 interacts with FLASH, and together they recruit the histone cleavage complex (HCC) composed of symplekin, CstF64, CPSF100, and CPSF73, the endonuclease that cleaves the pre-mRNA, to the U7 snRNP [321–324]. Processing by the HCC leaves the histone pre-mRNA with a 5'-ACCCA-3' tail (**Figure 29A**).

ERI1, which binds the 3' side of the histone pre-mRNA stem-loop, finalizes histone pre-mRNA processing by trimming 2 nucleotides from the 3' end [291,293]. ERI1 is most likely recruited to the stem-loop through its association with the U7 snRNP prior to HDE cleavage. SLBP further supports ERI1 recruitment, as SLBP and ERI1 both cooperatively bind the stem-loop *in vitro* [325]. If ERI1 further degrades the histone mRNA 3' end, the three-nucleotides length of the ssRNA tail is restored by addition of untemplated uridine by TUT7, an uridyl terminal transferase, thereby creating ACC, ACU or AUU 3' ends [326,327] (**Figure 29B**).

Following this processing of histone pre-mRNA, SLBP and ERI1 remain bound to the transcript, and the complex is exported to the cytoplasm. In the cytoplasm, SLBP interacts with SLIP1, which in turn interacts with translation initiation factors, thereby supporting histone mRNA translation [328]

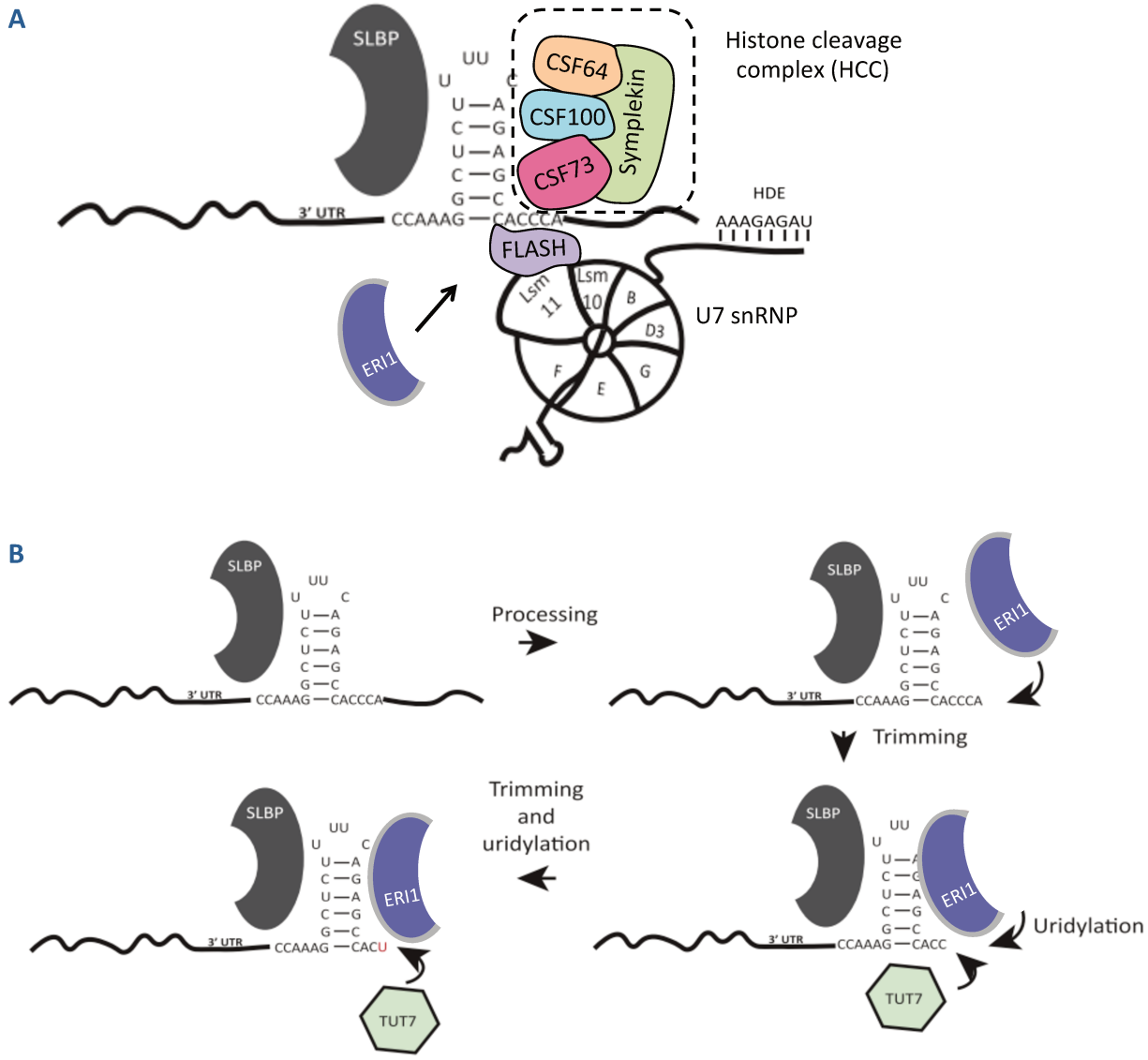

Figure 29: Histone mRNA 3' end formation.

A. The U7 snRNP composed of the heteroheptameric ring of Sm proteins along with the U7 snRNA, FLASH and the histone cleavage complex (HCC) are recruited to the HDE to promote histone pre-mRNA processing. ERI1 is recruited to the HDE most likely in an U7 snRNP dependent manner prior to HDE cleavage. **B.** After initial processing, the histone pre-mRNA is left ending with a 5'-ACCCA-3' sequence. ERI1 then trims two nucleotides from the 3' end tail. If trimming proceeds further, the length of the 3' end is restored by the TUT7 uridyl transferase. **Adapted from [311]**.

Histone mRNA decay

When DNA replication is inhibited or at the end of the S phase, histone mRNAs are rapidly degraded. ERI1 initiates degradation of histone mRNAs by removing five to seven nucleotides into the stem [329]. Once ERI1 has degraded into the stem, it can no longer bind to histone mRNA. This degradation intermediate is then heavily uridylated by TUT7 [326,330]. The UPF1 helicase, also involved in NMD, is required for histone mRNAs degradation and is recruited to histone mRNAs when DNA replication is inhibited. It interacts with SLBP and is most likely required to remove SLBP from the stem-loop [331].

Histone mRNAs uridylation leads to their degradation by the RNA exosome until a stalled ribosome is reached. The LSM1–7 ring (see sections III.1.a and III.1.e.), an activator of de-capping, which can bind oligo-uridylated sequences, is also required for the degradation of histone mRNAs. Since LSM4 was found to interact with both ERI1 and SLBP, this interaction could promote recruitment of the LSM1-7 complex to the 3’ end of the histone mRNA degradation intermediate, allowing subsequent degradation by the exosome [330,332].

Upon reaching a stalled ribosome, histone mRNAs degradation is stopped. Then, degradation intermediates are most likely, once again, uridylated before being further degraded [333]. Finally, complete degradation can proceed either from the 5’ end *via* de-capping or from the 3’ end, as both kinds of degradation intermediates have been observed [330] (**Figure 30**).

However, how initial degradation by ERI1 into the stem is activated and how TUT7 is recruited is not known. The helicase activity of UPF1, which interacts with ERI1 in an RNA dependent manner, is nonetheless required which could interfere with SLBP and the stem loop structure, allowing initial degradation by ERI1 [326,329].

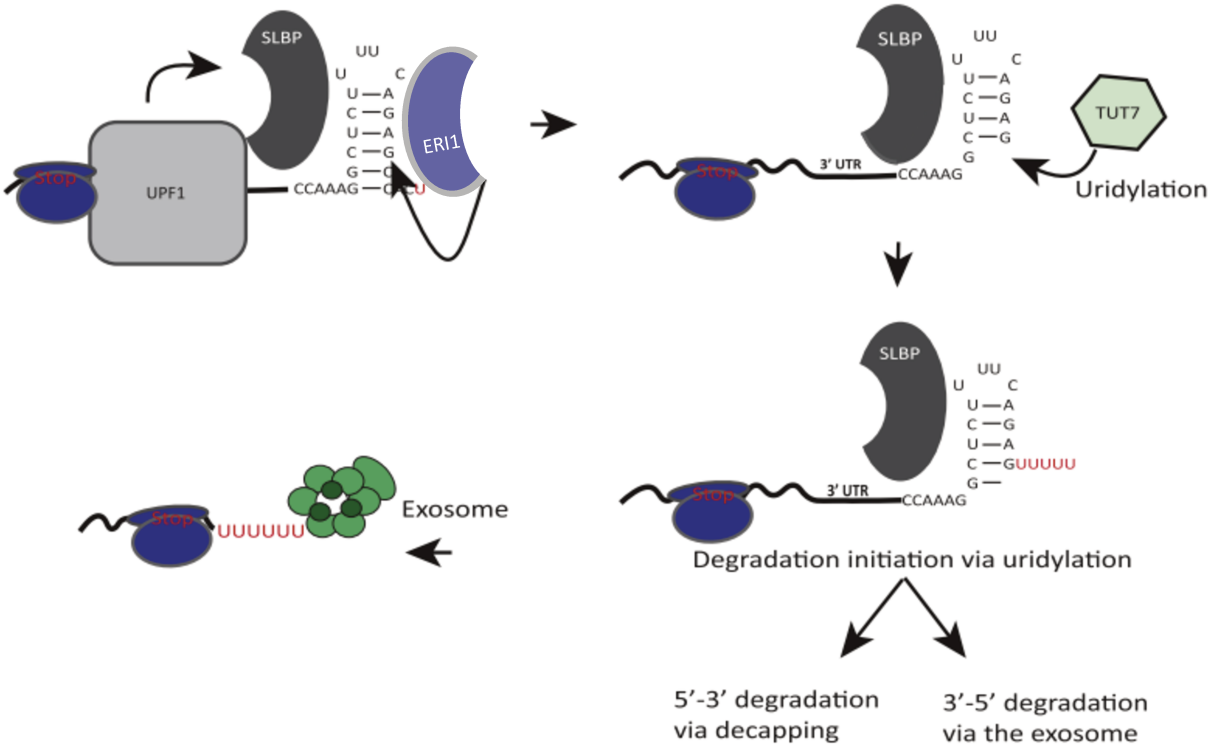

Figure 30: Histone mRNA decay.

When DNA replication is inhibited, UPF1 is recruited to the histone mRNA and is most likely required to remove SLBP from the stem-loop. ERI1 degrades into the stem until it cannot bind the stem anymore. The degradation intermediate is then uridylated by TUT7, which allows further degradation by the exosome until a stalled ribosome is reached. Upon stalling, the mRNA is re-uridylated and degradation can resume. Ribosomes are represented in blue, the exosome in green. **Adapted from [317].**

Aim of the work

RNA decay is a central cellular process as it regulates RNA stability and quality and thereby gene expression, which is essential to ensure proper cellular physiology and establishment of adapted responses to viral infection [211,212]. Moreover, global takeover of gene expression machineries and rewiring of the cellular environment is key to the success of viral infection. Growing evidence points towards the existence of a large interplay between eukaryotic RNA turnover machineries and viral proteins. Not only viruses have evolved mechanisms to evade those RNA degradation pathways, but they also manipulate them to promote viral replication [205–210].

Influenza A viruses (IAV) rely on cellular proteins to complete their multiplication cycle through complex and highly coordinated virus-host interactions, and many cellular proteins, including those belonging to the RNA decay machineries, have been reported to be involved in replication and transcription of the viral genome [152]. This led us to undertake a systematic screening of interactions between IAV proteins and a selected set of 75 cellular proteins carrying exoribonucleases activities or associated with RNA decay processes. A total of 18 proteins were identified as interactors of at least one viral protein tested. Moreover, analysis of the interaction network highlighted a specific and preferential targeting of RNA degradation pathways by IAV proteins.

A targeted siRNA screen on the recovered protein-protein interactions (PPIs) identified eight of the interacting factors as contributing to IAV multiplication. Among these, we focused on the 3'-5' exoribonuclease 1 (ERI1), identified in our screen as an interactor of several components of the vRNP: PB2, PB1 and NP.

We explored the interplay between ERI1 and viral proteins during the course of IAV infection through Protein Complementation Assay (PCA) and co-immunoprecipation experiments and further characterized the role of ERI1 during IAV infection through numerous RNAi experiments. Ultimately, our data point to a model where ERI1 associated to histone mRNA is co-opted by the transcribing viral polymerase, thereby promoting IAV multiplication.

Results

Deciphering the interplay between cellular and viral proteins is essential for a better understanding of the IAV life cycle. Several studies point to a targeting of cellular proteins involved in RNA decay machineries during IAV multiplication. However, the precise interplay between those cellular proteins and IAV proteins has never been specifically addressed. The protein-protein interaction screening of a dedicated set of cellular proteins involved in RNA decay and the subsequent RNAi screening performed on the recovered hits are presented in the first section, while the characterization of ERI1, a major hit of both the interactomics and RNAi screenings, is presented in the second section.

I. Screening of the ExoRDec library

1. GPCA screening of the ExoRDec library

a. *The Gaussia princeps Protein Complementation Assay (GPCA)*

The *Gaussia princeps* Protein Complementation Assay (GPCA) is based on the reconstitution of a full-length reporter protein, the *G. princeps* luciferase, upon interaction of the two protein partners tested [334] (**Figure 31**). In this assay, the two proteins tested are respectively fused to the N-terminal (Gluc1) or C-terminal (Gluc2) fragment of the *G. princeps* luciferase. If the two proteins tested interact, a full length *G. princeps* luciferase is reconstituted and a luminescent signal can be detected. Overall, this assay allows the detection of binary protein-protein interactions (PPIs) in mammalian cells and has previously successfully been used to accurately identify interactions with a low false positive rate [335,336].

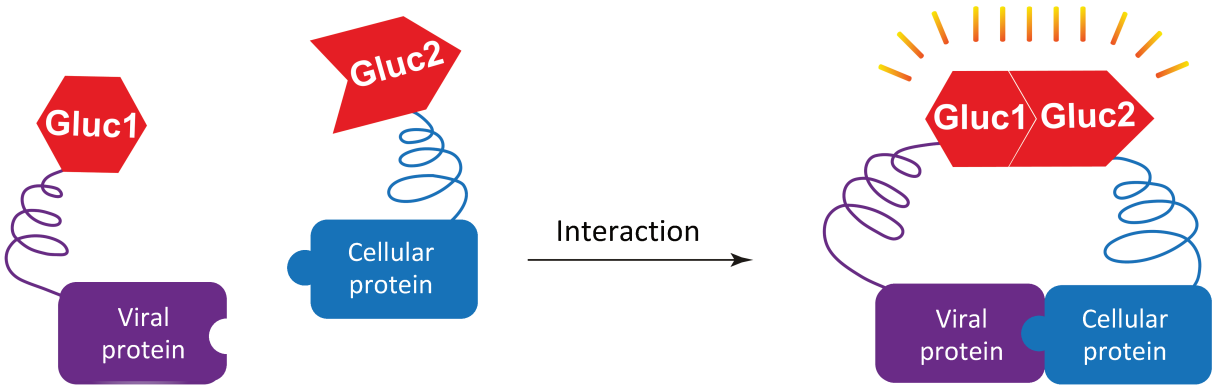

Figure 31: *Gaussia princeps* Protein Complementation Assay (GPCA) principle.
Viral proteins are fused to the Gluc1 fragment, while the cellular proteins of the exploratory set are fused to the Gluc2 fragment of the *G. princeps* luciferase. Gluc1 and Gluc2 fragments are complementary. If the two tested proteins interact, a full-length *G. princeps* luciferase is reconstituted and a luminescent signal can be detected upon addition of coelenterazine, the substrate of the *G. princeps* luciferase. **Adapted from Elise Biquand [337]**.

b. *Screening of the ExoRDec library*

A set of 75 cellular proteins was selected by choosing GO terms associated to exoribonuclease (Exo) activities or to RNA decay (RDec) processes to form the ExoRDec library (**Table 3 & Annex 1**). Each cellular protein was fused at its C-terminus to the C-terminal Gluc2 fragment of the *G. princeps* luciferase, and screened against a set of viral proteins fused at their N-terminus, or at its C-terminus for M1, to the N-terminal Gluc1 fragment. We chose viral proteins known to be part of the vRNPs and involved in viral transcription and/or replication (PB2, PB1, PA, NP), indirectly involved in transcription and/or replication (NS1, NEP) or interacting with the vRNPs (M1), from two strains of IAV: A/Paris/650/2004(H1N1) (sH1N1) and A/Bretagne/7608/2009(H1N1pdm09) (pH1N1).

GoTerm Name	GoTerm ID
3'-5' exonuclease activity	GO:0008408
5'-3' exonuclease activity	GO:0008409
exosome (RNase complex)	GO:0000178
negative regulation of single stranded viral RNA replication via double stranded DNA intermediate	GO:0045869
CCR4-NOT complex	GO:0030014
exonucleolytic catabolism of deadenylated mRNA	GO:0043928
hydrolase activity	GO:0016787
deaminase activity	GO:0019239

Table 3: GO Terms of the ExoRDec library.

IAV strains sH1N1 and pH1N1 selected for the screening of the ExoRDec library are drastically different in terms of origin and of time of circulation in the human population. Those two strains therefore provide an interesting basis for a comparative interactomic study to assess the conservation of virus-host interactions among IAV strains.

The sH1N1 virus circulated in the human population since its reintroduction in 1977 and was later replaced in 2009 by the pH1N1 virus. The sH1N1 virus is derived from the 1918 H1N1 pandemic virus, while the pH1N1 arose after multiple reassortment events between IAV strains from swine, avian and human origin (see section I.3.c. of the introduction for detailed origin and **Figure 5**). Interestingly, between the sH1N1 and pH1N1 strains, the segments encoding the proteins we chose to focus on for this study have a different origin.

For the GPCA screen, a positive threshold (PT) was calculated as previously described in [335] for each viral protein. Moreover, the validity of our assay was monitored using as controls two proteins belonging to the positive reference set (PRS) (proteins from the literature known to be interacting with the viral protein tested) as well as four proteins belonging to the random reference set (RRS) (proteins that are *a priori* not interacting with the viral protein tested) (**Figure 32A, B**). The PT was calculated for each viral protein, based on the distribution of the luminescence values generated by each protein pair tested. This PT corresponded to the third quartile + 1.5 the interquartile space (PT = Q3 + 1,5 IQR) [335]. For each viral protein tested, ExoRDec factors generating values that were higher than the calculated threshold were selected as putative interactors.

Luminescence values measured for the proteins of the RRS set were systematically below the PT, therefore validating our assay and the selection of the putative interactors. Furthermore, some PRS consistently generated luminescence values below the PT, underlying the high stringency of our assay.

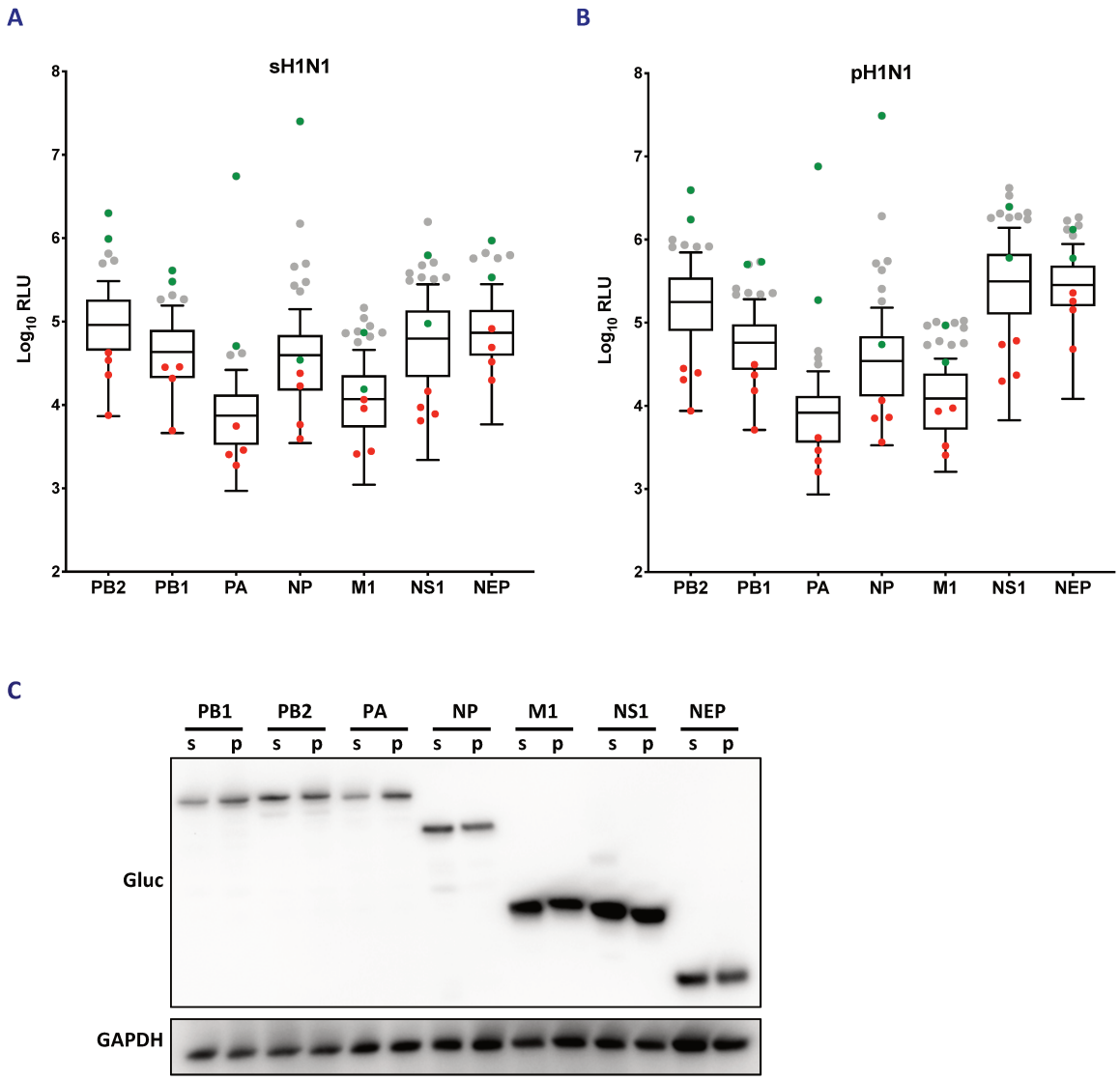

Figure 32: Systematic screening of the ExoRDec library.

A., B. For each viral protein tested (**A.** sH1N1; **B.** pH1N1), distributions of luminescence values (RLU – relative luminescence unit) are represented. The RRS (random reference set) and PRS (positive reference) values (red and green dots, respectively) were plotted. Outlier RLU (grey dots) were selected as putative interactors of the viral protein tested. The distribution of the relative luminescence values is represented by whisker plot boxes. The whisker length corresponds to 1.5 times the interquartile range (IQR), which equals the difference between the upper and lower quartiles (IQR = Q3 - Q1). The upper whisker, defined by the third quartile (Q3) plus 1.5 times the IQR, was defined as the Positive Threshold (PT) as follows: PT = Q3 + 1,5 (IQR) as described in [335]. A PT was calculated for each tested viral protein. **C.** HEK 293T cells were transfected with Gluc1-PB2, -PB1, -PA, -NP, -NS1, -NEP or M1-Gluc1 from sH1N1 (s) or pH1N1 (p) in the same conditions used for the GPCA screening. At 24hpt total cell extracts were prepared and Gluc1 protein expression levels were analyzed by immunoblot.

For each viral protein tested, quantities of transfected plasmids were optimized to achieve similar protein expression levels between the two tested virus strains (**Figure 32C**). On average, for a given viral protein, luminescence values were comparable for the two tested virus strains (**Figure 32A, B**). However, PA and M1 proteins were systematically associated to lower luminescence values compared to the other five viral proteins tested, even though they were expressed at levels relatively similar (PA) or higher than most of the other tested viral proteins (M1) (**Figure 32C**). Yet, this disparity did not appear to alter the sensitivity of our GPCA screen as similar numbers of putative interactors were selected for all viral proteins tested (**Figure 32A, B**). This preliminary screening allowed us to select, for each viral protein tested, between two or three (PA) and eight or nine (M1, NS1) cellular proteins as putative interacting partners, which only represents a small fraction of the initial library.

c. *Post-screening retesting of the recovered PPIs*

Using the NLR (Normalized Luminescence Ratio) method of the GPCA assay as described in [334], the putative interactions found in the preliminary screen were retested (**Figure 33**). By taking into account the background noise of interaction of each tested partner, this method accurately discriminates between true interacting partners and false positives, thereby increasing the robustness of our assay.

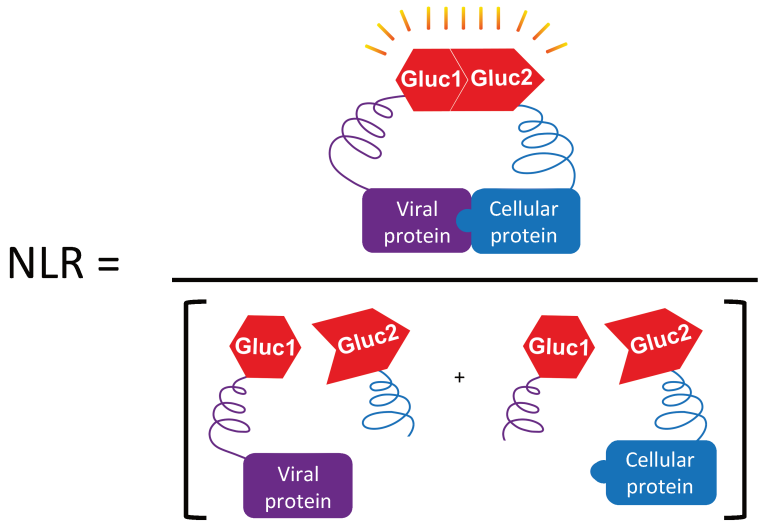

Figure 33: Calculation of the Normalized Luminescence Ratio (NLR).
For each assessed PPI, NLR is calculated as the luminescence value measured for the two tested partners divided by the sum of the luminescence values obtained for each partner tested against the other empty half of the *G. princeps* luciferase. **Adapted from Elise Biquand [337].**

To allow proper comparison between sH1N1 and pH1N1 interaction profiles, for a given viral protein, all putative interactors were retested applying the NLR method in three independent biological replicates, independently of their initial pattern of selection (*i.e.* if a protein was originally selected only as a putative interactor of one given protein for one strain, it was retested in the NLR assay with said protein of both strains). For each viral protein, the NLRs obtained with the eleven RRS were used to calculate a 99.73% confidence interval as described in [335]. The upper limit of this confidence interval was set as positive threshold to select positive interactions. Furthermore, a given interaction was considered positive when its NLR value was above the calculated threshold in at least two out of the three independent experiments. Accordingly, 19 ExoRDec proteins were validated as interactors of at least one viral protein tested (**Annex 2**).

It should be noted that most of the initially identified putative interactions were validated after NLR retesting, highlighting the stringency and robustness of our initial screening method. However, this also implies that our initial selection may have been too stringent and that some relevant interactions may have been overlooked.

Most of the interactions that were not validated after NLR retesting were putative interactions with M1. As already mentioned above, M1 was associated to low luminescence values. Furthermore, most of the NLR values obtained for putative M1 interactions were close to the calculated threshold. Indeed, among the eight putative interactions tested, only two (sH1N1) and three (pH1N1) displayed NLR values that were at least twice the value of the calculated positive threshold, while for the other viral proteins assessed (except for PA), NLR values of selected interactions are in most cases far above threshold (**Annexe 2**). Therefore, GPCA - at least in the experimental settings used here -, may not be an appropriate method to look for M1 interactions. Overall, due to their relatively high NLR value compared to the calculated positive threshold, only ADAR and ERI1 can be considered with high confidence as interactors of M1. Moreover, for the other tested viral proteins, only a few factors were not validated three times out the three performed experiments. This suggests that wrong selection of putative interactors due to a high background noise of interaction only occurs in a minority of cases in the initial screening, thereby further validating the use of GPCA as a reliable screening method to assess protein-protein interactions.

2. Network and enrichment analysis of the recovered PPIs

A differential enrichment analysis was used to identify cellular processes specifically targeted by the viral proteins. To do so, we looked at the interaction map of ExoRDec factors with the human proteome using the APID2net database [338] to identify their first neighbors and next considered two distinct clusters: cluster 1 contains ExoRDec factors that are not interacting with viral proteins and their first neighbors in the human proteome; cluster 2 contains factors identified as interactors and their first neighbors in the human proteome.

KEGG pathways analysis revealed that cluster 1 (*i.e.* the cluster not targeted by viral proteins) was specifically enriched in 18 distinct KEGG pathways including some linked to RNA processing or RNA decay (*i.e.*, “Spliceosome”, “Ribosome”, “RNA transport”, “mRNA surveillance pathway”, “Ribosomal biogenesis in eukaryotes”, “Basal transcription factors”, “Pyrimidine metabolism”, “RNA polymerase”, or “Mismatch repair”). On the other hand, KEGG pathways analysis of cluster 2 (*i.e.* the cluster targeted by viral proteins) strikingly indicated a single and specific enrichment in the KEGG RNA degradation pathway, with more than 50% of the proteins of this cluster found to be associated with this term (**Figure 34**).

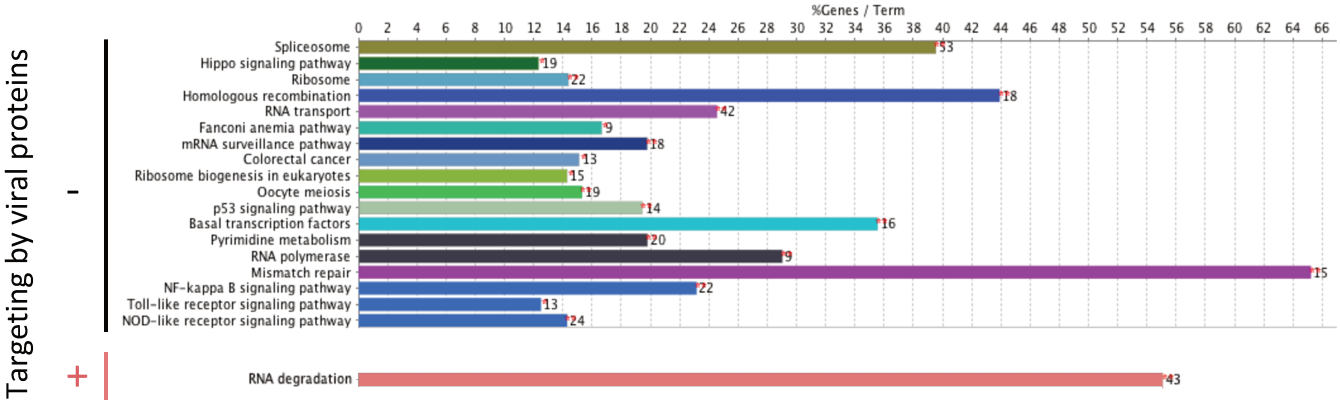

Figure 34: KEGG pathways enrichment analysis.
The ExoRDec library and its associated proteome was divided into two clusters, 1 and 2, respectively not targeted and targeted by viral proteins (% of genes associated to each term are shown). Numbers associated to each bar indicate the number of genes within a given cluster associated to a specific term. Enrichment analysis was carried out using the ClueGO plug-in of Cytoscape [339].

Although some terms enriched in cluster 1 can be linked to RNA degradation (such as “mRNA surveillance pathway” or “mismatch repair”), only cluster 2 is specifically enriched for the whole RNA degradation pathway. This further supports the existence of a large and intricate interplay between IAV viral proteins and RNA decay machineries.

The interaction profiles between pH1N1 and sH1N1 were almost identical, and several ExoRDec factors were found to interact with more than one viral protein (**Figure 35**). Only the interactions of APEX1 with M1 and NEP as well as the interaction between ADAR and M1 were found to be specific to pH1N1. However, as already discussed above, those interactions validated with M1 were associated to low NLR values, hardly lying above the calculated positive threshold (**Annex 2**). Likewise, the interaction between APEX1 and NEP was associated to a low NLR value. Therefore, such low NLR values question the overall validity of those identified interactions. Altogether the interaction profiles of sH1N1 and pH1N1 are certainly identical, suggesting that the identified interactions are most likely essential to the IAV life cycle.

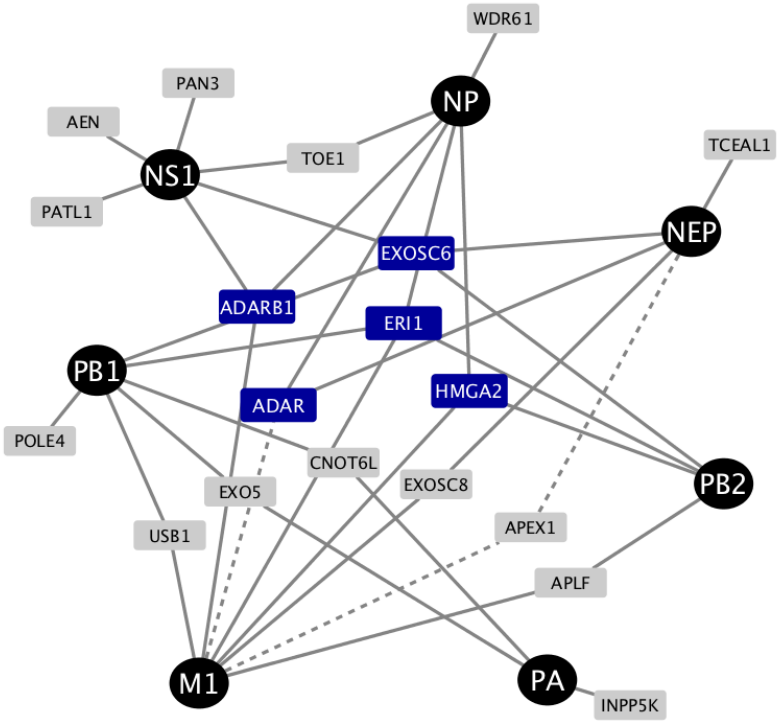

Figure 35: Interaction network of recovered PPIs after NLR retesting.
Viral proteins are indicated in black circles and proteins of the exploratory set in grey boxes. Redundant targeting (*i.e.* cellular protein targeted by three or more viral proteins) is depicted with blue boxes. Edges (*i.e.* interactions) that were only found with viral proteins of pH1N1 are indicated with dashed lines.

The most connected cellular proteins, ADAR, ADARB1, HMGA2, ERI1 and EXOSC6 were found to interact with three (ADAR, HMGA2) or four (ADARB1, ERI1, EXOSC6) viral proteins. This redundant targeting may reflect an important need to hijack these factors during infection.

3. RNAi screening of the recovered PPIs identifies ERI1 as required for IAV cycle

a. *RNAi screening of the recovered PPIs*

To assess the biological and functional relevance of the identified interactions we next performed a targeted RNAi screen and measured infectious viral particle production upon silencing of the different identified interactors. Small interfering RNAs (siRNAs) targeting ExoRDec proteins were transfected in A549 cells. Since the interaction profiles were found to be similar between sH1N1 and pH1N1, this RNAi screen was only performed with sH1N1.

A549 cells treated with siRNAs were infected at a low multiplicity of infection (moi) with sH1N1 and production of infectious viral particles was measured by plaque assay at 24 hpi. Upon siRNA knock-down of the ExoRDec factors, cell viability remained above 80% compared to the non-target treated cells, except in cells silenced for INPP5K (**Annex 3**). Taking into account the efficiency of siRNA knock-down to remove potential off-target effects (**Annex 3**), out of the 20 identified interactors, knock-down of eight ExoRDec proteins was associated to a statistically significant impairment of IAV replication (**Figure 36**). Three factors from the literature, COPS5, FANCG and NUP62, known to be required for IAV multiplication were used as internal controls to validate our assay [148,336].

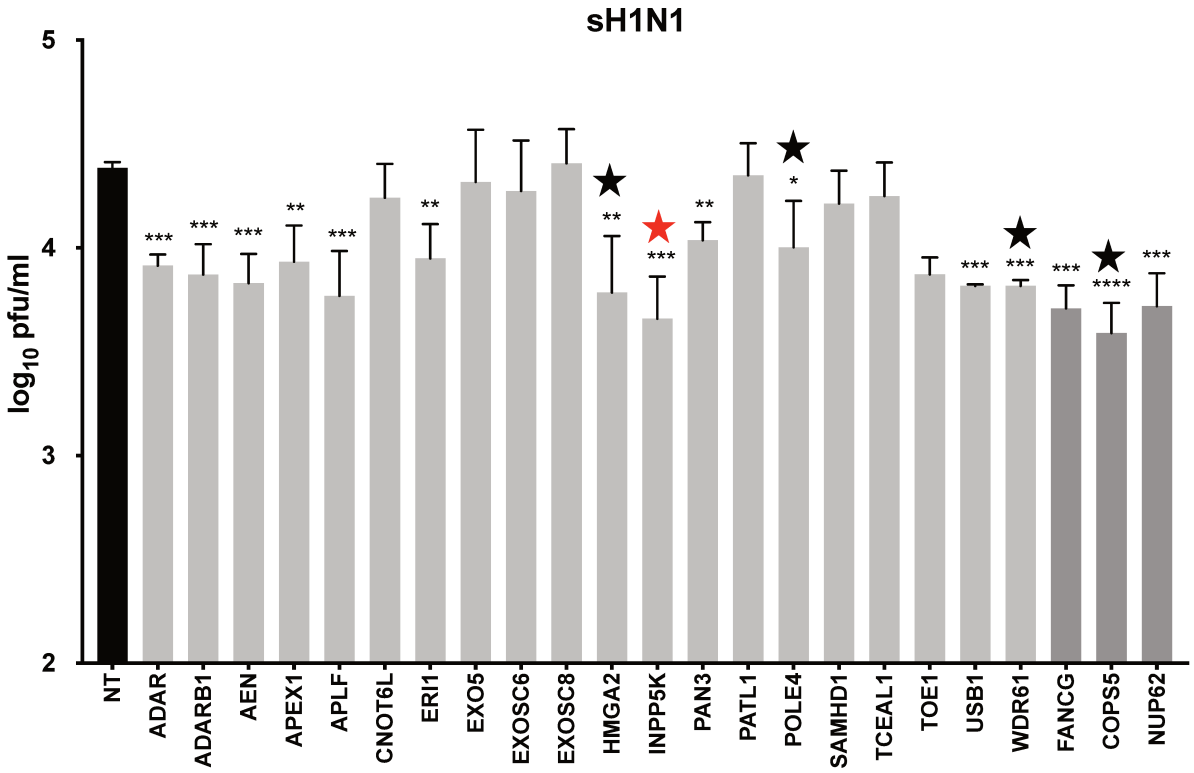

Figure 36: Functional evaluation of the involvement of the ExoRDec PPIs in the multiplication of sH1N1 virus.

A549 cells were transfected with non-target siRNAs (NT) (black bar) or with pools of siRNAs targeting the ExoRDec factors (grey bars) or control factors from the literature (dark grey bars). At 48 hpt cells were infected with sH1N1 at an moi of 10^{-3} pfu/cell for 24 h. Viral titers were determined by plaque-forming assay on MDCK-Siat cells. Effects potentially associated to siRNA toxicity are indicated with a red star, while effects potentially linked to an off-target effect of siRNA (*i.e.* poor knock-down efficiency, see **Annex 3**) are indicated with a black star. The results are expressed as the mean ± SEM of triplicates and the significance was tested with an unpaired, 2-tailed Student t test using GraphPad Prism software (*p < 0.05, ** p< 0.001, *** p< 0.0001, **** p< 0.0001).

Silencing of the ExoRDec factors was associated to a moderate decrease in infectious viral particle production, comparable to what was found with the positive controls from the literature. On average, silencing of the ExoRDec factors by siRNA lead to a one log reduction of the measured viral titer compared to control cells. Remarkably, none of the validated interactors were identified as putative "anti-viral" factors as, in all cases, silencing of the ExoRDec factors was associated to a decrease in infectious viral particle production (*i.e.* therefore being "pro-viral" factors).

b. *ERI1 is required for IAV replication*

Among the factors found to be required for IAV replication in our RNAi screen, we identified the cellular exonuclease ERI1 (**Figure 36**). We confirmed the involvement of ERI1 in the IAV life cycle using four different individual siRNAs to rule-out any potential off-target effect. Upon ERI1 silencing, with three individual siRNAs among the four tested, we observed a decrease in sH1N1 infectious viral particle production (**Figure 37**). The effect observed upon silencing of ERI1 using individual siRNAs is in line with what we observed in the initial RNAi screen using a pool of siRNAs, with an average three fold decrease in infectious viral particles production compared to cells treated with non-target siRNA.

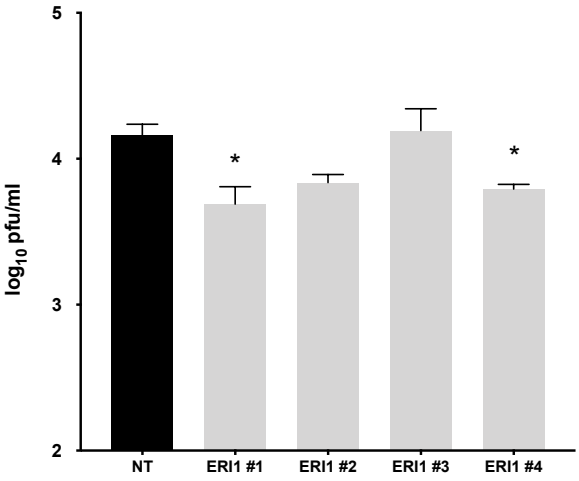

Figure 37: Effect of ERI1 silencing on sH1N1 replication using individual siRNAs.
A549 cells were transfected with non-target (NT) (black bar) or individual siRNAs targeting ERI1 (grey bars). At 48 hpt cells were infected with sH1N1 at an moi of 10^{-3} pfu/cell. Supernatants were collected 24hpi and viral titers were determined by plaque-forming assay. The results are expressed as the mean ± SEM of triplicates and the significance was tested with an unpaired, 2-tailed Student t test using GraphPad Prism software (*$p < 0.05$).

Individual siRNAs targeting ERI1 used here were associated to a moderate knock-down efficiency. For the experiments presented afterwards, siRNAs with the same sequence as those used in **Figure 37** were ordered from a different company. Those siRNAs were associated to a much more satisfying knock-down efficiency, while cell viability remained unaffected. Consequently, the effect of ERI1 depletion on infectious virus particles production was also more marked (more than one log decrease) (see below and especially **Figure 40**).

II. Characterization of the role of ERI1 in the IAV life cycle

1. ERI1, an interactor of the vRNPs required for viral multiplication

a. *ERI1 interacts with viral proteins PB2, PB1, NP and M1*

ERI1 was identified in our GPCA screening and then confirmed by NLR retesting as an interactor of viral proteins PB2, PB1, NP and M1. For PB2 and NP proteins the NLR values measured were far above the positive threshold suggesting a strong association. On the other hand, the lower NLR generated with PB1 and especially M1, suggests a weaker association of ERI1 with those factors (**Figure 38A, B**).

Interactions of those viral proteins with ERI1 were subsequently orthogonally validated using co-immunoprecipitation experiments. HEK 293T cells were transfected with Strep-tagged ERI1 or Strep-tagged mCherry as a negative control, along with Gluc1-PB2, Gluc1-PB1, Gluc1-PA, Gluc1-NP and M1-Gluc1. PA, which was not found to interact with ERI1 in our GPCA screen was used as an internal negative control. The PB2, PB1, NP and M1 proteins specifically co-purified with Strep-ERI1, while only marginal or significantly lower amounts of the viral proteins were retrieved upon Strep-mCherry purification (**Figure 38C**). In contrast, a similar fraction of PA was retrieved upon Strep-ERI1 or -mCherry purification, indicating non-specific binding, and therefore corroborating the lack of interaction of PA with ERI1, as already observed in GPCA (**Figure 38C**). Furthermore, lower amounts of M1 were retained compared to PB2, PB1 and NP upon Strep-ERI1 purification, further supporting the weaker interaction with ERI1, as already seen in GPCA (**Figure 38A, B**).

Altogether, our results point to the components of vRNPs PB2, PB1 and NP as the primary targets for ERI1.

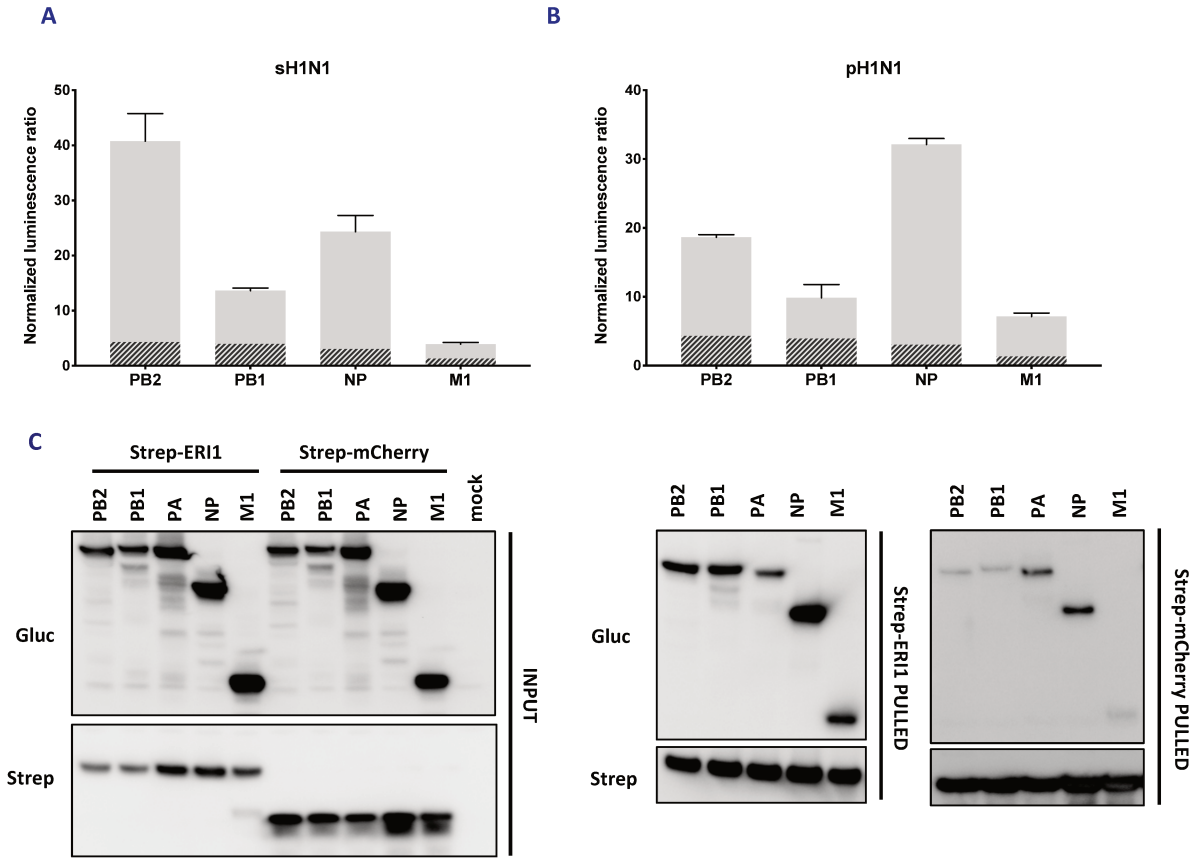

Figure 38: ERI1 primarily interacts with vRNP components PB2, PB1 and NP.

A., B. Interaction of ERI1 with viral proteins from sH1N1 (**A**) and pH1N1 (**B**) was tested by applying the NLR (Normalized Luminescence Ratio) method of the GPCA that takes into account the background noise of interaction of the Gluc1 or Gluc2 fusion partners. Positive threshold value, represented by hatched bars, was calculated as in [335]. The results are expressed as the mean ± SEM of triplicates**. C.** HEK 293T cells were co-transfected with Strep-ERI1 or Strep-mCherry as a control and Gluc1-PB2, -PB1, -PA or -NP or M1 -Gluc1. At 24hpt, Strep-tagged proteins were purified with sepharose streptactin beads. Inputs and Strep-tagged eluates were analyzed by immunoblot to detect Strep and Gluc1 tagged proteins. Results representative of two independent experiments are shown.

PB2 appeared in our GPCA screen to be a major interactor of ERI1, as it was associated to a high NLR value (*i.e.* sH1N1: NLR ≈ 40, PT ≈ 4; pH1N1; NLR ≈ 19, PT ≈ 4). According to the structure of the IAV polymerase, PB2 provides a large and flexible surface accessible for interactions with host proteins (see **Figure 10** and section II.1.d. of the introduction). We thus next wanted to characterize further the interface of interaction between ERI1 and PB2 by GPCA. To this end we used two PB2 constructs expressing either PB2 Nter or PB2 Cter fused to Gluc2 (**Figure 39A**). ERI1 was found to specifically interact with PB2 Cter, as NLR

values obtained with the Cter part were similar to those obtained with full-length PB2, while no interaction was detected with the PB2 Nter (**Figure 39B, C**). Interestingly, PB2 Cter is subject to multiple conformational rearrangements during the transcription and replication steps and notably comprises the cap-binding domain, which is essential for viral transcription.

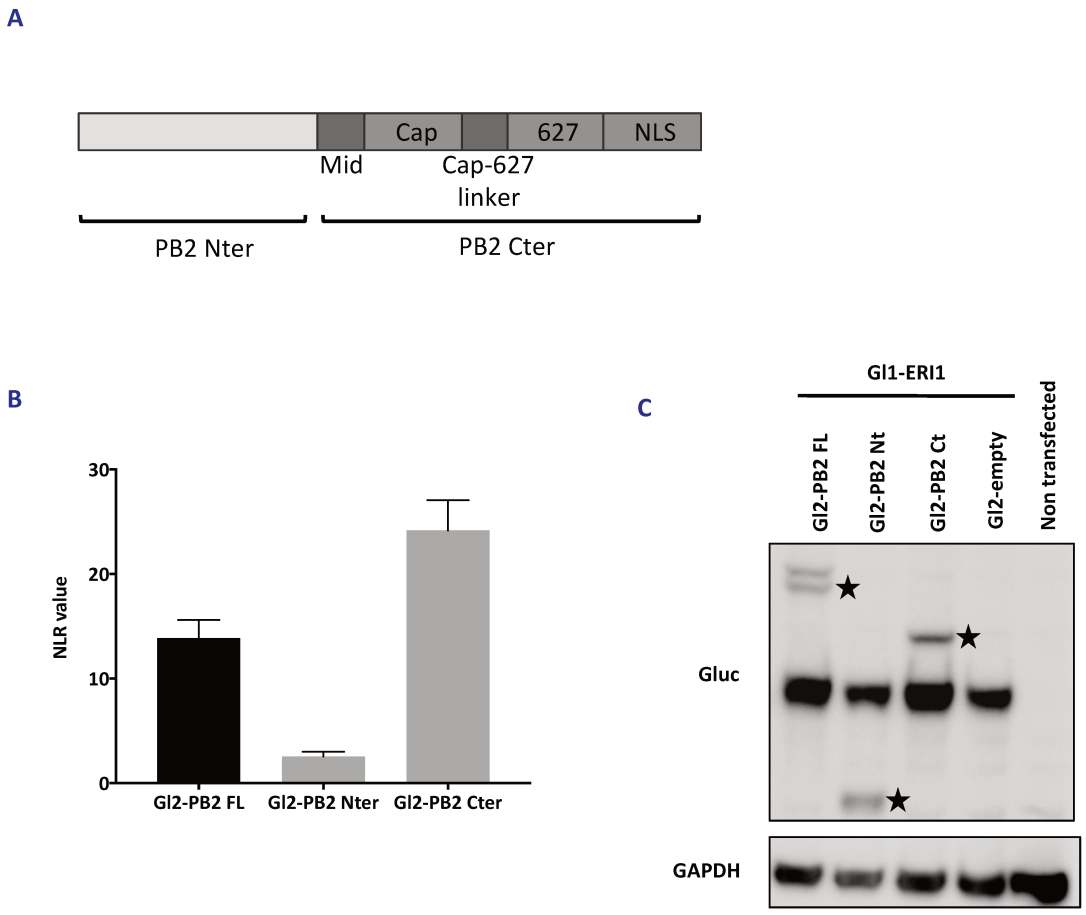

Figure 39: ERI1 interacts with PB2 through its C-terminal part.

A. Schematic organization of PB2 depicting its Nter and Cter parts. PB2 Cter notably contains the mid-Cter, cap-binding, 627 and NLS domains. **B., C.** HEK 293T cells were transfected with Gluc1-ERI1 and Gluc2-PB2-WSN constructs: full length (PB2) (FL), N-terminal (Nter), C-terminal (Cter) or Gluc2-empty. For each condition NLR values were calculated as described before (**B**) and expression levels of Gluc2 and Gluc1 constructs were analyzed by immunoblot to detect Gluc1-ERI1 and Gluc2-PB2 FL, Nt and Ct (**C.**). On the blot, the different PB2 constructs are indicated with a star.

b. *Infectious viral particle production is impaired in ERI1 silenced cells*

ERI1 was identified in our RNAi screen as required for the replication of sH1N1 (**Figure 36**). The specificity of the observed effect was subsequently confirmed using individual siRNAs targeting ERI1 (**Figure 37**). Involvement of ERI1 in IAV multiplication was further confirmed using different IAV strains, the lab adapted strain H1N1 WSN, the seasonal H1N1 (sH1N1), as well as the H1N1pdm09 (pH1N1), using the two best individual siRNAs targeting ERI1 (**Figure 40 A-C**).

For all tested IAV strains, viral titers measured in supernatants collected from ERI1 silenced cells were lower compared to those measured in the supernatants of cells treated with non-target siRNAs. The siRNA ERI1 #2 was associated to a lower knock-down efficiency compared to siRNA ERI1 #1 (**Figure 40E**) and its effect on viral replication was accordingly lower compared to siRNA ERI1 #1 (**Figure 40A-C**), whilst cell viability associated to both siRNAs was comparable (**Figure 40F**). Furthermore, the effect of ERI1 depletion was more marked on the replication of the sH1N1 and pH1N1 strains compared to H1N1 WSN. At 24hpi, sH1N1 and pH1N1 viral titers measured in supernatants of cells treated with siRNA ERI1 #1 were more than one log lower compared to titers measured in the supernatants of non-target siRNAs treated cells. However, less than a log difference was measured for the cells infected with H1N1 WSN. Remarkably, titers measured in non-target siRNAs treated cells are around 0.5 log higher in cells infected with H1N1 WSN compared to those infected with sH1N1 or pH1N1. Therefore, faster replication kinetics of the H1N1 WSN strain, allowing it to overcome more quickly the effect of ERI1 depletion, may explain the differences observed here.

In addition, pH1N1 multiplication was monitored at 18, 24, 36, 48 and 72hpi in ERI1 silenced cells. The effect of ERI1 depletion on virus production is lasting over time as, for all measured time points, except for the 72hpi time point, significantly less infectious viral particles were produced in ERI1 knock-down cells compared to control cells (**Figure 40D**).

As ERI1 siRNA #1 was associated with the better knock-down efficiency and the stronger effect on IAV replication as compared to ERI1 siRNA #2, experiments presented afterwards were carried out solely using siRNA #1.

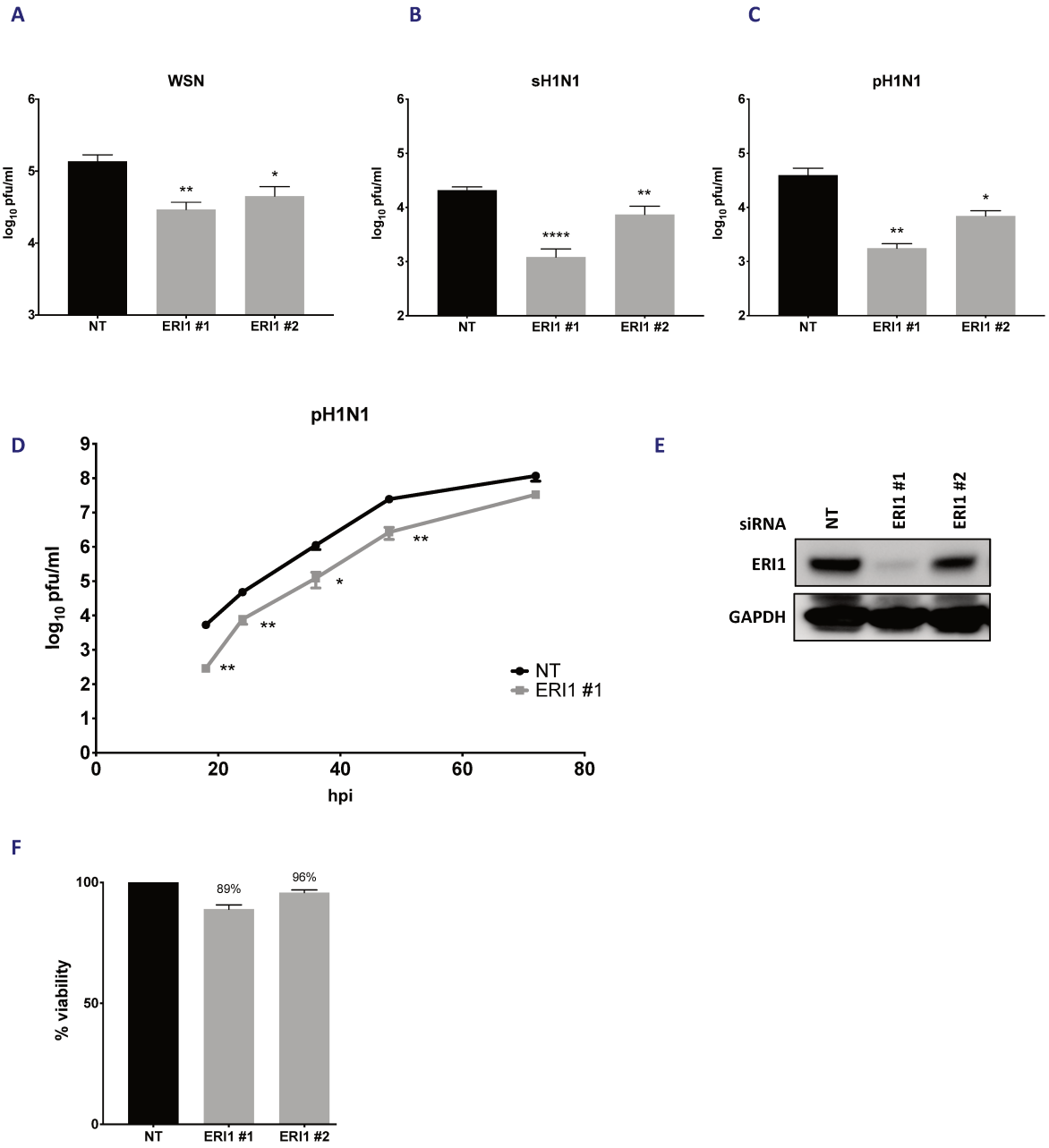

Figure 40: Viral replication is impaired in ERI1 silenced cells.

A-D. A549 cells were treated with non-target siRNAs (NT, dark grey) or single siRNAs targeting ERI1 (ERI1 #1 and ERI1 #2) (light grey) and infected with the following viruses at the indicated moi: A/WSN/33(H1N1) (WSN, 10^{-4} pfu/cell); A/Paris/650/2004(H1N1) (sH1N1, 10^{-3} pfu/cell); A/Centre/7608/2009(H1N1) (pH1N1, 10^{-3} pfu/cell). At 24hpi (**A-C**), or at several time points post-infection (18 hpi, 24 hpi, 36 hpi, 48 hpi, 72 hpi) (**D**) the viral titers were determined by plaque assay on MDCK-Siat cells. The results are expressed as the mean ± SEM of triplicates and the significance was tested with an unpaired, 2-tailed Student t test using GraphPad Prism software (*$p < 0.05$, ** $p < 0.001$). **E.** At 48 hpt, the levels of ERI1 protein after siRNA treatment were evaluated by immunoblot in cells transfected either with control non-target siRNAs or with individual siRNAs targeting ERI1. **F.** At 48 hpt, toxicity of individual siRNAs targeting ERI1 was measured using the CellTiter-Glo Luminescent Viability Assay kit (Promega) according to the manufacturer's instructions.

c. *Viral protein accumulation is impaired in ERI1 silenced cells*

To characterize further the role of ERI1 on IAV replication we monitored the accumulation of viral proteins in ERI1 depleted cells during a single cycle infection. In ERI1 silenced cells, the accumulation of early viral proteins PB2, NP and NS1 was greatly reduced at 3 hpi. Such decrease was less obvious by 6 hpi, at which point accumulation of late viral proteins M1 and NA was slightly reduced (**Figure 41**). The effects of ERI1 depletion are thus primarily detected during the initial steps of viral protein accumulation, suggesting an involvement of ERI1 in early stages of the viral cycle, although its involvement later in the viral life cycle is also possible.

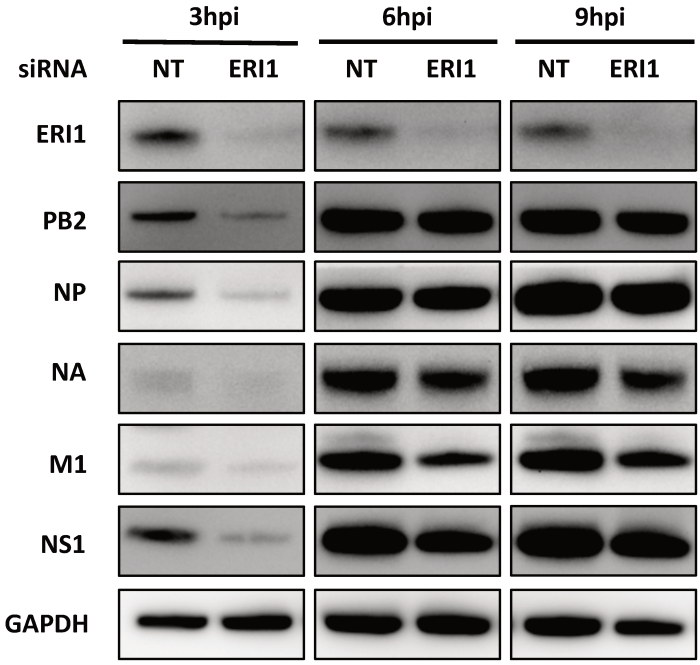

Figure 41: Viral protein accumulation is impaired in ERI1 silenced cells.
A549 cells were treated with non-target (NT) or ERI1 siRNAs and infected 48hpt with H1N1 WSN at an moi of 3 pfu/cell. Total extracts were prepared at the indicated times post-infection and analyzed by immunoblot using antibodies directed against the indicated proteins. Results representative of three independent experiments are shown.

d. *Viral transcription is impaired in ERI1 silenced cells*

As ERI1 appears to be required for the early stages of the viral cycle, we next examined whether viral transcription was affected, by measuring the mRNA to vRNA ratio in A549 cells. This ratio allows a normalized measurement of mRNAs produced from the incoming vRNAs at early time points of the viral cycle.

Starting from 2 hpi, mRNA production was reduced in ERI1 silenced cells compared to control cells. The greatest impairment of viral transcription was observed at 4 hpi (4 fold and 1.6 fold decrease for NP and NA mRNA/vRNA ratios, respectively), which also corresponds to

the peak in viral transcription [340]. At 6 hpi, mRNA to vRNA ratios were slightly higher in ERI1 silenced cells compared to control cells (**Figure 42A, B**). Indeed, delayed accumulation of mRNAs results in delayed accumulation of vRNAs in ERI1 silenced compared to NT treated cells, thereby explaining the higher ratio measured at 6 hpi in ERI1 silenced cells.

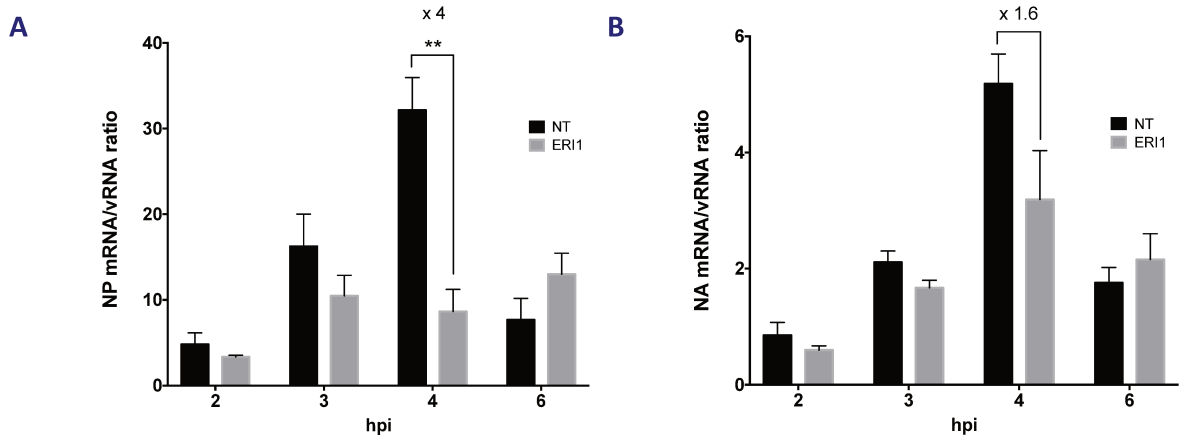

Figure 42: Viral transcription is impaired in ERI1 silenced cells.

A., B. A549 cells treated with non-target (NT (black bars)) or ERI1 (grey bars) siRNAs were infected with H1N1 WSN at an moi of 3 pfu/cell. Total RNAs were extracted at the indicated times post infection and the levels of NP (**A**) or NA (**B**) mRNAs and vRNAs were determined by strand specific RT-qPCR. The results are expressed as the mean ratios of mRNA/vRNA ± SEM determined in three independent experiments. The significance was tested with an unpaired t test using GraphPad Prism Software (*$p < 0.05$; **$p < 0.01$; ***$p < 0.001$).

We further characterized the role of ERI1 in viral transcription by looking at the effect of ERI1 overexpression on viral transcription in HEK 293T cells. For those overexpression experiments we had to use HEK 293T cells as, in our hands, transfected A549 cells are poorly infected. It is worth mentioning that from our experience, the kinetics of viral replication is faster in HEK 293T compared to A549 cells. As impairment in viral transcription was most pronounced at 4 hpi in A549 cells (**Figure 42**), we assessed viral transcription at an earlier time point, *i.e.* 3.5 hpi, in HEK 293T cells. Overexpression of ERI1 led to a two-fold increase in viral transcription compared to cells transfected with an empty control, further supporting a role of ERI1 in viral transcription as already observed in A549 cells upon ERI1 silencing (**Figure 43**).

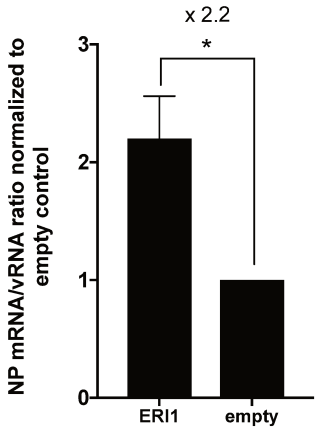

Figure 43: Overexpression of ERI1 is associated to an increased viral transcription.

HEK 293T cells were transfected with Strep-ERI1 or Strep-empty as a control and infected with H1N1 WSN at an moi of 3 pfu/cell. At 3.5 hpi total RNA was extracted and the levels of NP mRNAs and vRNAs were determined by strand specific RT-qPCR. The results are expressed as the mean ratios of mRNA/vRNA ± SEM normalized to empty control, determined in three independent experiments. The significance was tested with an unpaired t test using GraphPad Prism Software (*p < 0.05).

To better address viral cycle steps affected by ERI1 silencing, we then looked at primary transcription, *i.e.* transcription occurring from the incoming vRNPs thanks to the resident RdRp. As shown in **Figure 44B,** no viral protein was detectable at 6 hpi upon cycloheximide (CHX) treatment demonstrating that CHX effectively blocked *de novo* translation. Use of CHX allows addressing the transcription and replication steps separately. Indeed, given that IAV RNA replication (but not transcription) requires newly synthesized viral proteins, CHX, by blocking *de novo* translation, inhibits synthesis of cRNA and vRNA.

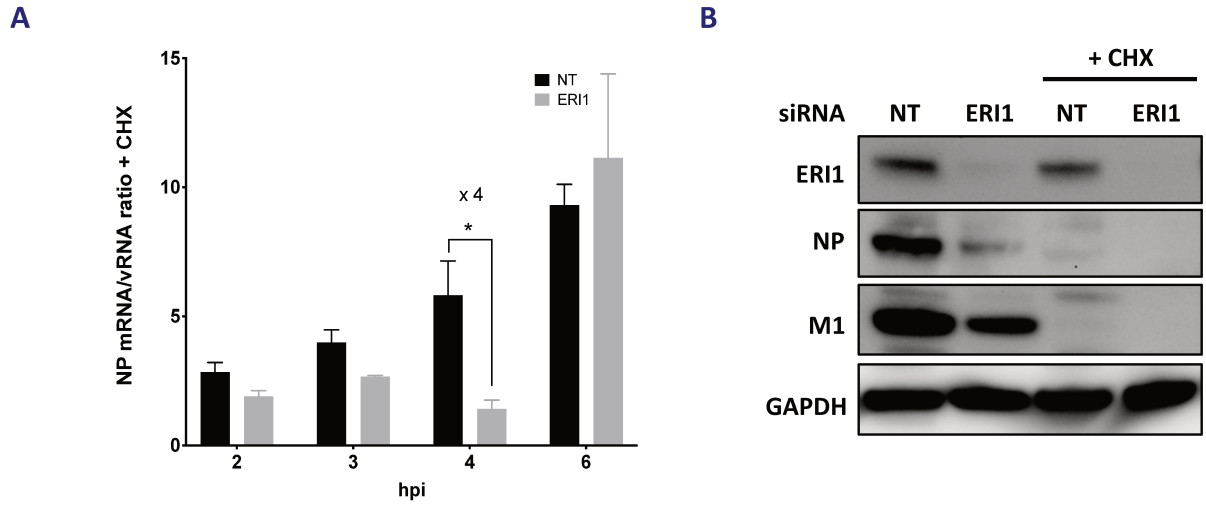

Figure 44: Primary viral transcription is impaired in ERI1 silenced cells.

A-B. A549 cells treated with non-target (NT (black bars)) or ERI1 (grey bars) siRNAs were infected with H1N1 WSN at an moi of 3 pfu/cell in the presence of cyclohexmide (CHX) (100µg/ml). **A.** Total RNA was extracted at the indicated times post infection and the levels of NP mRNAs and vRNAs were determined by strand specific RT-qPCR. The results are expressed as the mean ratios of mRNA/vRNA ± SEM determined in three independent experiments. The significance was tested with an unpaired t test using GraphPad Prism Software (*p < 0.05; **p < 0.01; ***p < 0.001). **B.** Total extracts from infected cells treated with non-target (NT) or ERI1 siRNAs and treated with CHX or not were prepared at 6 hpi and analyzed by immunoblot using antibodies directed against the indicated proteins.

In ERI1 silenced cells under CHX treatment, at all measured time points (except for the 6 hpi time point), mRNA/vRNA ratios were reduced compared to cells treated with control siRNA, thereby supporting a role of ERI1 in primary viral transcription (**Figure 44A**).

Altogether those data indicate that ERI1 has a role in early stages of the viral cycle, and most likely in viral transcription.

e. *Generation of ERI1 knock out cells by CRISPR-Cas9*

Using CRISPR Cas9 methodology we generated ERI1 knock out A549 and HEK 293T cell lines. ERI1 KO A549 cells were more difficult to obtain and required two successive rounds of CRISPR Cas9 transfection and selection. Indeed, clones obtained after the first selection only displayed reduced expression of ERI1 compared to their wild type counterpart. This is most likely explained by several ERI1 coding gene duplications as most of the A549 cells contain 66 chromosomes [341].

We first confirmed our previous results using siRNAs by looking at viral protein accumulation upon single cycle infection in ERI1 KO cells. As observed previously (**Figure 41**), viral proteins accumulated at a slower rate in ERI1 KO A549 and HEK 293T cell lines (**Figure 45A, B**).

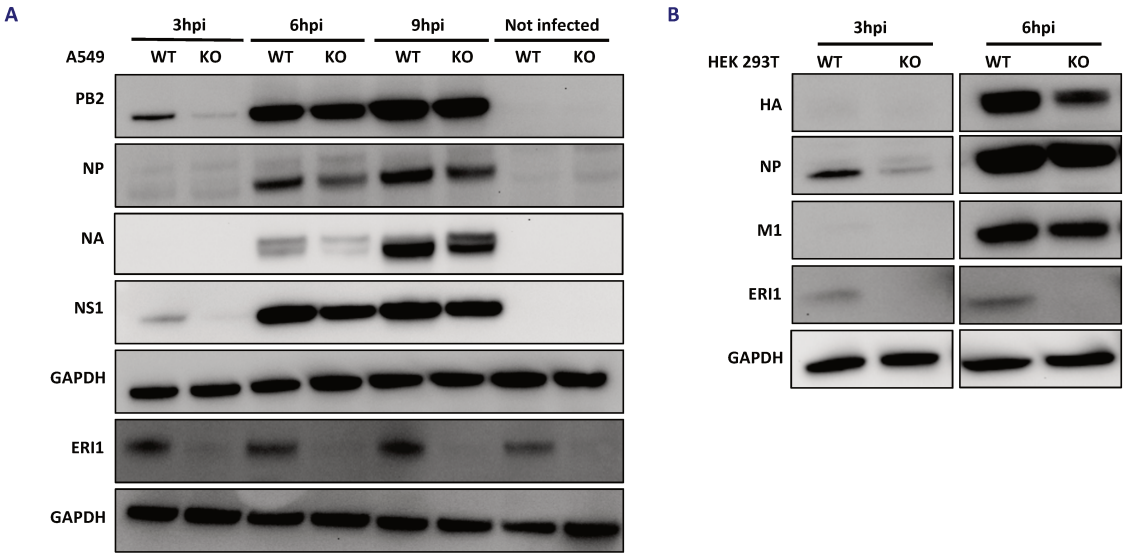

Figure 45: Viral protein accumulation is impaired in ERI1 knock-out cell lines.
ERI1 knock-out A549 (**A**) and HEK 293T (**B**) cells were infected with H1N1 WSN at an moi of 3 pfu/cell. Total extracts were prepared at the indicated times post-infection and analyzed by immunoblot using antibodies directed against the indicated proteins. Results representative of two independent experiments are shown.

For A549 cells, PB2 and NS1 accumulation was clearly reduced at 3 hpi. However, this reduced accumulation was less pronounced at 6 hpi, when a reduction in the accumulation of NP and NA was detected. For HEK 293T cells, accumulation of NP was reduced at 3 hpi but was no longer evident at 6 hpi, when only accumulation of HA and M1 was reduced. Thus, in ERI1 knock-out cell lines, the kinetics of viral protein production appeared to be delayed as seen previously in ERI1 silenced cells (**Figure 41**).

We took advantage of our easily transfectable HEK 293T ERI1 KO cell line to assess the effect of ERI1 depletion on the viral polymerase activity. Cells were transfected with viral polymerase PB2, PB1, PA and NP expressing plasmids, along with a plasmid directing the expression of a mini-genome including a firefly luciferase reporter whose expression is driven by the viral polymerase and a CMV renilla expression plasmid, used as a transfection control to normalize transfection efficiency between conditions. At 24 hpt, luciferase and renilla activities were measured in transfected cell lysates and the polymerase activity was measured relative to the transfection control (*i.e.* firefly luciferase to renilla ratio). This assay thereby allows to explore the transcription/replication activity of the polymerase complex. Interestingly, in HEK 293T ERI1 KO cells, activity of the viral polymerase was reduced two-fold compared to wt cells (**Figure 46**). This result further confirmed the impaired viral transcription already observed in ERI1 silenced cells (**Figure 42, 43 and 44**).

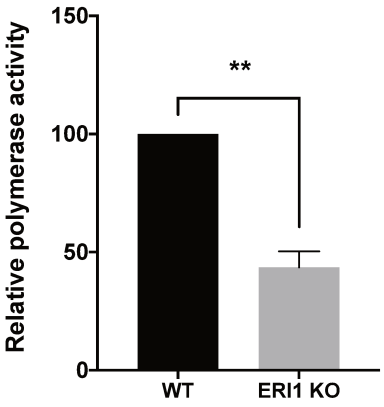

Figure 46: Transcription/replication activity of the IAV polymerase is reduced in HEK 293T ERI1 KO cells.
Wild-type (wt) and HEK 293T ERI1 KO cells were transfected with a plasmid directing the expression of a firefly reporter mini-genome, plasmids encoding the viral proteins PB2, PB1, PA and NP as well as a renilla reporter plasmid to assess transfection efficiency. 24 hpt, firefly activity was measured and normalized using the measured renilla activity. Each ratio was then expressed as a percentage of the wt activity measured in wt HEK 293T cells. The results are expressed as the mean ± SEM of three independent experiments and the significance was tested with an unpaired t test using GraphPad Prism Software (**$p < 0.01$).

Unfortunately, our ERI1 KO cell lines quickly compensated the loss of ERI1. Indeed, after a few passages, IAV replication was no longer impaired in our KO cell lines thereby rendering them unusable for the rest of our study. Nonetheless, those ERI1 KO cells lines allowed us to confirm the requirement of ERI1 in the IAV life cycle, already observed using siRNAs.

2. ERI1 RNA binding and exonuclease activities are both required to promote viral transcription

ERI1 can be schematically divided in two domains, the N-terminal domain containing a SAP domain (Acinus and PIAS), which binds nucleic acids, and the C-terminal domain containing the exonuclease activity (**Figure 47**). Those two domains are connected by a small interdomain spacer (see section IV.1.a. of the introduction). The function of ERI1 has been extensively studied in histone mRNA metabolism, and mutants for RNA binding (ΔSAP) or DEDDh exonuclease activity (D134A+E136A, *i.e.* "no DE") showed a strong defect in histone mRNA decay and binding [293,329].

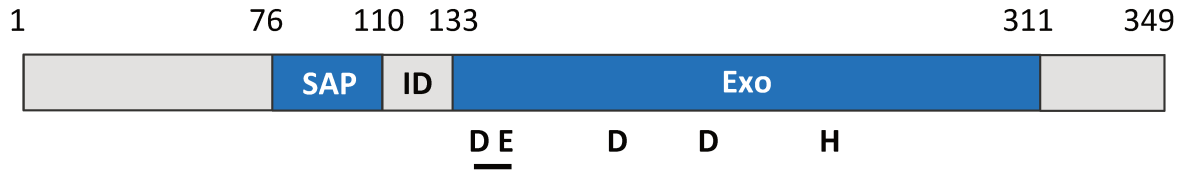

Figure 47: ERI1 schematic organization.
The conserved "SAF-box, Acinus and PIAS" (SAP), inter-domain (ID) and DEDDh exonuclease (Exo) (D134, E136, D234, D298 and H293) domains are represented. Amino acid numbers and conserved residues of the catalytic core are indicated. Residues mutated in the "no DE" mutant are underlined.

To decipher whether those activities contribute to the role of ERI1 in the IAV life cycle, we performed overexpression experiments with ERI1 mutants. HEK 293T cells were transfected with optimized amounts of ERI1 mutants expressing plasmids and infected 24 hpt with H1N1 WSN. At 3.5 hpi cells were lysed and vRNAs and viral mRNAs were quantified.

Overexpression of wild type ERI1 led to a two-fold increase in viral transcription as already presented in **Figure 43**. However, overexpression of ΔSAP or no DE mutants was not associated with such increase in viral transcription, even though all mutants accumulated at

the same level as ERI1 wt (**Figure 48A, B**). Overexpression of the no DE mutant even led to a slight decrease in viral transcription (**Figure 48A**). Thus, both RNA binding and exonuclease activities appear to be required for IAV transcription.

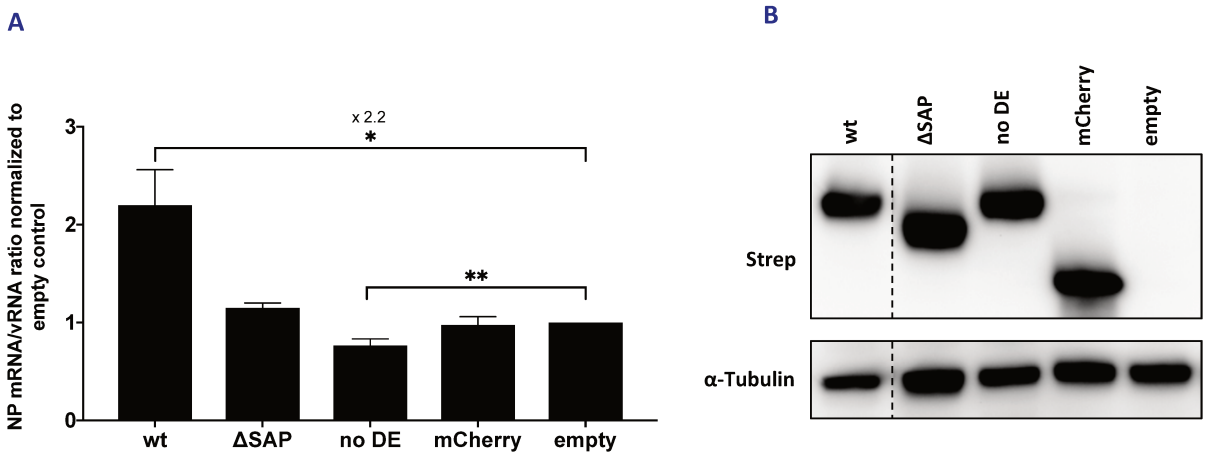

Figure 48: ERI1 RNA binding and exonuclease activities are both required to promote IAV transcription.

HEK 293T cells were transfected with Strep-ERI1, Strep-ERI1 mutants (ΔSAP, D134A+E136A *i.e.* "no DE") or Strep-mCherry as a control and infected with H1N1 WSN at an moi of 3 pfu/cell. **A.** At 3.5 hpi total RNA was extracted and the levels of NP mRNAs and vRNAs were determined by strand-specific RT-qPCR. The results are expressed as the mean ratios of mRNA/vRNA ± SEM normalized to empty control, determined in three independent experiments. The significance was tested with an unpaired t test using GraphPad Prism Software (*p < 0.05, ** p< 0.001). **B.** Total cell extracts of transfected HEK 293T cells were prepared and analyzed by immunoblot to detect Strep and GAPDH. Dashed lines indicate where the blots have been cropped.

3. ERI1 interplay with viral proteins during infection

a. *Transcribing IAV vRNPs are associated with ERI1 during infection*

ERI1 was found in our GPCA screen and by co-immunoprecipitation as interacting primarily with the vRNP components PB2, PB1 and NP (**Figure 38**). To confirm this interaction profile in an infectious context we looked at the interaction of the endogenous ERI1 with viral proteins in infected cells.

Upon ERI1 purification in H1N1 WSN infected cells, PB2 and NP proteins were specifically co-immunoprecipitated (**Figure 49A**). The interaction with PB2 was further confirmed by performing the reverse co-immunoprecipitation in H1N1 WSN infected HEK 293T cells that had been previously transfected with Strep-ERI1 or Strep-mCherry as a control. Upon PB2 immunoprecipitation, Strep-ERI1 was specifically retrieved in the eluates (**Figure 49B**). Altogether, those observations suggest that ERI1 most likely interacts with the viral polymerase during infection.

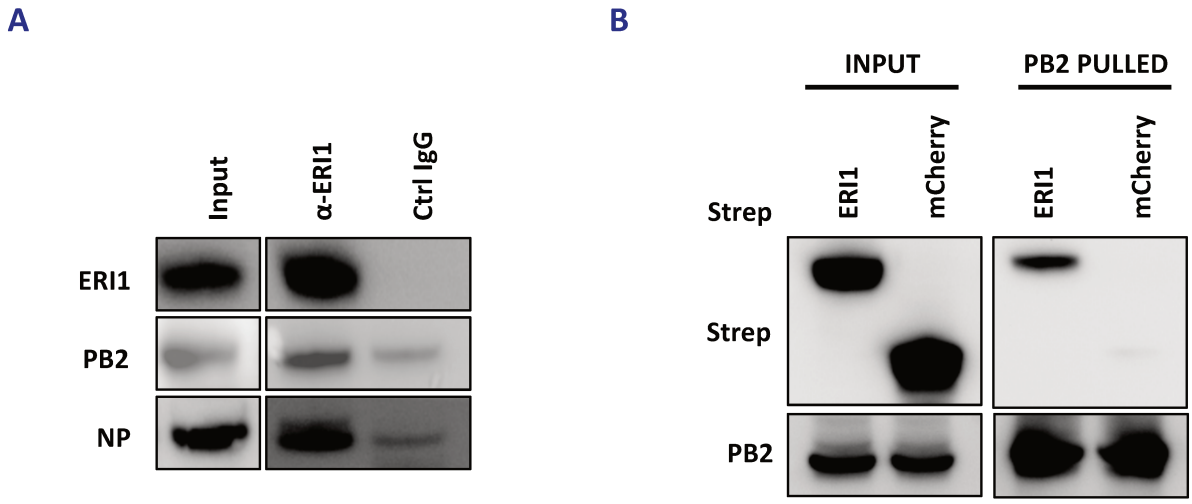

Figure 49: The viral polymerase interacts with ERI1 during infection.
A. HEK 293T cells were infected with H1N1 WSN (3 pfu/cell). At 3 hpi, ERI1 proteins were purified using anti-ERI1 antibodies (α-ERI1) or control immunoglobulins (Ctrl IgG). Input and α-ERI1 or Ctrl IgG eluates were analyzed by immunoblot to detect ERI1, PB2 and NP. Results representative of two independent experiments are shown. **B.** HEK 293T cells were transfected with Strep-ERI1 or Strep-mCherry and infected with H1N1 WSN (3 pfu/cell). At 6 hpi, PB2 proteins were purified using anti PB2 antibodies. Inputs and anti-PB2 eluates were analyzed by immunoblot to detect ERI1 and PB2. Results representative of two independent experiments are shown.

We previously showed that ERI1 RNA binding activity is required for viral transcription (**Figure 48**) and that ERI1 most likely interacts with the vRNPs (**Figure 49**). We thus next sought to look at the requirement of RNA for the interaction between ERI1 and viral proteins. HEK 293T cells were transfected with Strep-ERI1 or Strep-empty as a control and infected 24 hpt with H1N1 WSN. Remarkably, upon RNAse treatment of the infected cell lysate, viral proteins were no longer co-purified along with Strep-tagged ERI1. However, in

the condition where RNA integrity was preserved by addition of RNAse inhibitors, PB2 and NP were still co-purified (**Figure 50**). These results suggest that the interaction between ERI1 and the viral proteins during the course of infection is RNA dependent.

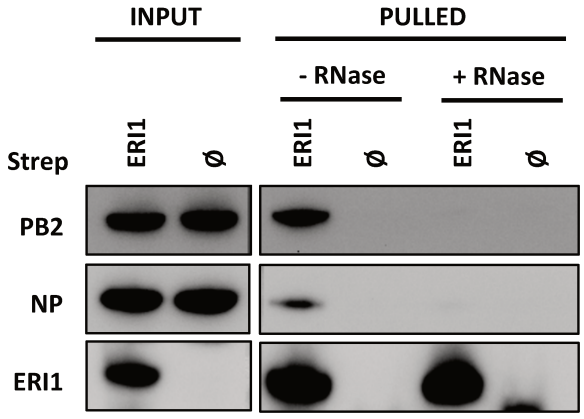

Figure 50: Interaction of ERI1 with viral proteins in infected cells is RNase sensitive.
HEK 293T cells were transfected with Strep-ERI1 or Strep-empty (Ø) and infected with H1N1 WSN (3 pfu/cell). At 6 hpi, Strep tagged proteins were purified with sepharose streptactine beads. Complexes bound to the beads were incubated with RNase A or without for 1 h. Inputs and Strep-tag eluates were analyzed by immunoblot to detect ERI1, PB2 and NP. Results representative of three independent experiments are shown.

The interaction between ERI1 and the viral proteins being RNase sensitive, this implies that RNA, either viral or cellular, might bridge the interaction. Furthermore, ERI1 interacts with the viral polymerase during IAV infection (**Figure 49**) and appears to be required for viral transcription (**Figure 41, 42, 43**). One hypothesis connecting all these results would be that ERI1 interacts with the transcribing vRNPs. To test this hypothesis, we wondered whether viral RNAs would co-purify with ERI1 in infected cells.

For that purpose, we quantified NP mRNA and vRNA co-purified with Strep-ERI1 or Strep-empty as a control in H1N1 WSN infected cell lysates. Strep-ERI1 eluates were enriched in NP vRNA and mRNA compared to the Strep-empty control eluates (6×10^3 vs 9.9×10^2 copies of vRNA and 1.6×10^5 vs 6×10^3 copies of mRNA in Strep-ERI1 and Strep-empty eluates respectively), indicating that indeed viral RNAs are associated with ERI1 during infection (**Figure 51A**). Moreover, the proportion of mRNAs co-purified with ERI1 was significantly higher than that of the vRNAs (43 fold vs 6 fold, **Figure 51B**).

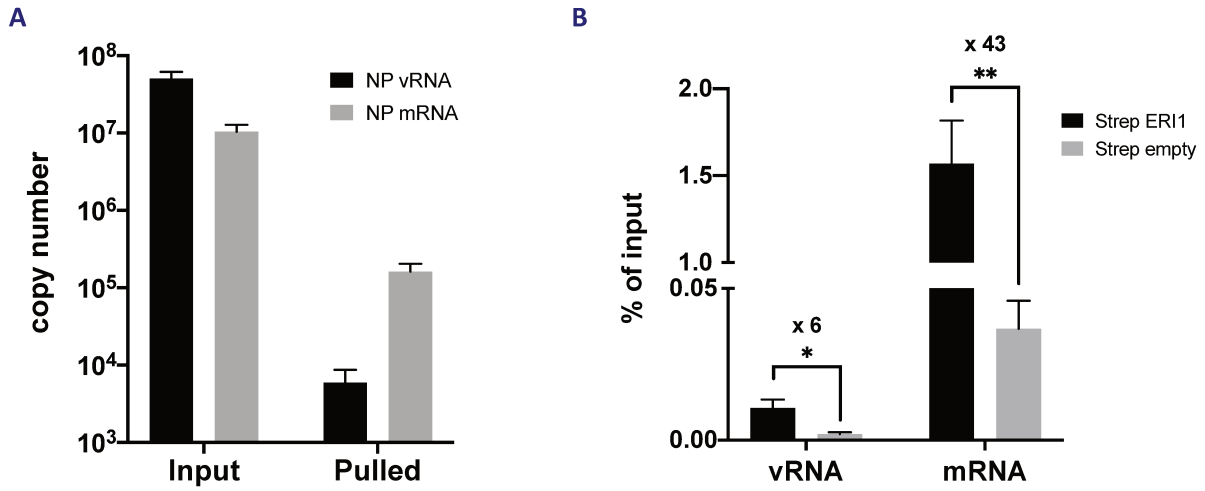

Figure 51: Viral RNAs co-purify with ERI1 in infected cells.

A. HEK 293T cells were transfected with Strep-ERI1 or Strep-empty and infected with H1N1 WSN (3 pfu/cell). At 6 hpi the levels of NP vRNAs (black bars) and mRNAs (grey bars) co-purified with Strep-ERI1 were quantified by strand-specific RT-qPCR. Levels of co-purified viral RNAs are expressed as the mean ± SEM of three independent experiments. The background level of detection in Strep-empty eluates was 9.9×10^2 and 6×10^3 copies for NP vRNAs and NP mRNAs, respectively. **B.** Viral RNAs co-immunoprecipitated with Strep-ERI1 and Strep-empty as a control quantified in **A.** were expressed as a ratio of the viral RNAs quantified in the input. The significance was tested with an unpaired t test using GraphPad Prism Software (*$p<0.05$, **$p < 0.01$).

ERI1 is known to associate with several cellular RNAs, including histone mRNAs and rRNAs [288]. Moreover, interaction between ERI1 and viral proteins is RNase sensitive (**Figure 50**). To determine whether cellular RNAs could play a role in the interaction we looked at the interaction profile between ERI1 and the viral proteins in non-infected cells. As presented in **Figure 38**, HEK 293T cells were transfected with Strep-tagged ERI1 or Strep-tagged mCherry as a control, along with Gluc1-PB2, Gluc1-PB1, Gluc1-PA, Gluc1-NP and M1-Gluc1 and cell lysates were treated with RNase or with RNase inhibitors. PA, found as a non interacting partner, was again used as an internal negative control. As presented in **Figure 38**, the PB2, PB1, NP and M1 proteins specifically co-purified with Strep-ERI1, while only marginal or significantly lower amounts of the viral proteins were retrieved upon Strep-mCherry purification. However, upon RNase treatment of the cell lysates, a substantial part of the interaction was lost. This was especially clear for PB1, NP and M1 for which the amount of Gluc1 tagged proteins co-purified with Strep-ERI1 was greatly reduced in the RNase treated condition (**Figure 51**).

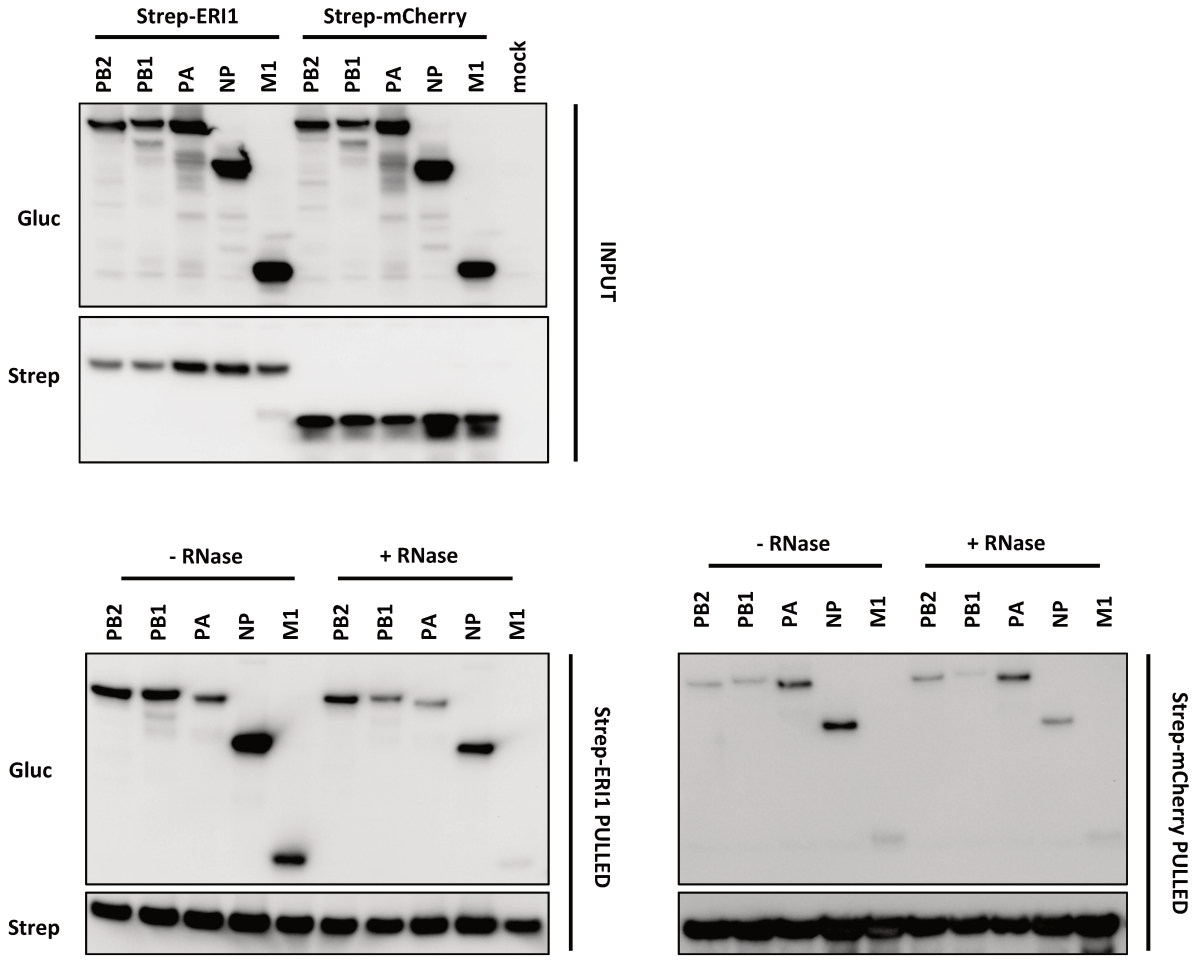

Figure 52: Interaction between ERI1 and viral proteins is partially RNase sensitive in a non-infectious context.

HEK 293T cells were co-transfected with Strep-ERI1 or Strep-mCherry as a control and Gluc1-PB2, -PB1, -PA, -NP or M1-Gluc1. At 24 hpt, cell lysates were retrieved and Strep-tagged proteins were purified with sepharose streptactin beads. Complexes bound to the beads were incubated with RNase A or Rnasine for 1 h. Inputs and Strep-tag eluates were analyzed by immunoblot to detect Strep and Gluc1 tagged proteins. Results representative of two independent experiments are shown.

Taken together, these results indicate that viral RNAs associate with ERI1 during infection, with viral mRNAs being the major form of ERI1 associated viral RNAs. This may highlight a prominent connection between ERI1 and the transcribing vRNPs, in line with the role of ERI1 in viral transcription.

Furthermore, the interaction being RNase sensitive in both infectious and non-infectious contexts, this supports a model where cellular RNAs could promote the interaction between ERI1 and viral proteins. However, our binary interaction GPCA results associated with the

fact that the loss of binding to viral proteins upon RNase treatment in a non-infectious context was only partial, suggest that, in addition to an evident role of RNA, the interaction between ERI1 and viral proteins is also supported by direct protein-protein interactions.

b. *vRNPs associate with the SLBP-ERI1 histone mRNA processing factors*

As previously shown, ERI1 interaction with viral proteins is RNA dependent in an infectious context, and also partially RNA dependent in a non-infectious context. These results suggest that rather than viral RNAs, cellular RNAs may instead support this interaction. Viral transcription occurs in the nucleus of infected cells. Furthermore, in the nucleus, histone mRNAs are associated to ERI1 and SLBP, both involved in their processing [291]. Moreover, both ERI1 activities – RNA binding and exonuclease – are not only required for viral transcription as previously shown here, but are also required for histone mRNA binding and processing [293,329]. We therefore wondered whether ERI1 forms that are associated to histone mRNAs in the nucleus could be preferentially targeted by the virus. If viral proteins interact with histone mRNAs associated with ERI1 and SLBP, we should be able retrieve both ERI1 and SLBP upon PB2 purification in infected cells.

We thus performed PB2 purification in H1N1 WSN infected cells co-transfected with Strep-ERI1 and 3XFlag-SLBP, or with Strep-ERI1 or 3XFlag-SLBP alone. Upon PB2 purification, ERI1 as well as SLBP were recovered (**Figure 53A**). Moreover, like the interaction between ERI1 and viral proteins, the interaction of SLBP with PB2 and NP was RNase sensitive (**Figure 53B**). Hence, disrupting the ERI1/SLBP/histone mRNA complex by RNase digestion leads to a loss of the interaction between viral proteins and ERI1.

Finally, further supporting the importance of histone mRNA in the interaction, PB2 eluates were found to be specifically enriched in HIST1H2AB mRNA compared to control eluates (**Figure 53C**).

Altogether, our results support a model in which ERI1 is recruited by IAV transcribing vRNPs in a form that is bound to histone mRNA and associated with SLBP.

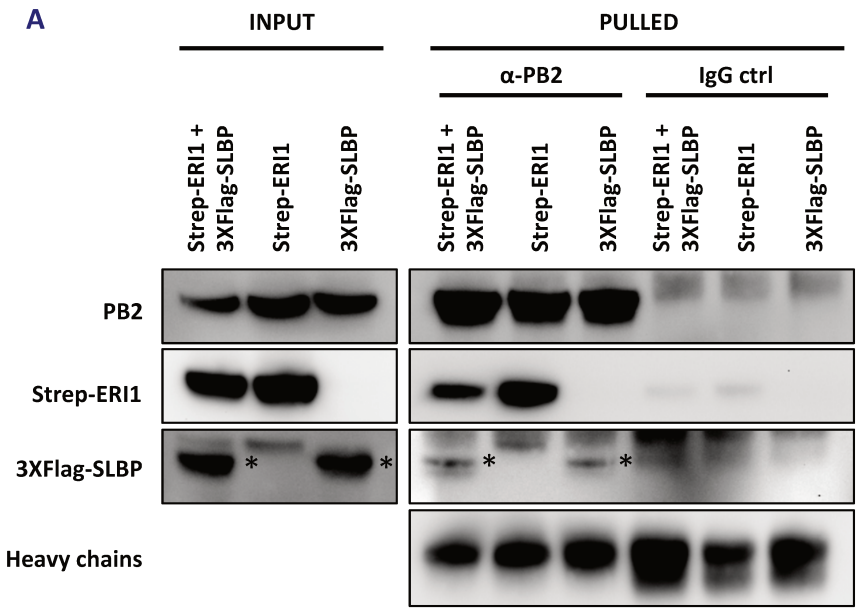
A
INPUT
PULLED
α-PB2
IgG ctrl
Strep-ERI1 + 3XFlag-SLBP
Strep-ERI1
3XFlag-SLBP
Strep-ERI1 + 3XFlag-SLBP
Strep-ERI1
3XFlag-SLBP
Strep-ERI1 + 3XFlag-SLBP
Strep-ERI1
3XFlag-SLBP
PB2
Strep-ERI1
3XFlag-SLBP
Heavy chains

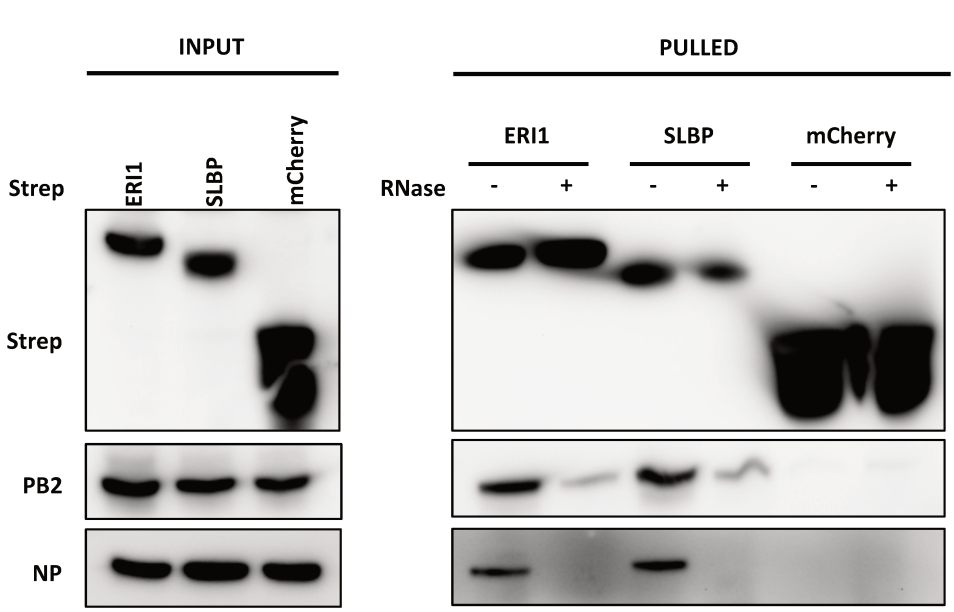
B
INPUT
PULLED
Strep
ERI1
SLBP
mCherry
RNase
ERI1
SLBP
mCherry
- + - + - +
Strep
Strep
PB2
NP

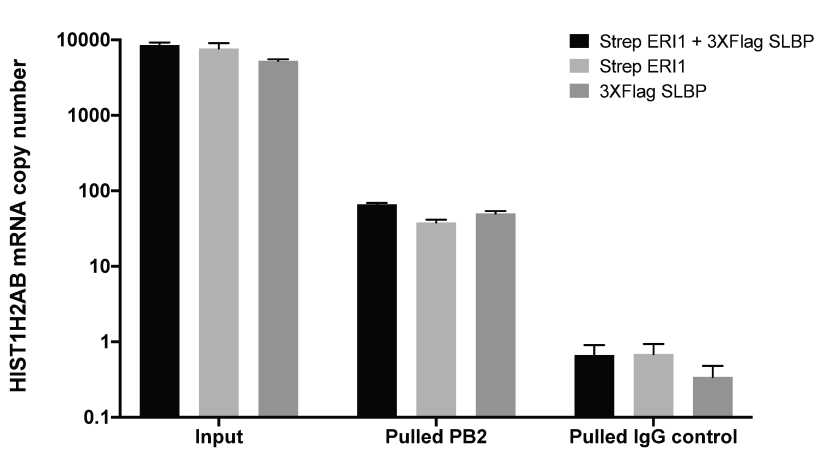
C
HIST1H2AB mRNA copy number
10000
1000
100
10
1
0.1
Strep ERI1 + 3XFlag SLBP
Strep ERI1
3XFlag SLBP
Input
Pulled PB2
Pulled IgG control

Figure 53: vRNPs associate with histone mRNA processing factors.

A. HEK 293T cells were co-transfected with Strep-ERI1 and 3XFlag-SLBP, or transfected with either Strep-ERI1 or 3XFlag-SLBP and infected with H1N1 WSN (3 pfu/cell). At 6 hpi, PB2 proteins were purified using anti PB2 antibodies. Inputs and anti-PB2 eluates were analyzed by immunoblot to detect Strep-ERI1, 3XFlag-SLP and PB2. Results representative of three independent experiments are shown **B.** HEK 293T cells were transfected with Strep-ERI1, Strep-SLBP or Strep-mCherry and infected with H1N1 WSN (3 pfu/cell). At 6 hpi, Strep tagged proteins were purified with sepharose streptactin beads. Complexes bound to the beads were incubated with RNase A or Rnasine for 1 h. Inputs and Strep-tag eluates were analyzed by immunoblot to detect Strep-ERI1, Strep-SLBP, PB2 and NP. Results representative of two independent experiments are shown. **C.** HEK 293T cells were co-transfected with Strep-ERI1 and 3XFlag-SLBP, or transfected with either Strep-ERI1 or 3XFlag-SLBP and infected with WSN (3 pfu/cell). At 6 hpi, PB2 proteins were purified using anti PB2 antibodies. The levels of HIST1H2AB mRNA detected by RT-qPCR co-purified with PB2 are expressed as the mean ± SEM of three independent experiments.

c. *ERI1 mutants impaired for association to histone mRNA are also impaired in viral RNAs association*

Our data point towards a recruitment of ERI1 bound to histone mRNAs to the transcribing vRNPs. To further support this hypothesis, we next examined the ERI1 interaction profile with viral proteins in infected cells using ERI1 mutants invalidated for histone mRNA binding. ERI1 SAP domain is involved in RNA binding and the ERI1 ΔSAP mutant was reported to no longer bind histone mRNAs [293]. Although the SAP domain constitutes a major part of the whole protein, its deletion does not cause major structural alterations of ERI1 as ERI1 ΔSAP mutants still bear a functional exonuclease domain as reported by Yang and colleagues [293].

HEK 293T cells were transfected with Strep-ERI1, Strep-ERI1 ΔSAP, or Strep-mCherry and Strep-empty as a control and were infected 24 hpt with H1N1 WSN. Upon Strep-tag purification, we were able to retrieve the interactions with the viral proteins PB2 and NP for ERI1 wt as already described in **Figure 49**. In contrast, for the ERI1 ΔSAP mutant, the amount of co-purified viral proteins was comparable to the mCherry control, demonstrating that deletion of the SAP domain abolished the interaction between ERI1 and the viral proteins (**Figure 54**).

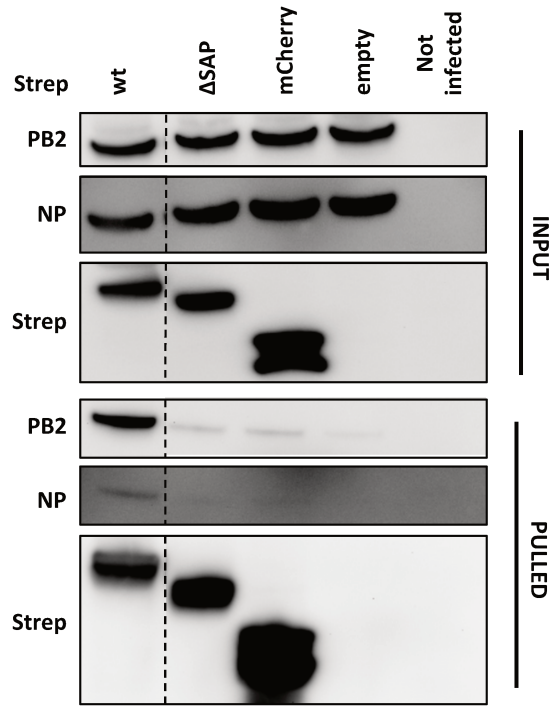

Figure 54: ERI1 ΔSAP mutant looses the ability to interact with viral proteins during infection.
HEK 293T cells were co-transfected with Strep-ERI1, Strep-ERI1 ΔSAP or Strep-mCherry and Strep-empty as controls and infected with H1N1 WSN (3 pfu/cell). At 6 hpi, Strep-tagged proteins were purified with sepharose streptactin beads. Inputs and Strep-tag eluates were analyzed by immunoblot to detect Strep, PB2 and NP. Dashed lines indicate where the blots have been cropped.

Interestingly, the ERI1 ΔSAP mutant was also impaired for its association with viral RNAs. Deletion of the SAP domain was associated to a loss of binding to histone mRNA as 60 times less histone mRNA were co-purified with the Strep-ERI1 ΔSAP mutant compared to Strep-ERI1 wt, as already published (**Figure 55C**) [293]. Furthermore, upon Strep-ERI1 purification, respectively 12 and seven times less viral mRNAs and vRNAs were co-purified with ERI1 ΔSAP compared to ERI1 wt (**Figure 55A, B**). For both viral mRNAs and vRNAs the level of association with the ΔSAP mutant was close to the background noise level of interaction detected upon Strep-mCherry purification.

Altogether, these results suggest that an ERI1 mutant impaired for histone mRNA binding looses its capacity to interact with IAV vRNPs, which might suggest a histone mRNA dependency of the ERI1/vRNP association in the nucleus. Overall, this implies that, either histone mRNA is somehow important for the interaction between ERI1 and the transcribing vRNPs, or that a histone mRNA bound form of ERI1 is required for the interaction to occur.

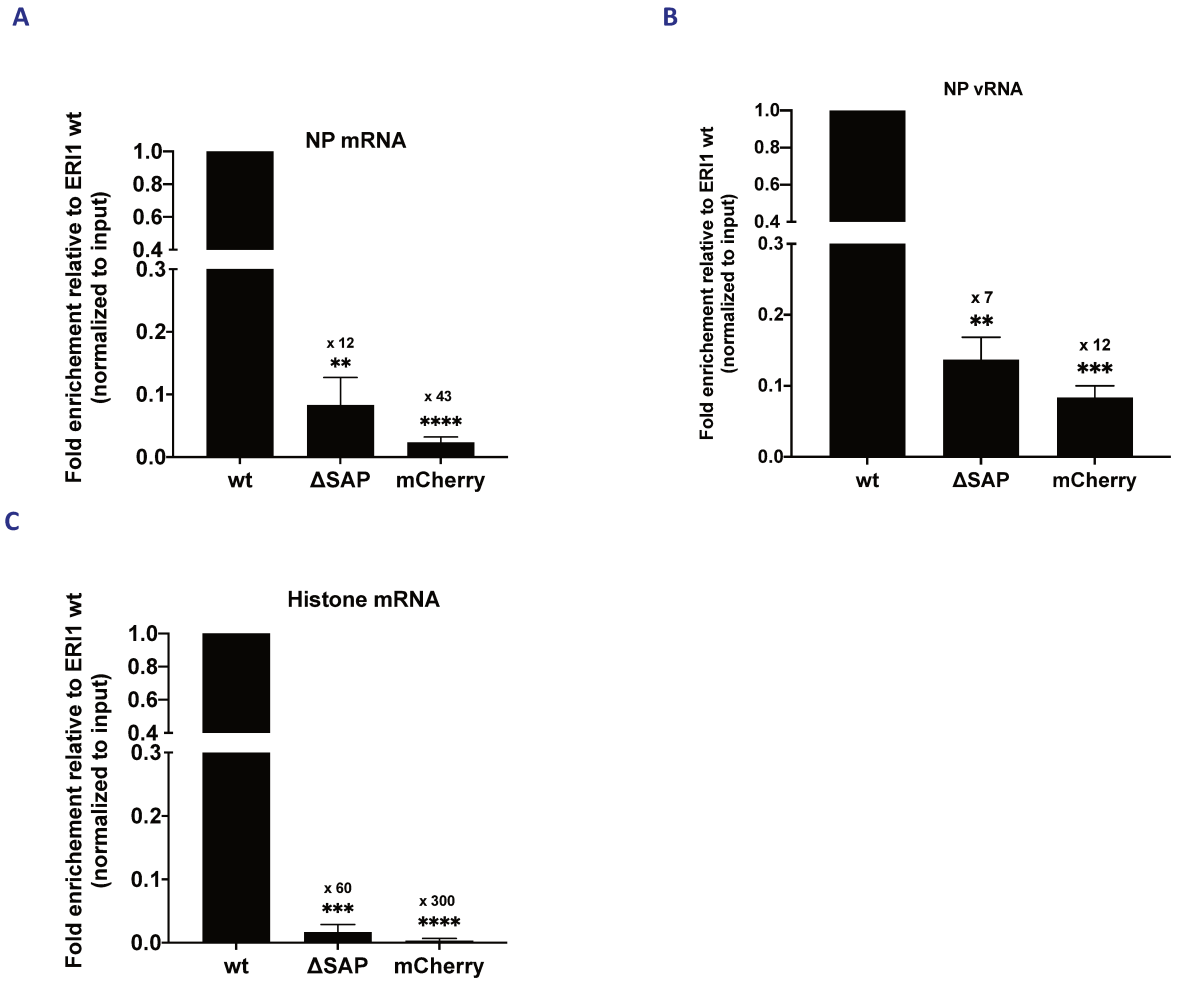

Figure 55: ERI1 RNA binding mutant unable to bind histone mRNA looses the ability to associate with vRNPs.

HEK 293T cells were co-transfected with Strep-ERI1 mutants or Strep-mCherry as a control and infected with H1N1 WSN (3 pfu/cell). At 6 hpi, Strep tagged proteins were purified with sepharose streptactin beads. The levels of NP mRNAs (**A**), vRNAs (**B**) and HIST1H2AB mRNA (**C**) co-purified with Strep-ERI1 are expressed as the mean ± SEM of three independent experiments normalized to Strep-ERI1 wt. The significance was tested with an unpaired t test using GraphPad Prism Software (**p<0.01, *** p< 0.0001, **** p< 0.0001).

d. *ERI1 no DE mutant is a dominant negative form*

Since we found that the ERI1 no DE mutant was unable to support viral transcription contrary to ERI1 wt, we wondered whether this could be explained by a loss of interaction with the viral proteins (**Figure 47**). HEK 293T cells were thus transfected with the Strep-ERI1 no DE mutant and infected with WSN. Upon Strep-purification similar amounts of viral

proteins were retrieved with Strep-ERI1 wt and the Strep-ERI1 no DE mutant, suggesting that the ERI1 no DE mutant was still able to interact with the viral proteins (**Figure 56**).

Interestingly, overexpression of the ERI1 no DE mutant led to a slight decrease in viral transcription suggesting that it might interfere with viral transcription. Therefore, as the no DE mutant retains the ability to bind viral proteins and histone mRNA [293] but is unable to support viral transcription, it may act as a dominant negative form of ERI1. Since the ERI1 exonuclease activity is required to promote histone pre-mRNA processing, taken together, our data also suggest that complete processing of histone pre-mRNA might somehow be required for efficient viral transcription. However we cannot also exclude that ERI1 exonuclease activity might be required for IAV transcription independently of its role in histone mRNA processing.

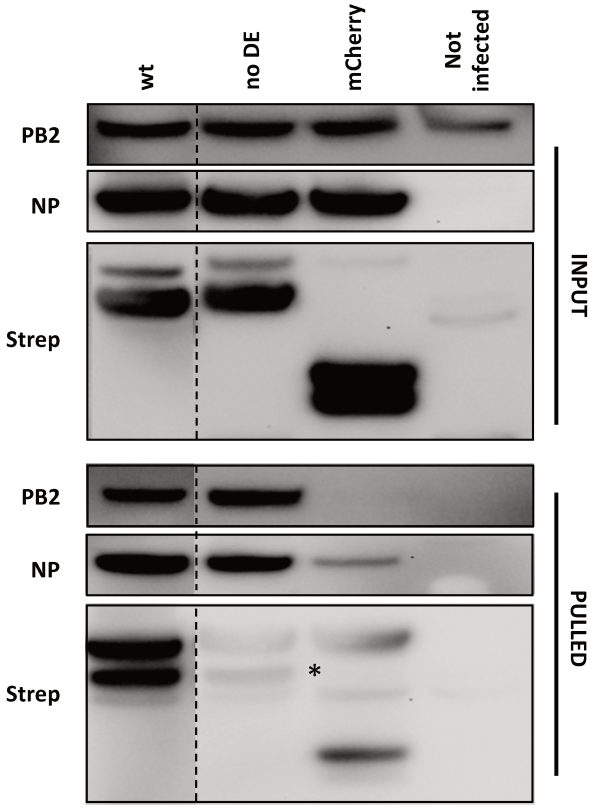

Figure 56: ERI1 no DE mutant retains the ability to interact with viral proteins during infection.
HEK 293T cells were co-transfected with Strep-ERI1, Strep-ERI1 no DE or Strep-mCherry as a control and infected with H1N1 WSN (3 pfu/cell). At 6 hpi, Strep tagged proteins were purified with sepharose streptactin beads. Inputs and Strep-tag eluates were analyzed by immunoblot to detect Strep, PB2 and NP. Dashed lines indicate where the blots have been cropped. Results representative of three independent experiments are shown.

Annexes

Annex 1

Protein Name	Synonyms	UniProt ID
ADAR	ADAR1, DSRAD, G1P1, IFI4	P55265
ADARB1	ADAR2, DRADA2, RED1	P78563
AEN	ISG20L1	Q8WTP8
AICDA	AID	Q9GZX7
APEX1	APE, APE1, APEX, APX, HAP1, REF1	P27695
APEX2	APE2, APEXL2, XTH2	Q9UBZ4
APLF	C2orf13, PALF, XIP1	Q8IW19
C1D		Q13901
CNOT10		Q9H9A5
CNOT11	C2orf29	Q9UKZ1
CNOT2	CDC36, NOT2	Q9NZN8
CNOT3	KIAA0691, LENG2, NOT3	O75175
CNOT4	NOT4	O95628
CNOT6	CCR4, CCR4a, KIAA1194	Q9ULM6
CNOT6L	CCR4B	Q96LI5
CNOT7	CAF1	Q9UIV1
CNOT9	RCD1, RQCD1	Q92600
DIS3	KIAA1008, RRP44	Q9Y2L1
DIS3L	DIS3L1, KIAA1955	Q8TF46
DIS3L2	FAM6A	Q8IYB7
ERCC3		O13768
ERI1	3'EXO, THEX1	Q8IV48
ERI2	EXOD1, KIAA1504	A8K979
ERI3	PINT1, PRNPIP, PRNPIP1	O43414
EXD1	EXDL1	Q8NHP
EXD2	C14orf114, EXDL2	Q9NVH0
EXD3		Q8N9H8
EXO1	EXOI, HEX1	Q9UQ84
EXO5	C1orf176, DEM1	Q9H790
EXOSC1	CSL4	Q9Y3B2
EXOSC10	PMSCL, PMSCL2, RRP6	Q01780
EXOSC2	RRP4	Q13868
EXOSC3	RRP40	Q9NQT5
EXOSC4	RRP41, SKI6	Q9NPD3
EXOSC5	CML28, RRP46	Q9NQT4
EXOSC6	MTR3	Q5RKV6
EXOSC7	KIAA0116, RRP42	Q15024
EXOSC8	OIP2, RRP43	Q96B26
EXOSC9	PMSCL1	Q06265
HLTF	HIP116A, RNF80, SMARCA3, SNF2L3, ZB	Q14527
HMGA2	HMGIC	P52926
INPP5K	PPS, SKIP	Q9BT40
ISG20	HEM45	Q96AZ6
ISG20L2		Q9H9L3
METTL3	Mta70	Q8C3P7
MPHOSPH6	MPP6	Q99547
MRE11A	HNGS1, MRE11A	P49959
MTREX	DOB1, KIAA0052, MTR4, SKIV2L2	P42285
PAN2	KIAA0710, USP52	Q504Q3
PAN3		Q58A45
PAPD7	PAPD7, POLS, TRF4	Q5XG87
PARN		Q21412
PATL1		Q86TB9
PDE12		Q6L8Q7
PNPT1	PNPASE	Q8TCS8
POLD1	POLD	P28340
POLE4		Q9NR33
POLR2I		P36954
RAD1	REC1	O60671
RAD54B		Q9Y620
RAD9A		Q99638
RAD9B		Q6WBX8
REXO2	SFN, SMFN	Q9Y3B8
SAMHD1	MOP5	Q9Y3Z3
SETX	ALS4, KIAA0625, SCAR1	Q7Z333
SNRNP200	ASCC3L1, HELIC2, KIAA0788	O75643
TCEA1	GTF2S, TFIIS	P23193
TCEAL1	SIIR	Q15170
TOE1		Q96GM8
TREX1		Q9NSU2
TREX2		Q9BQ50
TTC37	KIAA0372	Q6PGP7
USB1	C16orf57	Q9BQ65
WDR61		Q9GZS3
ZCCHC7		Q8N3Z6

Table 4: The ExoRDec library.

Summary of the 75 factors included in the ExoRDec library. For each factor, protein name, synonyms and UniProt ID are specified.

Annex 2

Cellular factors	sH1N1				pH1N1			
	Exp1	Exp2	Exp3	Validated**	Exp1	Exp2	Exp3	Validated **
	PB2							
ADARB1	82,08	30,16	57,03	**3/3**	46,85	45,81	33,45	**3/3**
APLF	37,61	17,74	32,26	**3/3**	30,19	23,32	28,24	**3/3**
ERI1	50,68	37,02	34,55	**3/3**	19,36	18,51	18,05	**3/3**
EXOSC6	28,85	25,45	46,57	**3/3**	15,06	14,87	24,76	**3/3**
HMGA2	58,35	41,36	64,15	**3/3**	37,07	22,22	37,25	**3/3**
PT*	**5,57**	**4,87**	**5,65**	**5/5**	**4,65**	**3,46**	**4,78**	**6/6**
	PB1							
CNOT6L	9,88	6,58	10,55	**3/3**	6,88	4,51	10,49	**3/3**
ERI1	14,55	13,37	12,96	**3/3**	9,03	6,98	13,53	**3/3**
EXO5	19,95	13,47	21,86	**3/3**	13,55	8,27	19,69	**3/3**
EXOSC6	21,06	16,40	29,40	**3/3**	14,08	11,55	26,42	**3/3**
POLE4	32,58	18,85	43,29	**3/3**	21,15	12,18	31,77	**3/3**
SKIV2L	23,89	15,09	25,46	**3/3**	18,31	12,49	21,57	**3/3**
USB1	5,99	3,81	7,66	**2/3**	5,73	6,34	8,44	**3/3**
PT*	**5,43**	**4,08**	**7,27**	**6/6**	**3,95**	**2,90**	**4,96**	**6/6**
	PA							
CNOT6L	2,51	1,53	3,18	**3/3**	3,41	2,73	1,96	**3/3**
EXO5	3,96	2,49	6,21	**3/3**	5,70	3,80	7,95	**3/3**
INPP5K	1,97	1,86	3,07	**3/3**	2,49	2,47	3,01	**3/3**
PT*	**1,08**	**0,85**	**1,17**	**3/3**	**1,27**	**0,88**	**1,23**	**6/6**
	NP							
ADAR	5,10	2,14	5,63	**3/3**	17,02	17,92	19,26	**3/3**
ADARB1	281,71	80,99	120,75	**3/3**	260,84	132,73	184,00	**3/3**
ERI1	30,21	20,85	21,88	**3/3**	31,07	31,42	33,85	**3/3**
HMGA2	24,06	13,68	17,55	**3/3**	27,86	19,21	27,17	**3/3**
TOE1	38,59	29,82	48,16	**3/3**	30,46	28,11	39,80	**3/3**
WDR61	3,25	2,65	3,66	**3/3**	2,70	2,72	3,14	**2/3**
PT*	**2,67**	**1,78**	**3,61**	**6/6**	**3,63**	**2,46**	**2,97**	**6/6**
	M1							
ADAR	0,71	0,31	0,98	**0/3**	2,16	2,27	2,37	**3/3**
ADARB1	5,89	3,31	3,65	**3/3**	9,15	3,29	4,53	**3/3**
APEX1	0,97	0,91	0,85	**0/3**	1,28	1,23	1,08	**1/3**
APLF	2,07	1,17	0,82	**2/3**	2,75	2,04	2,99	**3/3**
ERI1	4,21	3,35	4,23	**3/3**	7,68	6,12	7,59	**3/3**
EXOSC8	2,40	1,13	2,22	**3/3**	3,85	1,57	2,76	**3/3**
HMGA2	3,30	1,67	2,59	**3/3**	6,11	3,93	3,94	**3/3**
USB1	1,60	1,45	1,30	**2/3**	1,88	1,74	1,77	**3/3**
PT*	**1,66**	**1,05**	**1,21**	**6/9**	**1,69**	**1,06**	**1,20**	**7/8**
	NS1							
ADARB1	220,92	112,78	157,78	**3/3**	521,65	348,60	303,15	**3/3**
AEN	22,07	17,08	35,36	**3/3**	20,21	21,36	22,16	**3/3**
EXOSC6	24,35	29,81	30,12	**3/3**	76,85	75,24	87,48	**3/3**
PAN3	37,09	42,26	49,82	**3/3**	165,61	159,31	210,16	**3/3**
PATL1	35,12	27,89	38,66	**3/3**	98,62	105,83	133,01	**3/3**
TOE1	31,14	44,76	57,58	**3/3**	90,28	91,62	99,43	**3/3**
PT*	**5,42**	**3,02**	**3,51**	**6/6**	**6,55**	**5,90**	**6,05**	**6/6**
	NEP							
ADAR	9,31	3,24	7,75	**2/3**	16,14	11,24	19,55	**3/3**
APEX1	2,52	3,69	3,40	**0/3**	7,26	6,92	8,27	**2/3**
EXOSC6	6,01	8,53	9,84	**3/3**	20,28	18,87	16,53	**3/3**
EXOSC8	9,14	13,35	14,58	**3/3**	35,35	26,73	25,94	**3/3**
TCEAL1	7,47	6,64	5,56	**3/3**	13,65	11,92	12,05	**3/3**
PT*	**3,48**	**4,52**	**3,96**	**4/5**	**7,39**	**6,63**	**5,67**	**5/5**

Table 5: NLR retesting of the putative interactors.

The interactions selected from the initial screening were retested by applying the NLR method of the GPCA. Threshold value was calculated as in [335]. PPIs (protein-protein interaction) that were found ≥ 2/3 were considered as validated. Black cells indicate the number of validated interactions after NLR retesting.

*: The Positive Threshold (PT) is defined as the upper limit of the 99.73% confidence interval calculated from the NLR generated by a set of 11 RRS.

**: PPIs that were found in at least two of the three experiments were considered as validated.

Annex 3

A

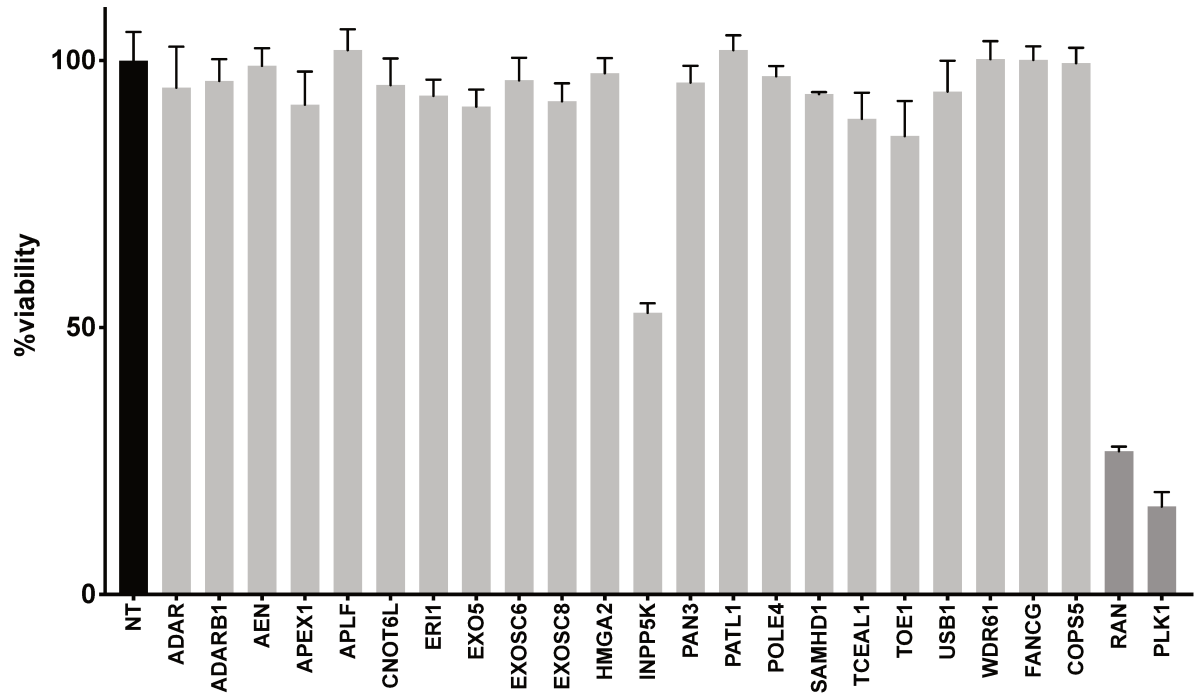
100
50
0
%viability
NT
ADAR
ADARB1
AEN
APEX1
APLF
CNOT6L
ERI1
EXO5
EXOSC6
EXOSC8
HMGA2
INPP5K
PAN3
PATL1
POLE4
SAMHD1
TCEAL1
TOE1
USB1
WDR61
FANCG
COPS5
RAN
PLK1

B

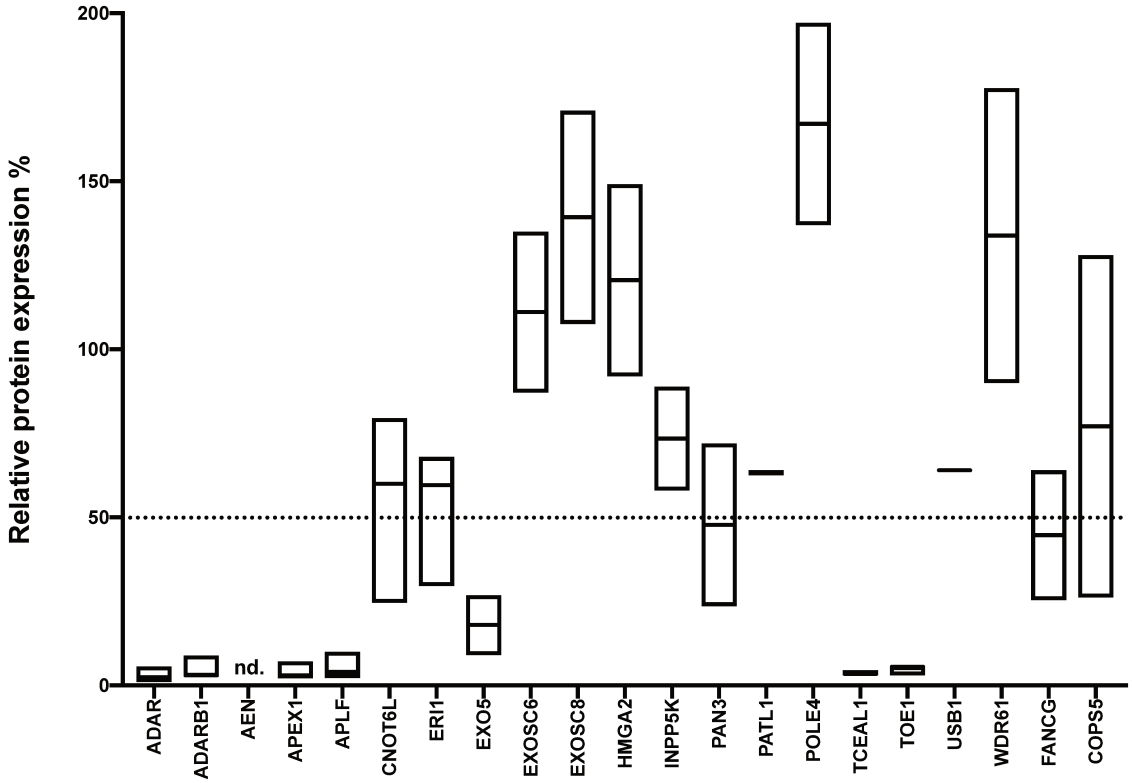
200
150
100
50
0
Relative protein expression %
nd.
ADAR
ADARB1
AEN
APEX1
APLF
CNOT6L
ERI1
EXO5
EXOSC6
EXOSC8
HMGA2
INPP5K
PAN3
PATL1
POLE4
TCEAL1
TOE1
USB1
WDR61
FANCG
COPS5

Figure 57: Cell viability and silencing efficiency upon transfection of siRNAs targeting the recovered PPIs of the ExoRDec library.

A. A549 cells were transfected with 25 nM of siRNAs and cell viability was determined at 72 hpt using the CellTiter-Glo Luminescent Viability Assay kit (Promega) following the manufacter's instructions. The results are expressed as the mean percentages ± SEM. siRNAs targeting RAN and Plk1 (dark grey) were used as toxicity controls. **B.** A549 cells were transfected with 25 nM of control or ExoRDec-targeting siRNAs and with plasmids encoding the corresponding ExoRDec protein fused with the full-length *Gaussia* luciferase (pGlucFL-ExoRDec). Ratios of the luciferase activities obtained in cells transfected with the ExoRDec-targeting siRNAs to the luciferase activity obtained in cells transfected with the control siRNAs are shown. The results are represented as floating bars with a line at the mean. The dashed line corresponds to a relative protein expression of 50% in silenced cells compared to control cells. n.d.: not determined.

Material & Methods

Cells, drugs and viruses. HEK 293T and A549 cells were grown in Dulbecco's modified Eagle's medium (DMEM) supplemented with 10% fetal calf serum (FCS). MDCK and MDCK Siat cells [342] were grown in Modified Eagle's Medium (MEM) supplemented with 5% FCS. Cycloheximide (CHX, Sigma) was added to the medium at the time of infection (100 µg/mL). The A/WSN/33(H1N1), A/Paris/650/2004(H1N1) and A/Bretagne/7608/2009(H1N1pdm09) viruses were produced by reverse genetics. For the siRNA experiments, cells were infected with A549 cell adapted H1N1pdm09 virus [335] obtained from reverse genetics.

Plasmids. The Gateway entry plasmids containing the ExoRDec ORFs were obtained from the human ORFeome resource. To generate vectors encoding Gluc1-, Gluc2-, GlucFL-, 3XFlag and Strep- fusion proteins, the ORFs were transferred respectively into a Gateway-compatible pGluc-GW, pCIneo3XFlag-GW or pIBA105-GW destination plasmid. All constructs were verified by Sanger sequencing. The sequences of the oligonucleotides used for amplification are available upon request.

HT-GPCA. HEK 293T cells were seeded into white 96-well plates at 3.10^4 cells/well. After 24 h, cells were transfected with linear PEI (polyethylenimine) with 200 ng of a plasmid expressing a viral protein fused to Gluc1 at its N-terminus (PB1, PB1, PA, NP, NS1, NEP) or at its C-terminus (M1) and 100 ng of a Gluc2-ExoRDec-expressing plasmid. At 24 h post-transfection, cells were washed with 100 µl of phosphate buffered saline and lysed with 40 µl of Renilla lysis buffer (Promega E2820) for 30 min at room temperature. *G. princeps* luciferase enzymatic activity was measured with a Berthold Centro LB960 luminometer by injecting 50 µl of luciferase substrate reagent (Promega E2820) per well and measuring luminescence for 10 s. Results were expressed in relative luminescence units.

NLR retesting. For the NLR method, the Gluc1-viral proteins/Gluc2-ExoRDec pairs were tested in HT-GPCA along with controls consisting of 200 ng of Gluc1-viral proteins plus 100

ng of Gluc2 and 200 ng of Gluc1 plus 100 ng of Gluc2-ExoRDec. The NLR was calculated as the fold change normalized over the sum of the controls. For a given protein pair A and B, NLR = (Glc1-A +Glc2-B)/[(Glc1-A + Glc2) + (Glc1 + Glc2-B)]. Retesting experiments were conducted independently three times for each ExoRDec factor. To estimate the significance of an NLR for a given protein-protein pair by comparison to the RRS sampling signal, a confidence interval was calculated for the RRS data set as described in [335], considering the estimated standard error (SE) and a confidence level of 99.73% (i.e., a risk α of 0.27%) by using the expression (μ - t.SE) + (μ - t.SE), where t is the critical value for a two-sided Student test and for n - 1 degrees of freedom. In a normally distributed population, a 99.73% confidence interval corresponds to the mean - 3 standard deviations. We considered the NLR of a new sample to be statistically significantly different from the RRS if its value was greater than the upper bound value of the confidence interval determined for the RRS data set. Furthermore, a given interaction was considered positive when, out of the three performed experiments, its obtained NLR value was two or three times above the calculated threshold.

KEGG pathways enrichment analysis. Enrichment analysis was performed using the ClueGO Cytoscape plug-in [339] and the KEGG pathway data base [343–345]. Two lists of ExoRDec factors and their first neighbors in the human proteome retrieved from the APID2net database [338], were generated according to whether they interact (294 proteins) or not (664 proteins) with viral proteins. ClueGO parameters were set as follows: Statistical Test Used = Enrichment/Depletion (Two-sided hypergeometric test), Correction Method Used = Benjamini-Hochberg, Min GO Level = 3, Max GO Level = 8, Combine Clusters With 'Or' = true, Percentage for a Cluster to be Significant = 75.0, GO Fusion = true, GO Group = true, Kappa Score Threshold = 0.45.

siRNA assays. siRNAs were purchased from Dharmacon (ON-TARGETplus SMARTpools and Nontargeting Control pool). Individual siRNAs targeting ERI1 were purchased from Sigma Aldrich. A549 cells were transfected with 25 nM siRNA with the Interferine transfection reagent (Polyplus). At 48 h post-transfection, cells were infected with H1N1 WSN (moi 10^{-4}

pfu/cell) or H1N1pdm09 (moi 10^{-3} pfu/cell) virus for 24 h. Plaque assays were performed on MDCK-Siat cells as described [346]. Cell viability was determined using the CellTiter-Glo Luminescent Viability Assay kit (Promega). To control the efficiency of siRNAs targeting ExoRDec genes, siRNA-treated A549 cells were transfected with plasmids encoding an ExoRDec protein fused with the full-length *Gaussia* luciferase (pGlucFL-ExoRDec) using polyethylenimine PEI (Polysciences Inc). The luciferase activity was measured 24 h later in cell lysates using the Renilla luciferase assay reagent (Promega) and a Berthold CentroXS luminometer.

Antibodies and immunoblots. Protein extracts were prepared in Laemmli buffer. Immunoblot membranes were incubated with primary antibodies directed against ERI1 (MABE894, Merck), A/PR/8/34 virions [347], NS1 (kindly provided by Daniel Marc, INRA-Tours, France), PB2 (GTX125926, GeneTex), NP (HT103, Kerafast), M1 (GA2B, Pierce), NA (GeneTex), GAPDH (Pierce), α-Tubulin (Sigma, T6199), *Gaussia* luciferase (New England Biolabs), and revealed with secondary antibodies (GE Healthcare) or peroxidase-conjugated Strep-Tactin (IBA), and with the ECL 2 substrate (Pierce). The chemiluminescence signals were acquired using a G-Box and the GeneSnap software (SynGene).

Overexpression experiments. HEK 293T cells were seeded in 24 well plates at 5.10^5 cells per well and transfected with 600 ng of Strep-ERI1 plasmids with linear PEI (polyethylenimine). At 24 hpt cells were infected at an moi of 5 pfu/cell with H1N1 WSN. At 3.5 hpi total RNA was extracted using the RNeasy mini kit (Qiagen).

RT-qPCR assays. RNAs were extracted using the RNeasy mini kit (Qiagen) from H1N1 WSN infected A549 cells. Strand-specific RT-qPCR for NP and NA vRNAs and mRNAs were performed as described in [348]. For HIST1H2AB mRNA amplification reverse transcription was carried out using random hexamer and SuperScript II following manufacter's instructions. qPCR was performed using SYBR green reagent (Agilent Technologies) on a Light Cycle 480 (Roche) using primers allowing the specific detection of NP and NA vRNA and

mRNA as in [348] or HIST1H2AB F (5'-cacacgccccaagagtttat-3') and HIST1H2AB R (5'-ctccgcaaaggcaactactc-3') primers to detect HIST1H2AB mRNA [317].

Strep-tag-mediated purifications. HEK 293T cells were transfected with Strep-ERI1 or Strep-empty expressing plasmids and infected at an moi of 5 pfu/cell with H1N1 WSN. Infected HEK 293T were resuspended in lysis buffer (20 mM MOPS-KOH pH 7.4, 120 mM KCl, 0.5% Igepal, 1X Protease Inhibitor Cocktail (Roche) supplemented with 200 U/mL RNasin (Promega) or 100 µg/mL RNase (Thermo Scientific). Clarified lysates were incubated with Strep-Tactin beads (StrepTactin Sepharose High Performance, GE Healthcare) for 1 h at 4°C. Beads were washed three times in lysis buffer. Protein complexes were eluted from StrepTactin beads with desthiobiotin (IBA). Pulled samples were either diluted in Laemmli sample buffer and analyzed by western blot or in RLT buffer (RNeasy mini kit, QIAGEN) for RNA analyzes.

PB2 purification. HEK 293T cells were transfected with Strep-ERI1 or Strep-empty expressing plasmids and infected at an moi of 5 pfu/cell with H1N1 WSN. Infected HEK 293T cells were resuspended in lysis buffer (20 mM MOPS-KOH pH 7.4, 120 mM KCl, 0.5% Igepal, 1X Protease Inhibitor Cocktail (Roche) supplemented with 200 U/mL RNasin (Promega) or 100 µg/mL RNase (Thermo Scientific). Clarified lysates were cleared for 1 h at 4°C with dynabeads protein A (Invitrogen) and then incubated with anti PB2 antibodies (GTX125926, Genetex) overnight at 4°C. Protein complexes were allowed to bind to dynabeads protein A for 1 h at 4°C. Beads were washed three times in lysis buffer. Pulled samples were either diluted in Laemmli sample buffer and analyzed by western blot or in RLT buffer (RNeasy mini kit, QIAGEN) for RNA analyzes.

Generation of ERI1 knock-out cell lines. HEK 293T or A549 cells were seeded into a 12 well plate to achieve 80% confluency the following day. 24 h later, cells were transfected with a combination of two different pSpCas9(BB)-2A-Puro plasmids containing a target sequence complementary to ERI1 using JetPrime. Primers containing guide sequences were as follows: 1st set: ERI1 F 5'- caccgtatgacttccgaatattgat-3', ERI1 R 5'- aaacatcaatattcggaagtcatac-3'; 2nd

set : ERI1 F 5’- caccgccggcaggctctttactctg-3’, ERI1 R 3’- aaaccagagtaaagagcctgccggc-5’. Once cells were fully confluent, the medium was replaced by complete DMEM containing 2 µg/ml puromycin for A549 cells or 2.5 µg/ml puromycin for HEK 293T cells to select for cells expressing Cas9. 72 h later, cells were diluted and seeded into a 96 well plate at 1 cell/well in complete DMEM. Wells that contained a single colony were expanded until enough cells were available for total cell extract. For each candidate knock-out cell line, extinction of ERI1 was monitored by western blot using anti ERI1 antibody (MABE894, Merck).

Minireplicon assay. Wild-type and HEK 293T ERI1 KO cells were transfected with a plasmid directing the expression of a firefly reporter minigenome (mini-replicon), with plasmids encoding the viral proteins PB2, PB1, PA and NP as well as with a renilla reporter plasmid to assess transfection efficiency. At 24 hpt Firefly and renilla activities were measured using the Dual-Glo luciferase assay system (Promega). Firefly activity was normalized using the measured renilla activity. Each ratio was then expressed as a percentage of the wt activity measured in wt HEK 293T cells.

Discussion

Deciphering virus-host interactions is crucial to a better understanding of the viral transcription and replication processes. Here, we detected binary protein-protein interactions between IAV proteins and a dedicated set of cellular proteins carrying exonucleases activities and/or associated to RNA decay (ExoRDec library). We looked for interactions between cellular proteins of the ExoRDec library and components of the vRNPs (PB2, PB1, PA and NP), viral proteins that associate to the vRNPs and are implicated in the regulation of transcription and replication (NS1 and NEP) or proteins that mediate nuclear export of neosynthesized viral vRNPs (M1 and NEP). This screen allowed the identification of several new candidate interactors of the viral proteins and highlighted a specific targeting of the RNA degradation pathway by IAV proteins. Through a targeted RNAi screen on the recovered PPIs we identified ERI1, a cellular exonuclease, as major cellular protein required for IAV multiplication. Further characterization of the role of ERI1 in the IAV life cycle showed that ERI1 was required for early viral transcription and recruited to transcribing vRNPs in a form that is bound to histone mRNA and associated to SLBP. Overall, our results provide new insights into the global hijacking of the RNA degradation pathway by IAVs and identified an original targeting of the cellular exonuclease ERI1 by the transcribing vRNPs.

In a first section we will discuss the PPI and RNAi screening strategies used as well as their outcome. The second section will more precisely address the role of ERI1 in the IAV life cycle and the questions arising from this work.

I. GPCA screening of the ExoRDec library and RNAi screening

1. Advantages and limitations of the main PPIs screening strategies

a. *Yeast two-hybrid assay and affinity purification followed by mass-spectrometry*

The main experimental techniques used for the identification of protein-protein interactions are the yeast two-hybrid assay (Y2H), which detects binary interactions, and affinity purification followed by mass spectrometry (AP-MS), which allows the identification of large complexes, and therefore of components that do not necessarily directly interact between each other. Due to the nature of the interaction they detect, theses techniques are complementary (reviewed in [349]). PPIs identified through those experimental approaches can further be supported by computational *in silico* techniques that can predict a full range of potential protein-protein interactions (structure or sequence based PPIs prediction for example) (reviewed in [350]).

Yeast two-Hybrid assay

Y2H is an *in vivo* method that relies on the association of two domains: a DNA binding domain, and an activation domain (responsible for activating DNA transcription), each fused to one of the tested protein. Upon interaction, both domains reconstitute a yeast transcription factor that allows subsequent transcription of a reporter gene. However, many false negatives and false positives can arise from such technique. The tested proteins need to both localize to the nucleus in order to elicit activation of the reporter gene transcription. Furthermore, interactions are studied in a yeast environment, which differs from a mammalian cell environment, especially in terms of post-translational modification or protein folding. Therefore, proteins that require specific post-translational modifications to carry out their function are unlikely to behave or interact in yeast the same way as they would in a mammalian cell environment [351]. Consequently, Y2H is associated to high rates of non specific interactions, and according to some studies, up to 50% of Y2H identified interactions may not be reliable [352]. However, Y2H still remains a widely used and powerful tool for high-throughput library screening. Mammalian Protein-Protein Interaction

Trap (MAPPIT) is an alternative two-hybrid technology based on the functional complementation of a cytokine receptor-signaling pathway [351]. This assay allows the exploration of PPIs in the cytoplasmic compartment and can be performed in mammalian cells, thereby avoiding caveats of post-translational issues reported in Y2H.

Affinity Purification followed by Mass-Spectrometry

Affinity Purification followed by Mass-Spectrometry (AP-MS) relies on the affinity purification (AP) of a bait protein, either by using an antibody targeting the endogenous protein, or by using over-expression of the tagged protein of interest, coupled with an antibody targeting the tag used. To gain specificity in the recovered complexes, purification is often realized using two sequential purification steps thanks to the TAP (Tandem Affinity Purification) tag, which consists of two sequential tags spaced by a viral protease cleavage site [353]. Complexes bound to the bait protein are then identified by mass-spectrometry (MS). As it relies on the purification of the endogenous protein, or of proteins overexpressed in mammalian cells, AP-MS avoids some of the limitations associated to Y2H, such as post-translational modifications or correct intracellular localization. However, during cell lysis, complexes can come into contact with irrelevant proteins, which may associate to the bait protein containing complexes, leading to identification of false positive interactors. Furthermore, due to the stringent lysis conditions generally used to reduce the identification of contaminating proteins as false positive interactors, AP-MS may not be a suitable methodology to detect transient interactions. Lastly, unlike Y2H, AP-MS can be biased towards the preferential detection of interactions between the bait protein and highly abundant cellular interactors (*i.e.* a protein expressed only to the level of a few molecules is less likely to be identified by MS than a highly abundant one) [349]. Methods such as SILAC (stable-isotope labeling by amino acids in cell culture) requiring the use of isotope labeled amino acids, are being used to increase AP-MS sensitivity and specificity [354]. Thus, AP-MS is a very powerful methodology to decipher the composition of complexes, however, it does not allow to precisely identify binary interactions within the identified protein complexes.

b. *GPCA*

Protein Complementation Assays (PCA) are based on the reconstitution of an active reporter protein upon interaction of the tested protein pair. PCA requires that the two fragments of the split reporter protein have no or very limited intrinsic activity on their own and that their reconstitution gives rise to a signal sensitive enough to be detected. Assays based on the reconstitution of a fluorescent protein *in vivo*, such as the Bimolecular Fluorescence Complementation (BiFC) assay, have been used for genome wide PPIs screening and have the advantage of allowing detection of PPIs directly in living cells [355]. However, the fluorescence intensity of the reconstituted reporter protein must be bright enough to be distinguished from the cell background signal. For the GPCA technique, the *G. princeps* luciferase is split into two fragments (Gluc1 and Gluc2) and each fragment is fused to one of the two proteins of interest [356]. Upon interaction of the two partners a complete *G. princeps* luciferase is reconstituted and a luminescent signal can be detected upon addition of coelenterazine, the substrate of the *G. princeps* luciferase [334,356].

Unlike, Y2H and AP-MS, GPCA allows the detection of binary interactions in a mammalian cellular environment. Furthermore, transient interactions are detectable in GPCA, contrary to Y2H and AP-MS, which are more suitable to detect stable interactions. This assay has successfully been used in the past, combined with Y2H, to compare interaction profiles of different Human Papilloma Virus (HPV) genotypes and more recently to compare interaction profiles between different IAV strains [335,357,358].

However, GPCA bears the limitation to be restricted to non-infectious contexts unlike AP-MS that can be performed in infected cells. Therefore, interactions that are specifically induced by changes in the cellular environment due to infection, or that rely on the assembly of viral protein complexes upon infection, may not be detected. This would be the case for instance, for the assembled trimeric IAV FluPol and/or the vRNPs. To avoid this bias, iPCA (infectious PCA) has been developed, where A/WSN/33 viruses expressing a PB2-, PB1- or PA-Gluc1 fusion protein provide a means to explore interactions between the viral polymerase and the host proteome in an infectious context. Furthermore, this method can address PPIs throughout the entire viral cycle allowing the identification of interactions that

are required for specific steps of the cycle. This method has been successfully used to identify cellular proteins interacting with viral proteins during IAV infection [336].

However, like Y2H and AP-MS, GPCA relies on the overexpression of tagged proteins, which implies the existence of potential bias. On the one hand, overexpression of recombinant proteins can alter subcellular localization or lead to subcellular expression patterns that do not reflect those of the endogenous protein. Furthermore, the overexpressed protein may not assemble properly into protein complexes as it would in physiological conditions or even induce cytotoxicity. All of those caveats can potentially lead to the identification of false positive interactions. On the other hand, addition of the Gluc1 or Gluc2 tag either fused to the Nter or Cter extremity of the protein of interest can alter its cellular localization, folding, turnover rate as well as its interactions. To reduce the potential bias associated to the addition of a tag and to increase the exhaustiveness of the detected interactions, PPI screening using GPCA should be applied using the four possible tag configurations (*i.e.* Gluc1 in Nter or Cter and Gluc2 in Nter or Cter, for the two tested proteins). New techniques combining different expression systems and assays as well as different tag configurations such as the novel NanoLuc two-hybrid (N2H) system (referred to as an “assayome”) that integrates 12 different assays and tag configurations allows maximal detection of positive interactions while avoiding detection of random protein pairs [359]. However, this multiplication of tag configurations and assays rapidly becomes out of reach for routine screening strategies and require high-throughput screening platforms. Therefore, hits identified through GPCA, like those identified through Y2H or AP-MS, need to be orthogonally validated using complementary techniques such as co-immunoprecipitation.

2. PPI screening unravels a specific targeting of RNA degradation pathways by IAV proteins

Viruses rely on host factors to complete their cycle. Moreover, creating a favorable environment for their replication and spreading, or counteracting cellular anti-viral responses, is key to a successful infection. Establishment of such favorable environment occurs notably through rewiring of cellular gene expression by usurping cellular RNA decay machineries (see section III. of the introduction). Such hijacking primarily relies on virus-host interactions, as PPIs can have multiple roles in regulating cellular pathways, modifying enzyme kinetic properties or inducing cellular relocalization. Therefore, identifying virus-host interaction networks is essential to decipher viral replication mechanisms, thereby providing substantial knowledge that can be later used for the development of antiviral strategies.

a. *PPI network is shared between seasonal H1N1 and H1N1pdm09*

We screened the ExoRDec library against IAV viral proteins selected for their involvement in viral replication and/or transcription: PB2, PB1, PA and NP are components of the vRNPs while M1 is involved in mRNA export, and NS1 and NEP also take part in the transcription/replication mechanism as co-factors (see **Table 1**).

We selected viral proteins of two different influenza strains: A/Paris/650/2004(H1N1) (sH1N1) and A/Bretagne/7608/2009(H1N1pdm09). We choose those two strains as, given their drastically different origin and history, they provide an interesting basis for comparative interactomics studies.

The sH1N1 virus has been circulating in the human population since its reintroduction in 1977, while H1N1pdm09 was newly introduced in the human population in 2009 (the isolate used as a basis for the construction of our viral protein expressing plasmids is actually from 2009). Introduction of H1N1pdm09 led to replacement of sH1N1 as the seasonal circulating strain in the human population. The sH1N1 virus derived from the 1918 H1N1 pandemic virus which either arose by reassortment between an avian and a mammalian virus or directly from an avian virus by gradual adaptation to human without reassortment [63,64].

Due to its long history of circulation in the human population, all segments of the sH1N1 can be considered as of human origin.

On the other hand, segments of the H1N1pdm09 are of multiple origin: the M segment originated from the H1N1 eurasian avian-swine virus while the PB2, PB1, PA, NP and NS segments all originated from the H1N2 triple reassortant virus (PB2 and PA segments came from the avian H1N1, the PB1 segment from seasonal H3N2 virus circulating in the human population, while the NP segment came from an H1N1 virus of the classical swine lineage) [4] (**Figure 58** and **Table 6**) (see section I.3.c. of the introduction). Therefore, PB2 and PA segments of the H1N1pdm09 virus are of avian origin, the PB1 segment is of human origin, while NP, M and NS segments are of swine origin.

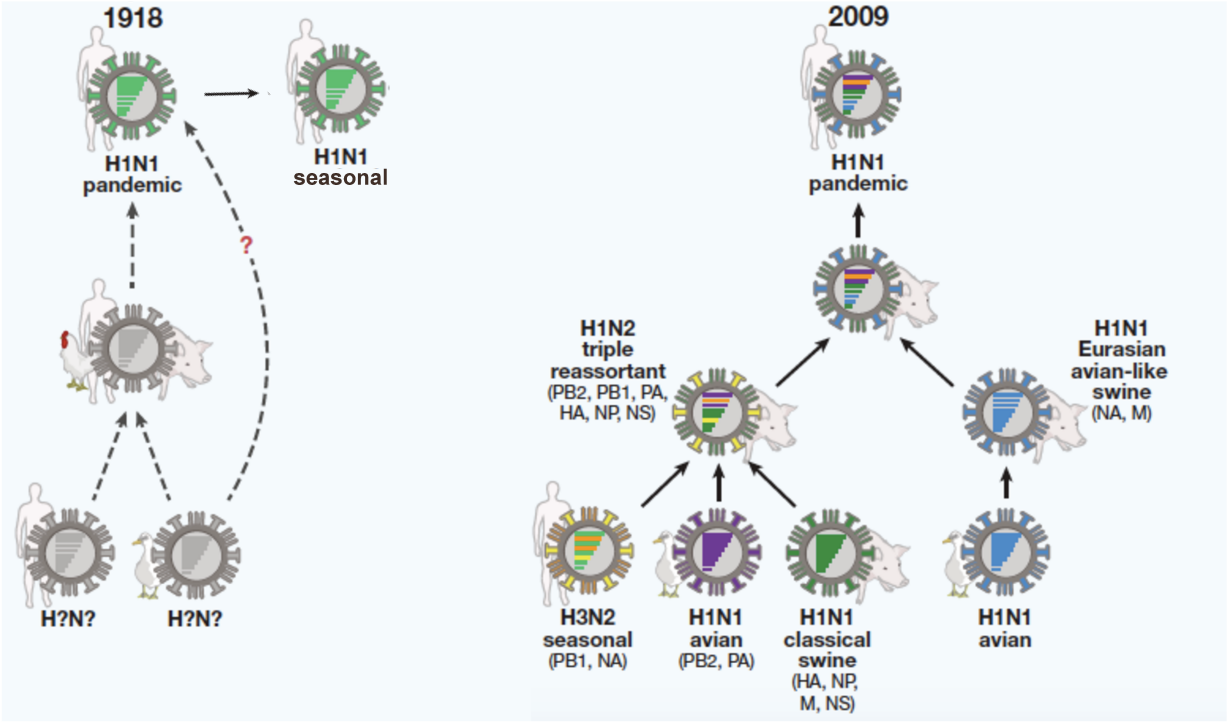

Figure 58: Origin of the sH1N1 and H1N1pdm09 viruses.
Reassortment history of seasonal H1N1 (sH1N1) and H1N1pdm09 is presented. sH1N1 originated from the 1918 pandemic H1N1 virus while the 2009 pandemic H1N1 virus originated from the reasortment between an H1N2 triple reassortant virus and an H1N1 eurasian avian-like swine virus. **Adapted from [4]**.

Segment	Virus	Host origin
PB2	H1N2 triple reassortant (avian H1N1)	Avian
PB1	H1N2 triple reassortant (seasonal H3N2)	Human
PA	H1N2 triple reassortant (avian H1N1)	Avian
NP	H1N2 triple reassortant (classical swine lineage H1N1)	Swine
M	Eurasian avian-like swine H1N1	Swine
NS	H1N2 triple reassortant (classical swine lineage H1N1)	Swine

Table 6: H1N1pdm09 segment origin.
Only segments encoding the proteins included in the screen are displayed.

Surprisingly, although all segments encoding the viral proteins included in our screen come from diverse origin, interaction profiles between sH1N1 and H1N1pdm09 were found to be very similar. Only three interactions were found with H1N1pdm09 but not with sH1N1: APEX1 with NEP and M1 as well as ADAR with M1. However, their relevance is questionable as NLR values obtained for those three interactions were just above or below the positive threshold, respectively for H1N1pmd09 and sH1N1 proteins. Furthermore, most of the interactions identified with the M1 proteins may not be reliable as NLR values and calculated positive threshold, were low overall. This could be due to the nature of the M1 protein, which forms oligomers. Oligomerization of M1 in the cell could mask or make inaccessible the Gluc1 tag, thereby making M1 less suitable as a bait for GPCA screening. Nonetheless, GPCA screening of the ExoRDec still identified robust interactors of M1. Indeed, ERI1 was originally identified in our GPCA screen as an interactor of M1 and was later confirmed in our study by an orthogonal validation method (co-immunoprecipation in both infectious and non-infectious contexts) as a true interactor of M1. Furthermore, GPCA may be optimized for the detection of M1 interactors, either by using a larger set of RRS, thereby increasing the robustness of the calculated positive threshold, or by applying a more stringent method to select positive interactions.

Among the identified hits of our screen, some proteins were highly targeted by viral proteins (*i.e.* targeted by three or more viral proteins): ADAR, ADARB1, ERI1, HMGA2 and EXOSC6. This could reflect the importance for the virus to target precise pathways in which those proteins are involved. Interestingly, EXOSC6, a subunit of the RNA exosome, was identified in another study by AP-MS as an interactor of PA [251]. In our screen, EXOSC6 was

identified as a highly confident interactor of PB2, PB1, NEP and NS1. Although Rialdi and colleagues did not identify EXOSC6 as an interactor of PB2 and PB1, they demonstrated that the FluPol hijacks the RNA exosome and recycles junk capped cellular RNAs, that would otherwise be targeted to degradation, to prime viral transcription (see section II.3.a. of the introduction) [251]. Components of the vRNPs, as well as NEP and NS1 proteins, are all involved in viral transcription. Therefore, it is not surprising that the RNA exosome, required for viral transcription, is highly targeted by viral proteins. This example clearly demonstrates the requirement for orthogonal validation to specifically define interactions networks and points to the limitations of the AP-MS and GPCA methods. Indeed, PB2 and PB1 may not have been recovered as interactors of EXOSC6 due to the limitations inherent to AP-MS: interaction between EXOSC6 and viral proteins may be too weak and were therefore lost due to the lysis conditions, or the interaction may be transient, and is consequently not detected through AP-MS but could however be detected by GPCA. One the other hand, this also points to the limits of GPCA, as we did not recovered PA as an interactor of EXOSC6. Interestingly, only three cellular proteins were identified as PA interactors and NLR values obtained with PA were very low. Therefore, PA, similarly to M1, may also not be a suitable bait for GPCA screening or its screening by GPCA may require specific optimizations.

Altogether, the interaction networks identified can be considered as highly similar when comparing both tested strains, suggesting a targeting of cellular pathways that are greatly conserved between IAVs, and might therefore play an essential role in the IAV life cycle. However, generalization of these observations will require analysis of the interaction network for other IAV strains of different host origins. It will also be of interest to determine whether the same pathways are prime targets for the other influenza virus types.

b. *A specific targeting of RNA degradation pathways by IAV viral proteins*

RNA decay is a central cellular mechanism as it controls RNA stability and thereby regulates gene expression in eukaryotic cells. Mounting of an efficient antiviral response relies on transcript stability regulation and efficient gene expression, while successful viral infection relies on a rewiring of the cellular environment, and therefore of cellular gene expression, to promote viral replication. Consequently, to control viral and cellular gene expression, interfacing with RNA decay machineries is inevitable. As discussed in depth in section III. of the introduction, not only have viruses evolved ways to escape host directed RNA degradation, but they have also evolved mechanisms to hijack RNA decay pathways to promote viral replication.

IAV interacts with many cellular exonucleases (such as ISG20, RNase L or components of the RNA exosome [251,273,282,284]). However, the interplay between IAV proteins and cellular RNA decay machineries has never been specifically addressed. Our systematic screening strategy allowed us to identified 19 robust interactors among the 75 tested proteins from the original ExoRDec library and highlighted a specific targeting of RNA degradation pathways by IAV proteins. It should be noted that some PRS (positive controls) regularly generated luminescence values under the positive threshold supporting the high stringency of our assay. Eight of the factors identified as interactors in our screen were also found to be required for viral replication underlying that such stringent PPI screen allows the identification of functionally relevant factors to IAV infection (see section I.3.). Those identified factors involved in RNA stability or decay have various cellular roles and their implication in the IAV cycle could be multiple.

Our KEGG pathways enrichment analysis on the recovered PPIs and their first neighbors found in the human proteome identified a specific targeting of RNA degradation pathways by IAV viral proteins. As several studies have already pointed to RNA decay as a pathway targeted and hijacked by other RNA viruses, the specific targeting of RNA degradation pathways by IAV highlighted here is not surprising (reviewed in [205–210]).

Although the cluster of non-interacting proteins was enriched, among others, in the mRNA surveillance pathway, which is a specific RNA degradation pathway, only the cluster of interacting proteins was specifically enriched in the overall RNA degradation pathway. The

latter includes, the RNA exosome and its associated cofactors, de-capping and de-adenylation complexes, exonucleases and cofactors involved in 5'-3' RNA decay, as well as factors involved in the mRNA surveillance pathway (**Figure 59**). This enrichment further supports a global targeting of the whole RNA degradation process by IAV, as already suggested by several independent studies, which reported a specific targeting of several components of the RNA degradation pathways by IAVs [121,251,273,281,282,284].

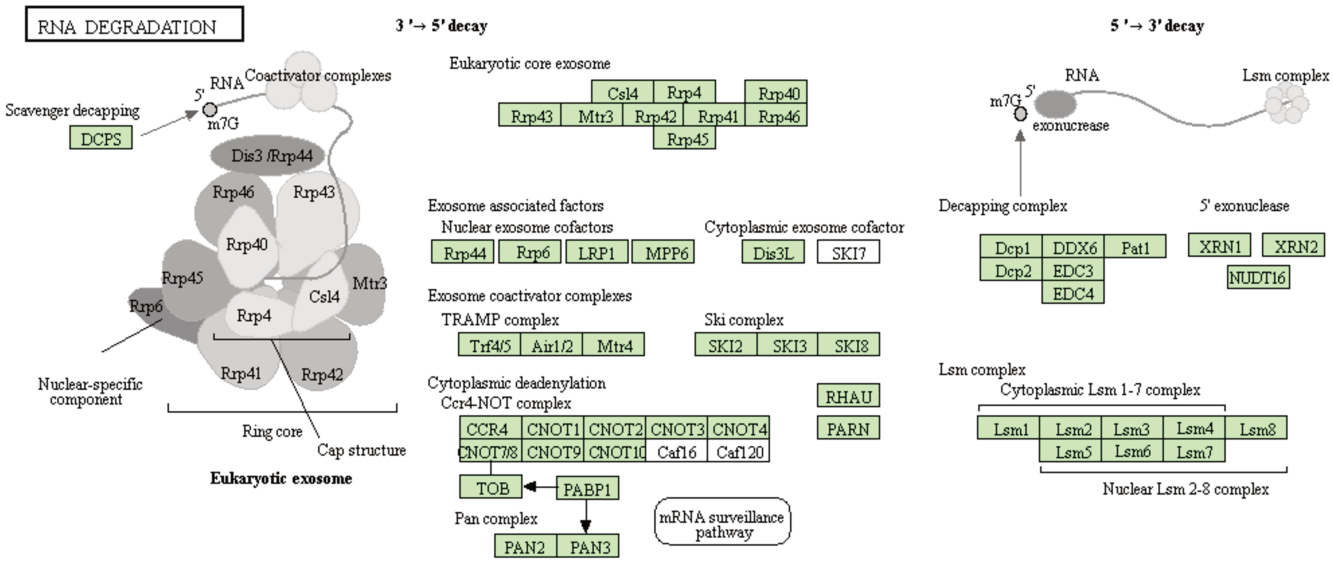

Figure 59: RNA Degradation KEGG Pathway.
RNA degradation KEGG pathway description, obtained **from [360]**, generated thanks to the KEGG pathway data base [343–345].

IAVs interact with several factors involved in RNA decay, as described in section II.3., and numerous examples point towards a wide targeting of the RNA degradation pathway during IAV infection. Notably, the de-adenylation factor PAN3 was identified in our screen as an interactor of NS1 in both tested IAV strains. This further supports the interplay between NS1 and cellular polyadenylation pathways, as the NS1 protein is already known to interfere with the 3' end formation of host mRNAs by interacting with the human cleavage-polyadenylation specificity factor 30 (CPSF30) [194,195]. Furthermore, de-adenylation factors are notably concentrated in cellular structures such as processing bodies, which regroup several mRNA decay enzymes. Interestingly, formation of RAP55 containing

processing bodies is blocked by IAV infection [281]. Therefore, the identification of PAN3 as an interactor of IAV proteins further supports the IAV interplay with processing bodies.

IAV polymerase also interacts with the RNA exosome, and hijacks capped host transcripts targeted to degradation which are then used as primers for viral transcription [251]. Remarkably we identified two subunits of the RNA exosome, EXOSC6 and EXOSC8 as interactors of viral proteins PB2, PB1, NS1 and NEP, or M1 and NEP, respectively. EXOSC8 was already identified in a Y2H assay as an interactor of M1 from the A/Puerto Rico/8/1934(H1N1) strain [361]. As previously mentioned in section I.2., such redundant targeting of the RNA exosome by viral proteins is not surprising given its essential role in viral transcription [251].

3. Functional relevance of identified factors

Overall, among the 19 recovered interactors, knock-down of eight of the ExoRDec proteins was found to significantly impair IAV multiplication which further highlights the performance of the stringent protein-protein interaction screen applied here for the identification of functionally relevant factors.

Among the factors required for IAV replication we identified the Double-stranded RNA-specific adenosine deaminase ADAR, already shown in a Y2H assay as an NS1 interactor and found to be required for IAV replication [362]. Furthermore, we reported that silencing of PAN3, a subunit of the PAN2-PAN3 de-adenylation complex, was associated with impaired viral replication. Interestingly, PAN2 was previously found in a screen to be necessary for the replication of three different IAV strains (H1N1 WSN, H1N1pdm09 and A/Centre/1003/2012(H3N2)) [335]. We also showed here the requirement of the U6 snRNA phosphodiesterase USB1, an exoribonuclease responsible for trimming the poly(U) tract of the pre-U6 snRNA molecule, required for the formation of mature U6 snRNA [363], previously identified in a CRISPR/Cas9 screen, and found to be essential for the replication of an avian H5N1 strain [151].

In addition, the Apoptosis-Enhancing Nuclease AEN, a nuclease required for p53 induced apoptosis, and the DNA-(apurinic or apyrimidinic site) lyase APEX1, a multi functional nuclease, besides their involvement shown here in IAV replication, were also described as

important for the replication of other RNA viruses such as the enterovirus EV71 or rotavirus and VSV respectively [364–366].

Finally, ERI1 was identified as a major hit of our screening strategy. ERI1 belongs to the DEDDh exoribonucleases family. Among this family, few exonucleases have been reported to be essential for RNA virus multiplication. However, an ERI1 homologue, the putative 3'-5' RNA exonuclease ERI3, is critical for DENV-2 RNA synthesis and viral particle production, and was found to associate with DENV-2 RNA [367]. Coronavirus nsp14 has been shown to carry an exoribonuclease activity required to maintain replication fidelity, while Lassa fever virus nucleoprotein possesses a DEDDh exonuclease activity essential to suppress host innate immune system activation [278,280].

The importance of DEDDh exoribonucleases reported for several major RNA viruses, thus prompted us to focus on the cellular exoribonuclease ERI1.

II. The cellular exonuclease ERI1 as a new factor required for IAV replication

The exoribonuclease ERI1 was found in our GPCA screen as an interactor of viral proteins PB2, PB1, NP and, to a lesser extent, M1. We later confirmed this interaction profile both in infectious and non-infectious context through co-immunoprecipitation experiments, which pointed to the vRNP components PB2, PB1 and NP as the major interactors of ERI1.

Furthermore, our RNAi screen identified ERI1 as required for IAV replication as silencing of ERI1 is associated to a reduced viral infectious particles production as well as to a reduced viral protein and viral RNAs accumulation.

1. Cellular impact of ERI1 knock-out

To further analyze the mechanisms by which ERI1 promotes IAV multiplication, we generated ERI1 knock-out A549 and HEK 293T cell lines through CRISPR-Cas9 technology. As mentioned in the results section, generation of ERI1 KO A549 cell lines was challenging as two rounds of CRISPR transfection and clonal selection were required to achieve complete ERI1 knock-out. This is most likely explained by the polyploidy of the A549 cell lines, rendering the targeting of the many copies of a given gene by the small guide RNAs and the Cas9 difficult [341]. Once obtained, ERI1 KO cell lines behaved similarly to wt cells in terms of growth rate.

We confirmed the requirement of ERI1 for IAV replication already observed *via* siRNA silencing, by comparing viral protein accumulation upon single cycle infection in KO and wt cell lines. However, it appeared that our ERI1 KO cell lines somehow quickly overcame the loss of ERI1 during cell culture. Defects in IAV replication were no longer evident in our KO cell lines, rendering them unusable for the rest of our study. Nonetheless, ERI1 deficiency appears to be well tolerated by cells and ERI1$^{-/-}$ mice have been successfully obtained [294]. However, such ERI1 deficiency in mice is associated with high rates of neonatal mortality (less than 10% of ERI1 KO mice survived to the weaning age and most of the mice died during the first two days post-partum), as well as growth defects (reduced body size that remained even in adult mice) [294]. Furthermore, murine embryonic fibroblasts from ERI1$^{-/-}$

mice also displayed slower doubling times than wt cells when cultured *in vitro.* Ansel and colleagues speculate that such defects observed in ERI1$^{-/-}$ mice may be linked to the role of ERI1 in 5.8s rRNA maturation as the ERI1$^{-/-}$ mice phenotype resembles phenotypes observed in patients and mice bearing mutations in ribosomal proteins [294]. ERI1 is also involved in miRNA homeostasis and lymphocytes from ERI1$^{-/-}$ mice display an increase in general miRNA abundance [302]. As miRNAs are also major regulators of cell and organ development [368], the ERI1$^{-/-}$ mice phenotype could alternatively be associated to an impaired regulation of miRNA abundance during development.

Histone mRNAs and protein level increase as cells enter S phase in order to meet the histone requirement during DNA replication. Conversely, their levels decrease at the end of the S phase. Equilibrium between DNA replication and histone synthesis is crucial, as improper balance leads to genomic instability [309]. Possible genomic instability in ERI1 KO cells could disturb those interactions essential for the IAV life cycle, thus interfering with viral replication. Viral transcription and replication are proposed to take place at nuclear matrix and/or near chromatin components [157]. Interactions between the FluPol and chromatin remodelers such as CHD1 and CHD6, nuclear matric protein 2 (NXP2) and hCLE, which modulates RNA Pol II activity, have been reported [159,160,162,163]. Furthermore, proper chromatin dynamics and architecture are crucial as they modulate the initiation and elongation steps of transcription and RNA Pol II recruitment, and active transcription is known to be required for cap-snatching to prime IAV transcription [369]. Nevertheless, our ERI1 KO cell lines quickly compensated the loss of ERI1. As ERI1 deficient cells have been reported to normally progress in the cell cycle [329], alternative mechanisms such as inhibition of histone mRNA translation or alternative pathways of histone mRNA degradation could have appeared in ERI1 KO cells, preventing genomic instability and thereby allowing efficient IAV replication. Such possibility would strongly support a model where the role of ERI1 in histone pre-mRNAs processing and/or histone mRNAs decay is required for IAV replication.

2. ERI1 functions and IAV cycle

Silencing of ERI1 or ERI1 knock-down is associated to a reduced viral infectious particles production, and a reduced viral protein and viral RNAs accumulation. This effect is most pronounced at early times of the IAV life cycle as seen for the early viral proteins PB2, NP and NS1. At later times of the viral cycle, *i.e.* 6 hpi in single cycle infection, the effect on early viral proteins is no longer detected but a decrease in the late proteins M1 and NA is observed. Furthermore, silencing of ERI1 has a lasting effect in multi cycle infection, where a delay in viral infectious particles production is maintained up to 72 hpi.

ERI1 involvement in viral transcription was further confirmed thanks to cycloheximide experiments. Indeed, as cycloheximide blocks *de novo* translation, synthesis of cRNA and vRNA, which requires newly synthesized viral proteins, is blocked, therefore allowing to specifically and solely address viral transcription. The role of ERI1 in viral transcription was further supported by the preferential interaction of ERI1 with the PB2 Cter detected in GPCA experiments. Indeed, ERI1 does not interact with PB2 Nter while it strongly interacts with PB2 Cter, which notably encompasses the PB2 cap-binding domain essential for cap-snatching and therefore, for viral transcription.

The functions of ERI1 have been extensively documented thanks to studies addressing its role in histone mRNA decay and rRNA processing. Those studies characterized two main functions of ERI1: RNA binding and 3'-5' exonuclease. Using overexpression experiments we showed that both ERI1 activities were crucial to its role in IAV transcription.

a. *ERI1 RNA binding activity*

We further addressed the requirement of ERI1 RNA binding activity by first characterizing more in depth the interplay between ERI1 and the viral proteins. We showed that ERI1 interaction with viral proteins; both in infectious and non-infectious context, was RNase sensitive. While treatment with RNase of the infected cell lysates almost completely abrogated interaction between ERI1 and viral proteins, the same treatment in non-infected cells only led to a partial lose of the interaction. Although the interaction is RNase sensitive, we therefore cannot exclude that the interaction between ERI1 and viral proteins is also, to some extent, supported by direct protein-protein interactions.

Interestingly, we found that viral RNAs were co-purified with ERI1 in infected cells. Greater amounts of viral mRNAs were retrieved upon ERI1 purification compared to vRNAs. This specific enrichment, coupled to our interactomics data and the role of ERI1 in viral transcription points to a specific targeting of ERI1 by the transcribing vRNPs. As ERI1 interacts with viral RNAs, this could be an easy explanation for the RNase sensitivity of the interaction. However, interaction between ERI1 and viral proteins is also partially RNase sensitive in a non-infectious context, rather pointing to the role of a cellular RNA in the interaction. IAV transcription occurs in the nucleus of infected cells. In the nucleus, ERI1 is known to bind histone mRNA, participating in its processing along with SLBP. Upon PB2 purification in infected cells, ERI1 and SLBP as well as histone mRNAs are retrieved. Furthermore, the interaction between SLBP and viral proteins is also sensitive to RNase treatment, similarly to what we described for ERI1. Altogether, this suggests that the viral polymerase specifically targets ERI1 forms that are in complex with histone mRNAs in the nucleus.

To further address the potential interaction of the viral polymerase with an histone mRNA bound form of ERI1, we took advantage of the ERI1 ΔSAP mutant, reported to no longer bind histone mRNAs, while maintaining an intact exonuclease activity [293]. Remarkably, the ERI1 ΔSAP mutant was impaired for binding to histone mRNAs but also for its association with viral RNAs further highlighting the importance of ERI1 RNA binding activity.

Altogether, our data point to a model where the role of ERI1 in the IAV life cycle and its interaction with viral proteins require a tight association with histone mRNAs. This interaction is greatly dependent on RNA and is probably also stabilized by direct protein/protein interactions. However this complex pattern of interaction does not allow us to discriminate between two possibilities. i) ERI1, bound to histone mRNA, could directly bind viral mRNAs in the nucleus and/or interact with the transcribing vRNPs. In this model, histone mRNAs are simply an obligatory by-stander due to their natural interaction with ERI1. Such direct interaction between ERI1 and the viral RNAs would also require a displacement of ERI1 from histone mRNAs to viral RNAs. ii) Alternatively, we could hypothesize that histone mRNAs associated to ERI1 and SLBP are targeted by viral proteins *via* their association with ERI1 for some, yet to be addressed, purpose. Both hypotheses are in line with our RNase digestion experiments, which both lead to the disassembly of the

transcribing vRNPs and of the histone mRNA/ERI1/SLBP complex, and to the loss of the ERI1/viral proteins interaction (**Figure 60**).

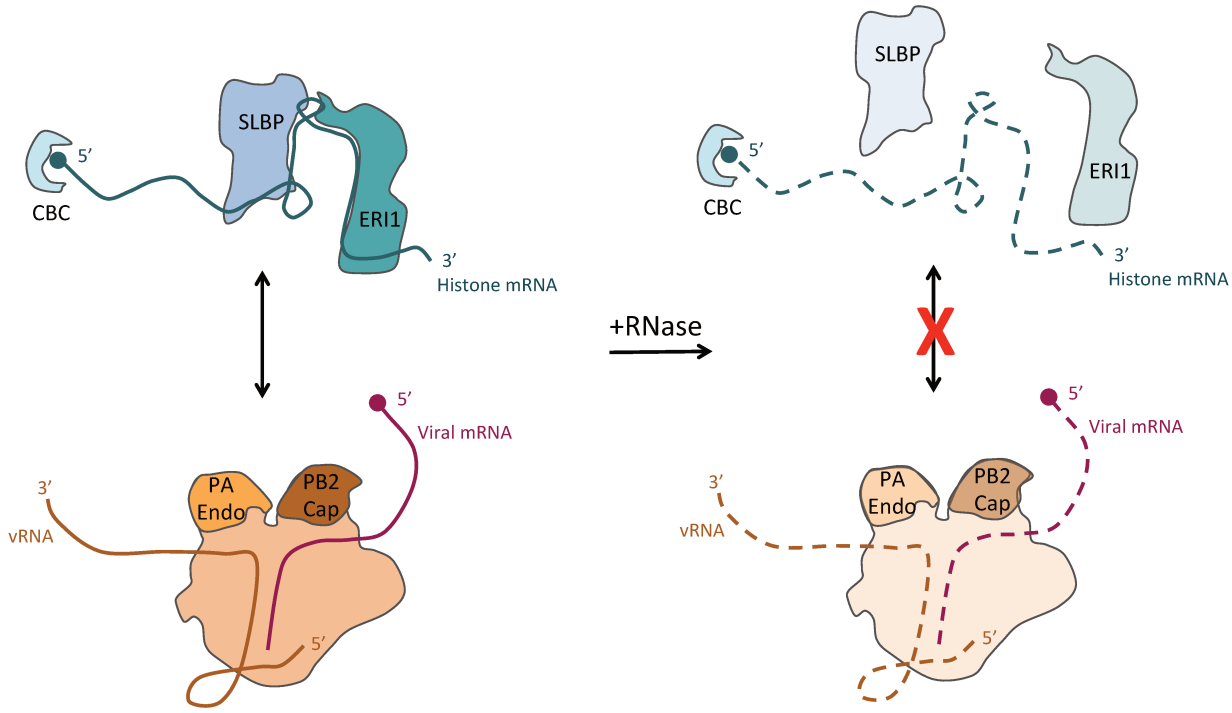

Figure 60: Model of the RNase sensitive interaction between ERI1 and viral proteins.
In the nucleus, capped histone mRNAs are bound by SLBP and ERI1. The transcribing vRNPs contacts ERI1 bound to histone mRNAs. Upon RNase treatment, SLBP and ERI1 are dissociated from histone mRNAs. RNase treatment also destabilizes the transcribing vRNPs and the dynamic configuration of the FluPol is rearranged due to loss of binding to viral RNA. Ultimately, this leads to the loss of interaction between ERI1 and the viral proteins. CBC: cap binding complex, PA Endo: Endonuclease domain of PA, PB2 Cap: Cap-binding domain of PB2.

b. *ERI1 exonuclease activity and substrates*

The ERI1 exonuclease activity was required to promote IAV transcription. Furthermore, as it retained the ability to interact with viral proteins without supporting viral transcription, the ERI1 no DE mutant even appeared to act as a dominant negative form of ERI1.

So far, all described ERI1 processing mechanisms point to a prime role of ERI1 in 3’ end trimming. As already mentioned, ERI1 in involved in the 3’ end trimming of histone pre-mRNAs leading to their full maturation and is also involved in initiating histone mRNAs decay by degrading their 3’ end. In addition, loss of ERI1 in the mouse model is associated with a two fold increase in general miRNA abundance [302]. However, the mechanism involved in

miRNA regulation is not clear, but trimming of miRNA 3' overhangs by ERI1 could be involved (see section IV.2.a. and b. of the introduction) [288]. Finally, ERI1 also mediates the cytoplasmic trimming of 5.8S rRNA. By base pairing with the 5' end of the 28S rRNA, the 3' end of the 5.8S rRNA forms a duplex, leaving a 3' ssRNA overhang cleaved by ERI1 [294].

Trimming of histone pre-mRNAs by ERI1 requires the recognition of the 3' stem loop. However, ERI1 trimming of other RNA species such as 5.8S rRNA, siRNA or miRNA does not seem to require neither a specific RNA sequence nor structure aside from the existence of a 3' ssRNA overhang. Therefore, multiple RNA species can be potential ERI1 substrates. As ERI1 exonuclease is required for efficient viral transcription, either the trimming of one of its known targets, and/or trimming of a yet to be characterized cellular or viral target, is important for IAV transcription.

Viral substrates

Viral mRNAs or small viral RNAs (svRNAs) could be envisioned as potential ERI1 substrates. svRNAs are 22 to 27 nucleotides long viral RNAs corresponding to the 5' end of genomic viral RNA, generated from cRNA during viral replication and thought to promote the transcription/replication switch (see section II.2.c. of the introduction) [134,135]. However, since our data suggest that ERI1 is most likely involved in viral transcription, it is hard to reconcile our results with a model where ERI1 would take part in svRNAs processing. Although IAV mRNAs are mostly unfolded *in vivo*, they display a few stably-folded structural motifs, including some stem loop structures, localized close to transcripts ends, that could be a basis for ERI1 binding and processing [370]. Therefore, it would be interesting to analyze the sequence and length of the 3' end of viral mRNAs for possible ERI1 trimming as well as the svRNA repertoire upon ERI1 silencing.

Cellular substrates

Considering known cellular targets of ERI1, it is interesting to note that some studies reported that 5.8S rRNA processing as well as histone mRNA decay only require small amounts of ERI1 suggesting that silencing by siRNA usually would not affect those processes [294,330]. However, miRNA processing by ERI1 seems to be more sensitive to ERI1 silencing, as heterozygous ERI1$^{+/-}$ mice show alteration in miRNA abundance [302]. Furthermore, some

miRNAs have been reported to interfere with IAV replication, such as miR-584-5p and miR-1.249, or miR-323, miR-491, and miR-654, respectively inhibiting H5N1 and H1N1, by targeting PB2 and PB1 genes, respectively [371,372]. ERI1 could therefore be recruited by viral proteins to target specific miRNA degradation and thus promote viral replication. It would thus be interesting to compare miRNA abundance and viral mRNA stability in infected cells silenced for ERI1 or treated with non-target siRNAs.

The defect observed in viral transcription in ERI1 silenced cells is unlikely to be linked to ERI1 role in 5.8S rRNA processing. First, ERI1 silencing is associated to impaired viral transcription. However, a defect in ribosomal biogenesis would rather lead to impaired viral translation without impairing viral transcription. Furthermore, Ansel and colleagues reported that upon overexpression of ERI1 mutants defective in RNA binding, efficient trimming of 5.8S rRNA was still observed, and that the SAP domain only increases the efficiency of this 3' end processing [294]. However, we do not observe such effect here, as overexpression of ERI1 RNA binding mutants is not associated to an increased viral transcription unlike what is observed upon overexpression of ERI1 wt.

Our data showed that ERI1 is required for viral transcription and vRNPs are co-purified in an RNase sensitive manner with SLBP and ERI1, as well as with histone mRNAs in infected cells. Hence, requirement of the exonuclease activity of ER1 to promote viral transcription may be merely linked to its role in histone mRNA processing.

3. Possible hypothesis for IAV targeting of histone mRNA processing factors

a. *ERI1 and cap-snatching*

Both histone pre-mRNA processing by U7 snRNP and cap-snatching occur co-transcriptionally [116,373], and ERI1 is recruited to histone pre-mRNAs co-transcriptionally in a U7 dependent manner [374]. Moreover, we found that ERI1 preferentially binds to the PB2 Cter, which notably contains the cap-binding domain [375]. Hence, we can hypothesize that interaction of FluPol with ERI1 could contribute to efficiently target sites of RNA Pol II transcription, and that histone mRNAs could represent a profuse source of capped primers used to prime viral transcription. A similar mechanism has been proposed to explain the requirement of the Ribosomal RNA Processing 1 Homolog B protein (RRP1B) in IAV cycle.

Upon IAV infection, RRP1B is relocalized from the nucleolus to the nucleoplasm where viral transcription most likely occurs [164]. Depletion of RRP1B significantly impairs viral infectious particles production and viral transcription. Furthermore, RRP1B has been reported to interact with PB2 and PB1 and to specifically enhance the recruitment of the FluPol to cellular mRNAs, thereby promoting cap-snatching and viral transcription [164] (**Figure 61**). Such hypothesis could be addressed by looking at FluPol binding to capped mRNAs in cells silenced for ERI1 as well as *in vitro* in the presence or absence of ERI1.

b. *ERI1, cell cycle and IAV infection*

In addition, the role of ERI1 in controlling histone mRNA decay during the cell cycle might contribute to ERI1 requirement in the IAV life cycle. Transcription activity of RNA Pol II is much higher in the G1 phase than in any other phase and several studies have reported that IAV infection induces a G0/G1 cell cycle arrest [376–380]. Histone mRNAs are however heavily synthesized as cells enter the S phase making histone gene clusters hot spots of transcription by RNA Pol II [381]. Hence targeting of ERI1 by viral proteins could recruit vRNPs to hot spots of RNA Pol II transcription, where capped primers are available in abundance, as cells enter the S phase, thereby promoting viral transcription, even outside of the G1 phase (**Figure 61**).

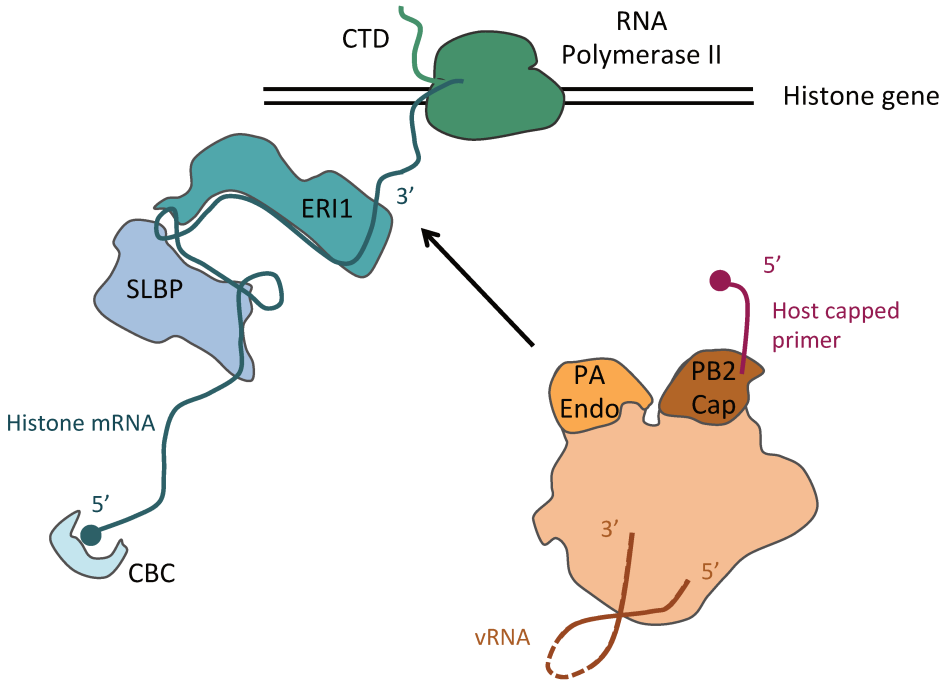

Figure 61: Proposed hypothesis explaining the role of ERI1 in the IAV life cycle.
Viral transcription initiation requires host capped primers acquired through cap-snatching. Before cells enter the S phase, histone genes are heavily transcribed to meet the histone demand. Targeting of ERI1 could therefore help localize the vRNPs close to hot spots of RNA Pol II transcription, thereby creating a favorable environment for cap-snatching, and promoting viral transcription. Moreover, we found that ERI1 preferentially binds to PB2 Cter, which contains the cap-binding domain. Hence, we can hypothesize that FluPol interaction with ERI1 could contribute to efficiently target FluPol to capped histone mRNAs to promote cap-snatching, thereby promoting viral transcription.

c. *ERI1 and IAV induced host shut-off*

In addition, ERI1 requirement for IAV transcription could be an indirect effect of its involvement in histone mRNAs degradation. IAV induced host shut-off occurs through two main mechanisms: i) inhibition of production of host mRNAs and ii) PA-X mediated host transcripts degradation.

Replication dependent histone mRNAs have unique features among cellular mRNAs as they are non-polyadenylated intronless transcripts which are heavily transcribed during specific stages of the cell cycle [311]. Hence, as mentioned above, due to their abundance during the S phase they could represent a proficient source of capped primers. According to one of the proposed models explaining RNA Pol II termination, the torpedo model,

transcription termination is triggered by degradation of uncapped RNA fragments by XRN2. Unprotected uncapped histone mRNAs generated through cap-snatching could likewise be targeted by XRN2 [121,193]. RNA Pol II termination further leads to RNA Pol II removal from the DNA template which is thus freed to reinitiate elsewhere, thereby providing more capped primers to fuel viral transcription.

We can otherwise hypothesize that ERI1 could be involved in histone mRNA degradation induced by PA-X. PA-X targets RNA Pol II transcripts, including polyadenylated cellular mRNAs and histone mRNAs, as reporters bearing the canonical polyadenylation signal or the histone stem loop at their 3' end are equally inhibited by PA-X [330]. XRN1 is involved in histone mRNA degradation as its silencing partially stabilizes histone mRNA [330]. Furthermore, XRN1 is required to finalize degradation of cellular transcripts initially fragmented by PA-X [273]. Recent findings suggest that intronless mRNAs are considerably less sensitive to PA-X degradation compared to exon containing transcripts and that PA-X is most likely targeted to cellular transcripts through the splicing machinery [287]. However, as histone mRNAs can be targeted and degraded by PA-X, alternative mechanisms, which might involve interaction with ERI1, could promote PA-X dependent histone mRNAs degradation. Furthermore, XRN1 may stall on the histone mRNAs stem loop leading to improper degradation. Indeed, RNA structures such as the one found in the 5' and 3'UTR regions of flaviviruses or less elaborated structures such as the two hairpins separated by a short spacer found in the 3'UTR of some beny- and cucumoviruses have been shown to efficiently stall XRN1 [241,243,245,246,382]. The 3'-5' exonuclease activity of ERI1 might thus be required to degrade into the stem loop, allowing further degradation of histone mRNAs by XRN1.

Overall, histone mRNAs thus represent an interesting mRNA repertoire to target during the IAV life cycle, with either direct or indirect involvement of ERI1 in promoting IAV transcription.

III. Conclusion and perspectives: ERI1 as a new member of the growing family of RNA decay factors involved in IAV cycle

Altogether, several other studies and ours highlight the existence of a wide interplay between IAV and RNA degradation pathways (*i.e.* processing bodies, RNA exosome and the cellular exonucleases XRN1 and XRN2) during viral replication. This interplay allows IAV to hijack RNA decay components to promote viral replication, and to globally rewire cellular gene expression, thereby creating a cellular environment favorable to viral replication.

Our study identified ERI1, which can process small regulatory RNAs, rRNAs and histone mRNA and has therefore a pivotal role in the control of cellular gene expression, as a major interactor of vRNPs required for IAV multiplication and more specifically to promote viral transcription. We also showed that both ERI1 activities - RNA binding and exonuclease - are required for viral transcription. Moreover, we found that a complex composed of at least, the transcribing IAV polymerase, ERI1, SLBP and histone mRNA exists during IAV infection. However, the mechanisms by which ERI1 promotes viral transcription, the implication of the ERI1/SLBP/histone mRNA complex in the IAV cycle as well as the role and substrate of the exonuclease activity of ERI1 found to be required for viral transcription, remain to be determined.

As previously discussed, ERI1 could have multiple roles in the IAV cycle. Several of our hypotheses converge to a potential implication of ERI1 in viral transcription mechanisms. A proficient pool of capped mRNA primers is essential for viral transcription. Access to host capped transcripts is achieved through a close interaction between the viral polymerase and the RNA Pol II. However, given the importance of such mechanism for IAV multiplication, alternative interactions could also further support and promote IAV cap-snatching. Therefore, interaction between the transcribing vRNPs and ERI1 could have multiple purposes. Cellular transcripts are heavily synthesized during G0/G1 phases of the cell cycle and IAV infection has been shown to induce a G0/G1 cell cycle arrest. However, such cell cycle arrest takes time to establish and it is critical for the outcome of the infection to efficiently transcribe the viral genome outside of the G0/G1 phase. On the other hand, histone mRNAs are synthesized as cells enter the S phase. Hence, ERI1 targeting by the

transcribing polymerase could promote an efficient targeting of RNA Pol II transcription hot spots, especially outside of the G0/G1 phase, to promote cap-snatching. Monitoring viral transcription in cell cycle synchronized cells silenced or not for ERI1 could provide further insights into the relevance of such possibility. Alternatively, ERI1 could be targeted by the viral polymerase to promote histone mRNAs degradation, which would participate to host shut-off and would free RNA Poll from DNA template, which would subsequently be able to reinitiate elsewhere, leading to the generation of more capped primers to fuel viral transcription.

Although our data point to a role of ERI1 in early viral transcription, we cannot exclude the possibility that ERI1 might be involved in other steps of the IAV cycle. As ERI1 binds histone mRNAs in the nucleus and is exported along with it in the cytoplasm, one could suggest that FluPol targets ERI1 already in the cytoplasm as a means to target capped histone transcripts, thereby allowing transcription to occur before vRNPs enters the nucleus. Even though the current model for IAV transcription involved a co-transcriptional cap-snatching in close association with the RNA Pol II in the nucleus, other RNA viruses relying on cap-snatching for their transcription, such as Bunyaviruses, snatch caps from cellular transcripts in the cytoplasm. Addressing such hypothesis would require nucleocytoplasmic fractionation assays and quantification of viral mRNAs at very early time points post infection in the cytoplasmic compartment. Alternatively, ERI1 could be recruited by the viral polymerase to protect viral transcripts from miRNA dependent decay, as ERI1 has been shown to be required for miRNA degradation. Comparing viral transcripts stability in cells silenced for ERI1 or not, as well as sequencing the miRNAs repertoire upon ERI1 silencing would help addressing a potential role of ERI1 in miRNA homeostasis during IAV infection.

Interestingly, PA-X is tightly associated to RNA decay as it is involved in host transcripts degradation, which requires the involvement of the host exonuclease XRN1, and ultimately leads to host shut-off. Therefore, screening of the ExoRDec for interaction with PA-X could be of great interest. However, as PA-X shares the Nter domain of PA, and PA was found to be a poor bait to assess PPI using GPCA, our screening strategy might not be recommended and methods such as Y2H or AP/MS should be considered.

Overall, our work, through targeted interactomic and RNAi screens, provides a better understanding of the IAV cycle and highlights the RNA degradation pathway as a major player in IAV multiplication. Our initial interactomic strategy was remarkably efficient as a

considerable proportion of the identified interactors were found to be involved in IAV multiplication. Therefore, our ExoRDec library could be repurposed and used for the identification of cellular factors involved in the life cycle of other viruses. Indeed, controlling cellular gene expression is essential to the success of viral infection and establishing a large interplay with host RNA decay machineries appears to be a shared feature between many RNA viruses (reviewed in [205–210]). Altogether, deciphering host-virus interactions, and more specifically the interplay with RNA decay machineries, is essential to acquire better knowledge of the viral cycle as well as of the infection induced cellular environment rewiring, which are both critical for the development of effective anti-viral strategies.

References

1. Hause BM, Collin EA, Liu R, Huang B, Sheng Z, Lu W, et al. Characterization of a novel influenza virus in cattle and Swine: proposal for a new genus in the Orthomyxoviridae family. MBio. American Society for Microbiology (ASM); 2014;5: e00031-14. doi:10.1128/mBio.00031-14

2. Krammer F, Smith GJD, Fouchier RAM, Peiris M, Kedzierska K, Doherty PC, et al. Influenza. Nat Rev Dis Prim. Nature Publishing Group; 2018;4: 3. doi:10.1038/s41572-018-0002-y

3. Tong S, Zhu X, Li Y, Shi M, Zhang J, Bourgeois M, et al. New World Bats Harbor Diverse Influenza A Viruses. Subbarao K, editor. PLoS Pathog. Public Library of Science; 2013;9: e1003657. doi:10.1371/journal.ppat.1003657

4. Wendel I, Matrosovich M, Klenk HD. SnapShot: Evolution of Human Influenza A Viruses. Cell Host Microbe. 2015;17: 416-416.e1. doi:10.1016/j.chom.2015.02.001

5. Noda T. Native morphology of influenza virions. Front Microbiol. Frontiers Media SA; 2011;2: 269. doi:10.3389/fmicb.2011.00269

6. Shaw ML, Stone KL, Colangelo CM, Gulcicek EE, Palese P. Cellular Proteins in Influenza Virus Particles. Früh K, editor. PLoS Pathog. Public Library of Science; 2008;4: e1000085. doi:10.1371/journal.ppat.1000085

7. Hutchinson EC, Charles PD, Hester SS, Thomas B, Trudgian D, Martínez-Alonso M, et al. Conserved and host-specific features of influenza virion architecture. Nat Commun. Europe PMC Funders; 2014;5: 4816. doi:10.1038/ncomms5816

8. Vahey MD, Fletcher DA. Low-Fidelity Assembly of Influenza A Virus Promotes Escape from Host Cells. Cell. Cell Press; 2018; doi:10.1016/J.CELL.2018.10.056

9. Noda T, Murakami S, Nakatsu S, Imai H, Muramoto Y, Shindo K, et al. Importance of the 1+7 configuration of ribonucleoprotein complexes for influenza A virus genome packaging. Nat Commun. Nature Publishing Group; 2018;9: 54. doi:10.1038/s41467-017-02517-w

10. Richardson JC, Akkina RK. NS2 protein of influenza virus is found in purified virus and phosphorylated in infected cells. Arch Virol. Springer-Verlag; 1991;116: 69–80. doi:10.1007/BF01319232

11. Nakajima N, Hata S, Sato Y, Tobiume M, Katano H, Kaneko K, et al. The first autopsy case of pandemic influenza (A/H1N1pdm) virus infection in Japan: detection of a high

copy number of the virus in type II alveolar epithelial cells by pathological and virological examination. Jpn J Infect Dis. 2010;63: 67–71. Available: http://www.ncbi.nlm.nih.gov/pubmed/20093768

12. Noda T, Sugita Y, Aoyama K, Hirase A, Kawakami E, Miyazawa A, et al. Three-dimensional analysis of ribonucleoprotein complexes in influenza A virus. Nat Commun. Nature Publishing Group; 2012;3: 639. doi:10.1038/ncomms1647

13. de Graaf M, Fouchier RAM. Role of receptor binding specificity in influenza A virus transmission and pathogenesis. EMBO J. John Wiley & Sons, Ltd; 2014;33: 823–841. doi:10.1002/embj.201387442

14. Skehel JJ, Wiley DC. Receptor Binding and Membrane Fusion in Virus Entry: The Influenza Hemagglutinin. Annu Rev Biochem. Annual Reviews 4139 El Camino Way, P.O. Box 10139, Palo Alto, CA 94303-0139, USA ; 2000;69: 531–569. doi:10.1146/annurev.biochem.69.1.531

15. Sriwilaijaroen N, Suzuki Y. Molecular basis of the structure and function of H1 hemagglutinin of influenza virus. Proc Jpn Acad Ser B Phys Biol Sci. The Japan Academy; 2012;88: 226–49. doi:10.2183/pjab.88.226

16. Matlin KS, Reggio H, Helenius A, Simons K. Infectious entry pathway of influenza virus in a canine kidney cell line. J Cell Biol. Rockefeller University Press; 1981;91: 601–613. doi:10.1083/JCB.91.3.601

17. de Vries E, Tscherne DM, Wienholts MJ, Cobos-Jiménez V, Scholte F, García-Sastre A, et al. Dissection of the Influenza A Virus Endocytic Routes Reveals Macropinocytosis as an Alternative Entry Pathway. Pekosz A, editor. PLoS Pathog. Public Library of Science; 2011;7: e1001329. doi:10.1371/journal.ppat.1001329

18. Sieczkarski SB, Whittaker GR. Influenza virus can enter and infect cells in the absence of clathrin-mediated endocytosis. J Virol. American Society for Microbiology Journals; 2002;76: 10455–64. doi:10.1128/jvi.76.20.10455-10464.2002

19. White JM, Whittaker GR. Fusion of Enveloped Viruses in Endosomes. Traffic. John Wiley & Sons, Ltd (10.1111); 2016;17: 593–614. doi:10.1111/tra.12389

20. Pinto LH, Holsinger LJ, Lamb RA. Influenza virus M2 protein has ion channel activity. Cell. Cell Press; 1992;69: 517–528. doi:10.1016/0092-8674(92)90452-I

21. Bui M, Whittaker G, Helenius A. Effect of M1 protein and low pH on nuclear transport of influenza virus ribonucleoproteins. J Virol. American Society for Microbiology Journals; 1996;70: 8391–401. Available: http://www.ncbi.nlm.nih.gov/pubmed/8970960

22. Eisfeld AJ, Neumann G, Kawaoka Y. At the centre: influenza A virus

ribonucleoproteins. Nat Rev Microbiol. Nature Publishing Group; 2015;13: 28–41. doi:10.1038/nrmicro3367

23. Pflug A, Lukarska M, Resa-Infante P, Reich S, Cusack S. Structural insights into RNA synthesis by the influenza virus transcription-replication machine. Virus Res. 2017; doi:10.1016/j.virusres.2017.01.013

24. Fodor E. The RNA polymerase of influenza A virus: mechanisms of viral transcription and replication. Acta Virol. 2013;57: 113–122. doi:10.4149/av_2013_02_113

25. York A, Fodor E. Biogenesis, assembly, and export of viral messenger ribonucleoproteins in the influenza A virus infected cell. RNA Biol. Taylor & Francis; 2013;10: 1274–1282. doi:10.4161/rna.25356

26. Huet S, Avilov S V., Ferbitz L, Daigle N, Cusack S, Ellenberg J. Nuclear Import and Assembly of Influenza A Virus RNA Polymerase Studied in Live Cells by Fluorescence Cross-Correlation Spectroscopy. J Virol. American Society for Microbiology Journals; 2009;84: 1254–1264. doi:10.1128/jvi.01533-09

27. Li J, Yu M, Zheng W, Liu W. Nucleocytoplasmic shuttling of influenza A virus proteins. Viruses. Multidisciplinary Digital Publishing Institute (MDPI); 2015;7: 2668–82. doi:10.3390/v7052668

28. Amorim MJ, Bruce EA, Read EKC, Foeglein A, Mahen R, Stuart AD, et al. A Rab11- and microtubule-dependent mechanism for cytoplasmic transport of influenza A virus viral RNA. J Virol. American Society for Microbiology Journals; 2011;85: 4143–56. doi:10.1128/JVI.02606-10

29. Momose F, Sekimoto T, Ohkura T, Jo S, Kawaguchi A, Nagata K, et al. Apical Transport of Influenza A Virus Ribonucleoprotein Requires Rab11-positive Recycling Endosome. Darlix J-LEPH, editor. PLoS One. Public Library of Science; 2011;6: e21123. doi:10.1371/journal.pone.0021123

30. de Castro Martin IF, Fournier G, Sachse M, Pizarro-Cerda J, Risco C, Naffakh N. Influenza virus genome reaches the plasma membrane via a modified endoplasmic reticulum and Rab11-dependent vesicles. Nat Commun. Nature Publishing Group; 2017;8: 1396. doi:10.1038/s41467-017-01557-6

31. Gavazzi C, Yver M, Isel C, Smyth RP, Rosa-Calatrava M, Lina B, et al. A functional sequence-specific interaction between influenza A virus genomic RNA segments. Proc Natl Acad Sci U S A. National Academy of Sciences; 2013;110: 16604–9. doi:10.1073/pnas.1314419110

32. Dadonaite B, Gilbertson B, Knight ML, Trifkovic S, Rockman S, Laederach A, et al. The structure of the influenza A virus genome. Nat Microbiol. Nature Publishing Group; 2019; 1. doi:10.1038/s41564-019-0513-7

33. Air GM. Influenza neuraminidase. Influenza Other Respi Viruses. Wiley-Blackwell; 2012;6: 245–56. doi:10.1111/j.1750-2659.2011.00304.x

34. Du R, Cui Q, Rong L, Du R, Cui Q, Rong L. Competitive Cooperation of Hemagglutinin and Neuraminidase during Influenza A Virus Entry. Viruses. Multidisciplinary Digital Publishing Institute; 2019;11: 458. doi:10.3390/v11050458

35. Böttcher-Friebertshäuser E, Garten W, Matrosovich M, Klenk HD. The Hemagglutinin: A Determinant of Pathogenicity. Springer, Cham; 2014. pp. 3–34. doi:10.1007/82_2014_384

36. Dou D, Revol R, Östbye H, Wang H, Daniels R. Influenza A Virus Cell Entry, Replication, Virion Assembly and Movement. Front Immunol. Frontiers Media SA; 2018;9: 1581. doi:10.3389/fimmu.2018.01581

37. Vasin A V, Petrova A V, Egorov V V, Plotnikova MA, Klotchenko SA, Karpenko MN, et al. The influenza A virus NS genome segment displays lineage-specific patterns in predicted RNA secondary structure. BMC Res Notes. 2016/05/22. 2016;9: 279. doi:10.1186/s13104-016-2083-6

38. Dubois J, Terrier O, Rosa-Calatrava M. Influenza viruses and mRNA splicing: doing more with less. MBio. American Society for Microbiology; 2014;5: e00070-14. doi:10.1128/mBio.00070-14

39. Chen W, Calvo PA, Malide D, Gibbs J, Schubert U, Bacik I, et al. A novel influenza A virus mitochondrial protein that induces cell death. Nat Med. Nature Publishing Group; 2001;7: 1306–1312. doi:10.1038/nm1201-1306

40. Krumbholz A, Philipps A, Oehring H, Schwarzer K, Eitner A, Wutzler P, et al. Current knowledge on PB1-F2 of influenza A viruses. Med Microbiol Immunol. Springer-Verlag; 2011;200: 69–75. doi:10.1007/s00430-010-0176-8

41. Wise HM, Foeglein A, Sun J, Dalton RM, Patel S, Howard W, et al. A Complicated Message: Identification of a Novel PB1-Related Protein Translated from Influenza A Virus Segment 2 mRNA. J Virol. 2009;83: 8021–8031. doi:10.1128/JVI.00826-09

42. Jagger BW, Wise HM, Kash JC, Walters K-A, Wills NM, Xiao Y-L, et al. An overlapping protein-coding region in influenza A virus segment 3 modulates the host response. Science. American Association for the Advancement of Science; 2012;337: 199–204. doi:10.1126/science.1222213

43. Muramoto Y, Noda T, Kawakami E, Akkina R, Kawaoka Y. Identification of novel influenza A virus proteins translated from PA mRNA. J Virol. American Society for Microbiology Journals; 2013;87: 2455–62. doi:10.1128/JVI.02656-12

44. Shih SR, Nemeroff ME, Krug RM. The choice of alternative 5’ splice sites in influenza

virus M1 mRNA is regulated by the viral polymerase complex. Proc Natl Acad Sci U S A. National Academy of Sciences; 1995;92: 6324–8. doi:10.1073/pnas.92.14.6324

45. Wise HM, Hutchinson EC, Jagger BW, Stuart AD, Kang ZH, Robb N, et al. Identification of a Novel Splice Variant Form of the Influenza A Virus M2 Ion Channel with an Antigenically Distinct Ectodomain. Pekosz A, editor. PLoS Pathog. Public Library of Science; 2012;8: e1002998. doi:10.1371/journal.ppat.1002998

46. Selman M, Dankar SK, Forbes NE, Jia J-J, Brown EG. Adaptive mutation in influenza A virus non-structural gene is linked to host switching and induces a novel protein by alternative splicing. Emerg Microbes Infect. Taylor & Francis; 2012;1: 1–10. doi:10.1038/emi.2012.38

47. Yamayoshi S, Watanabe M, Goto H, Kawaoka Y. Identification of a Novel Viral Protein Expressed from the PB2 Segment of Influenza A Virus. J Virol. American Society for Microbiology Journals; 2016;90: 444–56. doi:10.1128/JVI.02175-15

48. Clifford M, Twigg J, Upton C. Evidence for a novel gene associated with human influenza A viruses. Virol J. BioMed Central; 2009;6: 198. doi:10.1186/1743-422X-6-198

49. Vasin A V, Temkina OA, Egorov V V, Klotchenko SA, Plotnikova MA, Kiselev OI. Molecular mechanisms enhancing the proteome of influenza A viruses: an overview of recently discovered proteins. Virus Res. 2014;185: 53–63. doi:10.1016/j.virusres.2014.03.015

50. Knipe DM, Howley PM. Fields Virology, 6th Edition. Fields Virology, 6th Edition. Lippincott Williams & Wilkins; 2013.

51. Diot C. Exploration of the Cellular DDX RNA Helicases – Influenza A Virus Interplay : Identification of a Major Role of DDX19 in the Nuclear Export of viral mRNAs. 2016.

52. Munster VJ, Baas C, Lexmond P, Waldenström J, Wallensten A, Fransson T, et al. Spatial, Temporal, and Species Variation in Prevalence of Influenza A Viruses in Wild Migratory Birds. PLoS Pathog. Public Library of Science; 2007;3: e61. doi:10.1371/journal.ppat.0030061

53. Webster R, Bean W. Evolution and ecology of influenza A viruses. Microbiol Rev. 1992;56: 152–179. Available: http://mmbr.asm.org/content/56/1/152.short

54. Krauss S, Walker D, Pryor SP, Niles L, Chenghong L, Hinshaw VS, et al. Influenza A Viruses of Migrating Wild Aquatic Birds in North America. Vector-Borne Zoonotic Dis. Mary Ann Liebert, Inc. 2 Madison Avenue Larchmont, NY 10538 USA ; 2004;4: 177–189. doi:10.1089/vbz.2004.4.177

55. Shi Y, Wu Y, Zhang W, Qi J, Gao GF. Enabling the “host jump”: structural determinants

of receptor-binding specificity in influenza A viruses. Nat Rev Microbiol. Nature Research; 2014;12: 822–831. doi:10.1038/nrmicro3362

56. Webster RG, Govorkova EA. Continuing challenges in influenza. Ann N Y Acad Sci. NIH Public Access; 2014;1323: 115. doi:10.1111/NYAS.12462

57. Steinhauer DA, Holland JJ. Rapid evolution of RNA viruses. Annu Rev Microbiol. 1987;41: 409–433. doi:10.1146/annurev.mi.41.100187.002205

58. Iuliano AD, Roguski KM, Chang HH, Muscatello DJ, Palekar R, Tempia S, et al. Estimates of global seasonal influenza-associated respiratory mortality: a modelling study. Lancet. Elsevier; 2018;391: 1285–1300. doi:10.1016/S0140-6736(17)33293-2

59. Killingley B, Nguyen-Van-Tam J. Routes of influenza transmission. Influenza Other Respi Viruses. Wiley-Blackwell; 2013;7 Suppl 2: 42–51. doi:10.1111/irv.12080

60. Mullooly JP, Bridges CB, Thompson WW, Chen J, Weintraub E, Jackson LA, et al. Influenza- and RSV-associated hospitalizations among adults. Vaccine. Elsevier; 2007;25: 846–855. doi:10.1016/J.VACCINE.2006.09.041

61. TAUBENBERGER JK, MORENS DM. Pandemic influenza - including a risk assessment of H5N1. Rev Sci Tech l'OIE. 2009;28: 187–202. doi:10.20506/rst.28.1.1879

62. Taubenberger JK, Kash JC. Influenza Virus Evolution, Host Adaptation, and Pandemic Formation. Cell Host Microbe. Cell Press; 2010;7: 440–451. doi:10.1016/J.CHOM.2010.05.009

63. Taubenberger JK, Reid AH, Lourens RM, Wang R, Jin G, Fanning TG. Characterization of the 1918 influenza virus polymerase genes. Nature. Nature Publishing Group; 2005;437: 889–893. doi:10.1038/nature04230

64. Smith GJD, Bahl J, Vijaykrishna D, Zhang J, Poon LLM, Chen H, et al. Dating the emergence of pandemic influenza viruses. Proc Natl Acad Sci U S A. National Academy of Sciences; 2009;106: 11709–12. doi:10.1073/pnas.0904991106

65. Neumann G, Noda T, Kawaoka Y. Emergence and pandemic potential of swine-origin H1N1 influenza virus. Nature. Nature Publishing Group; 2009;459: 931–939. doi:10.1038/nature08157

66. Yen H-L. Current and novel antiviral strategies for influenza infection. Curr Opin Virol. Elsevier; 2016;18: 126–134. doi:10.1016/J.COVIRO.2016.05.004

67. Furuta Y, Gowen BB, Takahashi K, Shiraki K, Smee DF, Barnard DL. Favipiravir (T-705), a novel viral RNA polymerase inhibitor. Antiviral Res. Elsevier; 2013;100: 446–454. doi:10.1016/J.ANTIVIRAL.2013.09.015

68. Clark MP, Ledeboer MW, Davies I, Byrn RA, Jones SM, Perola E, et al. Discovery of a Novel, First-in-Class, Orally Bioavailable Azaindole Inhibitor (VX-787) of Influenza PB2. J Med Chem. American Chemical Society; 2014;57: 6668–6678. doi:10.1021/jm5007275

69. Portsmouth S, Kawaguchi K, Arai M, Tsuchiya K, Uehara T. Cap-dependent Endonuclease Inhibitor S-033188 for the Treatment of Influenza: Results from a Phase 3, Randomized, Double-Blind, Placebo- and Active-Controlled Study in Otherwise Healthy Adolescents and Adults with Seasonal Influenza. Open Forum Infect Dis. Oxford University Press; 2017;4: S734–S734. doi:10.1093/ofid/ofx180.001

70. Fukao K, Ando Y, Noshi T, Kitano M, Noda T, Kawai M, et al. Baloxavir marboxil, a novel cap-dependent endonuclease inhibitor potently suppresses influenza virus replication and represents therapeutic effects in both immunocompetent and immunocompromised mouse models. Pöhlmann S, editor. PLoS One. Public Library of Science; 2019;14: e0217307. doi:10.1371/journal.pone.0217307

71. Haffizulla J, Hartman A, Hoppers M, Resnick H, Samudrala S, Ginocchio C, et al. Effect of nitazoxanide in adults and adolescents with acute uncomplicated influenza: A double-blind, randomised, placebo-controlled, phase 2b/3 trial. Lancet Infect Dis. 2014;14: 609–618. doi:10.1016/S1473-3099(14)70717-0

72. Organization WH. Weekly epidemiological record. Relev épidémiologique Hebd. 2012;47: 461–476. Available: http://www.who.int/immunization/policy/position_papers/influenza/en/

73. Rudenko L, Yeolekar L, Kiseleva I, Isakova-Sivak I. Development and approval of live attenuated influenza vaccines based on Russian master donor viruses: Process challenges and success stories. Vaccine. Elsevier; 2016;34: 5436–5441. doi:10.1016/j.vaccine.2016.08.018

74. Sridhar S, Brokstad KA, Cox RJ. Influenza Vaccination Strategies: Comparing Inactivated and Live Attenuated Influenza Vaccines. Vaccines. Multidisciplinary Digital Publishing Institute (MDPI); 2015;3: 373–89. doi:10.3390/vaccines3020373

75. Sautto GA, Kirchenbaum GA, Ross TM. Towards a universal influenza vaccine: different approaches for one goal. Virol J. BioMed Central; 2018;15: 17. doi:10.1186/s12985-017-0918-y

76. Harding AT, Heaton NS. Efforts to Improve the Seasonal Influenza Vaccine. Vaccines. Multidisciplinary Digital Publishing Institute (MDPI); 2018;6. doi:10.3390/vaccines6020019

77. WHO. Recommended composition of influenza virus vaccines for use in the 2018-2019 northern hemisphere influenza season. Available:

https://www.who.int/influenza/vaccines/virus/recommendations/2018_19_north/en/

78. Dwyer DE, Kirkland PD. Influenza: One Health in action. N S W Public Health Bull. CSIRO PUBLISHING; 2011;22: 123. doi:10.1071/NB11005

79. Wu WWH, Weaver LL, Panté; N. Purification and Visualization of Influenza A Viral Ribonucleoprotein Complexes. J Vis Exp. 2009; e1105. doi:10.3791/1105

80. Moeller A, Kirchdoerfer RN, Potter CS, Carragher B, Wilson IA. Organization of the Influenza Virus Replication Machinery. Science (80-). 2012;338: 1631–1634. doi:10.1126/science.1227270

81. Arranz R, Coloma R, Chichón FJ, Conesa JJ, Carrascosa JL, Valpuesta JM, et al. The structure of native influenza virion ribonucleoproteins. Science. American Association for the Advancement of Science; 2012;338: 1634–7. doi:10.1126/science.1228172

82. Bouvier NM, Palese P. The biology of influenza viruses. Vaccine. Elsevier; 2008;26: D49–D53. doi:10.1016/J.VACCINE.2008.07.039

83. Lee N, Le Sage V, Nanni A V., Snyder DJ, Cooper VS, Lakdawala SS. Genome-wide analysis of influenza viral RNA and nucleoprotein association. Nucleic Acids Res. Oxford University Press; 2017;45: 8968. doi:10.1093/NAR/GKX584

84. Gallagher JR, Torian U, McCraw DM, Harris AK. Structural studies of influenza virus RNPs by electron microscopy indicate molecular contortions within NP supra-structures. J Struct Biol. Academic Press; 2017;197: 294–307. doi:10.1016/J.JSB.2016.12.007

85. Ruigrok RWH, Baudin F. Structure of influenza virus ribonucleoprotein particles. II. Purified RNA-free influenza virus ribonucleoprotein forms structures that are indistinguishable from the intact influenza virus ribonucleoprotein particles. J Gen Virol. Microbiology Society; 1995;76: 1009–1014. doi:10.1099/0022-1317-76-4-1009

86. te Velthuis AJW, Fodor E. Influenza virus RNA polymerase: insights into the mechanisms of viral RNA synthesis. Nat Rev Microbiol. Nature Publishing Group; 2016;14: 479–493. doi:10.1038/nrmicro.2016.87

87. Pflug A, Guilligay D, Reich S, Cusack S. Structure of influenza A polymerase bound to the viral RNA promoter. Nature. Nature Publishing Group; 2014;516: 355–360. doi:10.1038/nature14008

88. Ferhadian D, Contrant M, Printz-Schweigert A, Smyth RP, Paillart J-C, Marquet R. Structural and Functional Motifs in Influenza Virus RNAs. Front Microbiol. Frontiers Media SA; 2018;9: 559. doi:10.3389/fmicb.2018.00559

89. Wang J, Li J, Zhao L, Cao M, Deng T. Dual Roles of the Hemagglutinin Segment-Specific Noncoding Nucleotides in the Extended Duplex Region of the Influenza A Virus RNA Promoter. J Virol. American Society for Microbiology (ASM); 2017;91. doi:10.1128/JVI.01931-16

90. Leahy MB, Dobbyn HC, Brownlee GG. Hairpin Loop Structure in the 3' Arm of the Influenza A Virus Virion RNA Promoter Is Required for Endonuclease Activity. J Virol. 2002;75: 7042–7049. doi:10.1128/jvi.75.15.7042-7049.2001

91. Ye Q, Guu TSY, Mata DA, Kuo R-L, Smith B, Krug RM, et al. Biochemical and structural evidence in support of a coherent model for the formation of the double-helical influenza A virus ribonucleoprotein. MBio. American Society for Microbiology; 2012;4: e00467-12. doi:10.1128/mBio.00467-12

92. Ye Q, Krug RM, Tao YJ. The mechanism by which influenza A virus nucleoprotein forms oligomers and binds RNA. Nature. Nature Publishing Group; 2006;444: 1078–1082. doi:10.1038/nature05379

93. Biswas SK, Boutz PL, Nayak DP. Influenza virus nucleoprotein interacts with influenza virus polymerase proteins. J Virol. American Society for Microbiology Journals; 1998;72: 5493–501. Available: http://www.ncbi.nlm.nih.gov/pubmed/9621005

94. Turrell L, Lyall JW, Tiley LS, Fodor E, Vreede FT. The role and assembly mechanism of nucleoprotein in influenza A virus ribonucleoprotein complexes. Nat Commun. Nature Publishing Group; 2013;4: 1591. doi:10.1038/ncomms2589

95. Cros JF, García-Sastre A, Palese P. An Unconventional NLS is Critical for the Nuclear Import of the Influenza A Virus Nucleoprotein and Ribonucleoprotein. Traffic. John Wiley & Sons, Ltd (10.1111); 2005;6: 205–213. doi:10.1111/j.1600-0854.2005.00263.x

96. Chan W-H, Ng AK-L, Robb NC, Lam MK-H, Chan PK-S, Au SW-N, et al. Functional Analysis of the Influenza Virus H5N1 Nucleoprotein Tail Loop Reveals Amino Acids That Are Crucial for Oligomerization and Ribonucleoprotein Activities. J Virol. 2010;84: 7337–7345. doi:10.1128/jvi.02474-09

97. Honda A, Ueda K, Nagata K, Ishihama A. RNA Polymerase of Influenza Virus: Role of NP in RNA Chain Elongation. J Biochem. Narnia; 1988;104: 1021–1026. doi:10.1093/oxfordjournals.jbchem.a122569

98. Götz V, Magar L, Dornfeld D, Giese S, Pohlmann A, Höper D, et al. Influenza A viruses escape from MxA restriction at the expense of efficient nuclear vRNP import. Sci Rep. Nature Publishing Group; 2016;6: 23138. doi:10.1038/srep23138

99. Gabriel G, Dauber B, Wolff T, Planz O, Klenk H-D, Stech J. The viral polymerase mediates adaptation of an avian influenza virus to a mammalian host. Proc Natl Acad Sci U S A. National Academy of Sciences; 2005;102: 18590–5.

doi:10.1073/pnas.0507415102

100. Kao RY, Yang D, Lau L-S, Tsui WHW, Hu L, Dai J, et al. Identification of influenza A nucleoprotein as an antiviral target. Nat Biotechnol. Nature Publishing Group; 2010;28: 600–605. doi:10.1038/nbt.1638

101. Gerritz SW, Cianci C, Kim S, Pearce BC, Deminie C, Discotto L, et al. Inhibition of influenza virus replication via small molecules that induce the formation of higher-order nucleoprotein oligomers. Proc Natl Acad Sci. 2011;108: 15366–15371. doi:10.1073/pnas.1107906108

102. Lejal N, Tarus B, Bouguyon E, Chenavas S, Bertho N, Delmas B, et al. Structure-Based Discovery of the Novel Antiviral Properties of Naproxen against the Nucleoprotein of Influenza A Virus. Antimicrob Agents Chemother. American Society for Microbiology Journals; 2013;57: 2231–2242. doi:10.1128/AAC.02335-12

103. Jin H, Lu B, Zhou H, Ma C, Zhao J, Yang C, et al. Multiple amino acid residues confer temperature sensitivity to human influenza virus vaccine strains (flumist) derived from cold-adapted a/ann arbor/6/60. Virology. Academic Press; 2003;306: 18–24. doi:10.1016/S0042-6822(02)00035-1

104. te Velthuis AJW, Robb NC, Kapanidis AN, Fodor E. The role of the priming loop in influenza A virus RNA synthesis. Nat Microbiol. 2016;1: 16029. doi:10.1038/nmicrobiol.2016.29

105. Reich S, Guilligay D, Pflug A, Malet H, Berger I, Crépin T, et al. Structural insight into cap-snatching and RNA synthesis by influenza polymerase. Nature. Nature Publishing Group; 2014;516: 361–366. doi:10.1038/nature14009

106. Biquand É, Demeret C. Structure resolution of the trimeric RNA-dependent RNA polymerase of influenza viruses: Impact on our understanding of polymerase interactions with host and viral factors. Virologie. 2016;20: 302–320. doi:10.1684/vir.2016.0672

107. Thierry E, Guilligay D, Kosinski J, Bock T, Gaudon S, Round A, et al. Influenza Polymerase Can Adopt an Alternative Configuration Involving a Radical Repacking of PB2 Domains. Mol Cell. Cell Press; 2016;61: 125–137. doi:10.1016/J.MOLCEL.2015.11.016

108. Subbarao EK, London W, Murphy BR. A single amino acid in the PB2 gene of influenza A virus is a determinant of host range. J Virol. American Society for Microbiology Journals; 1993;67: 1761–4. Available: http://www.ncbi.nlm.nih.gov/pubmed/8445709

109. Nilsson BE, te Velthuis AJW, Fodor E. The role of the PB2 627-domain in influenza A virus polymerase function. J Virol. 2017; JVI.02467-16. doi:10.1128/JVI.02467-16

110. Long JS, Giotis ES, Moncorgé O, Frise R, Mistry B, James J, et al. Species difference in ANP32A underlies influenza A virus polymerase host restriction. Nature. Nature Publishing Group, a division of Macmillan Publishers Limited. All Rights Reserved.; 2016;529: 101–104. Available: http://dx.doi.org/10.1038/nature16474

111. De Vlugt C, Sikora D, Pelchat M, De Vlugt C, Sikora D, Pelchat M. Insight into Influenza: A Virus Cap-Snatching. Viruses. Multidisciplinary Digital Publishing Institute (MDPI); 2018;10: 641. doi:10.3390/v10110641

112. Hsin J-P, Manley JL. The RNA polymerase II CTD coordinates transcription and RNA processing. Genes Dev. Cold Spring Harbor Laboratory Press; 2012;26: 2119–37. doi:10.1101/gad.200303.112

113. Martínez-Alonso M, Hengrung N, Fodor E. RNA-Free and Ribonucleoprotein-Associated Influenza Virus Polymerases Directly Bind the Serine-5-Phosphorylated Carboxyl-Terminal Domain of Host RNA Polymerase II. J Virol. American Society for Microbiology Journals; 2016;90: 6014–6021. doi:10.1128/JVI.00494-16

114. Lukarska M, Fournier G, Pflug A, Resa-Infante P, Reich S, Naffakh N, et al. Structural basis of an essential interaction between influenza polymerase and Pol II CTD. Nature. Nature Research; 2016; doi:10.1038/nature20594

115. Engelhardt OG, Smith M, Fodor E. Association of the influenza A virus RNA-dependent RNA polymerase with cellular RNA polymerase II. J Virol. American Society for Microbiology Journals; 2005;79: 5812–8. doi:10.1128/JVI.79.9.5812-5818.2005

116. Walker AP, Fodor E. Interplay between Influenza Virus and the Host RNA Polymerase II Transcriptional Machinery. Trends Microbiol. Elsevier Current Trends; 2019; doi:10.1016/J.TIM.2018.12.013

117. Serna Martin I, Hengrung N, Renner M, Sharps J, Martínez-Alonso M, Masiulis S, et al. A Mechanism for the Activation of the Influenza Virus Transcriptase. Mol Cell. Elsevier; 2018;70: 1101-1110.e4. doi:10.1016/j.molcel.2018.05.011

118. Sikora D, Rocheleau L, Brown EG, Pelchat M. Influenza A virus cap-snatches host RNAs based on their abundance early after infection. Virology. Elsevier Inc.; 2017;509: 167–177. doi:10.1016/j.virol.2017.06.020

119. Koppstein D, Ashour J, Bartel DP. Sequencing the cap-snatching repertoire of H1N1 influenza provides insight into the mechanism of viral transcription initiation. Nucleic Acids Res. 2015;43: 5052–5064. doi:10.1093/nar/gkv333

120. Gu W, Gallagher GR, Dai W, Liu P, Li R, Trombly MI, et al. Influenza A virus preferentially snatches noncoding RNA caps. RNA. Cold Spring Harbor Laboratory Press; 2015;21: 2067–75. doi:10.1261/rna.054221.115

121. Bauer DL V, Tellier M, Martínez-Alonso M, Nojima T, Proudfoot NJ, Murphy S, et al. Influenza Virus Mounts a Two-Pronged Attack on Host RNA Polymerase II Transcription. Cell Rep. Elsevier; 2018;23: 2119-2129.e3. doi:10.1016/j.celrep.2018.04.047

122. Datta K, Wolkerstorfer A, Szolar OHJ, Cusack S, Klumpp K. Characterization of PA-N terminal domain of Influenza A polymerase reveals sequence specific RNA cleavage. Nucleic Acids Res. Narnia; 2013;41: 8289–8299. doi:10.1093/nar/gkt603

123. Kouba T, Drncová P, Cusack S. Structural snapshots of actively transcribing influenza polymerase. Nat Struct Mol Biol. Nature Publishing Group; 2019; 1. doi:10.1038/s41594-019-0232-z

124. Poon LL, Pritlove DC, Fodor E, Brownlee GG. Direct evidence that the poly(A) tail of influenza A virus mRNA is synthesized by reiterative copying of a U track in the virion RNA template. J Virol. American Society for Microbiology (ASM); 1999;73: 3473–6. Available: http://www.ncbi.nlm.nih.gov/pubmed/10074205

125. Braam J, Ulmanen I, Krug RM. Molecular model of a eucaryotic transcription complex: Functions and movements of influenza P proteins during capped RNA-primed transcription. Cell. Cell Press; 1983;34: 609–618. doi:10.1016/0092-8674(83)90393-8

126. Reich S, Guilligay D, Cusack S. An *in vitro* fluorescence based study of initiation of RNA synthesis by influenza B polymerase. Nucleic Acids Res. Narnia; 2017;45: gkx043. doi:10.1093/nar/gkx043

127. Vreede FT, Brownlee GG. Influenza virion-derived viral ribonucleoproteins synthesize both mRNA and cRNA in vitro. J Virol. American Society for Microbiology (ASM); 2007;81: 2196–204. doi:10.1128/JVI.02187-06

128. York A, Hengrung N, Vreede FT, Huiskonen JT, Fodor E. Isolation and characterization of the positive-sense replicative intermediate of a negative-strand RNA virus. Proc Natl Acad Sci U S A. National Academy of Sciences; 2013;110: E4238-45. doi:10.1073/pnas.1315068110

129. Te Velthuis AJ, Robb NC, Kapanidis AN, Fodor E. The role of the priming loop in RNA synthesis. Nat Microbiol. 2016/06/09. 2016;1. doi:10.1038/nmicrobiol.2016.29

130. Zhang S, Wang J, Wang Q, Toyoda T. Internal initiation of influenza virus replication of viral RNA and complementary RNA in vitro. J Biol Chem. American Society for Biochemistry and Molecular Biology; 2010;285: 41194–201. doi:10.1074/jbc.M110.130062

131. Oymans J, te Velthuis AJW. A mechanism for prime-realignment during influenza A virus replication. J Virol. 2017; JVI.01773-17. doi:10.1128/JVI.01773-17

132. Jorba N, Coloma R, Ortín J. Genetic trans-Complementation Establishes a New Model for Influenza Virus RNA Transcription and Replication. Whelan SPJ, editor. PLoS Pathog. Public Library of Science; 2009;5: e1000462. doi:10.1371/journal.ppat.1000462

133. Robb NC, Vreede FT, Smith M, Fodor E. NS2/NEP protein regulates transcription and replication of the influenza virus RNA genome. J Gen Virol. Microbiology Society; 2009;90: 1398–1407. doi:10.1099/vir.0.009639-0

134. Perez JT, Varble A, Sachidanandam R, Zlatev I, Manoharan M, García-Sastre A, et al. Influenza A virus-generated small RNAs regulate the switch from transcription to replication. Proc Natl Acad Sci U S A. National Academy of Sciences; 2010;107: 11525–30. doi:10.1073/pnas.1001984107

135. Perez JT, Zlatev I, Aggarwal S, Subramanian S, Sachidanandam R, Kim B, et al. A small-RNA enhancer of viral polymerase activity. J Virol. American Society for Microbiology (ASM); 2012;86: 13475–85. doi:10.1128/JVI.02295-12

136. Newcomb LL, Kuo R-L, Ye Q, Jiang Y, Tao YJ, Krug RM. Interaction of the Influenza A Virus Nucleocapsid Protein with the Viral RNA Polymerase Potentiates Unprimed Viral RNA Replication. J Virol. 2009;83: 29–36. doi:10.1128/jvi.02293-07

137. Vreede FT, Ng AK-L, Shaw P-C, Fodor E. Stabilization of influenza virus replication intermediates is dependent on the RNA-binding but not the homo-oligomerization activity of the viral nucleoprotein. J Virol. American Society for Microbiology Journals; 2011;85: 12073–8. doi:10.1128/JVI.00695-11

138. Falcón AM, Marión RM, Zürcher T, Gómez P, Portela A, Nieto A, et al. Defective RNA replication and late gene expression in temperature-sensitive influenza viruses expressing deleted forms of the NS1 protein. J Virol. American Society for Microbiology Journals; 2004;78: 3880–8. doi:10.1128/jvi.78.8.3880-3888.2004

139. Vreede FT, Jung TE, Brownlee GG. Model suggesting that replication of influenza virus is regulated by stabilization of replicative intermediates. J Virol. American Society for Microbiology Journals; 2004;78: 9568–72. doi:10.1128/JVI.78.17.9568-9572.2004

140. Mayer D, Molawi K, Martínez-Sobrido L, Ghanem A, Thomas S, Baginsky S, et al. Identification of cellular interaction partners of the influenza virus ribonucleoprotein complex and polymerase complex using proteomic-based approaches. J Proteome Res. NIH Public Access; 2007;6: 672–82. doi:10.1021/pr060432u

141. Hao L, Sakurai A, Watanabe T, Sorensen E, Nidom CA, Newton MA, et al. Drosophila RNAi screen identifies host genes important for influenza virus replication. Nature. Nature Publishing Group; 2008;454: 890–893. doi:10.1038/nature07151

142. Jorba N, Juarez S, Torreira E, Gastaminza P, Zamarreño N, Albar JP, et al. Analysis of

the interaction of influenza virus polymerase complex with human cell factors. Proteomics. 2008;8: 2077–2088. doi:10.1002/pmic.200700508

143. Brass AL, Huang I-C, Benita Y, John SP, Krishnan MN, Feeley EM, et al. The IFITM proteins mediate cellular resistance to influenza A H1N1 virus, West Nile virus, and dengue virus. Cell. Howard Hughes Medical Institute; 2009;139: 1243–54. doi:10.1016/j.cell.2009.12.017

144. Karlas A, Machuy N, Shin Y, Pleissner K-P, Artarini A, Heuer D, et al. Genome-wide RNAi screen identifies human host factors crucial for influenza virus replication. Nature. Nature Publishing Group; 2010;463: 818–822. doi:10.1038/nature08760

145. König R, Stertz S, Zhou Y, Inoue A, Hoffmann H-H, Bhattacharyya S, et al. Human host factors required for influenza virus replication. Nature. Nature Publishing Group; 2010;463: 813–817. doi:10.1038/nature08699

146. Bortz E, Westera L, Maamary J, Steel J, Albrecht RA, Manicassamy B, et al. Host- and strain-specific regulation of influenza virus polymerase activity by interacting cellular proteins. MBio. 2011/08/19. 2011;2. doi:10.1128/mBio.00151-11

147. Bradel-Tretheway BG, Mattiacio JL, Krasnoselsky A, Stevenson C, Purdy D, Dewhurst S, et al. Comprehensive proteomic analysis of influenza virus polymerase complex reveals a novel association with mitochondrial proteins and RNA polymerase accessory factors. J Virol. American Society for Microbiology Journals; 2011;85: 8569–81. doi:10.1128/JVI.00496-11

148. Tafforeau L, Chantier T, Pradezynski F, Pellet J, Mangeot PE, Vidalain P-O, et al. Generation and Comprehensive Analysis of an Influenza Virus Polymerase Cellular Interaction Network. J Virol. American Society for Microbiology; 2011;85: 13010–13018. doi:10.1128/JVI.02651-10

149. Watanabe T, Kawakami E, Shoemaker JE, Lopes TJ, Matsuoka Y, Tomita Y, et al. Influenza virus-host interactome screen as a platform for antiviral drug development. Cell Host Microbe. 2014;16: 795–805. doi:10.1016/j.chom.2014.11.002

150. York A, Hutchinson EC, Fodor E. Interactome Analysis of the Influenza A Virus Transcription/Replication Machinery Identifies Protein Phosphatase 6 as a Cellular Factor Required for Efficient Virus Replication. J Virol. 2014; doi:10.1128/JVI.01813-14

151. Han J, Perez JT, Chen C, Li Y, Benitez A, Kandasamy M, et al. Genome-wide CRISPR/Cas9 Screen Identifies Host Factors Essential for Influenza Virus Replication. Cell Rep. Cell Press; 2018;23: 596–607. doi:10.1016/J.CELREP.2018.03.045

152. Shaw ML, Stertz S. Role of Host Genes in Influenza Virus Replication. Springer, Cham; 2017. pp. 151–189. doi:10.1007/82_2017_30

153. Zhao M, Wang L, Li S. Influenza A Virus-Host Protein Interactions Control Viral Pathogenesis. Int J Mol Sci. Multidisciplinary Digital Publishing Institute (MDPI); 2017;18. doi:10.3390/ijms18081673

154. Peacock TP, Sheppard CM, Staller E, Barclay WS. Host Determinants of Influenza RNA Synthesis Review 03.01.19. 2019; 1–19.

155. Chase GP, Rameix-Welti M-A, Zvirbliene A, Zvirblis G, Götz V, Wolff T, et al. Influenza Virus Ribonucleoprotein Complexes Gain Preferential Access to Cellular Export Machinery through Chromatin Targeting. Pekosz A, editor. PLoS Pathog. Public Library of Science; 2011;7: e1002187. doi:10.1371/journal.ppat.1002187

156. López-Turiso J, Martínez C, Toshiki T, Ortín J. The synthesis of influenza virus negative-strand RNA takes place in insoluble complexes present in the nuclear matrix fraction. Virus Res. 1990;16: 325–337. doi:10.1016/0168-1702(90)90056-H

157. Takizawa N, Watanabe K, Nouno K, Kobayashi N, Nagata K. Association of functional influenza viral proteins and RNAs with nuclear chromatin and sub-chromatin structure. Microbes Infect. Elsevier Masson; 2006;8: 823–833. doi:10.1016/J.MICINF.2005.10.005

158. Garcia-Robles I, Akarsu H, Müller CW, Ruigrok RWH, Baudin F. Interaction of influenza virus proteins with nucleosomes. Virology. Academic Press; 2005;332: 329–336. doi:10.1016/J.VIROL.2004.09.036

159. Marcos-Villar L, Pazo A, Nieto A. Influenza Virus and Chromatin: Role of the CHD1 Chromatin Remodeler in the Virus Life Cycle. J Virol. American Society for Microbiology (ASM); 2016;90: 3694. doi:10.1128/JVI.00053-16

160. Alfonso R, Lutz T, Rodriguez A, Chavez JP, Rodriguez P, Gutierrez S, et al. CHD6 chromatin remodeler is a negative modulator of influenza virus replication that relocates to inactive chromatin upon infection. Cell Microbiol. John Wiley & Sons, Ltd (10.1111); 2011;13: 1894–1906. doi:10.1111/j.1462-5822.2011.01679.x

161. Rodriguez A, Pérez-González A, Nieto A. Cellular human CLE/C14orf166 protein interacts with influenza virus polymerase and is required for viral replication. J Virol. American Society for Microbiology Journals; 2011;85: 12062–6. doi:10.1128/JVI.00684-11

162. Rodriguez-Frandsen A, de Lucas S, Pérez-González A, Pérez-Cidoncha M, Roldan-Gomendio A, Pazo A, et al. hCLE/C14orf166, a cellular protein required for viral replication, is incorporated into influenza virus particles. Sci Rep. Nature Publishing Group; 2016;6: 20744. doi:10.1038/srep20744

163. Ver LS, Marcos-Villar L, Landeras-Bueno S, Nieto A, Ortín J. The Cellular Factor NXP2/MORC3 Is a Positive Regulator of Influenza Virus Multiplication. J Virol.

American Society for Microbiology; 2015;89: 10023–30. doi:10.1128/JVI.01530-15

164. Su W-C, Hsu S-F, Lee Y-Y, Jeng K-S, Lai MMC. A Nucleolar Protein, Ribosomal RNA Processing 1 Homolog B (RRP1B), Enhances the Recruitment of Cellular mRNA in Influenza Virus Transcription. J Virol. American Society for Microbiology Journals; 2015;89: 11245–55. doi:10.1128/JVI.01487-15

165. Tsai P-L, Chiou N-T, Kuss S, García-Sastre A, Lynch KW, Fontoura BMA. Cellular RNA Binding Proteins NS1-BP and hnRNP K Regulate Influenza A Virus RNA Splicing. Pekosz A, editor. PLoS Pathog. Public Library of Science; 2013;9: e1003460. doi:10.1371/journal.ppat.1003460

166. Shih SR, Krug RM. Novel exploitation of a nuclear function by influenza virus: the cellular SF2/ASF splicing factor controls the amount of the essential viral M2 ion channel protein in infected cells. EMBO J. 1996;15: 5415–27. Available: http://www.ncbi.nlm.nih.gov/pubmed/8895585%0Ahttp://www.pubmedcentral.nih.gov/articlerender.fcgi?artid=PMC452284

167. Fournier G, Chiang C, Munier S, Tomoiu A, Demeret C, Vidalain P-O, et al. Recruitment of RED-SMU1 Complex by Influenza A Virus RNA Polymerase to Control Viral mRNA Splicing. Pekosz A, editor. PLoS Pathog. Public Library of Science; 2014;10: e1004164. doi:10.1371/journal.ppat.1004164

168. Landeras-Bueno S, Jorba N, Pérez-Cidoncha M, Ortín J. The Splicing Factor Proline-Glutamine Rich (SFPQ/PSF) Is Involved in Influenza Virus Transcription. Pekosz A, editor. PLoS Pathog. Public Library of Science; 2011;7: e1002397. doi:10.1371/journal.ppat.1002397

169. Hu Y, Liu X, Zhang A, Zhou H, Liu Z, Chen H, et al. CHD3 facilitates vRNP nuclear export by interacting with NES1 of influenza A virus NS2. Cell Mol Life Sci. Springer; 2015;72: 971–982. doi:10.1007/s00018-014-1726-9

170. Diot C, Munier S, van der Werf S, Naffakh N, Fournier G, Komarova A, et al. Influenza A Virus Polymerase Recruits the RNA Helicase DDX19 to Promote the Nuclear Export of Viral mRNAs. Sci Rep. Nature Publishing Group; 2016;6: 33763. doi:10.1038/srep33763

171. Kawaguchi A, Nagata K. De novo replication of the influenza virus RNA genome is regulated by DNA replicative helicase, MCM. EMBO J. European Molecular Biology Organization; 2007;26: 4566–75. doi:10.1038/sj.emboj.7601881

172. Momose F, Naito T, Yano K, Sugimoto S, Morikawa Y, Nagata K. Identification of Hsp90 as a stimulatory host factor involved in influenza virus RNA synthesis. J Biol Chem. American Society for Biochemistry and Molecular Biology; 2002;277: 45306–14. doi:10.1074/jbc.M206822200

173. Naito T, Momose F, Kawaguchi A, Nagata K. Involvement of Hsp90 in Assembly and Nuclear Import of Influenza Virus RNA Polymerase Subunits. J Virol. American Society for Microbiology Journals; 2007;68: 1819–1826. doi:10.1128/jvi.01917-06

174. Momose F, Basler CF, O'Neill RE, Iwamatsu A, Palese P, Nagata K. Cellular splicing factor RAF-2p48/NPI-5/BAT1/UAP56 interacts with the influenza virus nucleoprotein and enhances viral RNA synthesis. J Virol. American Society for Microbiology Journals; 2001;75: 1899–908. doi:10.1128/JVI.75.4.1899-1908.2001

175. Naito T, Kiyasu Y, Sugiyama K, Kimura A, Nakano R, Matsukage A, et al. An influenza virus replicon system in yeast identified Tat-SF1 as a stimulatory host factor for viral RNA synthesis. Proc Natl Acad Sci. National Academy of Sciences; 2007;104: 18235–18240. doi:10.1073/PNAS.0705856104

176. Zhou Z, Cao M, Guo Y, Zhao L, Wang J, Jia X, et al. Fragile X mental retardation protein stimulates ribonucleoprotein assembly of influenza A virus. Nat Commun. Nature Publishing Group; 2014;5: 3259. doi:10.1038/ncomms4259

177. Cao M, Wei C, Zhao L, Wang J, Jia Q, Wang X, et al. DnaJA1/Hsp40 is co-opted by influenza A virus to enhance its viral RNA polymerase activity. J Virol. American Society for Microbiology Journals; 2014;88: 14078–89. doi:10.1128/JVI.02475-14

178. Minakuchi M, Sugiyama K, Kato Y, Naito T, Okuwaki M, Kawaguchi A, et al. Pre-mRNA Processing Factor Prp18 Is a Stimulatory Factor of Influenza Virus RNA Synthesis and Possesses Nucleoprotein Chaperone Activity. J Virol. 2017;91: e01398-16. doi:10.1128/JVI.01398-16

179. Qiu L, Wang T, Tang Q, Li G, Wu P, Chen K. Long Non-coding RNAs: Regulators of Viral Infection and the Interferon Antiviral Response. Front Microbiol. Frontiers Media SA; 2018;9: 1621. doi:10.3389/fmicb.2018.01621

180. Wang J, Wang Y, Zhou R, Zhao J, Zhang Y, Yi D, et al. Host Long Noncoding RNA lncRNA-PAAN Regulates the Replication of Influenza A Virus. Viruses. Multidisciplinary Digital Publishing Institute; 2018;10: 330. doi:10.3390/v10060330

181. Wang J, Zhang Y, Li Q, Zhao J, Yi D, Ding J, et al. Influenza Virus Exploits an Interferon-Independent lncRNA to Preserve Viral RNA Synthesis through Stabilizing Viral RNA Polymerase PB1. Cell Rep. Elsevier; 2019;27: 3295-3304.e4. doi:10.1016/j.celrep.2019.05.036

182. Staller E, Sheppard CM, Neasham PJ, Mistry B, Peacock TP, Goldhill DH, et al. ANP32 proteins are essential for influenza virus replication in human cells. J Virol. American Society for Microbiology Journals; 2019; JVI.00217-19. doi:10.1128/JVI.00217-19

183. Sugiyama K, Kawaguchi A, Okuwaki M, Nagata K. pp32 and APRIL are host cell-derived regulators of influenza virus RNA synthesis from cRNA. Elife. 2015;4.

doi:10.7554/eLife.08939

184. Wei X, Liu Z, Wang J, Yang R, Yang J, Guo Y, et al. The interaction of cellular protein ANP32A with influenza A virus polymerase component PB2 promotes vRNA synthesis. Arch Virol. Springer Vienna; 2019;164: 787–798. doi:10.1007/s00705-018-04139-z

185. Baker SF, Ledwith MP, Mehle A. Differential splicing of ANP32A in birds alters its ability to stimulate RNA synthesis by restricted influenza polymerase. Cell Rep. ElsevierCompany.; 2018;24: 274613. doi:10.1101/274613

186. Long JS, Idoko-Akoh A, Mistry B, Goldhill D, Staller E, Schreyer J, et al. Species specific differences in use of ANP32 proteins by influenza A virus. Elife. 2019;8. doi:10.7554/eLife.45066

187. Giese S, Ciminski K, Bolte H, Moreira ÉA, Lakdawala S, Hu Z, et al. Role of influenza A virus NP acetylation on viral growth and replication. Nat Commun. Nature Publishing Group; 2017;8: 1259. doi:10.1038/s41467-017-01112-3

188. Kumar N, Liang Y, Parslow TG, Liang Y. Receptor Tyrosine Kinase Inhibitors Block Multiple Steps of Influenza A Virus Replication. J Virol. American Society for Microbiology Journals; 2011;85: 2818–2827. doi:10.1128/JVI.01969-10

189. Chen G, Liu C-H, Zhou L, Krug RM. Cellular DDX21 RNA Helicase Inhibits Influenza A Virus Replication but Is Counteracted by the Viral NS1 Protein. Cell Host Microbe. Cell Press; 2014;15: 484–493. doi:10.1016/J.CHOM.2014.03.002

190. Wang L, Fu B, Li W, Patil G, Liu L, Dorf ME, et al. Comparative influenza protein interactomes identify the role of plakophilin 2 in virus restriction. Nat Commun. Nature Publishing Group; 2017;8: 13876. doi:10.1038/ncomms13876

191. Thapa RJ, Ingram JP, Ragan KB, Nogusa S, Boyd DF, Benitez AA, et al. DAI Senses Influenza A Virus Genomic RNA and Activates RIPK3-Dependent Cell Death. Cell Host & Microbe. 2016. doi:10.1016/j.chom.2016.09.014

192. Rivas HG, Schmaling SK, Gaglia MM. Shutoff of Host Gene Expression in Influenza A Virus and Herpesviruses: Similar Mechanisms and Common Themes. Viruses. 2016/04/20. 2016;8. doi:10.3390/v8040102

193. Levene R, Gaglia M, Levene RE, Gaglia MM. Host Shutoff in Influenza A Virus: Many Means to an End. Viruses. Multidisciplinary Digital Publishing Institute; 2018;10: 475. doi:10.3390/v10090475

194. Nemeroff ME, Barabino SML, Li Y, Keller W, Krug RM. Influenza Virus NS1 Protein Interacts with the Cellular 30 kDa Subunit of CPSF and Inhibits 3’ End Formation of Cellular Pre-mRNAs. Mol Cell. Cell Press; 1998;1: 991–1000. doi:10.1016/S1097-2765(00)80099-4

195. Das K, Ma L-C, Xiao R, Radvansky B, Aramini J, Zhao L, et al. Structural basis for suppression of a host antiviral response by influenza A virus. Proc Natl Acad Sci U S A. National Academy of Sciences; 2008;105: 13093–8. doi:10.1073/pnas.0805213105

196. Fortes P, Beloso A, Ortín J. Influenza virus NS1 protein inhibits pre-mRNA splicing and blocks mRNA nucleocytoplasmic transport. EMBO J. John Wiley & Sons, Ltd; 1994;13: 704–712. doi:10.1002/j.1460-2075.1994.tb06310.x

197. Lu Y, Qian XY, Krug RM. The influenza virus NS1 protein: a novel inhibitor of pre-mRNA splicing. Genes Dev. Cold Spring Harbor Laboratory Press; 1994;8: 1817–28. doi:10.1101/gad.8.15.1817

198. Wang W, Krug RM. U6atac snRNA, the highly divergent counterpart of U6 snRNA, is the specific target that mediates inhibition of AT-AC splicing by the influenza virus NS1 protein. RNA. 1998;4: 55–64. Available: http://www.ncbi.nlm.nih.gov/pubmed/9436908%0Ahttp://www.pubmedcentral.nih.gov/articlerender.fcgi?artid=PMC1369596

199. Qiu Y, Nemeroff M, Krug RM. The influenza virus NS1 protein binds to a specific region in human U6 snRNA and inhibits U6-U2 and U6-U4 snRNA interactions during splicing. RNA. 1995;1: 304–16. Available: http://www.ncbi.nlm.nih.gov/pubmed/7489502

200. Chen Z, Li Y, Krug RM. Influenza A virus NS1 protein targets poly(A)-binding protein II of the cellular 3'-end processing machinery. EMBO J. John Wiley & Sons, Ltd; 1999;18: 2273–2283. doi:10.1093/emboj/18.8.2273

201. Hale BG, Randall RE, Ortin J, Jackson D. The multifunctional NS1 protein of influenza A viruses. J Gen Virol. Microbiology Society; 2008;89: 2359–2376. doi:10.1099/vir.0.2008/004606-0

202. Chan AY, Vreede FT, Smith M, Engelhardt OG, Fodor E. Influenza virus inhibits RNA polymerase II elongation. Virology. Academic Press; 2006;351: 210–217. doi:10.1016/J.VIROL.2006.03.005

203. Rodriguez A, Pérez-González A, Nieto A. Influenza virus infection causes specific degradation of the largest subunit of cellular RNA polymerase II. J Virol. American Society for Microbiology Journals; 2007;81: 5315–24. doi:10.1128/JVI.02129-06

204. Vreede FT, Chan AY, Sharps J, Fodor E. Mechanisms and functional implications of the degradation of host RNA polymerase II in influenza virus infected cells. Virology. Elsevier; 2010;396: 125. doi:10.1016/J.VIROL.2009.10.003

205. Gaglia MM, Glaunsinger BA. Viruses and the cellular RNA decay machinery. Wiley Interdiscip Rev RNA. John Wiley & Sons, Ltd; 2010;1: 47–59. doi:10.1002/wrna.3

206. Molleston JM, Cherry S. Attacked from All Sides: RNA Decay in Antiviral Defense.

Viruses. Multidisciplinary Digital Publishing Institute (MDPI); 2017;9. doi:10.3390/V9010002

207. Abernathy E, Glaunsinger B. Emerging roles for RNA degradation in viral replication and antiviral defense. Virology. Academic Press; 2015;479–480: 600–608. doi:10.1016/J.VIROL.2015.02.007

208. Balistreri G, Bognanni C, Mühlemann O, Balistreri G, Bognanni C, Mühlemann O. Virus Escape and Manipulation of Cellular Nonsense-Mediated mRNA Decay. Viruses. Multidisciplinary Digital Publishing Institute; 2017;9: 24. doi:10.3390/v9010024

209. Guo L, Vlasova-St Louis I, Bohjanen PR. Viral manipulation of host mRNA decay. Future Virol. NIH Public Access; 2018;13: 211–223. doi:10.2217/fvl-2017-0106

210. Moon SL, Wilusz J. Cytoplasmic Viruses: Rage against the (Cellular RNA Decay) Machine. Racaniello V, editor. PLoS Pathog. Public Library of Science; 2013;9: e1003762. doi:10.1371/journal.ppat.1003762

211. Łabno A, Tomecki R, Dziembowski A. Cytoplasmic RNA decay pathways - Enzymes and mechanisms. Biochim Biophys Acta - Mol Cell Res. Elsevier; 2016;1863: 3125–3147. doi:10.1016/J.BBAMCR.2016.09.023

212. Mugridge JS, Coller J, Gross JD. Structural and molecular mechanisms for the control of eukaryotic 5′–3′ mRNA decay. Nat Struct Mol Biol. Nature Publishing Group; 2018;25: 1077–1085. doi:10.1038/s41594-018-0164-z

213. Shoemaker CJ, Green R. Translation drives mRNA quality control. Nat Struct Mol Biol. Nature Publishing Group; 2012;19: 594–601. doi:10.1038/nsmb.2301

214. Decker CJ, Parker R. P-bodies and stress granules: possible roles in the control of translation and mRNA degradation. Cold Spring Harb Perspect Biol. Cold Spring Harbor Laboratory Press; 2012;4: a012286. doi:10.1101/cshperspect.a012286

215. Tsai W-C, Lloyd RE. Cytoplasmic RNA Granules and Viral Infection. Annu Rev Virol. NIH Public Access; 2014;1: 147–70. doi:10.1146/annurev-virology-031413-085505

216. Reineke LC, Lloyd RE. Diversion of stress granules and P-bodies during viral infection. Virology. Academic Press; 2013;436: 255–267. doi:10.1016/J.VIROL.2012.11.017

217. Dougherty JD, White JP, Lloyd RE. Poliovirus-mediated disruption of cytoplasmic processing bodies. J Virol. American Society for Microbiology Journals; 2011;85: 64–75. doi:10.1128/JVI.01657-10

218. Zheng D, Ezzeddine N, Chen C-YA, Zhu W, He X, Shyu A-B. Deadenylation is prerequisite for P-body formation and mRNA decay in mammalian cells. J Cell Biol. Rockefeller University Press; 2008;182: 89–101. doi:10.1083/JCB.200801196

219. Khong A, Jan E. Modulation of Stress Granules and P Bodies during Dicistrovirus Infection. J Virol. American Society for Microbiology Journals; 2011;85: 1439–1451. doi:10.1128/JVI.02220-10

220. Gillis P, Malter JS. The adenosine-uridine binding factor recognizes the AU-rich elements of cytokine, lymphokine, and oncogene mRNAs. J Biol Chem. 1991;266: 3172–3177.

221. Qiu Y, Ye X, Hanson PJ, Zhang HM, Zong J, Cho B, et al. Hsp70-1: upregulation via selective phosphorylation of heat shock factor 1 during coxsackieviral infection and promotion of viral replication via the AU-rich element. Cell Mol Life Sci. Springer International Publishing; 2016;73: 1067–1084. doi:10.1007/s00018-015-2036-6

222. Wong J, Si X, Angeles A, Zhang J, Shi J, Fung G, et al. Cytoplasmic redistribution and cleavage of AUF1 during coxsackievirus infection enhance the stability of its viral genome. FASEB J. Federation of American Societies for Experimental Biology Bethesda, MD, USA; 2013;27: 2777–2787. doi:10.1096/fj.12-226498

223. Friedrich S, Schmidt T, Schierhorn A, Lilie H, Szczepankiewicz G, Bergs S, et al. Arginine methylation enhances the RNA chaperone activity of the West Nile virus host factor AUF1 p45. RNA. Cold Spring Harbor Laboratory Press; 2016;22: 1574–91. doi:10.1261/rna.055269.115

224. Wolf J, Passmore LA. mRNA deadenylation by Pan2-Pan3. Biochem Soc Trans. Europe PMC Funders; 2014;42: 184–7. doi:10.1042/BST20130211

225. Collart MA. The Ccr4-Not complex is a key regulator of eukaryotic gene expression. Wiley Interdiscip Rev RNA. Wiley-Blackwell; 2016;7: 438–54. doi:10.1002/wrna.1332

226. Garneau NL, Sokoloski KJ, Opyrchal M, Neff CP, Wilusz CJ, Wilusz J. The 3' untranslated region of sindbis virus represses deadenylation of viral transcripts in mosquito and Mammalian cells. J Virol. American Society for Microbiology Journals; 2008;82: 880–92. doi:10.1128/JVI.01205-07

227. Huarte J, Stutz A, O'Connell ML, Gubler P, Belin D, Darrow AL, et al. Transient translational silencing by reversible mRNA deadenylation. Cell. Cell Press; 1992;69: 1021–1030. doi:10.1016/0092-8674(92)90620-R

228. Beggs JD. Lsm proteins and RNA processing. Biochem Soc Trans. Portland Press Limited; 2005;33: 433–8. doi:10.1042/BST0330433

229. Sharif H, Conti E. Architecture of the Lsm1-7-Pat1 Complex: A Conserved Assembly in Eukaryotic mRNA Turnover. Cell Rep. Cell Press; 2013;5: 283–291. doi:10.1016/J.CELREP.2013.10.004

230. Tharun S, Muhlrad D, Chowdhury A, Parker R. Mutations in the Saccharomyces

cerevisiae LSM1 gene that affect mRNA decapping and 3' end protection. Genetics. Genetics; 2005;170: 33–46. doi:10.1534/genetics.104.034322

231. Pannone BK, Kim SD, Noe DA, Wolin SL. Multiple functional interactions between components of the Lsm2-Lsm8 complex, U6 snRNA, and the yeast La protein. Genetics. Genetics; 2001;158: 187–96. Available: http://www.ncbi.nlm.nih.gov/pubmed/11333229

232. Jungfleisch J, Chowdhury A, Alves-Rodrigues I, Tharun S, Díez J. The Lsm1-7-Pat1 complex promotes viral RNA translation and replication by differential mechanisms. RNA. Cold Spring Harbor Laboratory Press; 2015;21: 1469–1479. doi:10.1261/RNA.052209.115

233. Mas A, Alves-Rodrigues I, Noueiry A, Ahlquist P, Díez J. Host Deadenylation-Dependent mRNA Decapping Factors Are Required for a Key Step in Brome Mosaic Virus RNA Replication. J Virol. American Society for Microbiology Journals; 2006;80: 246–251. doi:10.1128/JVI.80.1.246-251.2006

234. Noueiry AO, Diez J, Falk SP, Chen J, Ahlquist P. Yeast Lsm1p-7p/Pat1p deadenylation-dependent mRNA-decapping factors are required for brome mosaic virus genomic RNA translation. Mol Cell Biol. American Society for Microbiology Journals; 2003;23: 4094–106. doi:10.1128/MCB.23.12.4094-4106.2003

235. Galão RP, Chari A, Alves-Rodrigues I, Lobão D, Mas A, Kambach C, et al. LSm1-7 complexes bind to specific sites in viral RNA genomes and regulate their translation and replication. RNA. Cold Spring Harbor Laboratory Press; 2010;16: 817–27. doi:10.1261/rna.1712910

236. Jungfleisch J, Blasco-Moreno B, Díez J. Use of Cellular Decapping Activators by Positive-Strand RNA Viruses. Viruses. Multidisciplinary Digital Publishing Institute (MDPI); 2016;8. doi:10.3390/v8120340

237. Scheller N, Mina LB, Galao RP, Chari A, Gimenez-Barcons M, Noueiry A, et al. Translation and replication of hepatitis C virus genomic RNA depends on ancient cellular proteins that control mRNA fates. Proc Natl Acad Sci. National Academy of Sciences; 2009;106: 13517–13522. doi:10.1073/pnas.0906413106

238. Ward AM, Bidet K, Yinglin A, Ler SG, Hogue K, Blackstock W, et al. Quantitative mass spectrometry of DENV-2 RNA-interacting proteins reveals that the DEAD-box RNA helicase DDX6 binds the DB1 and DB2 3' UTR structures. RNA Biol. Taylor & Francis; 2011;8: 1173–1186. doi:10.4161/rna.8.6.17836

239. Chahar HS, Chen S, Manjunath N. P-body components LSM1, GW182, DDX3, DDX6 and XRN1 are recruited to WNV replication sites and positively regulate viral replication. Virology. Academic Press; 2013;436: 1–7.

doi:10.1016/J.VIROL.2012.09.041

240. Giménez-Barcons M, Alves-Rodrigues I, Jungfleisch J, Wynsberghe PM Van, Ahlquist P, Díez J. The Cellular Decapping Activators LSm1, Pat1, and Dhh1 Control the Ratio of Subgenomic to Genomic Flock House Virus RNAs. J Virol. American Society for Microbiology Journals; 2013;87: 6192–6200. doi:10.1128/JVI.03327-12

241. Silva PAGC, Pereira CF, Dalebout TJ, Spaan WJM, Bredenbeek PJ. An RNA pseudoknot is required for production of yellow fever virus subgenomic RNA by the host nuclease XRN1. J Virol. American Society for Microbiology Journals; 2010;84: 11395–406. doi:10.1128/JVI.01047-10

242. Chapman EG, Costantino DA, Rabe JL, Moon SL, Wilusz J, Nix JC, et al. The Structural Basis of Pathogenic Subgenomic Flavivirus RNA (sfRNA) Production. Science (80-). American Association for the Advancement of Science; 2014;344: 307–310. doi:10.1126/SCIENCE.1250897

243. Moon SL, Anderson JR, Kumagai Y, Wilusz CJ, Akira S, Khromykh AA, et al. A noncoding RNA produced by arthropod-borne flaviviruses inhibits the cellular exoribonuclease XRN1 and alters host mRNA stability. RNA. Cold Spring Harbor Laboratory Press; 2012;18: 2029–40. doi:10.1261/rna.034330.112

244. Pijlman GP, Funk A, Kondratieva N, Leung J, Torres S, van der Aa L, et al. A Highly Structured, Nuclease-Resistant, Noncoding RNA Produced by Flaviviruses Is Required for Pathogenicity. Cell Host Microbe. Cell Press; 2008;4: 579–591. doi:10.1016/J.CHOM.2008.10.007

245. Chapman EG, Moon SL, Wilusz J, Kieft JS. RNA structures that resist degradation by Xrn1 produce a pathogenic Dengue virus RNA. Elife. 2014;3. doi:10.7554/eLife.01892

246. Moon SL, Blackinton JG, Anderson JR, Dozier MK, Dodd BJT, Keene JD, et al. XRN1 Stalling in the 5' UTR of Hepatitis C Virus and Bovine Viral Diarrhea Virus Is Associated with Dysregulated Host mRNA Stability. Siddiqui A, editor. PLOS Pathog. Public Library of Science; 2015;11: e1004708. doi:10.1371/journal.ppat.1004708

247. Kilchert C, Wittmann S, Vasiljeva L. The regulation and functions of the nuclear RNA exosome complex. Nat Rev Mol Cell Biol. 2016/01/05. 2016; doi:10.1038/nrm.2015.15

248. Molleston JM, Sabin LR, Moy RH, Menghani S V., Rausch K, Gordesky-Gold B, et al. A conserved virus-induced cytoplasmic TRAMP-like complex recruits the exosome to target viral RNA for degradation. Genes Dev. Cold Spring Harbor Laboratory Press; 2016;30: 1658–1670. doi:10.1101/gad.284604.116

249. Moy RH, Cole BS, Yasunaga A, Gold B, Shankarling G, Varble A, et al. Stem-Loop Recognition by DDX17 Facilitates miRNA Processing and Antiviral Defense. Cell. Cell Press; 2014;158: 764–777. doi:10.1016/J.CELL.2014.06.023

250. Miyashita M, Oshiumi H, Matsumoto M, Seya T. DDX60, a DEXD/H Box Helicase, Is a Novel Antiviral Factor Promoting RIG-I-Like Receptor-Mediated Signaling. Mol Cell Biol. American Society for Microbiology Journals; 2011;31: 3802–3819. doi:10.1128/MCB.01368-10

251. Rialdi A, Hultquist J, Jimenez-Morales D, Peralta Z, Campisi L, Fenouil R, et al. The RNA Exosome Syncs IAV-RNAPII Transcription to Promote Viral Ribogenesis and Infectivity. Cell. 2017;169: 679-692.e14. doi:10.1016/j.cell.2017.04.021

252. Karousis ED, Nasif S, Mühlemann O. Nonsense-mediated mRNA decay: novel mechanistic insights and biological impact. Wiley Interdiscip Rev RNA. 2016;7: 661–682. doi:10.1002/wrna.1357

253. Schweingruber C, Rufener SC, Zünd D, Yamashita A, Mühlemann O. Nonsense-mediated mRNA decay — Mechanisms of substrate mRNA recognition and degradation in mammalian cells. Biochim Biophys Acta - Gene Regul Mech. Elsevier; 2013;1829: 612–623. doi:10.1016/J.BBAGRM.2013.02.005

254. Drazkowska K, Tomecki R. Cytoplasmic RNA Decay. eLS. Chichester, UK: John Wiley & Sons, Ltd; pp. 1–14. doi:10.1002/9780470015902.a0027365

255. Balistreri G, Horvath P, Schweingruber C, Zünd D, McInerney G, Merits A, et al. The Host Nonsense-Mediated mRNA Decay Pathway Restricts Mammalian RNA Virus Replication. Cell Host Microbe. Cell Press; 2014;16: 403–411. doi:10.1016/J.CHOM.2014.08.007

256. Nicholson P, Yepiskoposyan H, Metze S, Zamudio Orozco R, Kleinschmidt N, Mühlemann O. Nonsense-mediated mRNA decay in human cells: mechanistic insights, functions beyond quality control and the double-life of NMD factors. Cell Mol Life Sci. SP Birkhäuser Verlag Basel; 2010;67: 677–700. doi:10.1007/s00018-009-0177-1

257. Ramage HR, Kumar GR, Verschueren E, Johnson JR, Von Dollen J, Johnson T, et al. A combined proteomics/genomics approach links hepatitis C virus infection with nonsense-mediated mRNA decay. Mol Cell. NIH Public Access; 2015;57: 329–340. doi:10.1016/j.molcel.2014.12.028

258. Li M, Johnson JR, Truong B, Kim G, Weinbren N, Dittmar M, et al. Identification of antiviral roles for the exon–junction complex and nonsense-mediated decay in flaviviral infection. Nat Microbiol. Nature Publishing Group; 2019;4: 985–995. doi:10.1038/s41564-019-0375-z

259. Wu X, He W-T, Tian S, Meng D, Li Y, Chen W, et al. pelo Is Required for High Efficiency Viral Replication. Schneider DS, editor. PLoS Pathog. Public Library of Science; 2014;10: e1004034. doi:10.1371/journal.ppat.1004034

260. Hogg JR. Viral Evasion and Manipulation of Host RNA Quality Control Pathways. J

Virol. American Society for Microbiology Journals; 2016;90: 7010–7018. doi:10.1128/JVI.00607-16

261. Greenbaum BD, Levine AJ, Bhanot G, Rabadan R, Josse J, Kaiser A, et al. Patterns of Evolution and Host Gene Mimicry in Influenza and Other RNA Viruses. Holmes EC, editor. PLoS Pathog. Public Library of Science; 2008;4: e1000079. doi:10.1371/journal.ppat.1000079

262. Zhao L, Jha BK, Wu A, Elliott R, Ziebuhr J, Gorbalenya AE, et al. Antagonism of the interferon-induced OAS-RNase L pathway by murine coronavirus ns2 protein is required for virus replication and liver pathology. Cell Host Microbe. NIH Public Access; 2012;11: 607–16. doi:10.1016/j.chom.2012.04.011

263. Townsend HL, Jha BK, Han J-Q, Maluf NK, Silverman RH, Barton DJ. A viral RNA competitively inhibits the antiviral endoribonuclease domain of RNase L. RNA. Cold Spring Harbor Laboratory Press; 2008;14: 1026–36. doi:10.1261/rna.958908

264. Han J-Q, Barton DJ. Activation and evasion of the antiviral 2'-5' oligoadenylate synthetase/ribonuclease L pathway by hepatitis C virus mRNA. RNA. Cold Spring Harbor Laboratory Press; 2002;8: 512–25. doi:10.1017/s1355838202020617

265. Parrish S, Hurchalla M, Liu S-W, Moss B. The African swine fever virus g5R protein possesses mRNA decapping activity. Virology. Academic Press; 2009;393: 177–182. doi:10.1016/J.VIROL.2009.07.026

266. Rowe M, Glaunsinger B, van Leeuwen D, Zuo J, Sweetman D, Ganem D, et al. Host shutoff during productive Epstein-Barr virus infection is mediated by BGLF5 and may contribute to immune evasion. Proc Natl Acad Sci U S A. National Academy of Sciences; 2007;104: 3366–71. doi:10.1073/pnas.0611128104

267. Covarrubias S, Gaglia MM, Kumar GR, Wong W, Jackson AO, Glaunsinger BA. Coordinated Destruction of Cellular Messages in Translation Complexes by the Gammaherpesvirus Host Shutoff Factor and the Mammalian Exonuclease Xrn1. Renne R, editor. PLoS Pathog. Public Library of Science; 2011;7: e1002339. doi:10.1371/journal.ppat.1002339

268. Lee H, Patschull AOM, Bagnéris C, Ryan H, Sanderson CM, Ebrahimi B, et al. KSHV SOX mediated host shutoff: the molecular mechanism underlying mRNA transcript processing. Nucleic Acids Res. Oxford University Press; 2017;45: 4756–4767. doi:10.1093/nar/gkw1340

269. Feng P, Everly DN, Read GS. mRNA decay during herpes simplex virus (HSV) infections: protein-protein interactions involving the HSV virion host shutoff protein and translation factors eIF4H and eIF4A. J Virol. American Society for Microbiology Journals; 2005;79: 9651–64. doi:10.1128/JVI.79.15.9651-9664.2005

270. Page HG, Read GS. The Virion Host Shutoff Endonuclease (UL41) of Herpes Simplex Virus Interacts with the Cellular Cap-Binding Complex eIF4F. J Virol. American Society for Microbiology Journals; 2010;84: 6886–6890. doi:10.1128/JVI.00166-10

271. Parrish S, Resch W, Moss B. Vaccinia virus D10 protein has mRNA decapping activity, providing a mechanism for control of host and viral gene expression. Proc Natl Acad Sci U S A. National Academy of Sciences; 2007;104: 2139–44. doi:10.1073/pnas.0611685104

272. Parrish S, Moss B. Characterization of a second vaccinia virus mRNA-decapping enzyme conserved in poxviruses. J Virol. American Society for Microbiology (ASM); 2007;81: 12973–8. doi:10.1128/JVI.01668-07

273. Khaperskyy DA, Schmaling S, Larkins-Ford J, McCormick C, Gaglia MM. Selective Degradation of Host RNA Polymerase II Transcripts by Influenza A Virus PA-X Host Shutoff Protein. Palese P, editor. PLoS Pathog. 2016/02/06. 2016;12: e1005427. doi:10.1371/journal.ppat.1005427

274. Kamitani W, Huang C, Narayanan K, Lokugamage KG, Makino S. A two-pronged strategy to suppress host protein synthesis by SARS coronavirus Nsp1 protein. Nat Struct Mol Biol. Nature Publishing Group; 2009;16: 1134–1140. doi:10.1038/nsmb.1680

275. Huang C, Lokugamage KG, Rozovics JM, Narayanan K, Semler BL, Makino S. SARS Coronavirus nsp1 Protein Induces Template-Dependent Endonucleolytic Cleavage of mRNAs: Viral mRNAs Are Resistant to nsp1-Induced RNA Cleavage. Baric RS, editor. PLoS Pathog. Public Library of Science; 2011;7: e1002433. doi:10.1371/journal.ppat.1002433

276. Ferron F, Subissi L, Silveira De Morais AT, Le NTT, Sevajol M, Gluais L, et al. Structural and molecular basis of mismatch correction and ribavirin excision from coronavirus RNA. Proc Natl Acad Sci U S A. National Academy of Sciences; 2017; 201718806. doi:10.1073/pnas.1718806115

277. Herbert KM, Nag A. A Tale of Two RNAs during Viral Infection: How Viruses Antagonize mRNAs and Small Non-Coding RNAs in The Host Cell. Viruses. 2016/06/09. 2016;8. doi:10.3390/v8060154

278. Hastie KM, Kimberlin CR, Zandonatti MA, MacRae IJ, Saphire EO. Structure of the Lassa virus nucleoprotein reveals a dsRNA-specific 3’ to 5’ exonuclease activity essential for immune suppression. Proc Natl Acad Sci U S A. National Academy of Sciences; 2011;108: 2396–401. doi:10.1073/pnas.1016404108

279. Reynard S, Russier M, Fizet A, Carnec X, Baize S. Exonuclease domain of the Lassa virus nucleoprotein is critical to avoid RIG-I signaling and to inhibit the innate immune

response. J Virol. American Society for Microbiology (ASM); 2014;88: 13923–7. doi:10.1128/JVI.01923-14

280. Eckerle LD, Becker MM, Halpin RA, Li K, Venter E, Lu X, et al. Infidelity of SARS-CoV Nsp14-exonuclease mutant virus replication is revealed by complete genome sequencing. PLoS Pathog. 2010;6: 1–15. doi:10.1371/journal.ppat.1000896

281. Mok BW-Y, Song W, Wang P, Tai H, Chen Y, Zheng M, et al. The NS1 protein of influenza A virus interacts with cellular processing bodies and stress granules through RNA-associated protein 55 (RAP55) during virus infection. J Virol. American Society for Microbiology Journals; 2012;86: 12695–707. doi:10.1128/JVI.00647-12

282. Min J-Y, Krug RM. The primary function of RNA binding by the influenza A virus NS1 protein in infected cells: Inhibiting the 2′-5′ oligo (A) synthetase/RNase L pathway. Proc Natl Acad Sci. National Academy of Sciences; 2006;103: 7100–7105. doi:10.1073/PNAS.0602184103

283. Cheng A, Wong SM, Yuan YA. Structural basis for dsRNA recognition by NS1 protein of influenza A virus. Cell Res. Nature Publishing Group; 2009;19: 187–195. doi:10.1038/cr.2008.288

284. Qu H, Li J, Yang L, Sun L, Liu W, He H. Influenza A Virus-induced expression of ISG20 inhibits viral replication by interacting with nucleoprotein. Virus Genes. Springer US; 2016;52: 759–767. doi:10.1007/s11262-016-1366-2

285. Espert L, Degols G, Gongora C, Blondel D, Williams BR, Silverman RH, et al. ISG20, a new interferon-induced RNase specific for single-stranded RNA, defines an alternative antiviral pathway against RNA genomic viruses. J Biol Chem. American Society for Biochemistry and Molecular Biology; 2003;278: 16151–8. doi:10.1074/jbc.M209628200

286. Shi M, Jagger BW, Wise HM, Digard P, Holmes EC, Taubenberger JK. Evolutionary Conservation of the PA-X Open Reading Frame in Segment 3 of Influenza A Virus. J Virol. American Society for Microbiology Journals; 2012;86: 12411–12413. doi:10.1128/JVI.01677-12

287. Gaucherand L, Porter BK, Levene RE, Price EL, Schmaling SK, Rycroft CH, et al. The Influenza A Virus Endoribonuclease PA-X Usurps Host mRNA Processing Machinery to Limit Host Gene Expression. Cell Rep. Cell Press; 2019;27: 776-792.e7. doi:10.1016/J.CELREP.2019.03.063

288. Thomas MF, L'Etoile ND, Ansel KM. Eri1: A conserved enzyme at the crossroads of multiple RNA-processing pathways [Internet]. Trends in Genetics Elsevier Current Trends; Jul, 2014 pp. 298–307. doi:10.1016/j.tig.2014.05.003

289. Zuo Y, Deutscher MP. Exoribonuclease superfamilies: structural analysis and

phylogenetic distribution. Nucleic Acids Res. Narnia; 2001;29: 1017–1026. doi:10.1093/nar/29.5.1017

290. Kipp M, Göhring F, Ostendorp T, van Drunen CM, van Driel R, Przybylski M, et al. SAF-Box, a conserved protein domain that specifically recognizes scaffold attachment region DNA. Mol Cell Biol. American Society for Microbiology Journals; 2000;20: 7480–9. doi:10.1128/mcb.20.20.7480-7489.2000

291. Tan D, Marzluff WF, Dominski Z, Tong L. Structure of histone mRNA stem-loop, human stem-loop binding protein and 3'hExo ternary complex. Science. NIH Public Access; 2013;339: 318. doi:10.1126/SCIENCE.1228705

292. Dominski Z, Yang XC, Kaygun H, Dadlez M, Marzluff WF. A 3' exonuclease that specifically interacts with the 3' end of histone mRNA. Mol Cell. 2003;12: 295–305. doi:10.1016/S1097-2765(03)00278-8

293. Yang XC, Purdy M, Marzluff WF, Dominski Z. Characterization of 3'hExo, a 3' exonuclease specifically interacting with the 3' end of histone mRNA. J Biol Chem. 2006;281: 30447–30454. doi:10.1074/jbc.M602947200

294. Ansel KM, Pastor WA, Rath N, Lapan AD, Glasmacher E, Wolf C, et al. Mouse Eri1 interacts with the ribosome and catalyzes 5.8S rRNA processing. Nat Struct Mol Biol. Nature Publishing Group; 2008;15: 523–530. doi:10.1038/nsmb.1417

295. Kennedy S, Wang D, Ruvkun G. A conserved siRNA-degrading RNase negatively regulates RNA interference in C. elegans. Nature. Nature Publishing Group; 2004;427: 645–649. doi:10.1038/nature02302

296. Kupsco JM, Wu M-J, Marzluff WF, Thapar R, Duronio RJ. Genetic and biochemical characterization of Drosophila Snipper: A promiscuous member of the metazoan 3'hExo/ERI-1 family of 3' to 5' exonucleases. RNA. Cold Spring Harbor Laboratory Press; 2006;12: 2103–17. doi:10.1261/rna.186706

297. Cheng Y, Patel DJ. Crystallographic Structure of the Nuclease Domain of 3'hExo, a DEDDh Family Member, Bound to rAMP. J Mol Biol. Academic Press; 2004;343: 305–312. doi:10.1016/J.JMB.2004.08.055

298. Iida T, Kawaguchi R, Nakayama J ichi. Conserved Ribonuclease, Eri1, Negatively Regulates Heterochromatin Assembly in Fission Yeast. Curr Biol. 2006;16: 1459–1464. doi:10.1016/j.cub.2006.05.061

299. Kim DH, Rossi JJ. Strategies for silencing human disease using RNA interference. Nat Rev Genet. Nature Publishing Group; 2007;8: 173–184. doi:10.1038/nrg2006

300. Gabel HW, Ruvkun G. The exonuclease ERI-1 has a conserved dual role in 5.8S rRNA processing and RNAi. Nat Struct Mol Biol. Nature Publishing Group; 2008;15: 531–533.

doi:10.1038/nsmb.1411

301. Majumdar R, Rajasekaran K, Cary JW. RNA Interference (RNAi) as a Potential Tool for Control of Mycotoxin Contamination in Crop Plants: Concepts and Considerations. Front Plant Sci. Frontiers; 2017;8: 200. doi:10.3389/fpls.2017.00200

302. Thomas MF, Abdul-Wajid S, Panduro M, Babiarz JE, Rajaram M, Woodruff P, et al. Eri1 regulates microRNA homeostasis and mouse lymphocyte development and antiviral function. Blood. American Society of Hematology; 2012;120: 130–42. doi:10.1182/blood-2011-11-394072

303. Lee RC, Hammell CM, Ambros V. Interacting endogenous and exogenous RNAi pathways in Caenorhabditis elegans. RNA. Cold Spring Harbor Laboratory Press; 2006;12: 589–97. doi:10.1261/rna.2231506

304. Bian Y, Zhou W, Zhao Y, Li X, Geng W, Hao R, et al. High-Dose siRNAs Upregulate Mouse Eri-1 at both Transcription and Posttranscription Levels. Creighton C, editor. PLoS One. Public Library of Science; 2011;6: e26466. doi:10.1371/journal.pone.0026466

305. Hong J, Qian Z, Shen S, Min T, Tan C, Xu J, et al. High doses of siRNAs induce eri-1 and adar-1 gene expression and reduce the efficiency of RNA interference in the mouse. Biochem J. Portland Press Limited; 2005;390: 675–9. doi:10.1042/BJ20050647

306. Klinge S, Woolford JL. Ribosome assembly coming into focus. Nat Rev Mol Cell Biol. Nature Publishing Group; 2019;20: 116–131. doi:10.1038/s41580-018-0078-y

307. Thermann R, Hentze MW. Drosophila miR2 induces pseudo-polysomes and inhibits translation initiation. Nature. Nature Publishing Group; 2007;447: 875–878. doi:10.1038/nature05878

308. Pillai RS, Bhattacharyya SN, Artus CG, Zoller T, Cougot N, Basyuk E, et al. Inhibition of translational initiation by Let-7 MicroRNA in human cells. Science. American Association for the Advancement of Science; 2005;309: 1573–6. doi:10.1126/science.1115079

309. Herrero AB, Moreno S. Lsm1 promotes genomic stability by controlling histone mRNA decay. EMBO J. EMBO Press; 2011;30: 2008–2018. doi:10.1038/emboj.2011.117

310. Hoefig KP, Heissmeyer V. Degradation of oligouridylated histone mRNAs: See UUUUU and goodbye. Wiley Interdiscip Rev RNA. John Wiley & Sons, Ltd; 2014;5: 577–589. doi:10.1002/wrna.1232

311. Marzluff WF, Koreski KP. Birth and Death of Histone mRNAs. Trends Genet. Elsevier; 2017;33: 745–759. doi:10.1016/j.tig.2017.07.014

312. Marzluff WF. Metazoan replication-dependent histone mRNAs: a distinct set of RNA polymerase II transcripts. Curr Opin Cell Biol. Elsevier Current Trends; 2005;17: 274–280. doi:10.1016/J.CEB.2005.04.010

313. Wang ZF, Whitfield ML, Ingledue TC, Dominski Z, Marzluff WF. The protein that binds the 3' end of histone mRNA: A novel RNA-binding protein required for histone pre-mRNA processing. Genes Dev. 1996;10: 3028–3040. doi:10.1101/gad.10.23.3028

314. Sullivan KD, Mullen TE, Marzluff WF, Wagner EJ. Knockdown of SLBP results in nuclear retention of histone mRNA. RNA. Cold Spring Harbor Laboratory Press; 2009;15: 459–72. doi:10.1261/rna.1205409

315. Cakmakci NG, Lerner RS, Wagner EJ, Zheng L, Marzluff WF. SLIP1, a factor required for activation of histone mRNA translation by the stem-loop binding protein. Mol Cell Biol. American Society for Microbiology Journals; 2008;28: 1182–94. doi:10.1128/MCB.01500-07

316. Sànchez R, Marzluff WF. The stem-loop binding protein is required for efficient translation of histone mRNA in vivo and in vitro. Mol Cell Biol. American Society for Microbiology Journals; 2002;22: 7093–104. doi:10.1128/mcb.22.20.7093-7104.2002

317. Brodersen MML, Lampert F, Barnes CA, Soste M, Piwko W, Peter M. CRL4 WDR23 - Mediated SLBP Ubiquitylation Ensures Histone Supply during DNA Replication. Mol Cell. Elsevier Inc.; 2016;62: 627–635. doi:10.1016/j.molcel.2016.04.017

318. Whitfield ML, Zheng LX, Baldwin A, Ohta T, Hurt MM, Marzluff WF. Stem-loop binding protein, the protein that binds the 3' end of histone mRNA, is cell cycle regulated by both translational and posttranslational mechanisms. Mol Cell Biol. American Society for Microbiology Journals; 2000;20: 4188–98. doi:10.1128/mcb.20.12.4188-4198.2000

319. Dominski Z, Marzluff WF. Formation of the 3' end of histone mRNA: getting closer to the end. Gene. NIH Public Access; 2007;396: 373–90. doi:10.1016/j.gene.2007.04.021

320. Pillai RS, Grimmler M, Meister G, Will CL, Lührmann R, Fischer U, et al. Unique Sm core structure of U7 snRNPs: assembly by a specialized SMN complex and the role of a new component, Lsm11, in histone RNA processing. Genes Dev. Cold Spring Harbor Laboratory Press; 2003;17: 2321–2333. doi:10.1101/GAD.274403

321. Yang X, Xu B, Sabath I, Kunduru L, Burch BD, Marzluff WF, et al. FLASH is required for the endonucleolytic cleavage of histone pre-mRNAs but is dispensable for the 5' exonucleolytic degradation of the downstream cleavage product. Mol Cell Biol. American Society for Microbiology Journals; 2011;31: 1492–502. doi:10.1128/MCB.00979-10

322. Burch BD, Godfrey AC, Gasdaska PY, Salzler HR, Duronio RJ, Marzluff WF, et al. Interaction between FLASH and Lsm11 is essential for histone pre-mRNA processing in

vivo in Drosophila. RNA. Cold Spring Harbor Laboratory Press; 2011;17: 1132–47. doi:10.1261/rna.2566811

323. Skrajna A, Yang X-C, Bucholc K, Zhang J, Hall TMT, Dadlez M, et al. U7 snRNP is recruited to histone pre-mRNA in a FLASH-dependent manner by two separate regions of the stem-loop binding protein. RNA. Cold Spring Harbor Laboratory Press; 2017;23: 938–951. doi:10.1261/rna.060806.117

324. Sullivan KD, Steiniger M, Marzluff WF. A Core Complex of CPSF73, CPSF100, and Symplekin May Form Two Different Cleavage Factors for Processing of Poly(A) and Histone mRNAs. Mol Cell. Cell Press; 2009;34: 322–332. doi:10.1016/J.MOLCEL.2009.04.024

325. Yang X, Torres MP, Marzluff WF, Dominski Z. Three proteins of the U7-specific Sm ring function as the molecular ruler to determine the site of 3'-end processing in mammalian histone pre-mRNA. Mol Cell Biol. American Society for Microbiology Journals; 2009;29: 4045–56. doi:10.1128/MCB.00296-09

326. Lackey PE, Welch JD, Marzluff WF. TUT7 catalyzes the uridylation of the 3' end for rapid degradation of histone mRNA. RNA. Cold Spring Harbor Laboratory Press; 2016;22: 1673–1688. doi:10.1261/rna.058107.116

327. Welch JD, Slevin MK, Tatomer DC, Duronio RJ, Prins JF, Marzluff WF. EnD-Seq and AppEnD: sequencing 3' ends to identify nontemplated tails and degradation intermediates. RNA. Cold Spring Harbor Laboratory Press; 2015;21: 1375–89. doi:10.1261/rna.048785.114

328. von Moeller H, Lerner R, Ricciardi A, Basquin C, Marzluff WF, Conti E. Structural and biochemical studies of SLIP1–SLBP identify DBP5 and eIF3g as SLIP1-binding proteins. Nucleic Acids Res. Narnia; 2013;41: 7960–7971. doi:10.1093/nar/gkt558

329. Hoefig KP, Rath N, Heinz GA, Wolf C, Dameris J, Schepers A, et al. Eri1 degrades the stem-loop of oligouridylated histone mRNAs to induce replication-dependent decay. Nat Struct Mol Biol. 2013;20: 73–81. doi:10.1038/nsmb.2450

330. Mullen TE, Marzluff WF. Degradation of histone mRNA requires oligouridylation followed by decapping and simultaneous degradation of the mRNA both 5' to 3' and 3' to 5'. Genes Dev. Cold Spring Harbor Laboratory Press; 2008;22: 50–65. doi:10.1101/gad.1622708

331. Kaygun H, Marzluff WF. Regulated degradation of replication-dependent histone mRNAs requires both ATR and Upf1. Nat Struct Mol Biol. Nature Publishing Group; 2005;12: 794–800. doi:10.1038/nsmb972

332. Lyons SM, Ricciardi AS, Guo AY, Kambach C, Marzluff WF. The C-terminal extension of Lsm4 interacts directly with the 3' end of the histone mRNP and is required for

efficient histone mRNA degradation. Rna. Cold Spring Harbor Laboratory Press; 2014;20: 88–102. doi:10.1261/rna.042531.113

333. Slevin MK, Meaux S, Welch JD, Bigler R, Miliani de Marval PL, Su W, et al. Deep Sequencing Shows Multiple Oligouridylations Are Required for 3' to 5' Degradation of Histone mRNAs on Polyribosomes. Mol Cell. Cell Press; 2014;53: 1020–1030. doi:10.1016/J.MOLCEL.2014.02.027

334. Cassonnet P, Rolloy C, Neveu G, Vidalain P-O, Chantier T, Pellet J, et al. Benchmarking a luciferase complementation assay for detecting protein complexes. Nat Methods. Nature Publishing Group; 2011;8: 990–992. doi:10.1038/nmeth.1773

335. Biquand E, Poirson J, Karim M, Declercq M, Malausse N, Cassonnet P, et al. Comparative Profiling of Ubiquitin Proteasome System Interplay with Influenza A Virus PB2 Polymerase Humans. 2017;2: 1–14.

336. Munier S, Rolland T, Diot C, Jacob Y, Naffakh N. Exploration of binary virus-host interactions using an infectious protein complementation assay. Mol Cell Proteomics. American Society for Biochemistry and Molecular Biology; 2013;12: 2845–55. doi:10.1074/mcp.M113.028688

337. Biquand E. Delineating the interplay between the PB2 protein of influenza A viruses and the host Ubiquitin Proteasome System. 2017.

338. Alonso-López D, Gutiérrez MA, Lopes KP, Prieto C, Santamaría R, De Las Rivas J. APID interactomes: providing proteome-based interactomes with controlled quality for multiple species and derived networks. Nucleic Acids Res. Narnia; 2016;44: W529–W535. doi:10.1093/nar/gkw363

339. Bindea G, Mlecnik B, Hackl H, Charoentong P, Tosolini M, Kirilovsky A, et al. ClueGO: a Cytoscape plug-in to decipher functionally grouped gene ontology and pathway annotation networks. Bioinformatics. Oxford University Press; 2009;25: 1091–3. doi:10.1093/bioinformatics/btp101

340. Vester D, Lagoda A, Hoffmann D, Seitz C, Heldt S, Bettenbrock K, et al. Real-time RT-qPCR assay for the analysis of human influenza A virus transcription and replication dynamics. J Virol Methods. Elsevier; 2010;168: 63–71. doi:10.1016/J.JVIROMET.2010.04.017

341. ATCC. A549 (ATCC® CCL-185™), human lung carcinoma cells [Internet]. Available: https://www.lgcstandards-atcc.org/products/all/CCL-185.aspx?geo_country=fr#characteristics

342. Matrosovich M, Matrosovich T, Carr J, Roberts NA, Klenk H-D. Overexpression of the alpha-2,6-sialyltransferase in MDCK cells increases influenza virus sensitivity to neuraminidase inhibitors. J Virol. American Society for Microbiology (ASM); 2003;77:

8418–25. doi:10.1128/jvi.77.15.8418-8425.2003

343. Kanehisa M, Sato Y, Furumichi M, Morishima K, Tanabe M. New approach for understanding genome variations in KEGG. Nucleic Acids Res. Oxford University Press; 2019;47: D590–D595. doi:10.1093/nar/gky962

344. Kanehisa M, Furumichi M, Tanabe M, Sato Y, Morishima K. KEGG: new perspectives on genomes, pathways, diseases and drugs. Nucleic Acids Res. Oxford University Press; 2017;45: D353–D361. doi:10.1093/nar/gkw1092

345. Kanehisa M, Goto S. KEGG: kyoto encyclopedia of genes and genomes. Nucleic Acids Res. Oxford University Press; 2000;28: 27–30. doi:10.1093/nar/28.1.27

346. Matrosovich M, Matrosovich T, Garten W, Klenk H-D. New low-viscosity overlay medium for viral plaque assays. Virol J. BioMed Central; 2006;3: 63. doi:10.1186/1743-422X-3-63

347. Vignuzzi M, Gerbaud S, van der Werf S, Escriou N. Naked RNA immunization with replicons derived from poliovirus and Semliki Forest virus genomes for the generation of a cytotoxic T cell response against the influenza A virus nucleoprotein. J Gen Virol. Microbiology Society; 2001;82: 1737–1747. doi:10.1099/0022-1317-82-7-1737

348. Kawakami E, Watanabe T, Fujii K, Goto H, Watanabe S, Noda T, et al. Strand-specific real-time RT-PCR for distinguishing influenza vRNA, cRNA, and mRNA. J Virol Methods. Elsevier; 2011;173: 1–6. doi:10.1016/J.JVIROMET.2010.12.014

349. Berggård T, Linse S, James P. Methods for the detection and analysis of protein–protein interactions. Proteomics. John Wiley & Sons, Ltd; 2007;7: 2833–2842. doi:10.1002/pmic.200700131

350. Rao VS, Srinivas K, Sujini GN, Kumar GNS. Protein-protein interaction detection: methods and analysis. Int J Proteomics. Hindawi; 2014;2014: 147648. doi:10.1155/2014/147648

351. Lievens S, Lemmens I, Montoye T, Eyckerman S, Tavernier J. Two-hybrid and its recent adaptations. Drug Discov Today Technol. Elsevier; 2006;3: 317–324. doi:10.1016/J.DDTEC.2006.09.006

352. Deane CM, Salwiński Ł, Xenarios I, Eisenberg D. Protein interactions: two methods for assessment of the reliability of high throughput observations. Mol Cell Proteomics. American Society for Biochemistry and Molecular Biology; 2002;1: 349–56. doi:10.1074/mcp.m100037-mcp200

353. Rigaut G, Shevchenko A, Rutz B, Wilm M, Mann M, Séraphin B. A generic protein purification method for protein complex characterization and proteome exploration. Nat Biotechnol. Nature Publishing Group; 1999;17: 1030–1032. doi:10.1038/13732

354. Mann M. Functional and quantitative proteomics using SILAC. Nat Rev Mol Cell Biol. Nature Publishing Group; 2006;7: 952–958. doi:10.1038/nrm2067

355. Miller KE, Kim Y, Huh W-K, Park H-O. Bimolecular Fluorescence Complementation (BiFC) Analysis: Advances and Recent Applications for Genome-Wide Interaction Studies. J Mol Biol. Academic Press; 2015;427: 2039–2055. doi:10.1016/J.JMB.2015.03.005

356. Remy I, Michnick SW. A highly sensitive protein-protein interaction assay based on Gaussia luciferase. Nat Methods. Nature Publishing Group; 2006;3: 977–979. doi:10.1038/nmeth979

357. Neveu G, Cassonnet P, Vidalain P-O, Rolloy C, Mendoza J, Jones L, et al. Comparative analysis of virus–host interactomes with a mammalian high-throughput protein complementation assay based on Gaussia princeps luciferase. Methods. Academic Press; 2012;58: 349–359. doi:10.1016/J.YMETH.2012.07.029

358. Muller M, Jacob Y, Jones L, Weiss A, Brino L, Chantier T, et al. Large Scale Genotype Comparison of Human Papillomavirus E2-Host Interaction Networks Provides New Insights for E2 Molecular Functions. Roth FP, editor. PLoS Pathog. Public Library of Science; 2012;8: e1002761. doi:10.1371/journal.ppat.1002761

359. Choi SG, Olivet J, Cassonnet P, Vidalain P-O, Luck K, Lambourne L, et al. Towards an ”assayome” for binary interactome mapping. bioRxiv. Cold Spring Harbor Laboratory; 2019; 530790. doi:10.1101/530790

360. Https://www.genome.jp/kegg/. KEGG Pathways [Internet].

361. Shapira SD, Gat-Viks I, Shum BOV, Dricot A, de Grace MM, Wu L, et al. A Physical and Regulatory Map of Host-Influenza Interactions Reveals Pathways in H1N1 Infection. Cell. Cell Press; 2009;139: 1255–1267. doi:10.1016/J.CELL.2009.12.018

362. de Chassey B, Aublin-Gex A, Ruggieri A, Meyniel-Schicklin L, Pradezynski F, Davoust N, et al. The Interactomes of Influenza Virus NS1 and NS2 Proteins Identify New Host Factors and Provide Insights for ADAR1 Playing a Supportive Role in Virus Replication. Chanda SK, editor. PLoS Pathog. 2013/07/16. 2013;9: e1003440. doi:10.1371/journal.ppat.1003440

363. Nomura Y, Roston D, Montemayor EJ, Cui Q, Butcher SE. Structural and mechanistic basis for preferential deadenylation of U6 snRNA by Usb1. Nucleic Acids Res. Oxford University Press; 2018;46: 11488–11501. doi:10.1093/nar/gky812

364. Wu KX, Phuektes P, Kumar P, Goh GYL, Moreau D, Chow VTK, et al. Human genome-wide RNAi screen reveals host factors required for enterovirus 71 replication. Nat Commun. Nature Publishing Group; 2016;7: 13150. doi:10.1038/ncomms13150

365. Silva-Ayala D, Lopez T, Gutierrez M, Perrimon N, Lopez S, Arias CF. Genome-wide RNAi screen reveals a role for the ESCRT complex in rotavirus cell entry. Proc Natl Acad Sci. 2013;110: 10270–10275. doi:10.1073/pnas.1304932110

366. Lee AS-Y, Burdeinick-Kerr R, Whelan SPJ. A Genome-Wide Small Interfering RNA Screen Identifies Host Factors Required for Vesicular Stomatitis Virus Infection. J Virol. American Society for Microbiology (ASM); 2014;88: 8355. doi:10.1128/JVI.00642-14

367. Ward AM, Calvert MEK, Read LR, Kang S, Levitt BE, Dimopoulos G, et al. The Golgi associated ERI3 is a Flavivirus host factor. Sci Rep. Nature Publishing Group; 2016;6: 34379. doi:10.1038/srep34379

368. Ivey KN, Srivastava D. microRNAs as Developmental Regulators. Cold Spring Harb Perspect Biol. Cold Spring Harbor Laboratory Press; 2015;7: a008144. doi:10.1101/cshperspect.a008144

369. Fuda NJ, Ardehali MB, Lis JT. Defining mechanisms that regulate RNA polymerase II transcription in vivo. Nature. NIH Public Access; 2009;461: 186–92. doi:10.1038/nature08449

370. Simon LM, Morandi E, Luganini A, Gribaudo G, Martinez-Sobrido L, Turner DH, et al. In vivo analysis of influenza A mRNA secondary structures identifies critical regulatory motifs. Nucleic Acids Res. 2019; doi:10.1093/nar/gkz318

371. Wang R, Zhang Y-Y, Lu J-S, Xia B-H, Yang Z-X, Zhu X-D, et al. The highly pathogenic H5N1 influenza A virus down-regulated several cellular MicroRNAs which target viral genome. J Cell Mol Med. John Wiley & Sons, Ltd (10.1111); 2017;21: 3076–3086. doi:10.1111/jcmm.13219

372. Song L, Liu H, Gao S, Jiang W, Huang W. Cellular microRNAs inhibit replication of the H1N1 influenza A virus in infected cells. J Virol. American Society for Microbiology Journals; 2010;84: 8849–60. doi:10.1128/JVI.00456-10

373. Saldi T, Fong N, Bentley DL. Transcription elongation rate affects nascent histone pre-mRNA folding and 3’ end processing. Genes Dev. Cold Spring Harbor Laboratory Press; 2018;32: 297–308. doi:10.1101/gad.310896.117

374. Yang X, Torres MP, Marzluff WF, Dominski Z. Three proteins of the U7-specific Sm ring function as the molecular ruler to determine the site of 3’-end processing in mammalian histone pre-mRNA. Mol Cell Biol. American Society for Microbiology Journals; 2009;29: 4045–56. doi:10.1128/MCB.00296-09

375. Guilligay D, Tarendeau F, Resa-Infante P, Coloma R, Crepin T, Sehr P, et al. The structural basis for cap binding by influenza virus polymerase subunit PB2. Nat Struct Mol Biol. Nature Publishing Group; 2008;15: 500–506. doi:10.1038/nsmb.1421

376. Bertoli C, Skotheim JM, de Bruin RAM. Control of cell cycle transcription during G1 and S phases. Nat Rev Mol Cell Biol. Nature Publishing Group; 2013;14: 518–528. doi:10.1038/nrm3629

377. Yonaha M, Chibazakura T, Kitajima S, Yasukochi Y. Cell cycle-dependent regulation of RNA polymerase II basal transcription activity. Nucleic Acids Res. Narnia; 1995;23: 4050–4054. doi:10.1093/nar/23.20.4050

378. Jiang W, Wang Q, Chen S, Gao S, Song L, Liu P, et al. Influenza A virus NS1 induces G0/G1 cell cycle arrest by inhibiting the expression and activity of RhoA protein. J Virol. American Society for Microbiology Journals; 2013;87: 3039–52. doi:10.1128/JVI.03176-12

379. He Y, Xu K, Keiner B, Zhou J, Czudai V, Li T, et al. Influenza A virus replication induces cell cycle arrest in G0/G1 phase. J Virol. American Society for Microbiology (ASM); 2010;84: 12832–40. doi:10.1128/JVI.01216-10

380. Fan Y, Sanyal S, Bruzzone R. Breaking Bad: How Viruses Subvert the Cell Cycle. Front Cell Infect Microbiol. Frontiers; 2018;8: 396. doi:10.3389/fcimb.2018.00396

381. Marzluff WF, Wagner EJ, Duronio RJ. Metabolism and regulation of canonical histone mRNAs: life without a poly(A) tail. Nat Rev Genet. Nature Publishing Group; 2008;9: 843–854. doi:10.1038/nrg2438

382. Dilweg IW, Gultyaev AP, Olsthoorn RC. A widespread Xrn1-resistant RNA motif composed of two short hairpins. bioRxiv. Cold Spring Harbor Laboratory; 2019; 522318. doi:10.1101/522318